UNIVERSIDAD COMPLUTENSE DE MADRID

FACULTAD DE MEDICINA

TESIS DOCTORAL

Papel de la metilación de H3K9 en la mecánica nuclear y la migración de la leucemia linfoblástica aguda

MEMORIA PARA OPTAR AL GRADO DE DOCTOR

PRESENTADA POR

Elena Madrazo Béjar

DIRECTOR

Javier Redondo Muñoz

UNIVERSIDAD COMPLUTENSE DE MADRID
FACULTAD DE MEDICINA

TESIS DOCTORAL

PAPEL DE LA METILACIÓN DE H3K9 EN LA MECÁNICA NUCLEAR Y LA MIGRACIÓN DE LA LEUCEMIA LINFOBLÁSTICA AGUDA

MEMORIA PARA OPTAR AL GRADO DE DOCTORA

PRESENTADA POR

ELENA MADRAZO BÉJAR

DIRECTOR

JAVIER REDONDO MUÑOZ

UNIVERSIDAD COMPLUTENSE DE MADRID

FACULTAD DE MEDICINA

TESIS DOCTORAL

PAPEL DE LA METILACIÓN DE H3K9 EN LA MECÁNICA NUCLEAR Y LA MIGRACIÓN DE LA LEUCEMIA LINFOBLÁSTICA AGUDA

MEMORIA PARA OPTAR AL GRADO DE DOCTORA

PRESENTADA POR

ELENA MADRAZO BÉJAR

DIRECTOR

JAVIER REDONDO MUÑOZ

A mis padres,

AGRADECIMIENTOS

Agradecimientos

¡Por fin tengo entre mis manos los que pensaba que no iba a llegar nunca! Con esto se cierra una etapa y espero que se abran las puertas de otras. Quiero agradecer a todos los que han hecho que este largo camino haya sido un poco más fácil y que esta tesis haya sido posible.

En primer lugar, gracias a Javier por haber confiado y apostado en mí para comenzar su laboratorio, por haberme dado la oportunidad de desarrollar este proyecto y que esta tesis vea la luz.

También quiero agradecer a todos los que han pasado por el laboratorio (Estefanía, Carmen, Candido, Lucía, Celso, Andrea, David, Ander), porque, aunque haya sido más o menos tiempo todos han aportado su granito de arena y han hecho que los días sean mucho más amenos. A Ana por toda su ayuda en el final de mi tesis y comienzo de la tuya, porque su entusiasmo y sus ganas se contagian a los demás. Y en especial quiero dar las gracias a Raquel, porque desde que llegaste al labo has sido un apoyo fundamental para que esta tesis haya salido para delante, porque siempre estás dispuesta con una sonrisa a ayudar en lo que haga falta y porque durante todos estos años te has convertido en mucho más que una compañera, sé que vas a llegar donde te propongas.

Gracias a toda la gente del Gregorio Marañón por su acogida en los comienzos de esta tesis, en especial a Paloma por acogernos en su laboratorio, por cada comida o cada charla con ella en la que siempre aprendes algo nuevo. A Julia por cuidarnos tanto y estar siempre pendiente de todos y de todo. A Rafa por todos los conocimientos y ayuda con el confo, porque ha sido fundamental para esta tesis. A Amaya, a Raquel, a Mónica, a Balti, a Elena, a Ali, porque siempre me han recibido con una sonrisa y me han ayudado en lo que he necesitado. Y, por último, gracias a Alba, Celia y Sara porque sin ellas este camino no hubiera sido lo mismo, porque su apoyo al principio en el labo y después en la distancia ha sido fundamental para llegar hasta aquí.

Gracias a toda la gente de la UCM (Sergio, Óscar, Beas, Marta, etc) por su gran ayuda a ubicarme cuando llegamos allí, por estar siempre dispuestos a prestarnos cualquier cosa o explicarme donde estaba todo, por el buen ambiente diario.

A Manuel y su equipo del Niño Jesús por todas las muestras proporcionadas para el desarrollo de esta tesis, y en especial a África por su ayuda con los *in vivo*.

Agradecimientos

A Francisco Monroy y su labo por haberme enseñado y dejado trabajar con sus equipos, por haberme abierto las puertas desde el primer día y tratarme como una más allí.

A toda la gente del CIB, que, aunque hayamos coincidido al final de este camino, han aportado su granito de arena. A Joaquín y sus chicos, por su ayuda a ubicarnos en el nuevo labo y con los reactivos.

También quiero agradecer a todos los que fuera del mundo de la ciencia por todo lo que me han ayudado en este camino, porque sin todos vosotros esto no hubiera sido posible. Gracias a todos mis amigos por escucharme y animarme durante todo el tiempo, porque sin esos ratos con cada uno de vosotros esto hubiera sido mucho más duro. Gracias a Jose por su apoyo durante todos estos años, por creer en mí cuando yo no lo hacía, y por animarme y repetirme lo orgulloso que estabas de mí. A Goku porque entre tus lametones y paseos la escritura de esta tesis ha sido mucho más amena.

Gracias a mi familia por su interés y apoyo, por estar siempre dispuestos a escucharme y tener siempre una palabra de ánimo. A mi tía Yoli porque es una guerrera, porque a pesar de los baches del camino siempre tiene una buena palabra. A mi hermana porque te quiero y me has dado el regalo más bonito del mundo, Marcos. A Marcos por cada abrazo y cada beso para recargarme las pilas, por tus charlas y tu imaginación, ¡vas a comerte el mundo pequeño!

Y finalmente como no podía ser de otra manera, gracias a mis padres, porque sin ellos nada de esto hubiera sido posible. Por estar en cada segundo de mi vida ayudándome y facilitándome todo. Porque gracias a vosotros soy quien soy y he conseguido llegar hasta aquí.

¡GRACIAS!

ÍNDICE

ÍNDICE DE CONTENIDO

ÍNDICE DE FIGURAS

ÍNDICE DE TABLAS DE CONTENIDO

ABREVIATURAS

A

ACR: *Atypical chemokines receptors,* receptores de quimioquinas atípicos

ADN: Ácido desoxirribonucleico

ADP: Adenosin difosfato

AKT: *Protein kinase B,* proteína kinasa B

ARF: *ADP-ribosilation factor,* factor de ribosilación de ADP

ARN: Ácido ribonucleico

ARNm: Ácido ribonucleico mensajero

C

C-terminal: Carboxiterminal

Ca^{2+}: Calcio

CAR-T: *Chimeric antigen receptor T-cell,* receptor de antígeno quimérico de células T

CDKN2: *Cyclin dependent kinase inhibitor 2,* inhibidor de quinasa dependiente de ciclina 2

CXCL12: *C-X-C chemokine ligand type 12,* ligando de quimioquina C-X-C tipo 12

D

DAG: Diacilglicerol

DARC: *Duffy antigen receptor for chemokines*, antígeno Duffy receptor de quimioquinas

DRY: Aspartato-tirosina-arginina

E

EDTA: *Ethylenediamine tetraacetic acid*, ácido etilendiaminotetraacético

EGIL: *European group of immunological classification of leukemia,* grupo europeo de clasificación inmunológica de las leucemias

ERM: Enfermedad residual mínima

ESL-1: *E-selectin ligand 1*, ligando 1 de selectina E

EZH2: *Enhancer of zeste 2 polycomb repressive complex 2 subunit,* potenciador de la subunidad 2 del complejo represivo polycomb zeste 2

F

FAB: Franco-americano-británica

FN: Fibronectina

G

GLP: *G9a like protein*

GPCR: *G protein-coupled receptors*, receptores acoplados a proteínas G

GTP: *Guanosine triphosphate*, guanosín trifosfato

H

H3K9: *Histone H3 lysine 9,* histona H3 lisina 9

HDMs: *Histone demethylase,* demetilasa de histonas

Hep: Heparina

HKMTs: *Histone lysine methyltransferases,* metiltransferasa de lisina

HSCs: *Hematopoietic stem cells*, células madre hematopoyéticas

HS/PC: *Hematopoietic stem and progenitor cells*, células troncales y progenitoras

HTMs: *Histone methyltransferases*, metiltransferasas de histonas

I

ICAM-1: *Intercellular adhesion molecule 1*, molécula de adhesión endotelial 1

IIICS: *Alternatively spliced type III connecting segment,* segmento de conexión tipo III empalmado alternativamente

IL-1: *Interleukin-1*, interleuquina-1

IP3: *Inositol trisphosphate*, inositol trifosfato

J

JAK: *Janus kinase*, quinasa Jano

K

kDa: kiloDalton

L

LFA-1: *Lymphocyte function-associated antigen 1,* antigeno-1 asociado a la función linfocitaria

LINC: *Linker of nucleoskeleton and cytoskeleton*, enlazador de nucleoesqueleto y citoesqueleto

LLA: Leucemia linfoblástica aguda

LMA: Leucemia mieloblástica aguda

LMO2: *Lim Domain Only 2*

lncRNA: *Long non-coding RNAs,* ARN largos no codificantes

M

Mac-1*: Macrophage-1 antigen*, antígeno de macrófagos 1

MEC: Matriz extracelular

Mg^{2+}: Magnesio

miARNs: micro ARNs

MO: Médula ósea

MMP: *Matrix metalproteinase*, metaloproteinasa de matriz

MTE: Migración transendotelial

MTP-SURF: *Multiple particle tracking-Speeded up robust features*, rastreo de partículas múltiples-funciones robustas aceleradas

N

N-terminal: Aminoterminal

NK: *Natural killer*

O

OMS: Organización mundial de la salud

P

Pb: Pares de bases

PBL: *Peripheral blood lymphocytes,* linfocitos de sangre periférica

PCR: Reacción en cadena de la polimerasa

PDK-1: *Phosphoinositide-dependent kinase-1*, quinasa dependiente de fosfoinosítido-1

PECAM-1: *Platelet endothelial cell adhesion molecule,* molécula de adhesión de células endoteliales de plaquetas

Ph: *Philladelphia*

PI3K: *Phosphatidylinositol 3-kinases,* fosfoinositol-3 quinasa

PIP3: *Phosphatidylinositol (3,4,5)-trisphosphate* fofatidilinositol (3,4,5)-tifosfato

PKC: Proteína kinasa C

PMA: *Phorbol 12-myristate 13-acetate,* forbol 12-miristato 13-acetato

PRMTs: *Protein arginine methyltransferases*, metiltransferasas de proteína arginina

PS: *Phosphatidylserine*, fosfatidilserina

PSGL: *P-Selectin Glycoprotein Ligand 1,* ligando glicoproteico-1 de la P-selectina

PTM: *Post-Translational modifications*, modificaciones postraduccionales

R

RDM: *Arginine demethylase*, demetilasa de arginina

RETI-SEHOP: Registro español de tumores infantiles – Sociedad española de hematología y oncología pediátricas.

RGD: Arginina-glicina-aspártico

RISC: *RNA-induced silencing complex*, complejos de silenciamiento inducidos por ARN

S

SDF-1: *Stromal cell-derived factor 1*, factor derivado de células estromales 1

SET: *Su(var)3-9 enhancer of zeste and trithorax*

SLR: Supervivencia libre de recaídas

SNC: Sistema nervioso central

SSC: Supervivencia sin complicaciones

STAT: *Signal transducer and activator of transcription*, traductoras de señales y activadoras de transcripción

SUN: *Sad1 and UNC38 homology,* homología Sad1 y UNC38

T

TM: Transmembrana

TNF: *Tumor necrosis factor*, factor de necrosis tumoral

V

VCAM-1: *Vascular cell adhesion molecule-1,* molécula de adhesión de células vasculares 1

VE: Vascular endotelial

VEGF: *Vascular endothelial growth factor*, factor de crecimiento del endotelio vascular

VLA-4: *Very Late Antigen 4,* antígeno de activación tardía 4

W

WBC: *White blood cells,* glóbulos blancos

RESUMEN

INTRODUCCIÓN

La leucemia linfoblástica aguda (LLA) es el cáncer más común en la edad pediátrica. Se caracteriza por la acumulación de células leucémicas en sangre y su posterior infiltración en otros tejidos. La supervivencia actualmente es superior al 80% con los tratamientos actuales, sin embargo, un porcentaje de los pacientes siguen recayendo y no presenta buen pronóstico; por lo que se necesitan nuevos abordajes y terapias que mejoren la supervivencia y los efectos secundarios de los tratamientos actuales.

La migración celular es un proceso celular que es esencial para el desarrollo de los tejidos y la homeostasis celular, pero también desempeña un papel crucial durante otros procesos como la inflamación, respuesta inmunológica y la metástasis en el cáncer. En el proceso de migración celular intervienen numerosos receptores celulares, como las integrinas y receptores que quimioquinas, que juegan un importante en el microambiente tumoral, así como en la progresión e invasión de las células tumorales. Recientemente se ha descrito al núcleo como un componente clave en el proceso de migración, pudiendo tener un papel importante en la infiltración de la LLA. La cromatina es el componente principal del núcleo y sus cambios de conformación, debido a modificaciones epigenéticas, regulan la homeostasis del ADN y podrían afectar a las propiedades biomecánicas del núcleo y a la migración celular.

El estudio de la epigenética y cómo se modula la respuesta transcripcional celular en el transcurso de múltiples enfermedades ha aumentado considerablemente en los últimos años. Estudios recientes sugieren que las alteraciones epigenéticas podrían marcar el origen de algunos tumores, así como su desarrollo y progresión. En el caso de la LLA se ha visto que algunas de las enzimas que se encuentran sobreexpresadas son las metiltransferasas de H3K9 y podrían tener un papel importante en la infiltración de las células leucémicas en los tejidos.

OBJETIVOS

El objetivo principal de esta tesis es estudiar las acciones que las modificaciones epigenéticas pueden desempeñar en la migración y diseminación de las células de LLA, en particular por su conexión con la biomecánica del núcleo celular. Para llegar a este objetivo hemos determinado los siguientes objetivos específicos:

1. Estudiar el papel del microambiente en la modificación de histonas y por tanto en las propiedades físicas del núcleo y en la migración de las células de LLA.
2. Estudiar el impacto de modificaciones epigenéticas (metilación de histonas) en la migración transendotelial de células de LLA.
3. Desarrollar un método de análisis de las propiedades mecánicas del núcleo celular.

RESULTADOS Y DISCUSIÓN

Las quimioquinas tienen un papel muy importante en la infiltración y la progresión de la LLA. Las células de LLA expresan varios receptores de quimioquinas en su superficie, entre ellos CXCR4 que se asocia con una infiltración extramedular en pacientes pediátricos, y, por lo tanto, con

peor pronóstico. CXCL12 es el principal ligando de CXCR4, y representa un papel fundamental en la proliferación y supervivencia de las células de LLA. En esta tesis hemos comprobado cómo la estimulación con CXCL12 produce un aumento de H3K9me3 en células de LLA-T pero no en las B. Estos cambios en la cromatina inducidos por CXCL12 tienen un impacto directo en las propiedades mecánicas y en la deformabilidad nuclear en las células de LLA-T, lo que regula la capacidad invasiva de estas células *in vitro* y usando un modelo *in vivo*. Con todos estos resultados sugerimos que las metiltransferasas de H3K9, G9a y SUV39H1, podrían convertirse en posibles dianas terapéuticas interesantes para bloquear la infiltración y el desarrollo de la LLA-T.

Además de las quimioquinas, las integrinas y otras moléculas de adhesión tienen un papel fundamental en la infiltración de la LLA. La integrina VLA-4 actúa como marcador pronóstico en la LLA, por lo que decidimos estudiar la posible relación que existe entre VLA-4 y las metiltransferasas de H3K9. Comprobamos que existe una correlación negativa entre VLA-4 y G9a, por lo que podría ser más importante la conexión funcional que se da entre ambas moléculas que sus niveles de expresión. Además, hemos demostrado que el silenciamiento o inhibición de G9a bloquea la migración transendotelial de células LLA. Nuestros resultados demuestran que tiene una función clave en este proceso, ya que interviene en la deformabilidad nuclear necesaria para la migración a través de los poros. Por lo tanto, los mecanismos inducidos por G9a serían atractivos para abordar la diseminación de la leucemia.

Para determinar las propiedades biofísicas del núcleo celular hemos desarrollado un algoritmo MTP-SURF que permite detectar las trayectorias de puntos de cromatina y determinar las propiedades viscoelásticas asociadas a esta. Para estos ensayos hemos utilizado tanto núcleos celulares aislados de linfocitos normales y diferentes tipos de muestras leucémicas, como células intactas. Además, hemos sometidos ambos a estrés osmótico mediante la adicción de Mg^{2+} y de EDTA. Nuestros resultados demuestran que la adicción de Mg^{2+} provoca una condensación de la cromatina y por tanto una reducción del tamaño nuclear, y como consecuencia observamos que se produce un aumento significativo de la viscosidad de la cromatina. Realizamos este ensayo comparando distintos subtipos de LLA, y comprobamos que en las células de LLA de alto riesgo presentan valores más altos de viscosidad y menor densidad que PBL sanos, y, sin embargo, las LLA en recaída presentan mayor densidad nuclear. Por tanto, nuestros resultados demuestran que el método de análisis desarrollado podría facilitar la posibilidad de generar nuevas herramientas para determinar el pronóstico de células leucémicas.

ABSTRACT

INTRODUCTION

Acute lymphoblastic leukemia (ALL) is the most common cancer in the pediatric age group. It is characterized by the accumulation of leukemic cells in the blood and their subsequent infiltration of other tissues. Survival is currently over 80% with current treatments, however, a percentage of patients still relapse and do not have a good prognosis; therefore, new approaches and therapies are needed to improve survival and side effects of current treatments.

Cell migration is a cellular process essential for tissue development, inflammation, immune response and cell homeostasis. It also plays a crucial role during other pathological processes, such as cancer metastasis. Many cell receptors are involved in cell migration, including integrins and chemokine receptors that play an important role in the tumor microenvironment and the invasion of tumor cells. The nucleus has recently been described as a key component in the migration process and may play an important role in the infiltration of ALL. Chromatin is the main component of the nucleus and its conformational changes, due to epigenetic modifications, regulate DNA homeostasis and could affect the biomechanical properties of the nucleus and cell migration.

The study of epigenetics and how the transcriptional response is modulated in the course of multiple diseases has increased considerably in recent years. Many studies suggest that epigenetic alterations could mark the origin of some tumors, as well as their development and progression. In the case of ALL, some of the overexpressed enzymes are H3K9 methyltransferases, which could play an important role in the infiltration of leukemic cells in tissues.

OBJECTIVES

The main objective of this thesis is to study the actions that epigenetic modifications may play in the migration and dissemination of ALL cells, through their connection with the biomechanics of the cell nucleus. To reach this goal we have determined the following specific objectives:

1. To study the role of the microenvironment in histone modification and therefore in the physical properties of the nucleus and in the migration of ALL cells.
2. To study the impact of epigenetic modifications (histone methylation) on the transendothelial migration of ALL cells.
3. To develop a method for the analysis of the mechanical properties of the cell nucleus.

RESULTS ANS DISCUSSION

Chemokines play a very important role in the infiltration and progression of ALL. ALL cells express several chemokine receptors on their surface, including CXCR4, which is associated with

extramedullary infiltration in pediatric patients and, therefore, with a worse prognosis. CXCL12 is the main ligand of CXCR4 and plays a fundamental role in the proliferation and survival of ALL cells. In this thesis, we have verified how stimulation with CXCL12 produced an increment in H3K9me3 levels of T-ALL cells, but not in B-ALL cells. These changes in chromatin induced by CXCL12 had a direct impact on the mechanical properties and nuclear deformability in cells. This mechanism regulated the invasive capacity of T-ALL cells in vitro and in vivo. All together, we suggest that the H3K9, G9a and SUV39H1 methyltransferases could become potential interesting therapeutic targets to block the infiltration and development of T-ALL.

In addition to chemokines, integrins and other adhesion molecules play a key role in the infiltration of ALL. The integrin VLA-4 acts as a prognostic marker in ALL, so we decided to study the possible relationship between VLA-4 and H3K9 methyltransferases. We verified that a negative correlation between VLA-4 and G9a, son the functional connection between the two molecules may be more important than their expression levels. Furthermore, we have shown that silencing or inhibition of G9a blocked the transendothelial migration of ALL cells. Our results show that the nuclear deformability was necessary for ALL migration through the pores. Therefore, G9a-induced mechanisms would be attractive to address leukemia dissemination.

To determine the biophysical properties of the cell nucleus, we have developed an MTP-SURF algorithm that detects the trajectories of chromatin points and determines their viscoelastic properties. To perform this, we have used both isolated nuclei from normal lymphocytes and different types of ALL cells, as well as intact cells. In addition, we have subjected both to osmotic stress through the addition of Mg2+ and EDTA. Our results show that the addition of Mg2+ caused a condensation of the chromatin and a reduction in nuclear size; consequently, we observed a significant increase in the viscosity of the chromatin. By comparing different subtypes of ALL, we found that high-risk ALL cells had higher values of viscosity and lower density than normal lymphocytes; however, relapsed ALL showed higher nuclear density. Therefore, our results demonstrate that the analysis method developed could facilitate the possibility of developing new tools to determine the prognosis of leukemic cells.

INTRODUCCIÓN

1 LEUCEMIA LINFOBLÁSTICA AGUDA (LLA)

1.1 CARACTERÍSTICAS GENERALES

Las leucemias agudas constituyen un grupo heterogéneo de enfermedades neoplásicas caracterizadas por la expansión clonal de células derivadas de un progenitor hematopoyético inmaduro de línea linfoide (leucemia linfoblástica aguda, LLA) o mieloide (leucemia mieloblástica aguda, LMA). Dentro de las LLA, podemos distinguir en función del tipo celular al que este afectando en leucemias de línea B (LLA-B precursoras) y de línea T (LLA-T) (Brunning, 2003). Las leucemias son las neoplasias que presentan mayor frecuencia en edad pediátrica, alcanzando un 30% de los casos de tumores infantiles (RETI-SEHOP, 2014) (**figura 1**). El subtipo más común es la leucemia linfoblástica aguda (LLA) que supone el 78,4% de los tumores hematológicos diagnosticados en edad infantil. La LLA se da tanto en niños como en adultos, aunque alcanza su máxima incidencia entre los 2 y 5 años (Belson et al., 2007).

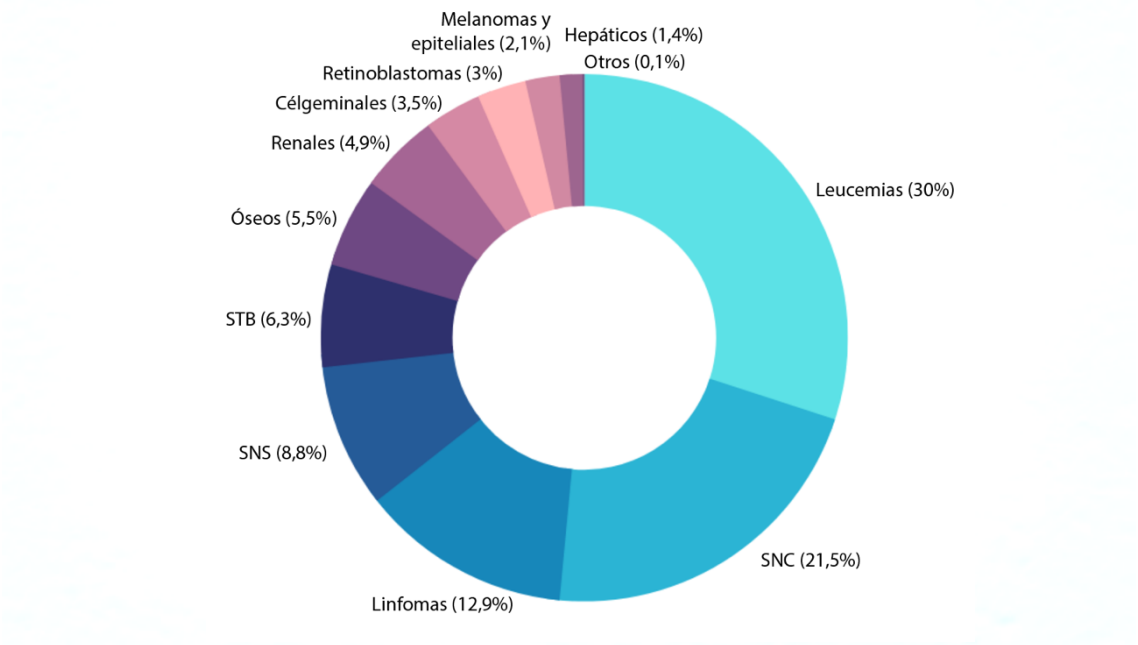

Figura 1. Distribución por grupo diagnóstico de los tumores infantiles en España, 0-14 años, 2000-2011 (figura adaptada de RETI-SEHOP, 2014).

La supervivencia de LLA ha aumentado significativamente en las últimas décadas, pasando de menos del 10% en los años 70 a más de un 80% de supervivencia con los tratamientos actuales (Miller et al., 2022). Sin embargo, entre un 10 y un 20% de los pacientes pediátricos siguen recayendo, y la cifra es aún mayor si hablamos de adultos o bebés (Hunger & Mullighan, 2015; Mullighan, 2010; Dinmohamed et al., 2016). Por lo que se necesitan enfoques innovadores para mejorar aún más la supervivencia, y reducir los efectos adversos de los tratamientos actuales, así como estudiar nuevos marcadores pronósticos y dianas terapéuticas para una medicina personalizada (Bassan & Hoelzer, 2011).

1.2 DIAGNÓSTICO Y CLASIFICACIÓN

El diagnóstico de LLA requiere la presencia del 20% o más de linfoblastos en médula ósea (Emadi & Law, 2022). En los años 70, el diagnóstico de LLA se basaba en la clasificación morfológica FAB (Franco-americano-británica) que define tres subtipos de LLA (L1, L2 y L3) en función del tamaño celular, el estado de la cromatina, la forma nuclear, la vacuolación del nucléolo, la cantidad de citoplasma y la basofilía (Bennet et al., 1976). Sin embargo, debido a la falta de valor pronóstico de estos criterios, en 1995 el grupo EGIL (*European Group of Immunological classification of Leukemias*) propuso una clasificación basada en las características inmunofenotípicas de los blastos de la LLA (Bene et al., 1995), en la que se sistematiza la LLA según el grado de madurez de la célula leucémica (**tablas 1 y 2**). En 2008, la Organización Mundial de la Salud (OMS) propuso una clasificación compuesta basada en las características citogenéticas e inmunofenotípicas combinadas de los blastos, reconociendo diferentes subgrupos de LLA (Swerdlow et al., 2008). En 2016 se hizo una revisión de esta última clasificación, en la que las LLA se clasifican en categorías linfoblásticas B y T con 2 nuevas entidades genéticas provisionales añadidas (**tabla 3**). La LLA de células B comprende aproximadamente el 85 % de los casos en niños y el 75 % en adultos, mientras que la LLA de células T comprende los casos restantes (Tasian et al., 2016; Terwilliger & Abdul-Hay, 2017).

LLA de línea B: CD19+ y/o CD22+ y/o CD79a+	
ProB (B-I)	TdT+, CD10-, Ig citoplasma -, Ig membrana -
Común (B-II)	TdT+, CD10+, Ig citoplasma -, Ig membrana -
Pre-B (B-III)	TdT+, CD10+, Ig citoplasma +, Ig membrana -
B madura (B-IV)	TdT+, CD10+, Ig citoplasma +, cadenas ligeras de superficie o citoplasmáticas kappa o lambda +

Tabla 1. Clasificación LLA-B según EGIL (tabla adaptada de Bene et al., 1995).

LLA de línea T: CD3 citoplasmático +	
ProT (B-I)	CD7+, CD2-, CD5-, CD8-, CD1a-
PreT (T-II)	CD2+ y/o CD5+ y/o CD8+, CD1a-, CD71+
Cortical (T-III)	CD1a+, CD71-
Madura (T-IV)	CD3 de superficie +, CD1a-

Tabla 2. Clasificación LLA-T según EGIL (tabla adaptada de Bene et al., 1995).

Leucemia/linfoma linfoblástico B, no especificado
Leucemia/linfoma linfoblástico B con alteraciones genéticas recurrentes
Leucemia/linfoma linfoblástica B con t(9;22)(q34;q11); BCR-ABL
Leucemia/linfoma linfoblástica B con t(v:11q23); reordenamiento del gen MLL
Leucemia/linfoma linfoblástica B con t(12;21)(p13;q22); ETV6-RUNX1 (TEL-AML1)
Leucemia/linfoma linfoblástica B con hiperdiploidía
Leucemia/linfoma linfoblástica B con hipodiploidía
Leucemia/linfoma linfoblástica B con t(5;14)(q31;q32); IL3-IGH
Leucemia/linfoma linfoblástica B con t(1;19)(q23;p13.3); TCF3-PBX1
Entidad provisional: Leucemia/linfoma BCR-ABL1-like
Entidad provisional: Leucemia/linfoma con iAMP21
Leucemia/linfoma linfoblástico T
Entidad provisional: Leucemia linfoblástica de precursores tempranos T
Entidad provisional: Leucemia/linfoma linfoblástica células NK (natural killer)

Tabla 3. Clasificación de la OMS de las neoplasias de precursores linfoides (tabla adaptada de Arber et al., 2016).

1.3 ORIGEN DE LA ENFERMEDAD

La etiología de la LLA es en gran parte desconocida, y la mayoría de los casos se creen que ocurren de forma esporádica (Pui et al., 2008). Sin embargo, existen algunas condiciones hereditarias predisponentes y factores de riesgo adquiridos asociados con una mayor incidencia de LLA. Menos del 5% de los casos se asocian con trastornos asociados con la inestabilidad cromosómica o la aneuploidía, como es el caso del Síndrome de Down (Schmidt et al., 2021). También ha habido algunas asociaciones entre distintos virus y la LLA; por ejemplo, entre el virus de Epstein-Barr y la LLA de células B maduras, el virus linfontrópico T humano tipo 1 y la LLA de células T de adulto, y el virus de la inmunodeficiencia humana en los trastornos linfoproliferativos (Guan et al., 2017; Xu et al., 2019). En el caso de las LLA pediátricas, se cree que el entorno fetal juega un papel vital en su desarrollo: durante la proliferación de las células en el desarrollo fetal ocurren alteraciones aleatorias que dan lugar a un clon preleucémico, que debido a la exposición a un patógeno durante los primeros años de la infancia conduce al desarrollo de la LLA (Raboso-Gallego et al., 2019). Por último, también se ha implicado la exposición a mutágenos como la quimioterapia o la radiación ionizante (Tebbi, 2021; Schmidt et al., 2021).

Existen lesiones genéticas específicas de LLA-B y LLA-T que no son compartidas entre ellas (Arber et al., 2016). Tradicionalmente se ha pensado que el origen tumoral estaba en una célula B o T comprometida, y por ello se desarrollaba un fenotipo u otro de LLA. Sin embargo, varios estudios (Raboso-Gallego et al., 2019; González-Herrero et al., 2018) han revelado que la transformación

celular esta mediada por un mecanismo de preparación epigenética que se establece por la lesión genética inicial, y va a imponer un programa de diferenciación celular específico en la célula cancerosa de origen que definirá el fenotipo posterior de las células tumorales. Hay que tener en cuenta que la alteración oncogénica inicial esencial para la iniciación del tumor no será necesaria una vez que se inicie el programa de diferenciación (**figura 2**).

En el caso de la LLA-B, la alteración cromosómica ETV6-RUNX1 es la alteración genética más común (Pui et al., 2019a). Esta lesión se encuentra en sangre del cordón umbilical en un 5% de los recién nacidos (Lausten-Thomsen et al., 2011; Schäfer et al., 2018), pero sólo unos pocos portadores de esta lesión desarrollaran la LLA. ETV6-RUNX1 actúa como un impulsor en la etapa inicial de la aparición de las células preleucémicas, pero son necesarios más señales secundarias para transformar la célula completamente en una célula leucémica. En este momento el gen de fusión ETV6-RUNX1 no será necesario ya para la propagación leucémica (Rodríguez-Hernández et al., 2017). El modelo ETV6-RUNX1 no es el único caso de cebado epigenético LLA-B. El BCR-ABLp190 también puede conferir susceptibilidad genética a LLA-B de manera similar a ETV6-RUNX1 (Martin-Lorenzo et al., 2018)

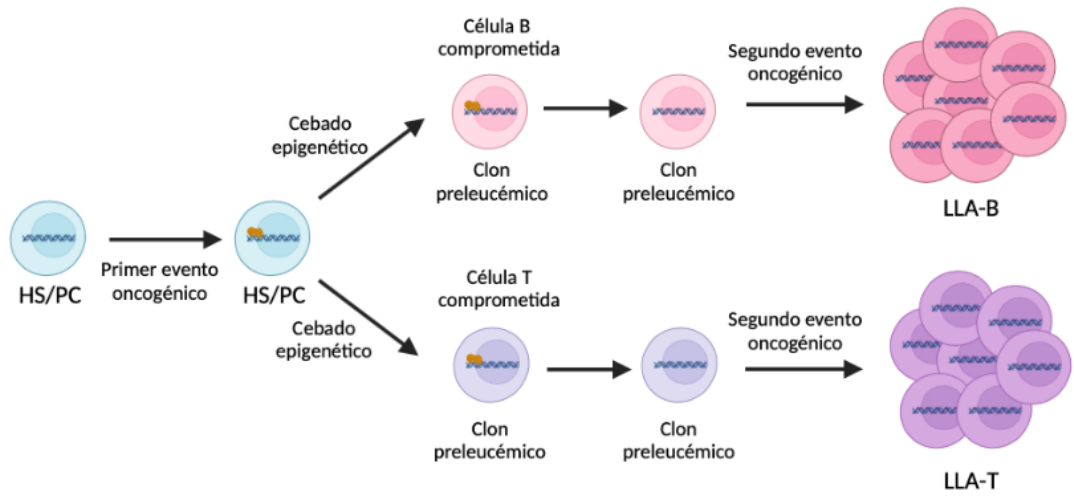

Figura 2. Evolución clonal de las LLA-T y B impuesta por el cebado epigenético (figura adaptada de Raboso-Gallego et al., 2019). El primer evento genético tiene lugar en una célula HS/PC, donde se induce un cebado epigenético específico que determinará el compromiso del fenotipo del clon preleucémico.

El oncogen LMO2 (*Lim Domain Only 2*) es uno de los impulsores más frecuentes de la LLA-T infantil (Van Vlierberghe et al., 2006; Qian et al., 2019). Según los estudios más recientes, el oncogén LMO2 es capaz de cebar las características fenotípicas del tumor en una célula T no comprometida. La expresión aberrante de LMO2 en células madre progenitoras hematopoyéticas (HS/PC) o en células T inmaduras (presentes en el timo) conduce a la acumulación temprana de precursores linfoides y la transformación a LLA-T (McCormack et al., 2010; Chambers & Rabbitts, 2015). Por lo tanto, las primeras etapas de la transformación estarían determinadas por el oncogen LMO2, pero el fenotipo final estaría determinado por

procedimientos oncogénicos secundarios, como las mutaciones de Notch1 (Garcia-Ramirez et al., 2018).

Muchos reguladores epigenéticos están implicados en la etiología de la enfermedad, así como en el diagnóstico, clasificación y pronóstico de los pacientes. La llegada de los estudios de asociación de todo el genoma permite la detección de un amplio número de modificaciones epigenéticas características de la LLA (**figura 3**), que reflejan la complejidad y heterogeneidad de la regulación epigenética en esta enfermedad. Además, el conocimiento de la epigenética de la LLA contribuirá a identificar dianas terapéuticas que podrían modificarse con tratamientos específicos, con la ventaja de que, a diferencia de las modificaciones genéticas, las alteraciones epigenéticas son reversibles (Navarrete-Meneses & Pérez-Vera, 2017).

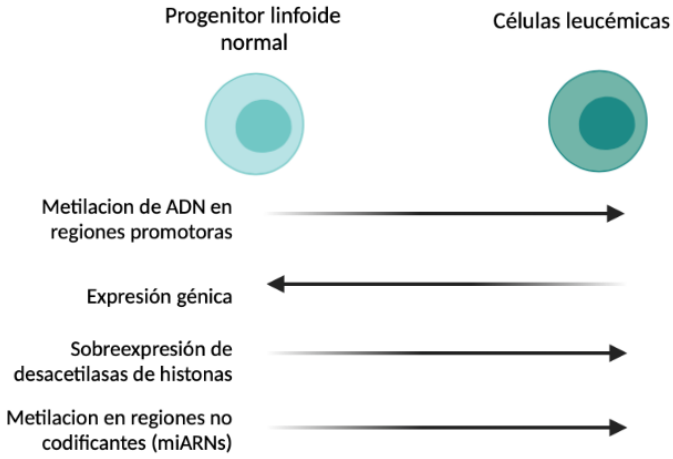

Figura 3. Diferencias epigenéticas entre progenitores linfoides normales y células leucémicas (figura adaptada de Navarrete-Meneses & Pérez-Vera, 2017).

1.4 PATOLOGÍA

La LLA representa un grupo de neoplasias malignas de células linfoides B o T en la etapa precursora que bloquea la diferenciación e impulsa la proliferación y supervivencia estas células (Zuckerman & Rowe, 2014). La presentación clínica es muy variable e inespecífica, y en la mayoría de los casos los síntomas al diagnóstico son secundarios a la infiltración de las células leucémicas en la médula ósea y otros órganos. Normalmente se presenta de forma aguda, con una historia de menos de 3 meses desde el inicio de los síntomas hasta el diagnóstico (Pui, 2012). Los síntomas iniciales más frecuentes son fiebre, cansancio, falta de apetito y pérdida de peso. La ocupación de blastos leucémicos en la medula ósea conduce a la supresión de la hematopoyesis, lo que hace que se produzca una anemia, neutropenia y trombocitopenia (Terwilliger & Abdul-Hay, 2017). Cuando los linfoblastos salen al torrente sanguíneo e invaden otros órganos se pueden apreciar adenopatías, hepatomegalia y esplenomegalia. Los linfoblastos también pueden invadir otros órganos como el SNC, los testículos o el timo (Pui, 2006; Deak et al., 2021; Nguyen et al., 2021).

En comparación con la LLA de linaje de células B más común, la LLA-T se define por características clínicas y biológicas distintas, como infiltración difusa de la médula ósea por linfoblastos T inmaduros, recuento alto de glóbulos blancos, masas mediastínicas con derrames pleurales, adenopatía voluminosa y infiltración del sistema nervioso central (Van Vlierberghe & Ferrando, 2012). A pesar de tener un mayor riesgo de recaída, el pronóstico de los pacientes con LLA-T ha mejorado notablemente en los últimos años debido a los nuevos tratamientos, y ahora superan el 85% (Belson et al., 2007; Kato & Namabe, 2018). Sin embargo, los pacientes con LLA-T primaria resistente siguen teniendo un resultado muy pobre y los efectos secundarios de estos tratamientos de quimioterapia son significativos tanto a corto como a largo plazo (Ness et al., 2012). Por lo tanto, los esfuerzos de investigación actuales se centran en la búsqueda de dianas para el desarrollo de fármacos antileucémicos más eficaces y menos tóxicos, y terapias de medicina personalizada (Aifantis et al., 2008; Van Vlierberghe & Ferrando, 2012).

Las leucemias linfoblásticas aguda de tipo B y tipo T son biológicamente distintas, y muestran diferentes patrones de respuesta a la enfermedad. En la LLA-B factores como la edad, el recuento de glóbulos blancos en el momento del diagnóstico (WBC) y la genética de los blastos son marcadores pronósticos de la enfermedad, sin embargo, en la LLA-T no ocurre lo mismo, por lo que no se pueden utilizar estas características para la estratificación del riesgo (Pullen J et al., 1999). En LLA-T se han identificado muchas translocaciones cromosómicas, sin embargo, no está clara la importancia pronóstica de esto y tampoco se utilizan estas características de citogenética para la estratificación del riesgo (Aifantis et al., 2008). El factor pronóstico determinante en la LLA-T es la respuesta de enfermedad residual mínima (ERM) al final de la inducción y al final de la fase de tratamiento (Campana, 2012). Estudios basados en la medición de la ERM en LLA-T han podido determinar que los pacientes con LLA-T que son negativos en ambos tiempos tienen un pronóstico muy bueno frente a la quimioterapia convencional, sin embargo, cuando los niveles de ERM son altos al segundo tiempo el pronóstico es desfavorable (Schrappe et al., 2012) La respuesta al tratamiento medida por PCR-ERM al final de la fase del tratamiento es el factor predictivo más importante de recaída, y permite identificar a los pacientes que podrían ser tratados con nuevos fármacos experimentales. (Schrappe et al., 2011).

1.5 INFILTRACIÓN

El concepto de leucemia implica que las células se originan en los sitios de desarrollo linfoide (médula ósea o timo), pero en el momento del diagnóstico, es común que haya infiltración leucémica en varios órganos como el hígado, bazo, los testículos y el SNC (Steinherz et al., 1998; Reiter et al., 1994, Burger et al., 2003). Tradicionalmente, la afectación extramedular en el momento del diagnóstico se ha asociado con un mal pronóstico y tiene gran importancia desde el punto de vista terapéutico. Los protocolos actuales de tratamiento incluyen la evaluación de la enfermedad testicular y en el SNC.

La afectación testicular se manifiesta en el 2% de los niños con LLA en el momento del diagnóstico y se asocia con un alto riego y una tasa significativamente más alta de recaída. La infiltración en el SNC sigue siendo una complicación y causa de mortalidad entre un 3 y un 8% de los pacientes (Pui et al., 2008). Las posibles vías de entradas de las células de LLA al SNC varían desde la médula ósea craneal a través de las venas puente, desde el líquido cefalorraquídeo a través del plexo coroideo, desde el parénquima cerebral a través de los capilares cerebrales, desde las meninges a través de lesiones óseas del cráneo, o mediante una punción lumbar traumática (Pui et al., 2008).

1.6 TRATAMIENTO

El tratamiento más común para la leucemia linfoblástica aguda generalmente incluye cuatro fases: inducción, consolidación, intensificación y mantenimiento a largo plazo (Stock, 2010). También se administra un tratamiento dirigido para prevenir la recaída en el SNC (Fullmer et al., 2015). El trasplante alogénico de células hematopoyéticas se reserva para pacientes con enfermedad de alto riesgo o enfermedad residual mínima (ERM) persistente (Shen et al., 2018). Este abordaje terapéutico intensivo ha llevado a una supervivencia global estimada a los 5 años del 90% en LLA pediátrica (Pui et al., 2011), sin embargo, en adultos el resultado es mucho más desalentador, con una supervivencia global a los 5 años menor al 45% (Bassan & Hoelzer, 2011). El desarrollo de tratamientos en adultos basados en los tratamientos pediátricos ha permitido aumentar la tasa de supervivencia a los 5 años a más del 50% en pacientes de entre 50 y 60 años (Huguet et al., 2009; Storring et al., 2009; DeAngelo et al., 2015), y al 70-80% en pacientes con factores que se asocian a un pronóstico favorable. Sin embargo, en pacientes mayores de 60 años los resultados siguen siendo bastante malos, con una supervivencia global a los 5 años inferior al 20% (Dores et al., 2012).

1.6.1 Fases del tratamiento

La primera fase de inducción tiene como objetivo erradicar la carga de la enfermedad y restaurar la hematopoyesis normal para lograr una remisión completa. El tratamiento en esta fase se basa en una combinación de quimioterapia, que generalmente incluye un glucocorticoide, vincristina, L-asparaginasa y una antraciclina. La segunda fase es la fase de consolidación que consiste en varias secuencias cortas de quimioterapia cada 2 semanas, en las que normalmente se usa citarabina, metotrexato en dosis altas, vincriscina, asparaginasa, mercaptopurina y glucocorticoides. A la fase de consolidación le sigue una fase de intensificación tardía (terapia de reinducción), en la que se incluyen fármacos similares a los de la primera fase. Y, por último, está la fase de mantenimiento que dura de 2 a 3 años después de la inducción, que consiste en mercaptopurina diaria, metotrexato semanal con o vincristina y pulsos de glucocorticoides cada 1-3 meses (Stock, 2010).

1.6.2 Nuevos abordajes terapéuticos

Durante la última década, se han desarrollado varias terapias dirigidas para el tratamiento de la LLA (Yan et al., 2011). Estas terapias han mejorado considerablemente en pacientes con LLA-B en recaída o refractaria. Las limitaciones de terapias con CAR-T y anticuerpos monoclonales es que son dependientes de la expresión de su antígeno diana, y la pérdida de estos sería un mecanismo que podría utilizar las células tumorales para escapar de la inmunoterapia (Shah & Fry, 2019). Por ellos, se están desarrollando terapias con CAR-T que se dirigen a distintas moléculas, como CD19 y CD22 (Yang et al., 2018). En el caso de la LLA-T se están investigado abordajes terapéuticos señalando como diana a Notch1 (Jang et al., 2019), debido a la alta frecuencia de mutaciones en esta vía oncogénica. Las terapias con CAR-T en LLA-T se encuentra en etapas de desarrollo inicial, debido a la dificultad de identificar un antígeno de superficie adecuado, ya que la expresión de la mayoría de los antígenos de superficie de las células de LLA-T se comparte con las células sanas (Hill et al., 2019).

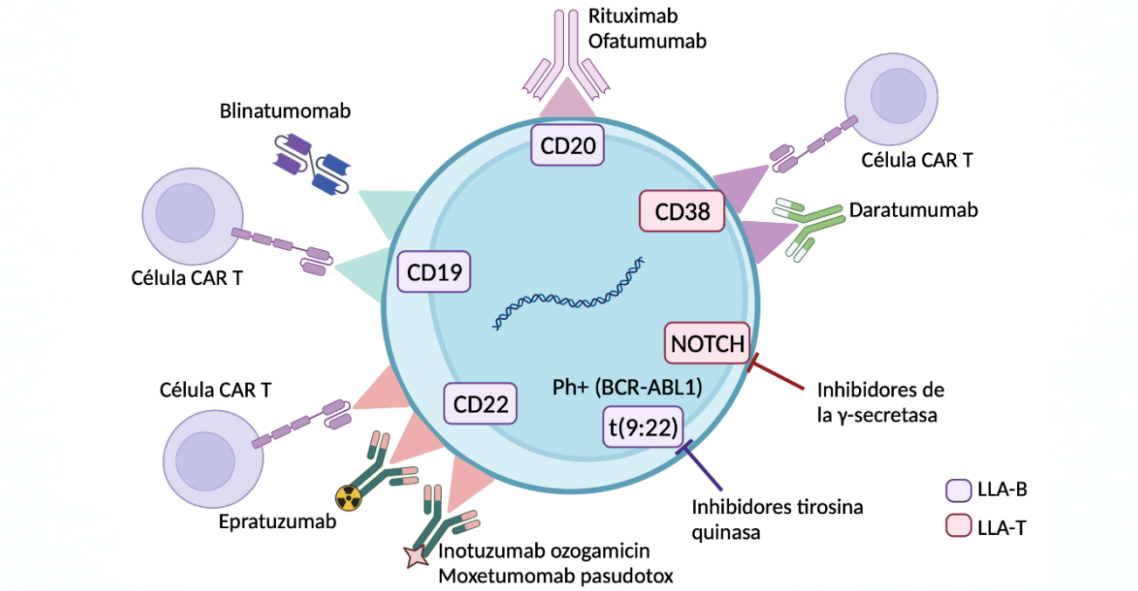

Figura 4. Nuevas terapias dirigidas para la LLA (figura adaptada de Malard & Mohty, 2020).

2 MIGRACIÓN TRANSENDOTELIAL

La migración transendotelial (MTE) es la etapa en la que los leucocitos atraviesan el revestimiento endotelial de los vasos sanguíneos a los tejidos secundarios y sitios de inflamación (Muller, 2013). Es un proceso formado por múltiples pasos, en el que cada uno de los pasos es orquestado por diferentes tipos de moléculas, incluyendo quimioquinas y moléculas de adhesión, e implica cambios morfológicos drásticos tanto en los leucocitos como en las células endoteliales (Barreiro et al., 2004). Constituye un proceso en el que se permite la llegada rápida y eficiente de los leucocitos a los focos inflamatorios o con daño tisular, sin comprometer la integridad de la barrera endotelial (Barreiro & Sánchez-Madrid, 2009). La expresión de estas moléculas de adhesión varía entre los diferentes tipos de leucocitos, el endotelio vascular, el

estímulo inflamatorio y la cronicidad de la respuesta inflamatoria (Muller, 2016). Además de ser un proceso altamente selectivo y regulador, también sirve para preparar a los leucocitos que se infiltran en los tejidos para proporcionar una respuesta inmunológica los más eficaz posible (Schimmel et al., 2017).

Los pasos de la migración endotelial son los siguientes:

1. Rodamiento: Este proceso se inicia por mediadores generados en respuesta a un daño tisular previo, estas señales (citoquinas y quimioquinas) producen una activación rápida de los leucocitos y las células endoteliales permitiendo el aumento de expresión de las selectinas (moléculas de adhesión responsables de este proceso. Se caracteriza por el establecimiento de interacciones adhesivas débiles y transitorias entre los leucocitos y las células de las paredes venulares poscapilares en las inmediaciones de los tejidos inflamados (Ley et al, 2007). Estas interacciones reversibles permiten establecer una estrecha unión de los leucocitos con el endotelio, permitiendo a la vez su desplazamiento sobre la superficie endotelial. La unión de selectinas con sus ligandos también activa diferentes rutas de señalización intracelular que tienen un efecto inductor de la activación de los leucocitos, aumentando la expresión de diferentes moléculas que están implicadas en los pasos siguientes del proceso de extravasación (Zarbock et al., 2011). Se ha demostrado la participación de las integrinas $\alpha 4$ en esta etapa, en concreto la que $\alpha 4\beta 1$ (VLA-4) y $\alpha 4\beta 7$, que median el rodamiento de eosinófilos y linfocitos respectivamente (McEver & Zhu, 2010). Además, también se ha descrito la participación de las integrinas β2 (αLβ2 (LFA-1) y αMβ2 (Mac-1)) que contribuyen a ralentizar el movimiento de los leucocitos sobre el endotelio (Dunne et al., 2002).

2. Activación: Las quimioquinas son producidas por varios tipos celulares en respuesta a patógenos o daño tisular (Turner et al., 2014). Cuando son secretadas se transportan a la superficie luminal de las células endoteliales de las vénulas poscapilares, donde son fijadas por los proteoglicanos. Los leucocitos en rodamiento expresan receptores específicos para estas quimioquinas. La interacción de las quimioquinas con sus receptores produce cambios conformacionales en las integrinas pasando de un estado de baja afinidad a un estado de alta afinidad (Abbas et al, 2021).

3. Adhesión: a la vez que se activan las integrinas, las citoquinas (TNFa e IL-1) aumentan la expresión endotelial de los ligandos de integrina, mayoritariamente de VCAM-1 (ligando de VLA-4) e ICAM-1 (ligandos de LFA-1 y Mac-1) (Muller, 2013). Esto permite que los leucocitos establezcan uniones firmes con el endotelio, reorganizando su citoesqueleto y extendiéndolo sobre la superficie endotelial (Abbas et al, 2021).

4. Migración: el último paso es la transmigración a través de la barrera endotelial. Esta puede darse de dos formas: paracelular o transcelular (Muller, 2013). El mecanismo más frecuente es el paracelular, que ocurre cuando los leucocitos atraviesan el endotelio por los espacios intercelulares, y depende de las integrinas y sus ligandos en las células endoteliales. Se produce una ruptura de las proteínas de unión intercelular transitoria y reversible,

principalmente el complejo cadherina vascular endotelial (Cadherina-VE); las quinasas fosforilan la cola citoplasmática de la Cadherina-VE y conducen a una ruptura reversible del complejo de unión (Shaw et al., 2001). En el caso de la migración transcelular, los leucocitos se mueven a través de las células endoteliales en vez de entre ellas, es un proceso muchos menos frecuente (Muller, 2013).

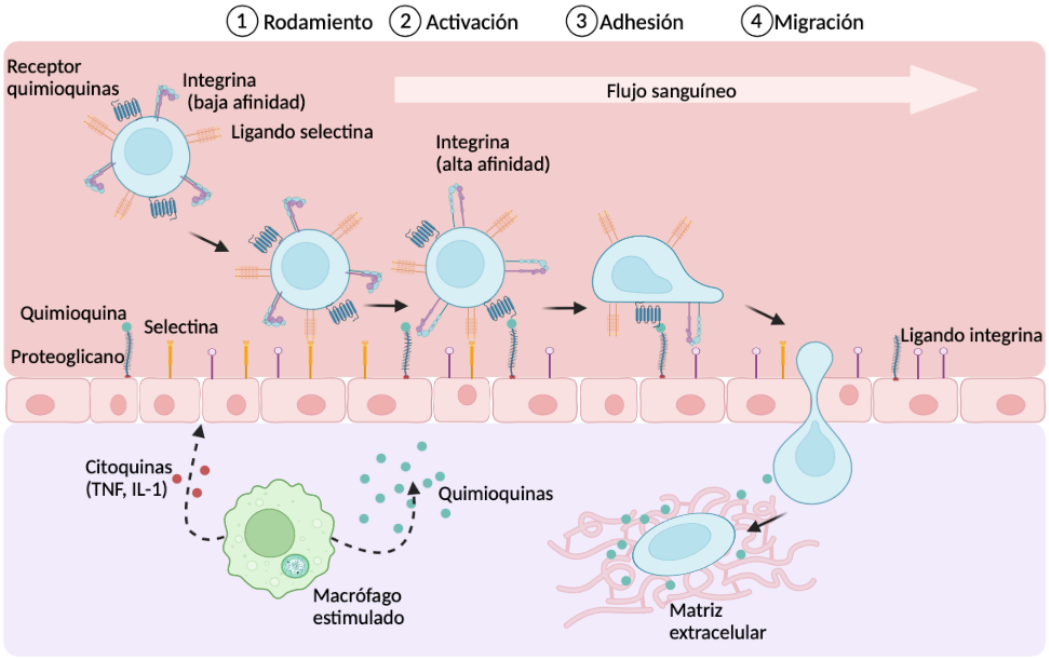

Figura 5. Pasos de la migración de los leucocitos a través del endotelio (figura adaptada de Elsevier 2018).

2.1 MOLÉCULAS IMPLICADAS EN ADHESIÓN Y MIGRACIÓN

Gracias a la eficacia de los tratamientos actuales en la LLA, la infiltración extramedular de células leucémicas ocurre con poca frecuencia; sin embargo, la infiltración en el SNC sigue ocurriendo en el 3-8% de los casos totales de leucemia, incluida la LLA (Pui & Howard, 2008). Aunque la expresión de las muchas moléculas entre LLA-T y LLA-B es similar, otras se expresan de forma diferencial y esto hace que haya diferencias en los mecanismos de infiltración en ambos subtipos de LLA.

2.1.1 Papel de las selectinas

El contacto y el rodamiento son los primeros pasos durante la extravasación de los leucocitos, como ya hemos mencionado antes. Esta etapa esta mediada principalmente por las selectinas. La P-selectina y la E-selectina se encuentran en el endotelio e interaccionan con ligandos que se encuentran en los leucocitos (PSGL y ESL-1, respectivamente); mientras que la L-selectina presente en los leucocitos e interacciona con ligandos que se encuentran en las células endoteliales activadas (PSGL-1, mucinas y otros ligandos glicosilados) (Barreiro & Sánchez-Madrid, 2009). Se ha demostrado que las células B-LLA se adhieren a las selectinas P y E principalmente por CD43 y no por PSGL-1, que solo se expresó a niveles muy bajos (Nomomura

et al., 2008). Mientras que en el caso de la LLA-T se ha estudiado que las selectinas E y L son las que median los primeros pasos de la transmigración por PSGL-1, CD43 y CD44 (Isikawa et al, 1993).

2.1.2 Papel de las integrinas

Las integrinas son la principal familia de receptores de la adhesión celular y median la unión de las células con la matriz extracelular (MEC), pero también participan en interacciones célula-célula (Hynes, 1992). Las integrinas se expresan en prácticamente todos los tipos celulares y están implicadas en muchos procesos celulares de gran importancia. Tanto las integrinas como sus ligandos desempeñan funciones clave en el desarrollo embrionario, respuestas inmunitarias, migración celular, proliferación o activación celular, pero también juegan un papel crítico en procesos patológicos como la invasión y metástasis de células tumorales, trombosis e inflamación (Hamidi et al., 2018).

i. Estructura y clasificación

Las integrinas son proteínas heterodiméricas formadas por dos subunidades (**figura 6**), una glicoproteína transmembrana α (120-180 KDa) y otra β (90-100 KDa) que forman un complejo no covalente. Cada subunidad contiene un gran dominio extracelular y otro pequeño citoplasmático, ambas subunidades contienen centros activos que contribuyen a la unión. Actualmente se conoce 18 subunidades α y 8 subunidades β, la combinación de ambas da lugar al menos a 24 integrinas diferentes (Plow et al., 2000).

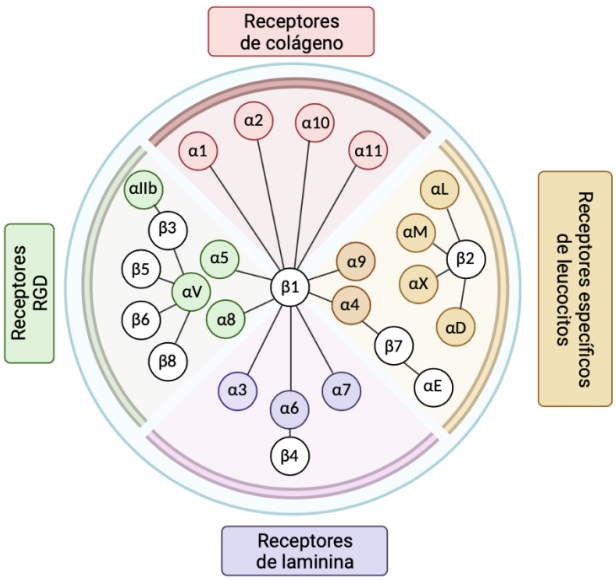

Figura 6. Clasificación de integrinas en mamíferos (figura adaptada de Hynes, 1992). Se muestran las posibles combinaciones entre las subunidades α y β. Las integrinas marcadas en amarillo se unen a colágeno; las marcadas en rojo a laminina; las marcadas en azul reconocen a la secuencia RGD presente en varias proteínas, y las integrinas de expresión restringida a leucocitos están marcadas en naranja.

ii. Integrina α4β1 (VLA-4)

La subunidad α4 se combina exclusivamente con las subunidades β1 y β7 dando lugar a las integrinas α4β1 y α4β7. La integrina $\alpha_4\beta_1$ (ó VLA-4) es un receptor de membrana que se expresa constitutivamente en alto grado en leucocitos mononucleares, monocitos, linfocitos, eosinófilos, basófilos, macrófagos y progenitores hematopoyéticos. La integrina α4β1 ó VLA-4 (*very late antigen-4*) tiene una gran importancia en procesos inflamatorios, recirculación linfocitaria, hematopoyesis y organogénesis (Imai et al, 2010). Los principales ligandos de la integrina α4β1 son VCAM-1 (*vascular cell adhesion molecule-1*) y fibronectina (FN), que es una glicoproteína de membrana perteneciente a la superfamilia de las inmunoglobulinas que se expresa fundamentalmente en células endoteliales activadas (Osborn *et al.*, 1989), en células estromales de médula ósea y bazo, y en células dendríticas (García-Castro et al., 1997; Jacobsen et al., 1996; Salomon et al., 1997; Salomon et al., 1994).

La fibronectina (FN) es una glicoproteína de 450 kDa presente tanto en la MEC como en forma soluble en plasma y otros fluidos. Está formada por dos cadenas polipeptídicas A y B unidas por puentes disulfuro en su extremo carboxilo-terminal. La FN media adhesión celular a través de dos regiones fundamentalmente: la región central de la molécula que contiene la secuencia RGD, capaz de unir las integrinas α5β1, αVβ3 y la integrina α4β1 en conformación activa (Sanchez-Aparicio et al., 1994), y la región IIICS con el sitio CS1 que es el principal ligando constitutivo de α4β1 (García-Pardo et al., 1990a). Existen además otras regiones de interacción con células, situadas en los dominios de unión a heparina HepI, HepII y HepIII (García-Pardo et al., 1990b; Moyano et al., 1999).

Las células LLA-T expresan LFA-1 en su conformación activa sin ningún estímulo adicional, este LFA-1 activo va a mediar la adhesión de las células T leucémicas a ICAM-1, lo que contribuye a la extravasación de LLA-T (Tanaka et al., 1998). En el caso de LLA-B se observan niveles altos de ICAM-1 y LFA-1 en los pacientes con recaídas, pero no en los primeros diagnósticos (Holland et al., 2011).

VLA-4 es una integrina que está implicada en procesos de adhesión, migración y supervivencia de los leucocitos y células madre hematopoyéticas (Wilson & Trumpp, 2006). Su expresión en el caso de las leucemias agudas es muy controvertida, ya que no actúa con el mismo criterio diagnóstico en los distintos tipos de leucemias. La expresión alta de VLA-4 en LMA es un marcador de buen pronóstico. Sin embargo, en la LLA la expresión alta de VLA-4 es un indicador de mal pronóstico, asociándolo con grupos de estratificación de alto riesgo y menor supervivencia libre de recaídas (SLR) en la edad infantil; además de presentar mayor resistencia a la quimioterapia (Shalapour et al., 2011).

2.1.3 Papel de las quimioquinas

Las quimioquinas son una familia de citoquinas de bajo peso molecular (8-12kDa) altamente conservadas que median muchos procesos biológicos (Miller & Mayo, 2017). Funcionan mediante la interacción con receptores acoplados a proteínas G en la superficie celular (Proudfoot 2002). Debido a su significancia en varios funciones biológicas y patologías, las quimioquinas y los receptores han sido un foco terapéutico para descubrir una diana para la intervención clínica (Miller & Mayo, 2017).

Las quimioquinas son esenciales para el funcionamiento del sistema inmunológico y juegan un papel importante en el microambiente tumoral (Bule et al., 2021). Entre sus principales funciones también destaca la capacidad de reclutar a diversos tipos celulares a sitios de inflamación (Müller et al., 2001); maduración, recirculación y activación leucocitaria (Zlotnik and Yoshie, 2000); hematopoyesis y angiogénesis (Moser et al., 2004); moduladoras de adhesión y migración (Grabovsky et al., 2000); y activación señalización intracelular a sus receptores (Mellado et al., 2001).

i. Estructura y clasificación

Las quimioquinas se definen por su secuencia de aminoácidos primaria y la disposición de residuos de cisteína específicos estructuralmente importante dentro de la proteína madura. Estos residuos forman enlaces disulfuro que mantienen la estructura del monómero de quimioquina, que consta de una hoja β central de tres hebras, una hélice α C-terminal superpuesta y un extremo N-terminal corto no estructurado que desempeña un papel fundamental en la activación del receptor (**figura 7**) (Kohidai, 2006). Además, sus estructuras terciarias conservadas permiten el intercambio de subunidades dentro y entre los miembros de la subfamilia, promoviendo así el concepto de un ‘’interactoma de quimioquinas’’. Las estructuras cuaternarias varían en función de cada subfamilia (Miller & Mayo, 2017).

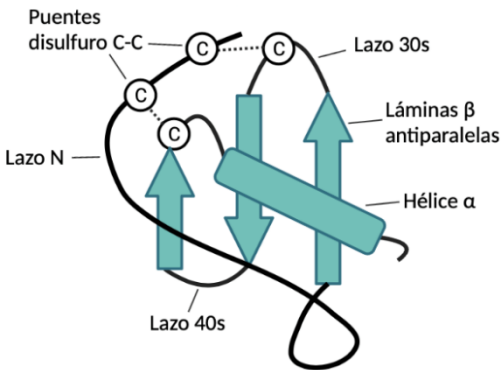

Figura 7. Estructura 3D de las quimioquinas (figura adaptada de Kohidai, 2006). Todas las quimiocinas comparten una estructura de clave griega típica que se estabiliza mediante enlaces disulfuro entre residuos de cisteína conservados.

Las quimioquinas se caracterizan por poseer 4 residuos cisteínas altamente conservados en el extremo N-terminal, y en función de la posición de las dos cisteínas más próximas al extremo N-terminal se van a categorizar en 4 subfamilias: XC, CXC, CC Y CX3C (**tabla 4**) (Miller & Mayo, 2017). En las dos grandes subfamilias, CC y CXC, las dos primeras cisteínas son adyacentes (motivo CC) o separadas por un residuo aminoácido (motivo CXC). La subfamilia XC es una excepción, solo posee una cisteína en el extremo amino-terminal, y la subfamilia CXC3 tienen tres aminoácidos entre el primer y segundo residuo cisteína (Zlotnik & Yoshie, 2000). Las quimioquinas se designan según su clasificación de subfamilia mediante nombres sistemáticos compuestos por un prefijo (CCL, CXCL, CX3CL o XCL; refiriéndose ''L'' a un ligando) seguido de un número de identificación. Sin embargo, la mayoría de las quimioquinas tienen también nombres comunes o históricos relacionados con sus primeras funciones caracterizadas (Stone et al., 2017). Las quimioquinas y sus receptores también se clasifican según su función en: homeostáticas e inflamatorias (Bendall, 2005).

ii. Receptores de quimioquinas

Los receptores de quimioquinas son receptores acoplados a proteínas G con 7 dominios transmembrana (**figura 8**) (Bendall, 2005). La unión de la quimioquina con su receptor da lugar a cambios conformacionales que dan lugar a la activación de efectores intracelulares (proteínas G o arrestinas β), el de vías de transducción de señales, y en ultima instancia respuesta celulares (Stone et al., 2017). Los receptores de quimioquinas son selectivos para miembros de una subfamilia de quimioquinas, por lo que se clasifican según la subfamilia de quimioquinas a la que pertenecen la mayoría de sus ligandos (Stone et al., 2017). Por lo tanto, se clasifican en CCR, CXCR, CX3CR y XCR seguidos de un número de identificación. Se han identificado al menos 18 receptores de quimioquinas, pero con existen casi 50 ligandos, por lo que la promiscuidad de los receptores es obvia.

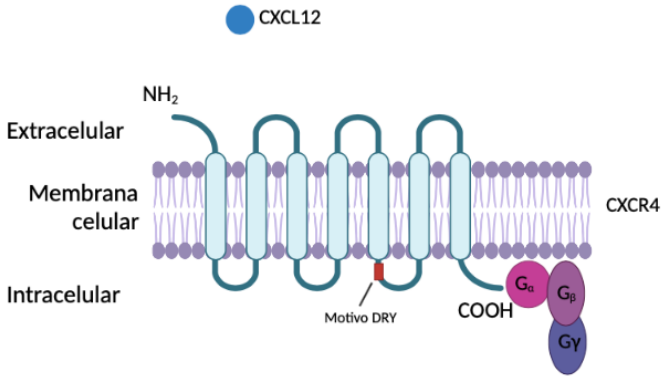

Figura 8. Estructura de los receptores de las quimioquinas. Los receptores de quimioquinas son receptores acoplados a proteínas G. Tienen siete dominios transmembrana (7TM) con siete regiones helicoidales que atraviesan la membrana. El extremo N y tres bucles extracelulares están expuestos fuera de la célula, mientras que el extremo C y tres bucles intracelulares se enfrentan al citoplasma. El extremo N-terminal del receptor se une a las quimioquinas. Las proteínas G se acoplan al extremo C-terminal. El segundo bucle intracelular tiene una secuencia de aminoácidos aspartato-arginina-tirosina (motivo DRY).

Subfamilia	Receptor	Ligando
CXC	CXCR1	CXCL6, CXCL8
	CXCR2	CXCL12, CXCL2, CXCL3, CXCL5, CXCL6, CXCL7, CXCL8
	CXCR3	CXCL9, CXCL10, CXCL11, CXCL4, CXCL4L1
	CXCR4	CXCL12
	CXCR5	CXCL13
	CXCR6	CXCL16
	CXCR7	CXCL11, CXCL12
XC	XCR1	XCL1, XCL2
CX3C	CX3CR1	CX3CL1
CC	CCR1	CCL3, CCL3L1, CCL4, CCL5, CCL6, CCL9, CCL10, CCL14, CCL15, CCL16, CCL23
	CCR2	CCL2, CCL7, CCL8, CCL11, CCL12, CCL13, CCL16
	CCR2b	CCL8
	CCR3	CCL5, CCL6, CCL7, CCL11, CCL13, CCL15, CCL16, CCL23, CCL24, CCL26, CCL28
	CCR4	CCL17, CCL22
	CCR5	CCL3, CCL3L1, CCL4, CCL5, CCL6, CCL8, CCL11, CCL12, CCL13, CCL16
	CCR6	CCL20
	CCR7	CCL19, CCL21
	CCR8	CCL1, CCL16
	CCR9	CCL25
	CCR10	CCL27, CCL28

Tabla 4. Clasificación de las quimioquinas y receptores en subfamilias. Familia y subfamilias de las quimioquinas en función de la posición relativa de las dos cisteínas del extremo amino-terminal. Se indica el nombre común y el receptor de cada una de ellas.

Se han identificado al menos 18 receptores de quimioquinas hasta la fecha, pero con casi 50 ligandos, la promiscuidad del receptor es obvia. Sin embargo, esta redundancia está restringida a familias con seis receptores que se unen a las quimioquinas CXC, 10 CC, y uno a cada una de las quimioquinas CX3C y C (Stone et al., 2017). No solo varias quimioquinas comparten un mismo receptor, sino que con frecuencia una misma quimioquina se une a múltiples receptores (Nomiyama et al., 2013). Existen también receptores de quimioquinas atípicos (ACRs), son receptores con siete dominios transmembrana homólogos a los receptores acoplados a proteínas G de quimioquinas (GPCR). Sin embargo, estos receptores ACRs no inducen la señalización clásica y las respuestas celulares posteriores características de los receptores GPCR. Estos receptores son DARC, D6, CXCR7, CCRL1 y CCRL2 (Ulvmar et al., 2011).

Durante el desarrollo de esta tesis nos hemos centrado en el papel de la quimioquina CXCL12 y su implicación en el aumento de la trimetilación en H3K9.

iii. Eje CXCR4/CXCL12

La quimioquina CXCL12, también conocida como SDF-1 (*stromal cell-derived factor-1*) es una quimioquina crucial en muchos procesos homeostáticos que se expresa de forma constitutiva en muchos tipos celulares y en más de 23 tipos de diferentes de cáncer (Zhou et al., 2019). CXCL12 destaca en comparación con otros miembros de la familia de quimioquinas CXC en cuanto a su ubicación cromosómica. Mientras que la mayoría de los genes de las quimioquinas

CXC se encuentran en el cromosoma 4q21, el gen que codifica CXCL12 está ubicado en el cromosoma 10q11 (Shirozu et al., 1995). Además, es la única quimioquina CXC con empalme diferencial de ARNm, identificándose seis variantes de empalme diferentes en humanos (CXCL12α a ϕ) y tres en ratones (CXCL12α a γ) (Yu et al., 2006).

CXCL12 desarrolla un papel fundamental en muchos procesos homeostáticos, como la neurogénesis, la embriogénesis, la angiogénesis y la linfopoyesis, y juega un papel en los procesos inflamatorios. La actividad de CXCL12 va a estar regulada a muchos niveles: transcripción, corte y empalme diferencias de ARNm, modificaciones postraduccionales, y disponibilidad y cooperatividad de proteínas (Janssens et al., 2018).

CXCR4 es el receptor de CXCL12, se expresa en múltiples tipos de células: linfocitos, células madre hematopoyéticas, células epiteliales, células endoteliales y células cancerosas (Teicher & Fricker, 2010). Existe otro receptor para CXCL12, denominado CXCR7 (también conocido como ACKR3). Este receptor también une la quimioquina CXL11 (Quinn et al., 2018). La expresión de CXCR7 está estrictamente regulada y aumenta durante procesos patológicos como la inflamación y el cáncer (Sánchez-Martín et al., 2013).

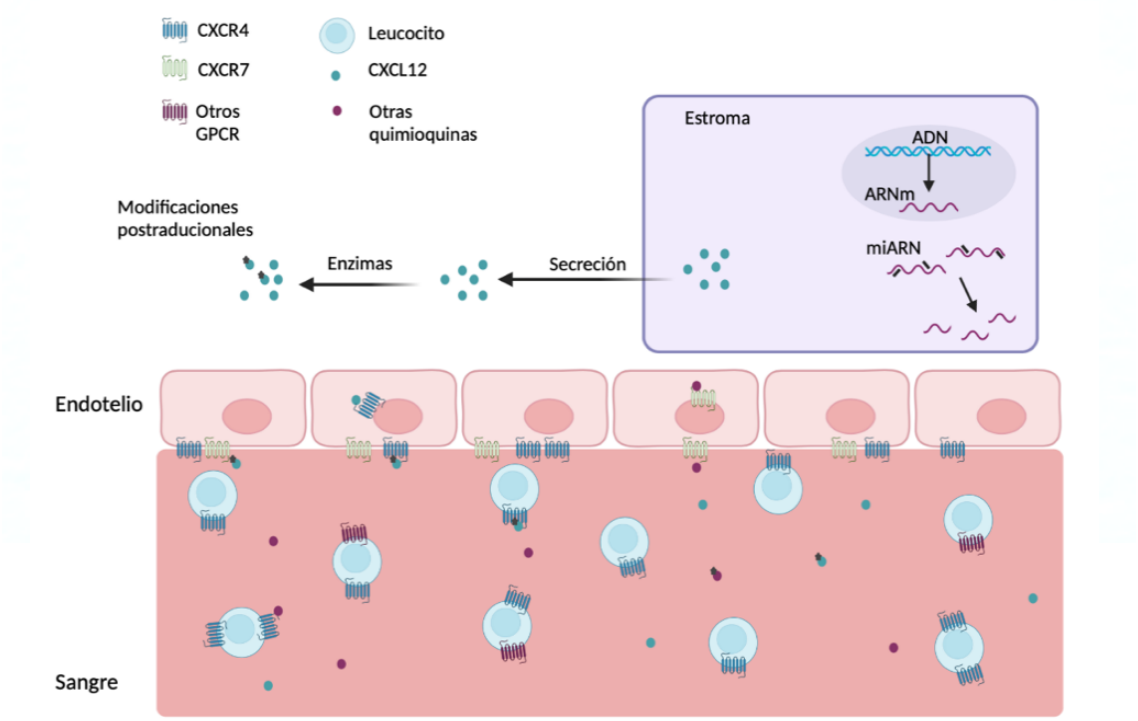

Figura 9. Niveles de regulación de la actividad CXCL12 (figura adaptada de Janssens et al., 2018). La actividad de CXCL12 se controla a múltiples niveles, comenzando con (a) transcripción controlada y empalme de ARNm de variantes de CXCL12 y (b) regulación posterior de la estabilidad del ARNm por microARN (miARN). Después de la traducción, CXCL12 y su receptor pueden ser modificados postraduccionalmente por varias enzimas o agentes químicos (c). En el endotelio, la interacción de CXCL12 con GAG es necesaria para su inmovilización en los vasos sanguíneos y su presentación a los leucocitos que pasan (d). Esta interacción GAG favorece la homo y heterodimerización de CXCL12 y protege a CXCL12 de

modificaciones postraduccionales. Los receptores de siete dominios transmembrana CXCR4 y ACKR3 son activados por CXCL12 y pueden formar homo o heterodímeros entre sí o con otros receptores de quimiocinas (f). ACKR3 internaliza CXCL12 y altera su gradiente (g), mientras que la sinergia entre CXCL12 y otras quimiocinas aumenta la respuesta de las células diana (h) (Janssens et al., 2018).

Tanto en LLA-T como en LLA-B se presentan unos altos niveles de expresión que se correlacionan con la infiltración en hígado, bazo, ganglios, SNC y testículos (Crazzolara et al., 2001). En el caso de la LLA-T se presentan también unos altos niveles de expresión de CCR7 y CCR10 que se relacionan con una mayor infiltración en ganglios linfáticos (Hasegawa et al., 2000) y en lesiones cutáneas (Harasawa et al., 2006), respectivamente. Las células de LLA-B expresan CXCR3 (Gómez et al., 2015). Las células de LLA-T expresan distintos receptores de quimioquinas como son CXCR4, CCR9, CXCR3 y CCR7 (Hong et al., 2021). Las quimioquinas y sus receptores juegan un papel extremadamente importante en la progresión y recaída de la LLA-T. La activación del eje CXCL12/CXCR4 está involucrada en varios aspectos de la progresión de la LLA, que incluyen proliferación, migración, infiltración y quimiorresistencia (Shi et al., 2020). CXCR4 se expresa en gran medida en la superficie de las células de LLA humanas y de ratón, y su alta expresión predice un mal pronóstico de los pacientes con LLA (Crazzolara et al., 2001;; Passaro et al., 2015).

En el caso del receptor CCR9 está altamente expresado en células T CD4 + LLA-T, y rara vez se expresa en células T CD4 + normales (Qiuping et al., 2003). CCR9 esta estrechamente relacionado con la infiltración de células de LLA, se ha demostrado que CCL25 induce la polarización de células LLA-T y la absorción de microvellosidades para participar en la infiltración y el trafico de LLA-T (Zhou et al., 2010; Zhang et al., 2011). Además, se ha comprobado que CCL25/CCR9 desempeña un papel antiapoptótico e induce un papel quimioresistente (Qiuping et al., 2004).

El eje CXCL10/CXCR3 puede promover la infiltración de células de ALL en el SNC (Zhou et al., 2019). La recaída de la LLA se asocia con la supervivencia de blastos en órganos como el SNC o los testículos (Martínez-Laperche et al., 2013), y CXCR3 se expresa en gran medida en los leucocitos del líquido cefalorraquídeo (LCR) y su ligando CXCL10 está regulado al alza en el LCR de pacientes con LLA-T (Gómez et al., 2015).

Se ha demostrado que CCR7 podría ser regulado positivamente por la vía Notch1, y jugar un pape clave en la infiltración del SNC en LLA (Buonamici et al., 2008). Se ha podido detectar CCL19 en secciones del cerebro de ratones leucémicos (Buonamici et al, 2009). Además, CCL19 también se expresa en gran medida en el microambiente esplénico, lo que podría promover el reclutamiento de células LLA-T con alta expresión de CCR7 al bazo (Ma et al., 2014).

Además de la expresión y activación de los receptores de adhesión y quimioquinas, las células LLA-T secretan factores solubles que facilitan la extravasación y la infiltración en órganos como las MMP (Kessenbrock et al., 2010).

2.1.4 Papel de las quinasas

Las vías intracelulares implicadas en la LLA son diversas, incluyendo la JAK-STAT (Mullighan et al., 2009), la PI3K-AKT Lee-Sherick et al., 2010), Ras-MAPK (Kindler et al., 2008) y las PKC (Jiffar et al., 2004), entre otros.

iv. Papel de las PKCs

Las proteínas quinasas C (PKC) constituyen un grupo de enzimas que fosforilan diversas proteínas específicamente en los residuos de serina y treonina (Webb et al., 2000). Se identificaron por primera vez en 1977 como una quinasa citoplasmática activada por calcio y regulada por fosfolípidos (Inoue y col., 1977). Están implicadas en diversas vías de transducción de señales, participando en multitud de funciones fisiológicas, como múltiples mecanismos de señalización que conducen a la mitogénesis y a la proliferación, en la apoptosis, en la activación plaquetaria, en el reordenamiento de citoesqueleto de actina (Kikkawa & Nishizuka, 1986; Nishizuka, 1988; Newton, 1995); así como en procesos patológicos, como diversos tumores y determinadas cardiopatías (Nishizuka, 1984; De Marchi et al., 2013). Las PKC son enzimas anfitrópicas, es decir, que puede existir en forma soluble en el citosol y en forma unida a la membrana (Sotiroudis et al., 1989). En el caso de la LLA, la inhibición de las PKC aumenta la sensibilidad en el tratamiento de la LLA-B (Ruiz-Aparicio et al., 2020). También se ha demostrado que la sobreexpresión de la PKCα promueve la fosforilación y quimioresistencia en las células de LLA (Jiffar et al., 2004).

3 NÚCLEO CELULAR EN LA MIGRACIÓN

En las células eucariotas, el núcleo se posiciona en un lugar específico dentro del citoplasma de acuerdo con diferentes procesos biológicos como la división, la diferenciación o la migración celular (Bone & Starr, 2016; Gundersen & Worman, 2013). La migración celular es un proceso celular que es esencial para el desarrollo de los tejidos y la homeostasis celular, pero también desempeña un papel crucial durante la metástasis e inflamación en el cáncer (Trepat el al., 2015). La migración e invasión celular requiere que las células atraviesen diferentes barreras como la matriz extracelular (MEC), muchas veces las células deben atravesar poros más pequeños que la propia célula. Mientras que el citoplasma, la membrana plasmática y la mayoría de los orgánulos de la célula pueden deformarse con facilidad para atravesar estos poros, el núcleo es el componente restrictivo en la migración por su tamaño y rigidez (Davidson et al., 2014; Wolf et al., 2013). El núcleo y su conexión con el citoesqueleto juegan un papel fundamental en la migración celular.

Durante el proceso de migración 3D, el núcleo tiene que coordinarse con la dinámica citoesquelética en los bordes anterior y posterior (**figura 10**). La migración celular 3D consta de cuatro pasos (Sneider et al., 2018):

1. Se forma una protuberancia en el borde de ataque seguido de la rotación del núcleo
2. Se produce el reposicionamiento nuclear e interacción con la MEC.

3. Contracción mediada por la red de actomiosina y degradación proteolítica de la MEC.
4. Liberación de adhesión en el extremo posterior y relajación nuclear.

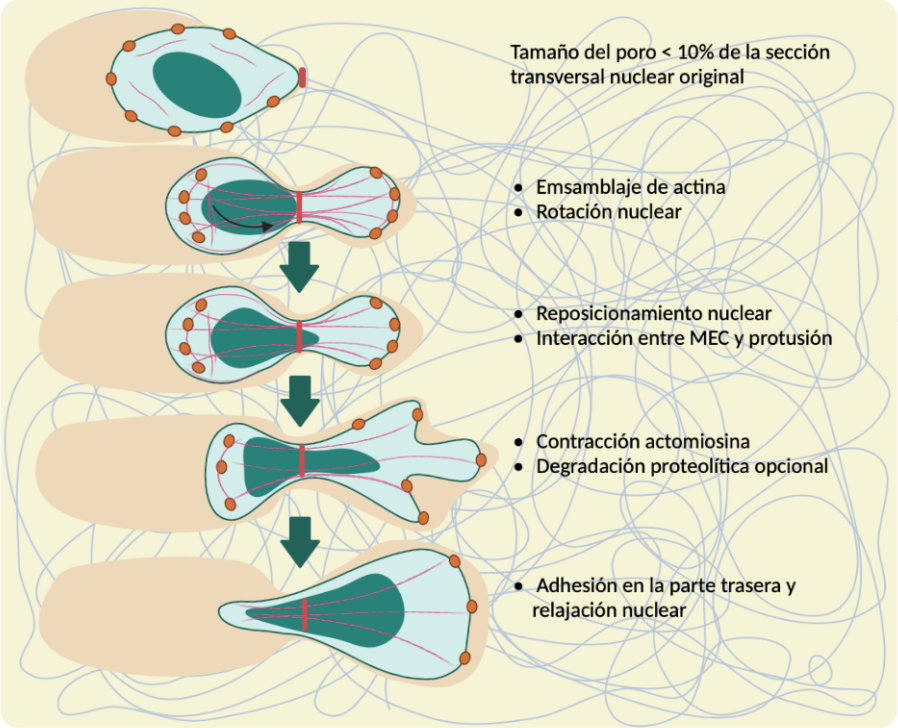

Figura 10. Deformación nuclear durante la migración celular a través de la matriz extracelular (figura adaptada de Sneider et al., 2018). La penetración celular en la matriz extracelular requiere múltiples pasos: formación de una protuberancia en el borde de ataque y rotación nuclear, reposicionamiento nuclear e interacción con la MEC, contracción dependiente de miosina, remodelación de la matriz y finalmente liberación de la fuerza de adhesión en la parte posterior de la célula.

Hay dos componentes principales del núcleo que van a determinar su viscosidad y rigidez: la lámina nuclear y la cromatina; interviniendo de forma directa en el proceso de migración celular. Los componentes principales de la lámina nuclear son los filamentos intermedios tipo V, las láminas A/C y la lámina B, formando todos ellos una red de citoesqueleto debajo de la envuelta nuclear (Adam, 2017). Las láminas A/C conecta el núcleo con el citoesqueleto a través del complejo LINC, ya que se une a las proteínas SUN (Chang et al., 2015). Las láminas A/C también regulan la forma y la rigidez del núcleo. Se ha demostrado que células con alta capacidad migratoria como las metastásicas tienen una subexpresión de láminas A/C (Chiotaki et al., 2014).La cromatina es el componente principal del núcleo, y se puede encontrar en dos conformaciones distintas: eucromatina o heterocromatina (Gordon et al., 2013). La eucromatina es la conformación transcripcionalmente activa, mientras que la heterocromatina es la forma condensada de la cromatina y se encuentra transcripcionalmente inactiva (Tamaru et al., 2010). Cada conformación esta asociada con una viscosidad diferente del núcleo, por lo que van a poder modular la rigidez del núcleo y afectar a la migración celular (Erdel et al., 2015). Los cambios entre los niveles de condensación de la cromatina van a deberse principalmente a

modificaciones epigenéticas, como modificaciones postraduccionales de histonas o metilación del ADN (Hieda et al., 2015). La forma condensada de la cromatina (heterocromatina) conduce a pensar que impediría la migración nuclear al estar el núcleo más rígido. Sin embargo, la cromatina condensada puede formar puntos de anclaje más fuertes con el complejo LINC, mejorando el acoplamiento del núcleo al citoesqueleto, lo que permitiría al citoesqueleto remodelar al núcleo más fácilmente y alterar su posición (Dupin & Etienne-Manneville, 2011).

4 EPIGENÉTICA

Históricamente, la palabra ‘’epigenética’’ se usó para describir eventos que no podían explicarse mediante principio genéticos. Conrad Waddington describió la epigenética como la rama de la biología que estudia las interacciones causales entre los genes y sus productos, que dan lugar a un fenotipo (Goldberg, et al., 2007). Actualmente, definimos epigenética como el estudio de los cambios heredables que regulan la expresión génica sin alterar la secuencia de ADN (Guil & Esteller, 2008). Las marcas epigenéticas pueden darse a distintos niveles (**figura 11**): a nivel de ADN (metilación del ADN), a nivel de cromatina (variantes de histonas o modificaciones post-traduccionales de histonas), a nivel de ARN no codificantes (microARNs) y a nivel de ARN (metilación del ARN) (Guil & Esteller, 2008; Liu et al., 2020). Los cambios epigenéticos por susceptibilidad genética y exposición ambiental pueden modular la expresión génica y alterar las funciones celulares sin alterar las secuencias genómicas (Baccarelli & Bollati, 2011). Por ello, la diferenciación celular puede considerarse un fenómeno epigenético (Goldberg, et al., 2007). El epigenoma de la célula es variable y va a ir cambiando según el estado de diferenciación de las células en respuesta de gran variedad de estímulos.

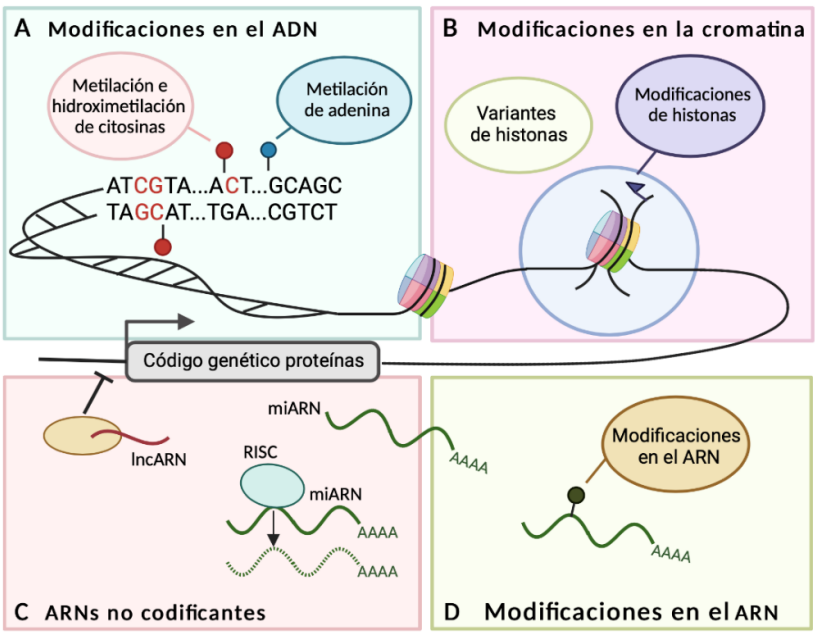

Figura 11. Mecanismos epigenéticos (figura adaptada de Aristizabal et al., 2020). (A) El ADN se puede modificar en los residuos de citosina y adenina mediante la adición de grupos

químicos. (B) Los nucleosomas pueden cambiar de posición para aumentar o disminuir la accesibilidad del ADN. Además, los nucleosomas pueden modificarse mediante la incorporación de variantes de histonas y la adición de modificaciones postraduccionales. (C) Los ARN no codificantes desempeñan un papel importante en la regulación de la transcripción. Dentro de los complejos de silenciamiento inducidos por ARN (RISC), los miARN median el reconocimiento y la unión de los ARN que se convierten en el objetivo de la degradación. Los lncARN están asociados con otros complejos y pueden activar o reprimir la transcripción. (D) Todos los nucleótidos de ARN pueden modificarse mediante la adición de grupos químicos.

4.1 HISTONAS

La cromatina es el complejo de ADN más proteínas que va a formar los cromosomas dentro del núcleo celular (Wolffe et al., 1997). El nucleosoma es la unidad estructural y funcional de la cromatina. El nucleosoma está formado por el ADN y las histonas (Longman, 1999). Las histonas son un grupo de proteínas de bajo peso molecular que se encargan de organizar y empaquetar el ADN. Los nucleosomas son octámeros de histonas, tienen dos copias de las histonas H2A, H2B, H3 y H4, y alrededor de este octámero de histonas se disponen 146 pared de base de ADN, dando 1,7 vueltas al octámero de histonas (Mariño-Ramírez et al., 2005). La histona H1, conocida como histona enlazadora, se une a los sitios de entrada y salida del ADN en la superficie del octámero de histonas, y completa el nucleosoma (Hergeth & Schneider, 2015). La histona H1 juega un papel esencial condensando a la cromatina en ordenes estructurales mayores (Zhou et al., 2019).

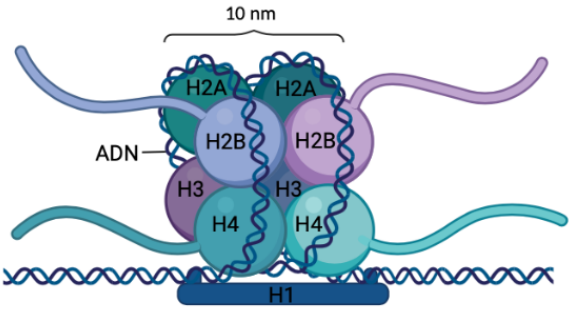

Figura 12. Estructura de un nucleosoma (figura adaptada de Longman, 1999). El nucleosoma está formado por 146 pb de ADN se asocian con un octámero de histonas. Entre cada nucleosoma hay aproximadamente 50 pb de ADN enlazador. Se cree que la histona H1 se une al ADN enlazador y funciona en la compactación de nucleosomas.

La estructura de todas las histonas que conforman el core del nucleosoma (H2A, H2B, H3 y H4) están altamente conservadas a lo largo de la evolución (**figura 12**). Las histonas H3 y H4 son las más conservadas, y tienen un papel central en el nucleosoma y en muchos procesos cromosómicos (Morgan et al., 1991). Las cuatro histonas presentan un dominio globular en el extremo C-terminal de la proteína, a través del cual se producen las interacciones histona-histona e histona-ADN. Además, tienen también un dominio amino-terminal, que contiene la mayoría de los residuos básicos, donde tienen lugar la mayoría de las modificaciones que se dan en las histonas (Jenuwein & Allis, 2001). Cada una de estas histonas tiene en el dominio estructural tres hélices α (α1, α2 y α3) separadas por dos lazos (L1 y L2), llamados pliegues de

histonas, los cuales facilitan la heterodimerización de la histona H2A con H2B y de la histona H3 con H4 (figura 13). Como resultado de esta organización estructural, el tetrámero H3-H4 forma un núcleo estable, mientras que los dos dímeros H2A-H2B pueden eliminarse más fácilmente (Kulaeva et al., 2010). Las colas N-terminales sufren varias modificaciones post-trasduccionales en aminoácidos específicos por proteínas reguladoras de la transcripción (Kuo, 1996). La histona H1 subdivide su estructura en tres dominios: el dominio amino-terminal, el dominio globular, y el dominio carboxi-terminal. La estructura tripartita de la H1 se debe a que cada dominio tiene funciones distintas; el dominio N-terminal estabiliza la unión del dominio globular, el dominio globular une la H1 al nucleosoma, mientras que el dominio C-terminal se asocia con la condensación de la cromatina ya que se une al ADN enlazado y neutraliza sus cargas. La histona H1 presenta múltiples isoformas (Wolffe, 1997).

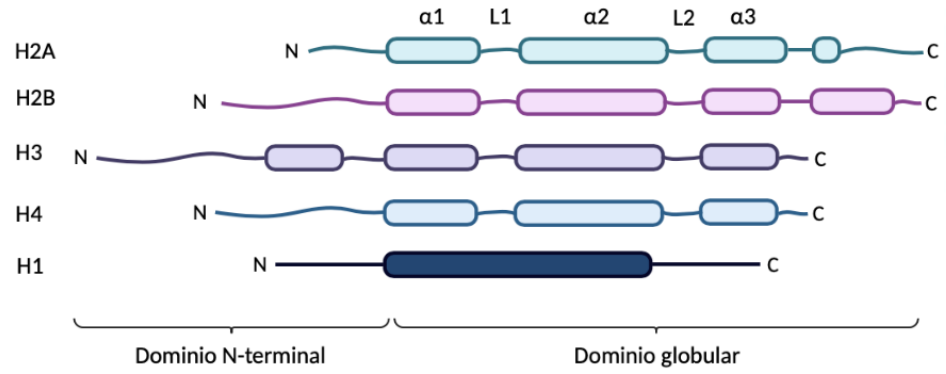

Figura 13. Arquitectura del pliegue de las histonas (figura adaptada de Luger et al., 2001). Descripción esquemática de las histonas H3, H4, H2A, H2B y H1. Las hélices del pliegue de las histonas se muestran como recuadros sólidos. Las colas de histonas se muestran como líneas.

4.2 MODIFICACIONES POSTRADUCCIONALES DE HISTONAS

Las modificaciones postraduccionales de histonas son modificaciones covalentes que tienen lugar en determinados residuos de las colas N-terminales de las histonas del core del nucleosoma y regulan la expresión génica. Las modificaciones de las histonas tienen el potencial de influir en muchos procesos biológicos fundamentales, algunos de los cuales pueden heredarse epigenéticamente (Kouzarides, 2007). Las PTMs se dan en los residuos de lisina, arginina, treonina, tirosina y serina de los extremos amino de las histonas. Al contrario que el ADN que sólo es modificado covalentemente mediante metilación o hidroximetilación, las PMTs pueden ser al menos ocho tipos diferentes de modificación (Dupont et al., 2009). Las PTMs más comunes son: metilación, acetilación, fosforilación, ubiquitinación, ADP ribosilación, sumoilación, deiminación e isomerización de la prolina (Kouzarides, 2007), entre otras. En la siguiente tabla (tabla 5) aparecen las diferentes modificaciones y qué funciones regulan. Todas estas PTMs van a actuar de una forma combinatoria y consistente, esto es lo que se conoce código de histonas (Jenuwein & Allis, 2001). Este código de histonas controla muchos procesos celulares como la activación o represión de la transcripción, la replicación o la reparación del

ADN. Alteraciones en el código de histonas pueden dar lugar a fallos en procesos celulares y, en consecuencia, desencadenar enfermedades en humanos, principalmente el cáncer (Munshi *et al.*, 2009).

Subfamilia	Receptor	Ligando
Acetilación	K-ac	Transcripción, Reparación, Replicación, Condensación
Metilación (lisinas)	K-me1 K-me2 K-me3	Transcripción, Reparación
Metilación (argininas)	R-me1 R-me2a R-me3s	Transcripción
Fosforilación	S-ph T-ph	Transcripción, Reparación, Condensación
Ubiquitinación	K-ub	Transcripción, Reparación
Sumoilación	K-su	Transcripción
ADP ribosilación	E-ar	Transcripción
Deiminación	R > Cit	Transcripción
Isomerización prolina	P-cis > P-trans	Transcripción

Tabla 5. Diferentes clases de modificaciones identificadas en histonas (tabla adaptada de Kouzarides, 2007). Resumen de diferentes clases de modificación identificadas en histonas. Se muestran las funciones que se han asociado con cada modificación.

4.3 METILACIÓN DE HISTONAS

La metilación de las histonas principalmente ocurre en los átomos de nitrógeno de los residuos de lisina y arginina de las cadenas laterales de las histonas. Estas modificaciones tienen una particularidad respecto al resto de modificaciones postraduccionales de histonas, y es que puede darse más de una vez en el mismo residuo. Las lisinas, pueden estar monometiladas, dimetiladas o trimetiladas; mientras que, las argininas se pueden monometilar o dimetilar simétrica o asiméticamente (Bannister and Kouzarides, 2011). De todas las PTMs existentes, la metilación y la acetilación en las histonas H3 y H4 son las más estudiadas (Chen et al., 2014).

Al contrario de otras PMTs, la metilación se asocia tanto con la activación como con la represión de la transcripción (Bannister and Kouzarides, 2005). Al ser un componente clave en la regulación de la expresión génica, resulta necesario una maquinaria eficiente que regule estas metilaciones. Las enzimas que se ocupan de regular la metilación de las histonas son: las HTMs (*histone methyltransferases*) que se encargan de añadir los grupos metilos a algunos aminoácidos de las histonas, y las HDMs (*histone demethylases*), que tienen como tareas

eliminar los grupos metilos de las histonas. Las metiltransferasas a su vez las podemos dividir en dos grupos: HKMTs (*histone lysine methyltransferases*) y PRMTs (*protein/histones arginine methyltransferases*) (Song et al., 2016). Las HDMs también las podemos dividir en: KDM (*lysine histone demethylase*) que van a retirar los grupos metilos de las lisinas (Trojer & Reinberg, 2006), y las RDM (*arginine histone demethylase*) descritas recientemente (Chang et al., 2007; Walport et al., 2016).

Las funciones opuestas entre HMTs y HDMs facilitan el mantenimiento de niveles equilibrados de metilación de histonas (Woo et al., 2017). Las metilaciones de histonas aberrantes se han encontrado con frecuencia en el cáncer, causadas por una mutación genética, translocación o expresión desregulada (Zhao & Shilatifard, 2019). Por lo tanto, muchas HMT y HDM podrían ser posibles dianas farmacológicas y los inhibidores de moléculas pequeñas de estas proteínas terapias potenciales (Cheng et al., 2019).

4.3.1 Metiltransferasas G9a y SUV39H1

Las metiltransferasas G9a y SUV39H1 pertenecen a la familia SUV39 de histona lisina metiltransferasas (HKMTs). Estas HKMTs median la metilación transfiriendo un grupo metilo de S-adenosil-L-metionina al grupo ε amino en los residuos de lisina en las proteínas diana (Rice et al., 2003). Muestran una alta especificidad por el residuo lisina del sustrato, y también tienen la capacidad de leer marcas de metilación (Wang et al., 2012).

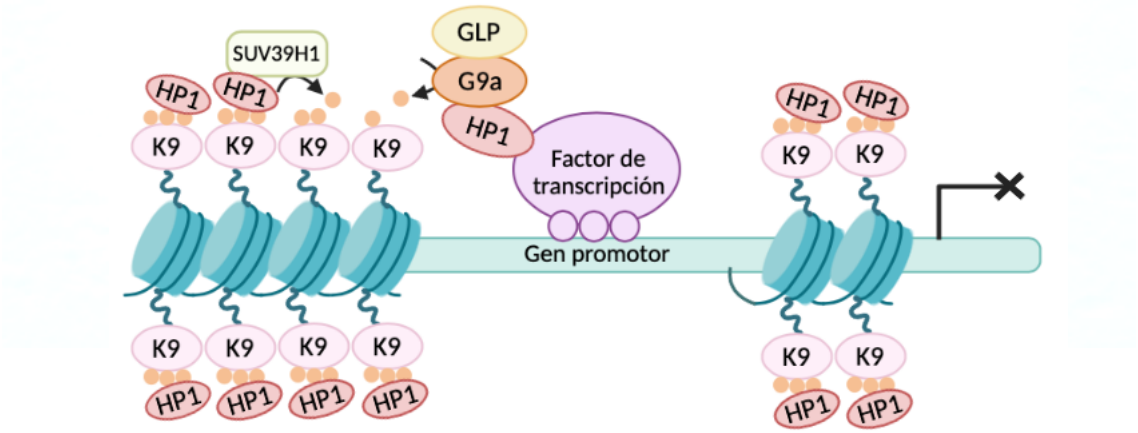

Figura 14. Metilación de H3K9 mediada por las metiltransferasas G9a y SUV39H1. La metiltransferasa cataliza la mono y dimetilación de H3K9, mientras que SUV39H1 cataliza la trimetilación. La trimetilación de H3K9 favorece la represión de la transcripción.

G9a cataliza principalmente la monometilación y dimetilación de la histona H3 en el residuo lisina 9 (Casciello et al., 2015). G9a está compuesto por un dominio SET catalítico, un dominio que contiene repeticiones de anquirina (involucradas en interacciones proteína-proteína) y señales de localización nuclear en la región N-terminal. El dominio SET es el responsable de la adición de grupos metilo en H3, mientras que las repeticiones de anquirina representan regiones

de unión de mono y dimetil lisinas (Estève et al., 2005). Por lo tanto, G9a no solo es capaz de metilar H3 lisina 9, sino que también reconoce esta modificación y recluta otras moléculas diana en la cromatina (**figura 14**) (Shahbazian et al., 2005). También se ha identificado una proteína similar a G9a (GLP), que interactúa activamente con G9a, formando un complejo heterodimérico (Shinkai & Tachibana, 2011). Se ha demostrado que la estructura heteromérica es la forma predominante, así como el estado activo, de la metiltransferasa in vivo. Sin embargo, la actividad enzimática de G9a es más importante para la función in vivo del complejo (Casciello et al., 2015). El complejo es responsable de la metilación de H3K9, una marca que es reconocida por la proteína heterocromatina 1 (HP1), lo que conduce al silenciamiento transcripcional (Tabichana et al., 2005).

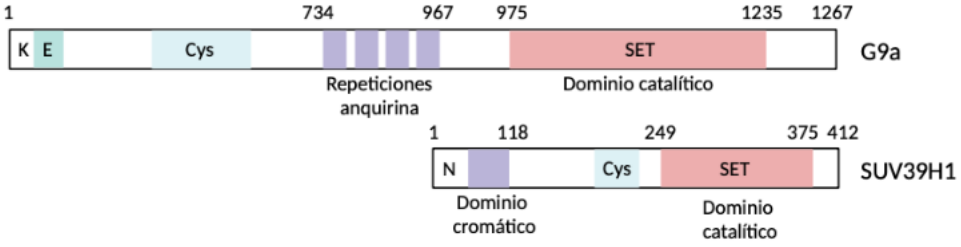

Figura 15. Estructura de las metiltranferasas G9a y SUV39H1 (figura adaptada de Melcher et al., 2000). A) La estructura de G9a se caracteriza por un sitio de autometilación en su extremo N-terminal, repeticiones de anquirina que reconocen la histona H3K9 mono y dimetilada y por un dominio SET catalítico, responsable de la actividad enzimática (adaptado de Collins & Cheng, 2010). B) La estructura SUV39H1 se caracteriza por un dominio cromático y un dominio SET catalítico encargado de la adición de grupos metilos.

SUV39H1 cataliza la trimetilación de la histona H3 lisina 9 al unirse preferiblemente a los residuos mono y dimetilados (Peters et al., 2003). La proteína SUV39H1 tiene varias regiones conservadas, un dominio cromático, el dominio SET, regiones ricas en cisteínas asociadas al dominio SET y una región N-terminal. El extremo N-terminal junto con el dominio cromático actúan como superficie de interacción con M31 (HP1β, miembro de la familia de proteínas de mamíferos H3 (**figura 15**) (Maison et al., 2016).

4.4 LAS MODIFICACIONES EPIGENÉTICAS EN LA LLA

Durante la transformación leucémica se desregulan algunos de los mecanismos implicados en el desarrollo de las células hematopoyéticas, como la modificación de las histonas, ARNs no condificantes o la metilación del ADN (Nordlund & Syvänen, 2017). Las modificaciones postraduccionales de las histonas en combinación con la metilación del ADN desempeñan un papel fundamental en la regulación de la expresión génica de las células. Sin embargo, mientras que la metilación del ADN es un mecanismo que se ha estudiado en múltiples ocasiones en LLA, las modificaciones de las histonas han sido mucho menos estudiadas (Xu et al., 2021). Las

alteraciones genéticas que impulsan la aparición de la leucemia infantil suelen implicar genes que alteran el patrón de metilación de determinadas histonas (de Barrios & Parra, 2021).

En los últimos años se ha demostrado que G9a desempeña un papel fundamental en el desarrollo y progresión de diferentes tipos de cáncer, entre los que se encuentran las leucemias (Chen et al., 2010). En la mayoría de los casos niveles altos de G9a se relacionan con un mal pronóstico de la enfermedad (Casciello et al., 2015). En el caso de la LLA, se ha demostrado que la inhibición de G9a favorece restaurar la sensibilidad de los LLA-B resistente al tratamiento (Poulard et al., 2018). En el caso de SUV39h1 también se ha implicado en el desarrollo de la LLA-T al ser recluida por PHF6 (Tsai et al., 2021). Sin embargo, el estudio de ambas metiltransferasas en relación con la LLA sigue siendo muy escaso, por lo que nos hemos planteado en esta tesis estudiar su posible papel en la migración celular.

OBJETIVOS

El objetivo principal de esta tesis ha sido estudiar las acciones que las modificaciones epigenéticas pueden desempeñar en la migración y diseminación de las células de LLA, en particular por su conexión con la biomecánica del núcleo celular. Para llegar a este objetivo hemos determinado los siguientes objetivos específicos:

1. Estudiar el papel del microambiente en la modificación de histonas y por tanto en las propiedades físicas del núcleo y en la migración de las células de LLA.
   1.1 Determinar la modificación de histonas inducida por la quimioquina CXCL12.
   1.2 Analizar cómo afecta a la cromatina la modificación de histonas inducida por CXCL12.
   1.3 Identificar que rutas moleculares podrían estar implicadas en la conexión entre la quimioquina CXCL12 y la maquinaria epigenética.
   1.4 Determinar cómo se ve afectada la migración de la LLA por estos cambios epigenéticos.

2. Estudiar el impacto de modificaciones epigenéticas (metilación de histonas) en la migración transendotelial de células de LLA.
   2.1 Determinar la relación entre la metiltransferasas de H3K9 y la integrina α4β1 en pacientes de LLA.
   2.2 Estudiar como la metiltransferasa G9a está implicada en la migración transendotelial de células de LLA.

3. Desarrollar un método de análisis de las propiedades mecánicas del núcleo celular.
   3.1 Evaluar la capacidad del método desarrollado para medir las propiedades físicas de núcleos sometidos a estrés osmótico.
   3.2 Determinar las propiedades biofísicas de los núcleos de diferentes subtipos de LLA.

MATERIAL Y MÉTODOS

Los materiales y métodos de empleados en esta tesis doctoral están detallados en los artículos presentados en la misma en el apartado de resultados.

RESULTADOS

La metilación rápida de H3K9 promovida por CXCL12 contribuye a los cambios nucleares y la invasión de las células de leucemia linfoblástica aguda T

La leucemia linfoblástica aguda T (LLA-T) es una neoplasia maligna hematológica agresiva que consiste en la acumulación de células T malignas. A pesar de las terapias actuales, el fracaso de los tratamientos convencionales y la recaída son frecuentes en niños con LLA-T. Se sabe que la quimioquina CXCL12 modula la supervivencia y diseminación de la leucemia; sin embargo, nuestro conocimiento sobre los mecanismos moleculares utilizados por las células LLA-T para infiltrarse y responder a las interacciones entre las células leucémicas y el microambiente aún es insuficiente. En el presente estudio, demostramos que CXCL12 promovió la metilación de H3K9 en líneas celulares y células LLA-T primarias en cuestión de minutos. De esta manera, identificamos que la metilación de H3K9 mediada por CXCL12 afectó la configuración global de la cromatina y la mecánica nuclear de las células LLA-T. Es importante destacar que caracterizamos los cambios en el perfil genómico de las células LLA-T asociadas con la estimulación rápida de CXCL12. Demostramos que el bloqueo de CXCR4 y la proteína quinasa C (PKC) disminuyó la metilación de H3K9 inducida por CXCL12 en las células LLA-T. Finalmente, el bloqueo de las metiltransferasas H3K9 redujo la eficiencia de las células LLA-T para deformar sus núcleos, migrar a través de espacios confinados y alojarse en el bazo y en la médula ósea en modelos *in vivo*. En conjunto, nuestros datos muestran nuevas funciones para CXCL12 como un regulador maestro de la deformabilidad nuclear y de los cambios epigenéticos en las células LLA-T, y su potencial como un objetivo farmacológico prometedor contra la diseminación de LLA-T.

Elena Madrazo #, Raquel González-Novo #, Cándido Ortiz-Placín, Mario García de Lacoba, África González-Murillo, Manuel Ramírez, Javier Redondo-Muñoz. Oncogene. 2022 Feb;41(9):1324-1336. doi: 10.1038/s41388-021-02168-8.

ARTICLE

Fast H3K9 methylation promoted by CXCL12 contributes to nuclear changes and invasiveness of T-acute lymphoblastic leukemia cells

Elena Madrazo[1,5], Raquel González-Novo[1,5], Cándido Ortiz-Placín[1], Mario García de Lacoba[2], África González-Murillo[3,4], Manuel Ramírez[3,4] and Javier Redondo-Muñoz[1]✉

T-acute lymphoblastic leukemia (T-ALL) is an aggressive hematological malignancy that comprises the accumulation of malignant T-cells. Despite current therapies, failure to conventional treatments and relapse are frequent in children with T-ALL. It is known that the chemokine CXCL12 modulates leukemia survival and dissemination; however, our understanding of molecular mechanisms used by T-ALL cells to infiltrate and respond to leukemia cells-microenvironment interactions is still vague. In the present study, we showed that CXCL12 promoted H3K9 methylation in cell lines and primary T-ALL cells within minutes. We thus identified that CXCL12-mediated H3K9 methylation affected the global chromatin configuration and the nuclear mechanics of T-ALL cells. Importantly, we characterized changes in the genomic profile of T-ALL cells associated with rapid CXCL12 stimulation. We showed that blocking CXCR4 and protein kinase C (PKC) impaired the H3K9 methylation induced by CXCL12 in T-ALL cells. Finally, blocking H3K9 methyltransferases reduced the efficiency of T-ALL cells to deform their nuclei, migrate across confined spaces, and home to spleen and bone marrow in vivo models. Together, our data show novel functions for CXL12 as a master regulator of nuclear deformability and epigenetic changes in T-ALL cells, and its potential as a promising pharmacological target against T-ALL dissemination.

Oncogene; https://doi.org/10.1038/s41388-021-02168-8

INTRODUCTION

Acute lymphoblastic leukemia (ALL) is an aggressive hematological disorder that represents the most common childhood cancer. ALL can be divided into B-ALL (80%) and T-ALL (20%) according to the malignant transformation of B- and T-cell precursors [1]. ALL dissemination remains a major clinical problem, as ALL cells respond to different microenvironmental signals and infiltrate various organs, including the spleen, lymph nodes, liver, and central nervous system [2, 3]. ALL resistance associates with these specific tissues where leukemia cells resist therapies. Thus, defining novel molecular mechanisms used by ALL cells is essential to target leukemia dissemination and reduce side effects of systemic treatment in patients.

Chemokines are chemotactic cytokines that regulate many cellular functions, including migration, survival, proliferation, and activation [4]. CXCL12 (CXC motif chemokine 12)/Stromal cell-derived factor-1 (SDF-1α) is a chemokine produced by several cell types (including CXCL12-abundant reticular/CAR, endothelial and stromal cells) that is critical for steady-state conditions of leukocytes and the homing of hematopoietic stem cells into the bone marrow (BM) [5]. In T-ALL cells, CXCL12 is critical for cells escaping from the thymus into the BM, for leukemia initiating cells, and for transendothelial migration and in vivo dissemination of T-ALL cells [6–8]. Studies blocking CXCL12 and its receptor CXCR4 have shown the potential effect of targeting this chemokine on leukemia maintenance and progression [9, 10]; however, the molecular implications of CXCL12 on leukemia cell biology remains intriguing and should be elucidated to maximize its potential as a therapeutic target in T-ALL.

Chromatin structure is regulated by multiple epigenetic alterations, including the methylation of histones, of which a key chromatin mark is the histone 3 lysine 9 (H3K9) methylation. [11]. Emerging evidence indicates that deformability and mechanical changes of the nucleus are crucial for cancer cell migration [12]. This nuclear deformability is regulated mainly by the expression of nuclear lamins and the chromatin structure [13, 14]. However, the molecular mechanisms by which CXCL12 might control H3K9 methylation and nuclear changes during T-ALL cell migration have not been reported.

In the present work, we demonstrated that CXCL12 induced H3K9 methylation in both cell lines and primary pediatric T-ALL cells. We described that H3K9 methylation induced by CXCL12 promoted global chromatin structure modification, which correlated with changes in the mechanical properties of the nucleus

[1]Department of Molecular Medicine, Centro de Investigaciones Biológicas Margarita Salas (CIB Margarita Salas-CSIC), Madrid, Spain. [2]Bioinformatics and Biostatistics Unit, Centro de Investigaciones Biológicas Margarita Salas (CIB Margarita Salas-CSIC), Madrid, Spain. [3]Department of Paediatric Haematology & Oncology, Hospital Universitario Niño Jesús, Madrid, Spain. [4]Health Research Institute La Princesa, Madrid, Spain. [5]These authors contributed equally: Elena Madrazo, Raquel González-Novo.
✉email: Javier.redondo@cib.csic.es

Received: 8 June 2021 Revised: 9 December 2021 Accepted: 22 December 2021
Published online: 08 January 2022

and the transcriptional profile of T-ALL cells. We showed that protein kinase C (PKC) inhibition impaired the CXCL12-mediated H3K9 methylation in T-ALL cells. Furthermore, targeting or blocking the enzymes involved in H3K9 methylation abrogated the migration and squeezing of T-ALL cells in vitro and in vivo systems. Taken together, our findings identified a critical role of CXCL12 on nuclear changes of T-ALL cells and suggested epigenetic changes induced by this chemokine as possible therapeutic targets to block T-ALL migration.

MATERIAL AND METHODS

Primary samples

Samples were obtained from Dr. Ramírez (Hospital Universitario Infantil Niño Jesús) with informed consent for research purposes, and the procedures were approved by the CSIC Ethics Committee and the Institutional Review Board of the Hospital Universitario Niño Jesús (R0070/15). A total of ten ALL patients under 14 years old were retrospectively included in this study. ALL diagnosis and treatment were defined according to SEHOP-Pethema 2013 (Spanish Program for the Treatment of Hematologic Diseases). Patients' characteristics are provided in Supplementary Table S1.

Cells

The human T-ALL cell lines (Jurkat and CCRF-CEM) and the B-ALL cell line (Reh). Cell lines and primary cells were cultured in RPMI 1640 with L-glutamine and $NaHCO_3$ (Sigma-Aldrich) and 10% fetal bovine serum (Sigma-Aldrich), in 5% CO_2 at 37 °C. Cells were routinely tested for mycoplasma contamination (Mycoplasma Gel Detection Kit, Biotools).

Cellular fractionation

Cells were lysed with buffer A (HEPES [pH 8.0] 10 mM, KCl 10 mM, $MgCl_2$ 1.5 mM, sucrose 0.34 M, glycerol 10%, DTT 1 mM, Tx-100 0.1%) for 5 min at 4 °C. Then, cytoplasmic fractions were collected from centrifugation at 3200 rpm for 5 min. The pellet was washed once with buffer A and resuspended in RIPA buffer (NaCl 1 M, NP-40 1%, Sodium deoxycholate 0.5%, SDS 0.1%, Tris-HCl [pH 7.4] 50 mM) with protease inhibitors. After 15 min, soluble nuclear fractions were collected from centrifugation (5 min, 4 °C, 13,500 rpm) and chromatin bound fractions were resuspended in sample buffer (VWR) and sonicated.

In vivo short-term leukemia homing assay

NOD.Cg-Prkdcscid Il2rgtm1Wjl/SzJ (NSG) mice were purchased from Charles River Laboratories and bred and maintained at the Servicio del Animalario del Centro de Investigaciones Energéticas, Medioambientales y Tecnológicas (CIEMAT) with registro 28079-21 A. All mice were used following guidelines issued by the European and Spanish legislation for laboratory animal care. All experiments involving animals were approved by the OEBA (Organ for Evaluating Animal Wellbeing) at CIEMAT and Madrid Regional Department of Environment, with reference PROEX 185/15. 2.5×10 6 control and BIX-01294 or chaetocin inhibited Jurkat cells were labeled with CFSE 5 μM or Far Red Cell Tracker 1 μM for 30 min in RPMI. Control and inhibited cells were mixed 1:1 and intravenously (IV) administrated into 10–12 weeks-old NSG male animals to compare the cell migration. Sacrifice was performed 3 h after inoculation. BMs from femurs and spleens were extracted, processed through mechanical disaggregation, and stained cells were resuspended in the PBS for flow cytometry (FACSCantoTM II, Becton Dickinson). Samples were acquired in a FacsCanto II (BD) cytometer and the number of Far Red cell tracker or CFSE positive cells analyzed using FacsDiva software.

RESULTS

CXCL12 promotes a fast H3K9 methylation in T-ALL cells

First, we analyzed H3K9me2/3 levels in primary samples from pediatric patients with ALL (Supplementary Table S1) and observed that 15 min of stimulation with CXCL12 upregulated the levels of H3K9me2/3 in T-ALL cells compared to untreated conditions (Fig. 1a). Interestingly, B-ALL cells downregulated H3K9me2/3 levels compared to control (unstimulated) conditions. We visualized H3K9me2/3 signal in ALL cell lines seeded on poly-lysine and found that CXCL12 stimulation increased the H3K9 methylation only in T-ALL (Jurkat and CCRF-CEM) but not in the B-ALL (Reh) cell lines (Fig. 1b, c). CXCL12 is mainly produced by resident cells in the BM microenvironment and its immobilization is fundamental for cell adhesion [15], we cultured ALL cells in the presence of soluble or immobilized CXCL12 and confirmed that both stimuli promoted H3K9 methylation in Jurkat and CCRF-CEM cells (Fig. 1d and Supplementary Fig. S1a). Furthermore, we confirmed that Reh cells did not upregulate H3K9 methylation in response to soluble or immobilized CXCL12 (Supplementary Fig. S1b). To explore whether this epigenetic change induced by CXCL12 only in T-ALL cells was reversible, Jurkat and CCRF-CEM cells were stimulated with CXCL12, washed, and cultured in fresh media without chemokine for an additional hour. CXCL12 stimulation increased the levels of H3K9me2/3 in both T-ALL cell lines within minutes, and these cells regained the basal level of H3K9me3 in the absence of the chemokine (Supplementary Fig. S1c, d). We also identified that H3K9 methylation induced by CXCL12 was associated with a reduction in the nuclear area (Supplementary Fig. S1e), suggesting that epigenetic changes induced by CXCL12 might regulate the nuclear morphology of ALL cells. Although no differences were found in the cell size distributions upon CXCL12 stimulation by flow cytometry (Fig. 1e); we observed that isolated nuclei from CXCL12-stimulated T-ALL cells were smaller than those from control cells (Fig. 1f). Furthermore, this only occurred in T- and not in B-ALL cells (Supplementary Fig. S1f). Together, our results indicated that CXCL12 promoted a fast and transient upregulation of H3K9me2/3 levels in T-ALL cells.

Fast epigenetic changes induced by CXCL12 regulate the genomic landscape of ALL cells

To investigate how H3K9 methylation induced by CXCL12 was associated with changes in the genomic landscape of T-ALL, we performed a chromatin immunoprecipitation assay (ChIP-seq) from control or CXCL12-stimulated Jurkat cells. We observed an upregulation of H3K9me3 peaks on the whole genome of Jurkat cells stimulated with CXCL12 compared to control cells (Fig. 2a) and mapped a total of 1739 differentially regulated H3K9me3 peaks, 1185 of which were upregulated upon CXCL12 stimulation (Fig. 2b). Overall, when we quantified the genomic location annotation of these H3K9me3 peaks, we found that most of them were located mainly at protein-coding regions belonging to genes or transcripts (Supplementary Fig. S2a, b). By focusing on these protein-coding regions, we observed that the biggest difference by K-means clustering corresponded to 45 regions (Supplementary Fig. S2c). GO-term enrichment showed differences in genes related to protein deglutamylathion, polarity and membrane-related signaling, calcium signaling, exocytosis among others (Supplementary Fig. S2d, Supplementary Table S2). To further identify the potential effects of CXCL12 stimulation on the transcriptional activity of T-ALL cells, we performed a whole transcriptome analysis of Jurkat cells stimulated with CXCL12. Consistent with the upregulation of H3K9me3 peaks, cells treated with CXCL12 showed that 149 and 212 genes to be significantly up- and downregulated, respectively (Fig. 2c and Supplementary Table S3), indicating that CXCL12 stimulation might repress transcription at short times. Among the top 20 most enriched GO terms were related to Ras activity, cation channels, calcium signaling, cell adhesion, and cell receptor signaling (Fig. 2d and Supplementary Table S4). Furthermore, gene set expression analysis (GSEA) showed a small set of genes altered in ChIP-seq and microarray analyses (Supplementary Table S5), without any correlation between H3K9me3 peaks resolved by ChIP-seq and the transcriptional analysis (Fig. 2e and Supplementary Fig. S2e). Together, these results indicate that CXCL12 promotes higher H3K9me3 occupancy at the whole genome, without significant changes at the transcriptional stage of ALL, suggesting that the relevance of this epigenetic change might be at a biomechanical level.

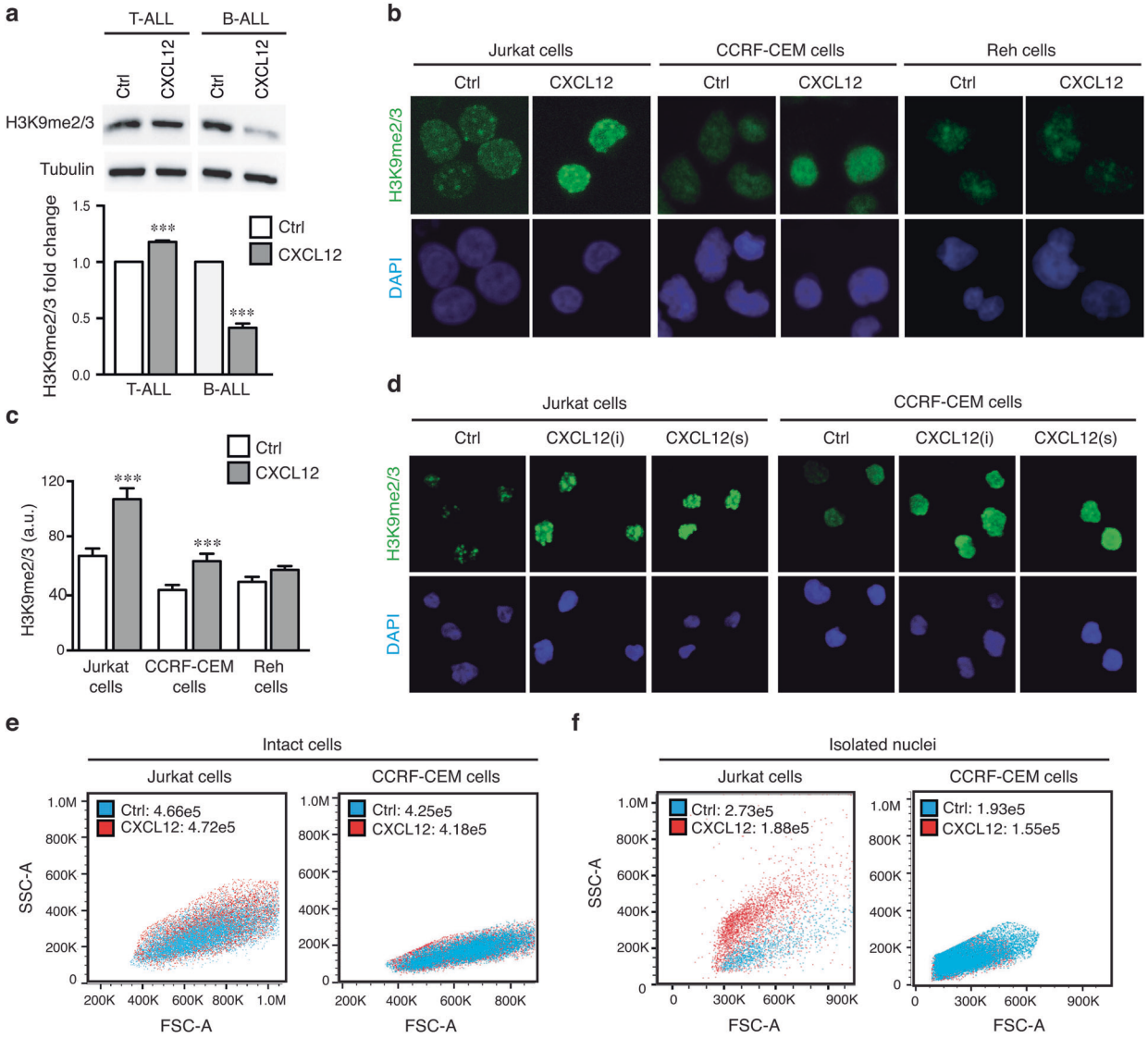

Fig. 1 CXCL12 promotes H3K9 methylation in T-ALL cells. a Primary ALL cells from patients were incubated for 15 min with CXCL12 (100 ng/ml). Subsequently, cells were lysed for detection of H3K9me2/3 levels by western blotting. Mean $n = 3 \pm$ SEM. **b** T- ALL (Jurkat and CCRF-CEM) and B-ALL (Reh) cell lines were seeded on poly-lysine coated coverslips and stimulated with CXCL12 (100 ng/ml) for 15 min. Then, cells were fixed, permeabilized and stained for the indicated markers. Confocal images show representative images of H3K9 methylation induced by CXCL12 in Jurkat and CCRF-CEM cells. **c** Graph shows the mean intensity (arbitrary units, a.u.) of H3K9me2/3 of ALL cell lines in (**b**). Mean $n =$ 60 cells ± SEM. **d** Jurkat and CCRF-CEM cells were seeded on poly-lysine coated coverslips in the absence or presence of immobilized (i) or soluble (s) CXCL12 for 15 min. Then, cells were fixed, permeabilized and stained for the indicated markers. **e** Jurkat and CCRF-CEM cells stimulated or not with CXCL12 for 15 min were analyzed by flow cytometry. The plot represents volume distributions of Ctrl (blue) and CXCL12-stimulated (red) cells measured by FSC-A and SSC-A. Values indicate the geometric mean. **f** Isolated nuclei from Jurkat and CCRF-CEM cells stimulated or not with CXCL12 for 15 min were analyzed by flow cytometry. The plot represents the volume distribution of Ctrl (blue) and CXCL12-stimulated (red) isolated nuclei measured by FSC-A and SSC-A. Values indicate the geometric mean. *P*-values are indicated by asterisks ***$P < 0.001$.

H3K9 methylation induced by CXCL12 alters the global chromatin conformation of ALL cells

As H3K9 methylation is a canonical marker for heterochromatin [16], we determined the level of chromatin compaction induced by CXCL12 in ALL cells. By using a DNAse I sensitivity assay [17], we observed that only T-ALL cells presented more resistance to DNA digestion upon CXCL12 stimulation (Fig. 3a, b). Then, we carried out in situ DNAse digestion of ALL cells upon CXCL12 stimulation to validate our findings. We found that CXCL12 induced the compaction and more resistant chromatin to DNAse I digestion in T- (Fig. 3c), but not in B-ALL cells (Supplementary Fig. S3a). Based on these results, we additionally measured the sensitivity of ALL cells to micrococcal nuclease (MNase), an enzyme that digests the nucleosome linker regions. We confirmed that CXCL12 stimulation also promoted a more compacted chromatin resistant to MNAse digestion in T-ALL cell lines (Fig. 3d, e). Chromatin compaction takes place during cell cycle progression, and it has been reported that CXCL12 promote cell proliferation [18]. As H3K9 methylation occurred within minutes, we speculated that it should not interfere with other prosurvival effects induced by this chemokine. To test this hypothesis, we evaluated the proliferation upon CXCL12 addition. As expected, CXCL12 stimulation increased slightly the proliferation ratio of all ALL cell lines tested (Supplementary Fig. S3b);

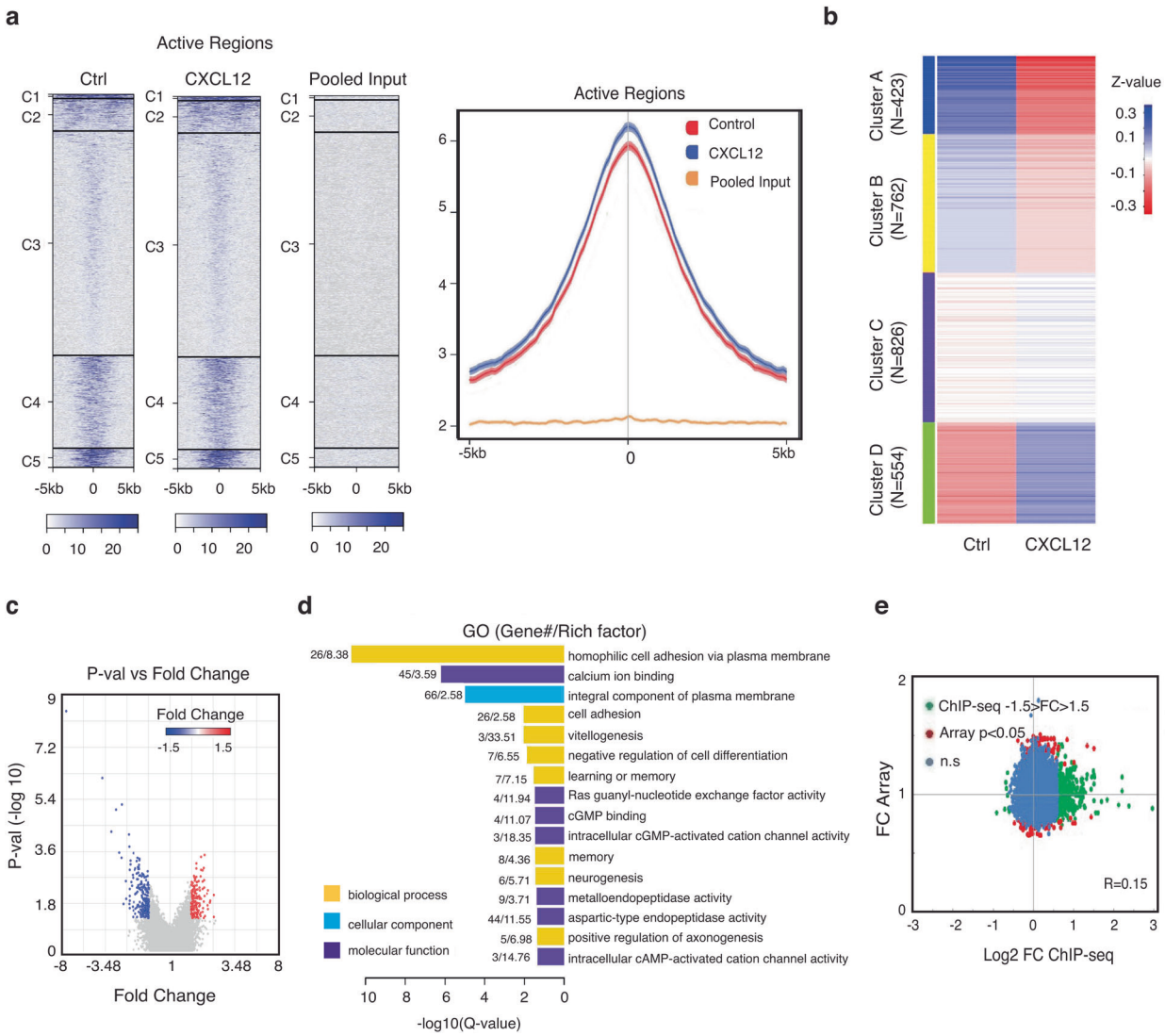

Fig. 2 CXCL12 alters the epigenetic and transcriptional landscape of T-ALL cells. a Jurkat cells were cultured in medium (Ctrl) or with CXCL12 (100 ng/ml) for 15 min, and H3K9 methylation changes were analyzed by ChIP-seq. Heatmaps for distance-base clustering of differential H3K9me3 tags across the whole genome and plots for their average values. **b** K-means clustering of genomic-wide changes relating to the H3K9me3 epigenetic signal induced by CXCL12. **c** Volcano-plot shows the differential expression of genes between control cells and stimulated cells by CXCL12 analyzed by microarray experiments. Red and blue dots are denoting up- and downregulated genes, respectively. **d** Jurkat cells were cultured without (Ctrl) with CXCL12 (100 ng/ml) for 15 min, and transcriptional changes were analyzed by microarray. Graph shows the GO-term analysis of altered genes in Jurkat cells upon CXCL12 stimulation from microarray experiments. **e** Correlation plot and quantification of H3K9me3 peaks resolved by ChIP-seq and differential gene expression obtained from the microarray.

although no significant differences were found in the S phase entry and G2 progression (Supplementary Fig. S3c). Together, these results suggest that CXCL12 stimulation was able to successfully induce a global condensation of chromatin in T-ALL cells.

CXCL12 stimulation induces a different mechanical behavior of the nucleus

Previous analyses have shown that chromatin changes contribute to the mechanical response of the cell nucleus [19, 20]. The chromatin compaction induced by CXCL12 in T-ALL cells suggested that the chromatin might be relevant for the mechanical response of leukemia cells. Consistent with this hypothesis, we tested a cell confiner developed to induce physical stress [21]. By using confocal stacks and reconstructed 3D renderings, we examined the area of isolated nuclei from control or CXCL12-stimulated Jurkat cells seeded on confinement plates of defined height (3 µm) (Fig. 4a, b). Under physical forces, isolated nuclei from control Jurkat cells showed a nuclear deformability ratio of 1.39, whilst those nuclei from cells upon CXCL12 stimulation revealed a less prominent ratio (Fig. 4c). We observed a similar effect on isolated nuclei of CCRF-CEM cells upon CXCL12 stimulation (Supplementary Fig. S4a, b), whilst Reh cells showed no differences in the nuclear deformability ratio of control and CXCL12-treated conditions (Supplementary Fig. S4c, d). Based on these findings, we measured the morphology of isolated nuclei from CXCL12-stimulated ALL cells under osmotic stress. Adding EDTA promoted more prominent nuclear swelling in control conditions than in isolated nuclei from CXCL12-stimulated cells. Consistent with the mechanical compression and nuclear compaction, we observed this phenomenon in T- but not in B-ALL cells (Fig. 4d, e). Together, these results revealed that

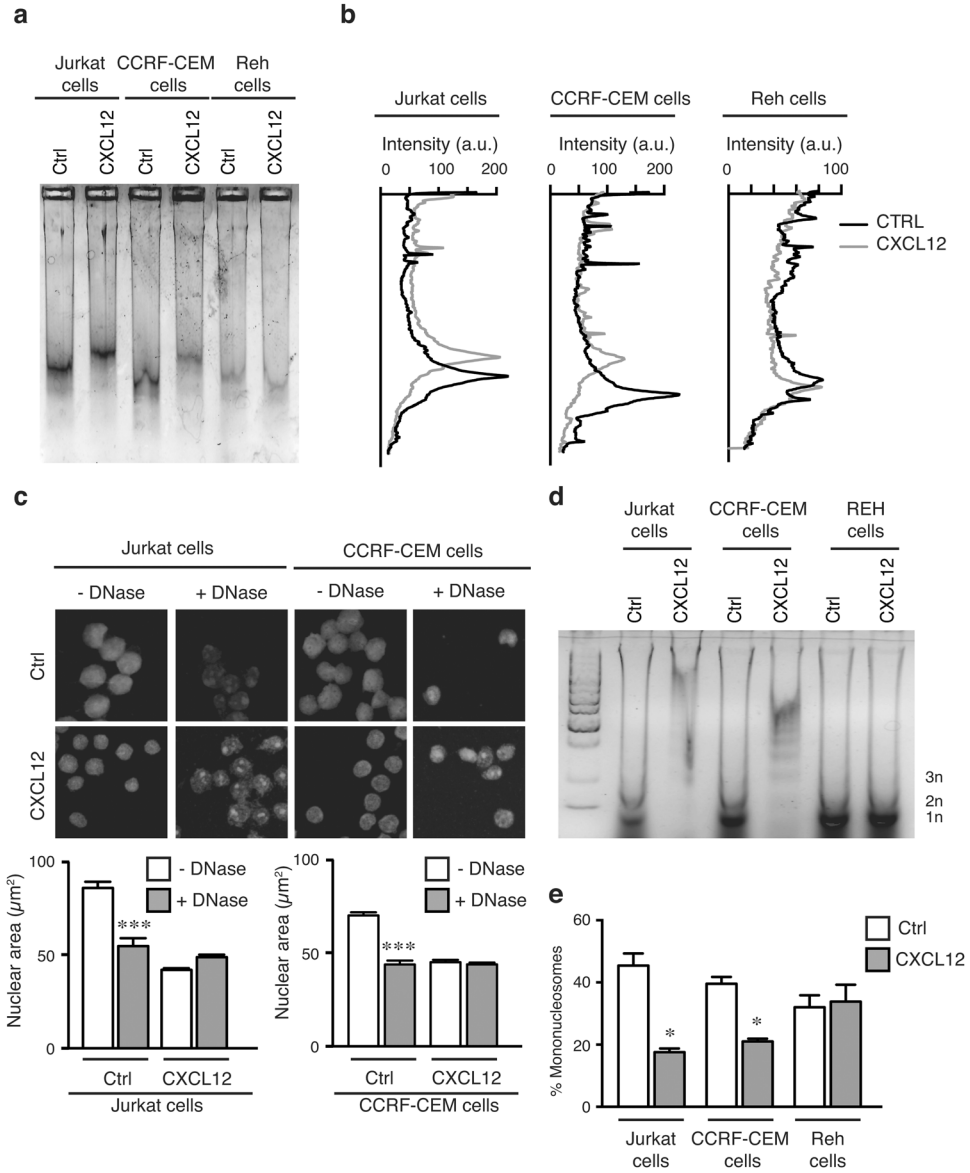

Fig. 3 CXCL12 induces global chromatin compaction in T-ALL cells. a Jurkat, CCRF-CEM and Reh cells were in fresh medium (Ctrl) or with CXCL12 (100 ng/ml) for 15 min. Then, cells were collected, lysed and DNA was digested with DNAse I for 15 min. Gel image shows chromatin degradation upon DNAse activity. **b** Graph shows the digested DNA profiles. Black line indicates control (Ctrl) conditions and gray line indicates upon CXCL12 stimulation. **c** Jurkat and CCRF-CEM cells were seeded on poly-lysine coated coverslips, and cultured in fresh medium (Ctrl) or stimulated with CXCL12 (100 ng/ml) for 15 min. Then, cells were subjected to in situ DNase I digestion, fixed, and stained with DAPI. Graph shows the nuclear projected area. Mean n = 30 ± SEM. **d** Jurkat, CCRF-CEM and Reh cells were in fresh medium (Ctrl) or with CXCL12 (100 ng/ml) for 15 min. Cells were lysed, and chromatin was digested by micrococcal DNAse (MNase) for 15 min. Nucleosome releasing was resolved on 2% agarose gels. Lines indicate mono- (1n), di- (2n) and tri- (3n) nucleosomes upon MNAse digestion. **e** Graph shows the percentage of released mononucleosomes upon MNAse digestion. Mean $n = 3 \pm$ SEM. *P*-values are indicated by asterisks ***$P < 0.001$.

chromatin changes induced by CXCL12 had a direct impact on the mechanical properties and the deformability of the nucleus of T-ALL cells.

PKC activity regulates the H3K9 methylation induced by CXCL12 in T-ALL cells

There are two cell receptors for CXCL12, CXCR4, and CXCR7, and both have relevance for ALL cell migration and invasiveness [22, 23]. As only T-ALL cells upregulated H3K9 methylation in response to CXCL12, we treated Jurkat with AMD3100 and CCX771 (CXCR4 and CXCR7 inhibitors, respectively) and observed that only CXCR4 inhibition abrogated the effect of CXCL12 on H3K9me2/3 levels (Fig. 5a, b). Similar results were observed in CCRF-CEM cells (Supplementary Fig. S5a, b). It is well known that CXCR4/CXCL12 axis promotes cell migration through multiple signaling pathways, including PKC activation [24]. We determined that inhibitors against conventional PKC prevented the H3K9 methylation induced by CXCL12 in T-ALL cell lines (Fig. 5c). By using Phorbol 12-myristate 13-acetate (PMA), we observed that PKC activation induced upregulation of H3K9 methylation in both T- (Fig. 5d, e) and, interestingly, also in B-ALL cells (Supplementary Fig. S5c). We examined the nuclear pattern of conventional PKC localization in ALL cells and found that PKCβ was expressed both in the cytoplasm and the nucleus of ALL cells, whilst most PKCα showed a cytoplasmic localization (Supplementary Fig. S5d). To confirm that this nuclear localization of PKCβ was not a microscopy artifact, we analyzed the subcellular localization of PKC in T- and B-ALL cells and confirmed that PKCα was detected primarily in the

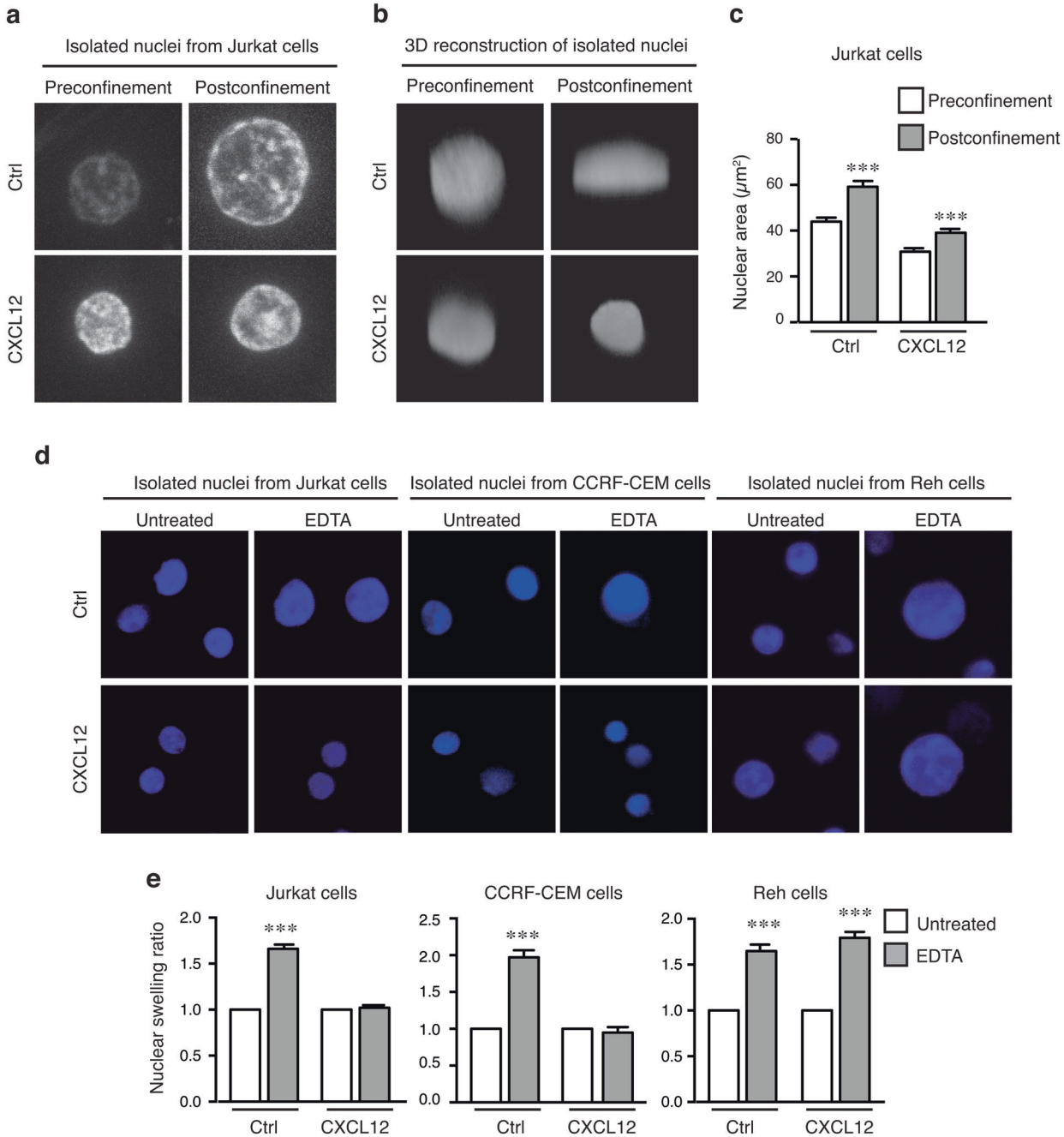

Fig. 4 Fast CXCL12 stimulation promotes mechanical changes in the nucleus of T-ALL cells. a Representative images from nuclei of Jurkat cells cultured in the absence (Ctrl) or presence of CXCL12 for 15 min. Nuclei were isolated, stained and seeded on poly-lysine-coated coverslips. Subsequently, confocal images were acquired before and after confinement conditions (3 µm height). **b** Reconstruction of 3D surface rendering of representative isolated nuclei in (**a**). **c** Graph shows the quantification of nuclear projected areas from isolated nuclei in pre- and post-constrained conditions. Mean $n = 50$ nuclei ± SEM. **d** Jurkat, CCRF-CEM, and Reh cells were cultured without (Ctrl) or with CXCL12 (100 ng/ml) for 15 min. Then, nuclei were isolated and treated with EDTA to induce nuclear swelling. **e** Graph shows the quantification of nuclear area of isolated nuclei. Mean $n = 80$ nuclei ± SEM. *P*-values are indicated by asterisks ***$P < 0.001$.

cytosol of ALL cells, whilst a significant amount of the total endogenous PKCβ partitioned to the nuclear fraction of ALL cells (Supplementary Fig. S5e, f). Mechanistically, we checked whether CXCL12 stimulation might promote nuclear PKC accumulation, although we found no differences in the nuclear translocation of conventional PKC isoforms upon CXCL12 stimulation in Jurkat cells (Supplementary Fig. S5g). We pretreated T-ALL cells with PKC inhibitors and confirmed that blocking conventional PKC activity reduced Jurkat and CCRF-CEM migration in response to CXCL12 (Fig. 5f). Together, our data suggested that CXCR4 was the key receptor for the H3K9 methylation induced by CXCL12 and that conventional PKC activity was necessary for this nuclear change in T-ALL cells.

H3K9 methyltransferases control epigenetic changes induced by CXCL12 in T-ALL cells

Several H3K9 (histone H3 at the residue lysine K9) methyltransferases, such as suv39h1 and G9a, have been proposed as therapeutic targets against cancer cell progression and migration, including hematological malignancies [25, 26]. To identify how

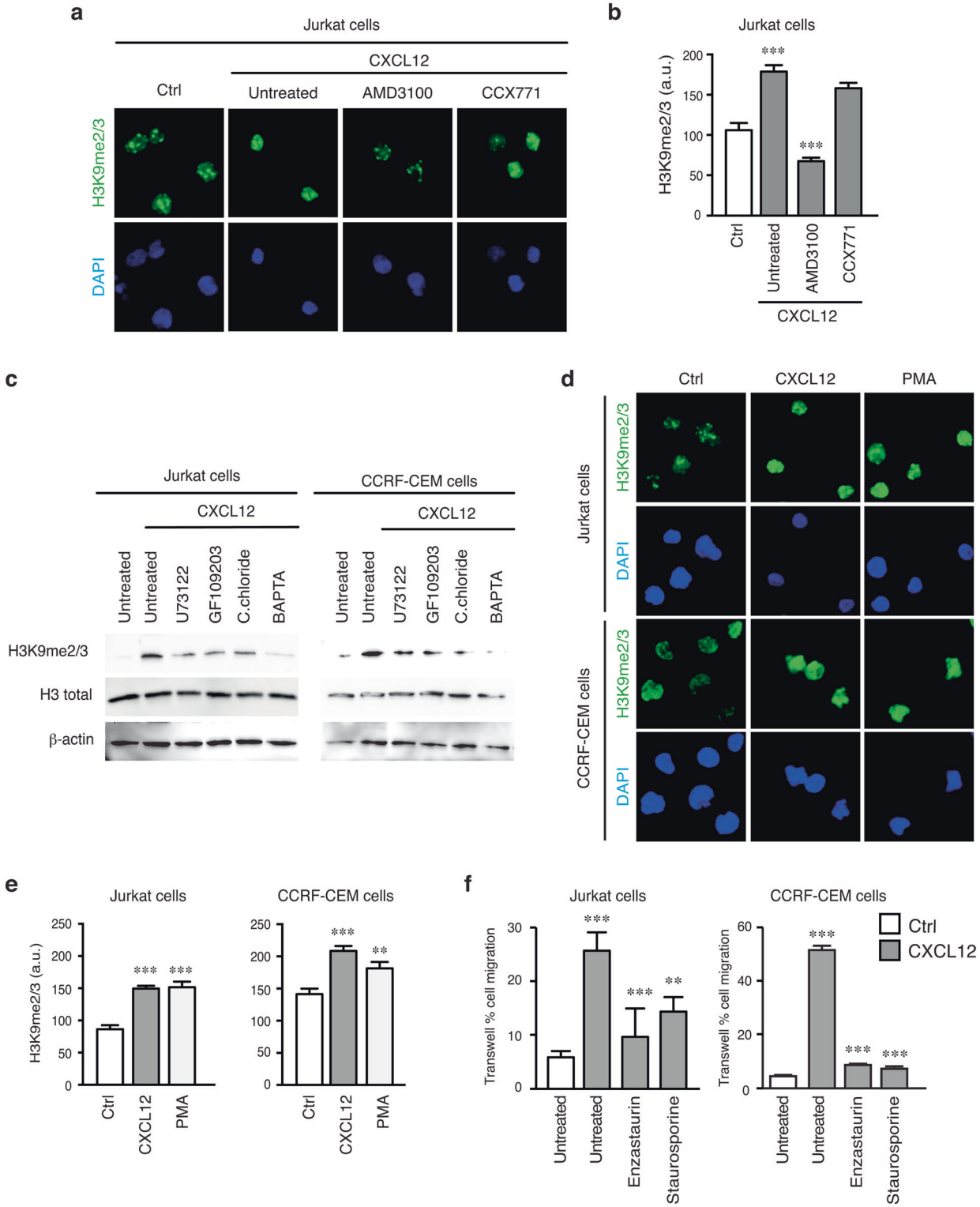

Fig. 5 Conventional PKC regulates CXCL12-medited H3K9 methylation in T-ALL cells. a Jurkat cells were preincubated with AMD3100 (1 μM), CCX771 (1 μM), for 30 min before culturing without (Ctrl) or with CXCL12. Then, cells were fixed, permeabilized and stained for the indicated markers. Confocal images show representative images of H3K9 methylation induced by CXCL12 in Jurkat and CCRF-CEM cells. **b** Graph shows the mean intensity (arbitrary units, a.u.) of H3K9me2/3 of ALL cell lines in (**a**). Mean $n = 60$ cells ± SEM. **c** Jurkat and CCRF-CEM cells were preincubated with U73122 (5 μM), GF109203 (2 μM), chelerythrine chloride (5 μM) and BAPTA (1 μM) for 30 min before culturing without (Ctrl) or with CXCL12. Cells were lysed, and H3K9me2/3 levels analyzed by western blotting. **d** Jurkat and CCRF-CEM cells were seeded on poly-lysine coated coverslips and stimulated with PMA (50 ng/ml) or CXCL12 (100 ng/ml) for 15 min. Then, cells were fixed, permeabilized and stained for the indicated markers. **e** Graph shows the mean intensity (arbitrary units, a.u.) of H3K9me2/3 of ALL cell lines in (**d**). Mean $n =$ 60 cells ± SEM. **f** Jurkat and CCRF-CEM cells were pretreated with the PKC (staurosporine, 2 nM) and PKCβ (enzastaurin, 50 nM) inhibitors for 30 min. After 24 h cells in the bottom chamber were collected and counted to calculate the migration index. Mean $n = 3$ ± SEM. *P*-values are indicated by asterisks *P*-values are indicated by asterisks $^{**}P < 0.01$, $^{***}P < 0.001$.

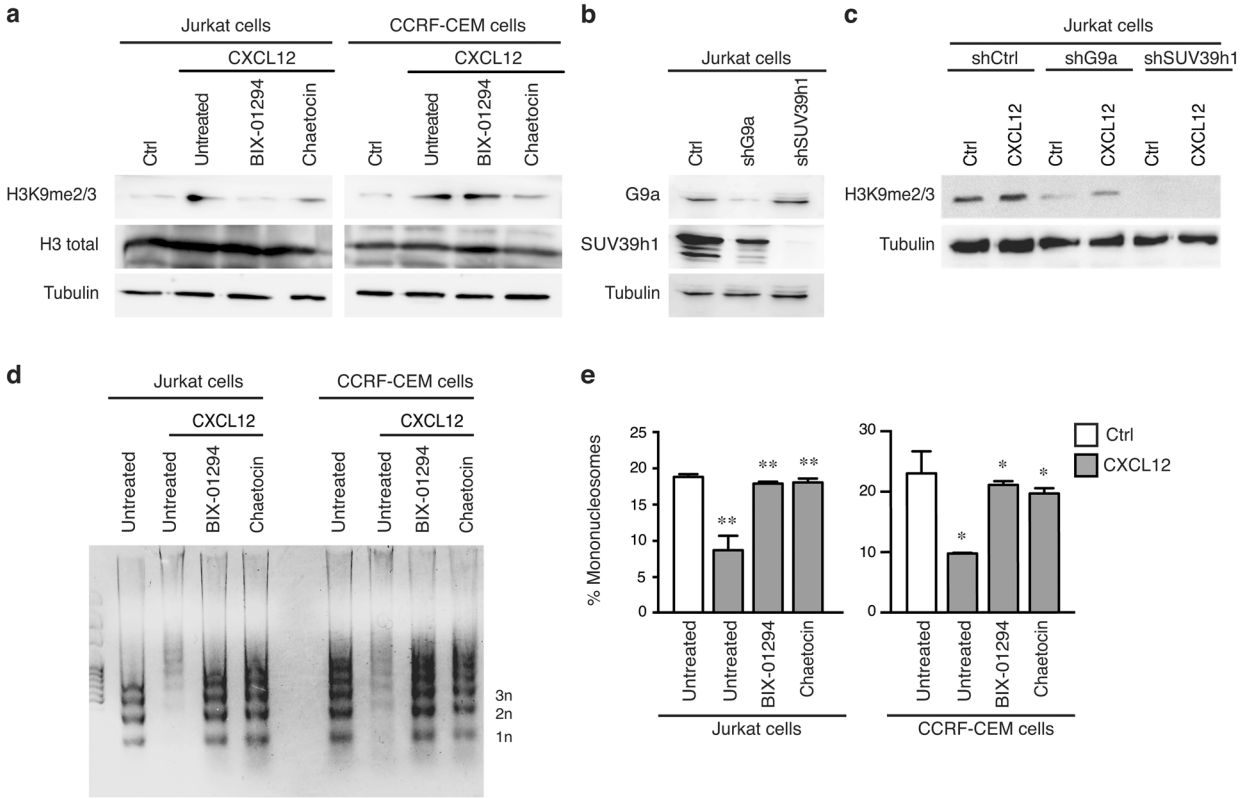

Fig. 6 The H3K9 methyltransferases G9a and suv39h1 regulate the H3K9 methylation induced by CXCL12 in T-ALL cells. a Jurkat and CCRF-CEM cells were preincubated or not with the H3K9 methyltransferase inhibitors, chaetocin (suv39h1 inhibitor 1 μM) and BIX-01294 (G9a inhibitor, 1 μM). After 30 min, cells were cultured in the absence (Ctrl) or presence of CXCL12 (100 ng/ml) for 15 min. Then, levels of H3K9me2/3 were resolved by western blotting. **b** Control, suv39h1- and G9a-depleted Jurkat cells were lysed and protein silencing was resolved by western blotting. **c** Control, suv39h1- and G9a-depleted Jurkat cells were cultured in the absence (Ctrl) or presence of CXCL12 (100 ng/ml) and their lysates analyzed by western blotting. **d** Jurkat and CCRF-CEM cells were preincubated or not with the H3K9 methyltransferase inhibitors, chaetocin (1 μM) and BIX-01294 (1 μM). After 30 min, cells were cultured with CXCL12 (100 ng/ml) for 15 min, lysed, and chromatin was digested by micrococcal DNAse (MNase) for 15 min. Nucleosome releasing was resolved on 2% agarose gels. Lines indicate mono- (1n), di- (2n) and tri- (3 N) nucleosomes upon MNAse digestion. **e** Graph shows the percentage of mononucleosomes (1n) from (**d**). *$P < 0.05$; **$P < 0.01$.

H3K9 methyltransferases might catalyze the epigenetic change induced by CXCL12, we used specific inhibitors to block suv39h1 (chaetocin) and G9a (BIX-01294) activities and found that both treatments reduced significantly the H3K9 methylation induced by CXCL12 in T-ALL cells (Fig. 6a). We next examined stable Jurkat cells depleted for G9a and Suv39h1 (Fig. 6b), and confirmed that the knocking-down of these proteins abrogated the H3K9 methylation induced by CXCL12 (Fig. 6c). Given that CXCL12 stimulation promoted chromatin compaction, we investigated whether suv39h1 and G9a activities might be necessary for the protective role of CXCL12 to MNAse digestion. We pretreated T-ALL cells with chaetocin and BIX-01294 and observed that both inhibitors increased the sensitivity of CXCL12-stimulated cells to DNA digestion (Fig. 6d, e), confirming that CXCL12 induced H3K9 methylation was dependent on suv39h1 and G9a activities. Together, these results strongly indicate the physiological relevance of H3K9 HMTs to control epigenetic changes and chromatin compaction induced by CXCL12 in T-ALL cells.

Targeting H3K9 methylation reduces the invasiveness of ALL cells in vitro and in vivo

Nuclear constrictions are related to cell migration and promote the redistribution of multiple nuclear components, including histone markers [27]. We then sought to quantify the distribution of H3K9 methylation in migrating ALL cells by determining the nuclear signal of H3K9me2/3 and the nuclear contour. We found that deformable migrating cells showed higher H3K9me2/3 intensity in those areas corresponding to active nuclear squeezing through 3 μm Transwell pores in response to CXCL12 gradient (Supplementary Movie S1, Fig. 7a, b). Furthermore, constricted migration of CCRF-CEM and Reh cells also promoted the polarization of H3K9me2/3 signal at the nuclear front of migrating cells (Supplementary Fig. S6a). To address how the nuclear changes induced by CXCL12 might impact the ALL cell capacity to migrate through small pores, we analyzed the chemotactic response of T- and B-ALL cells through 3 μm pores and found that Jurkat and CCRF-CEM cells increased their migration index (2 and 1.6 times, respectively) in response to CXCL12 for 3 h, whilst Reh cells did not alter their migration index (Supplementary Fig. S6b). We analyzed the chemotactic response at longer times (24 h) of primary cells from patients with ALL and confirmed that T-ALL cells increased their migration (Fig. 7c). Based on these findings, we quantified the cell migration of T-ALL cells upon blocking or silencing H3K9 methyltransferases. We found that targeting H3K9 methylation impaired Jurkat cell migration in response to CXCL12 (Fig. 7d, e). Similarly, we confirmed that chaetocin or BIX-01294 treatments reduced the migration of CCRF-CEM cells induced by CXCL12 (Supplementary Fig. S6c), confirming that H3K9 methylation activity might play a fundamental role in CXCL12-mediated migration of T-ALL cells through constricted conditions.

Constricted microchannels have been developed to mimic rigid environments that require the active deformability of migrating cells [28]. We observed that pretreatment with H3K9 methyltransferase inhibitors reduced the total number of Jurkat cells coming into the microchannels (Fig. 8a, Supplementary Movies S2–S4). To further elucidate whether H3K9 methylation might regulate nuclear

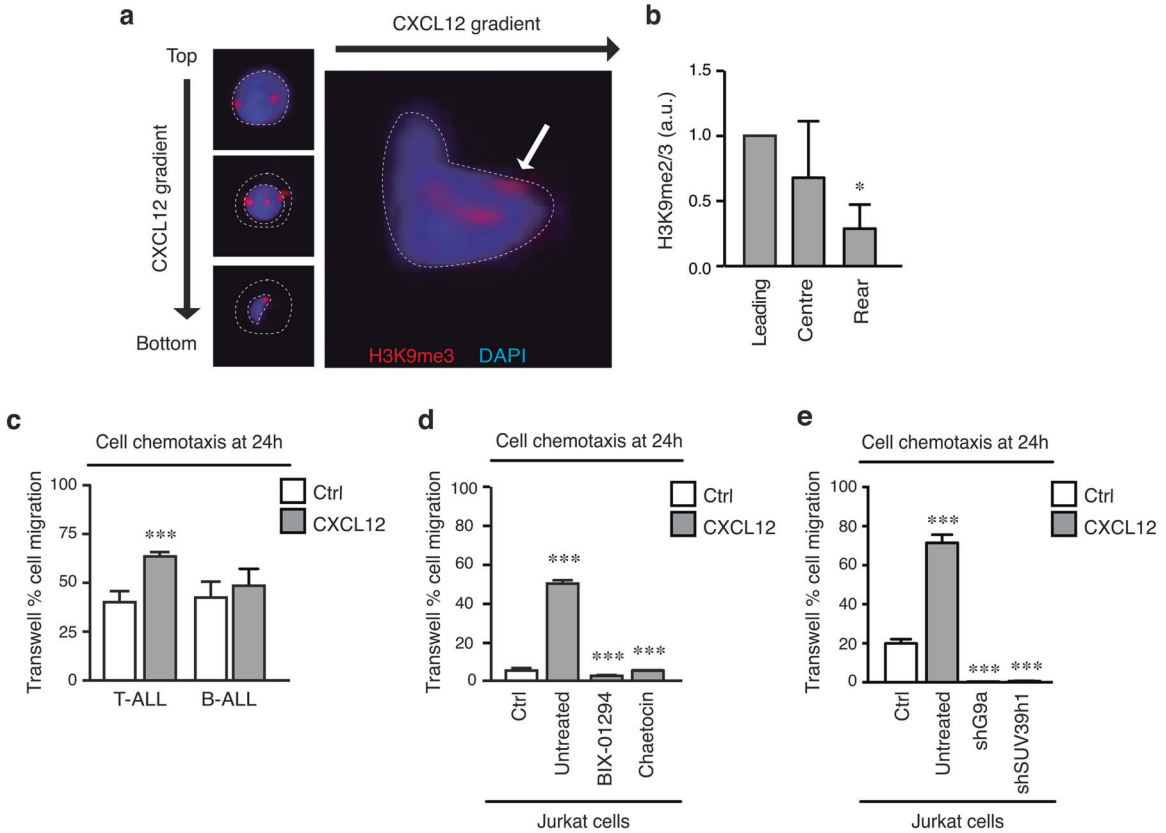

Fig. 7 H3K9 methylation controls T-ALL chemotaxis through rigid pores in response to CXCL12. a Representative image of a Jurkat cell migrating through a 3 µm pore in response to CXCL12 gradient. Cells were fixed, permeabilized and stained for the indicated proteins. White lines indicate the nuclear area and the nuclear constriction through the small pore. Right panel shows a 3D reconstruction of migrating cell nucleus squeezing, and white arrows indicates H3K9me3 signal accumulating at the nuclear constriction. **b** Graph shows the H3K9me2/3 ratio normalized to DAPI at the leading area of the nucleus (highly deformable region). H3K9 methylation accumulates mainly at the nuclear front during cell deformation across the small pore. **c** Chemotaxic migration of primary T- and B-ALL cells through 3 µm pore transwells towards CXCL12 (100 ng/ml) gradient. After 24 h, cells were collected from the bottom chamber and counted to calculate the migration index. Mean $n = 3 \pm$ SEM. **d** Jurkat cells were pretreated or not with chaetocin (1 µM) and BIX-01294 (1 µM) for 1 h prior to adding them in the upper chamber of the transwell. Then, cells were allowed to migrate through 3 µm pore transwells toward CXCL12 (100 ng/ml) gradient. After 24 h, cells were collected from the bottom chamber and counted to calculate the migration index. Mean $n = 3 \pm$ SEM. **e** Control, suv39h1- and G9a-depleted Jurkat cells were seeded in the upper chamber of the transwell and CXCL12 (100 ng/ml) was added to the bottom chamber. After 24 h, cells were collected from the bottom chamber and counted to calculate the migration index. Mean $n = 3 \pm$ SEM. *P*-values are indicated by asterisks $^*P < 0.05$; $^{***}P < 0.001$.

deformability and cell migration across confined spaces, we investigated the percentage of migrating cells that penetrate and deform effectively across constrictions. We observed that cell invasiveness (defined as cells migrating through constrictions) was reduced by chaetocin or BIX-01294 treatments (Fig. 8b). Together, our results suggested that H3K9 methylation played a fundamental role in CXCL12-mediated migration and deformability of T-ALL cells. To evaluate the therapeutic potential of H3K9 methyltransferase inhibitors against leukemia dissemination, we mixed control and pretreated Jurkat cells with H3K9 methyltransferase inhibitors, ad injected them into immunodeficient recipient mice. At 3 h after transplantation, we compared the presence of control and pretreated cells into the BM and spleen by flow cytometry (Fig. 8c). We observed that H3K9 methyltransferase inhibition impaired the homing of Jurkat cells into the spleen and BM compared to untreated cells (Fig. 8d, e). Finally, to confirm the consequences of the in vivo effects of H3K9 methyltransferase inhibitors in T-ALL cell migration, we pretreated CCRF-CEM cells with BIX-01294 and chaetocin, and analyzed the homing of leukemic cells into the spleen and BM at 3 h after inoculation (Supplementary Fig. S7a). We demonstrated that both inhibitors also reduced significantly the number of CCRF-CEM cells that reached the BM and spleen (Supplementary Fig. S7b, c). Together, these data suggested that H3K9 methylation plays a role in cell squeezing and migration of T-ALL cells.

DISCUSSION

T-ALL cells have to penetrate physical barriers to infiltrate various organs (including lymph nodes, liver, spleen, BM, and central nervous system) [29]. These places serve as protected niches against conventional chemotherapies and facilitate ALL recurrence and relapse [30, 31]. Here, we demonstrated that CXCL12 determines the H3K9 methylation, the biomechanical response and the invasiveness of T-ALL cells in vitro and in vivo.

Several chemokines mediate the infiltration and progression of ALL pathology [32]. CXCL12 produced by resident cells at tumor niches plays a critical role in the homing, proliferation, and survival of ALL cells into the BM, liver, CNS, etc. [22, 33, 34]. We observed that CXCL12 promoted rapid epigenetic changes within minutes in leukemia cells. Strikingly, only T-ALL cells upregulated H3K9me2/3 levels, while B-ALL cells showed diminished levels of H3K9 methylation upon CXCL12 stimulation. Differences in the epigenetic stage of B- or T-ALL cells have been previously pointed, including the hypermethylation of Notch factors and that only

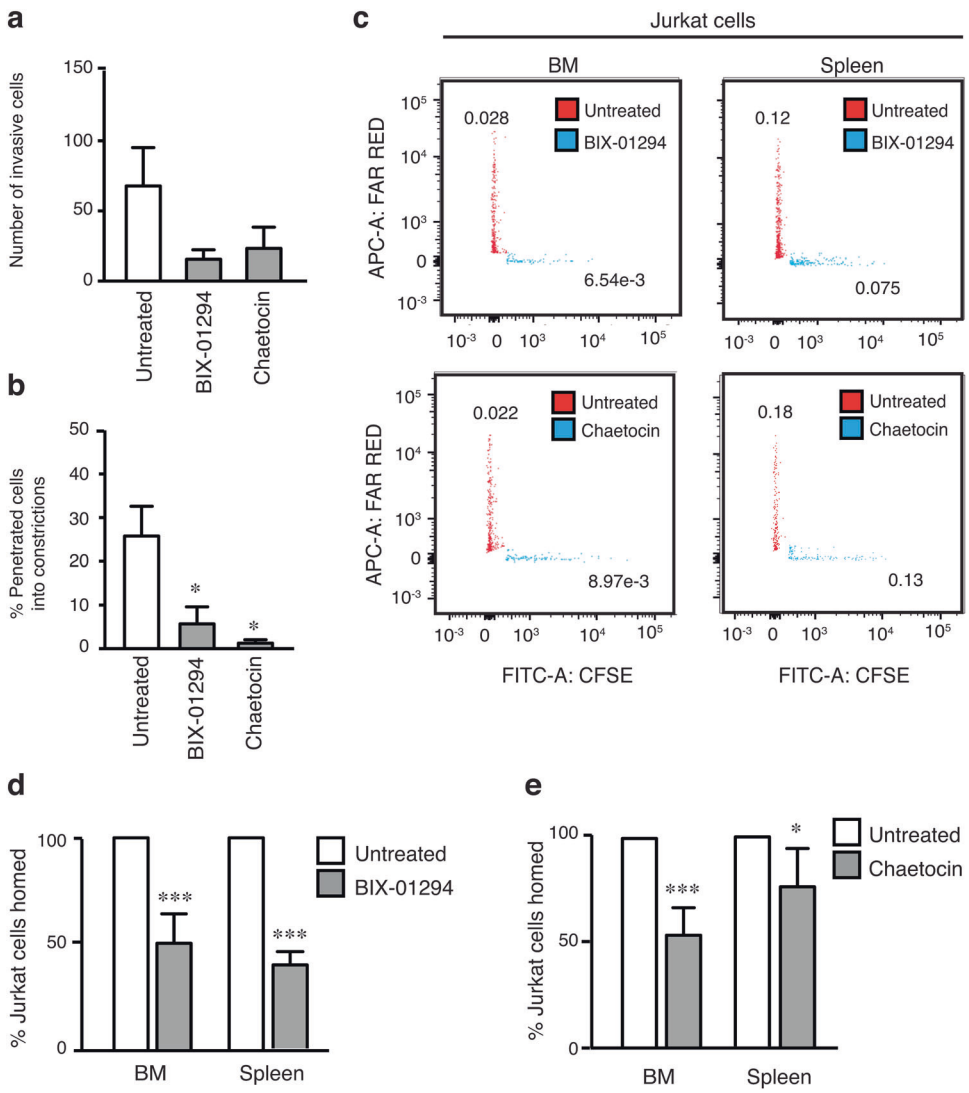

Fig. 8 H3K9 methylation regulates nuclear constrictions and T-ALL migration in vitro and in vivo systems. a Jurkat cells were pretreated or not with chaetocin (1 μM) and BIX-01294 (1 μM) for 1 h prior adding them into the microchannel chamber. Cells were allowed to enter in the microchannel upon CXCL12 stimulation for 8 h. Graph represents the total number of cells migrating into the microchannels Mean $n = 3 \pm$ SEM. **b** Graph shows the percentage of cells that effectively entered in the microchannel and crossed through constrictions. Mean $n = 3 \pm$ SEM. **c** Jurkat cells were labeled with 5 μM CFSE (for BIX-01294- or chaetocin-pretreated cells) and 1 μM Far Red Cell Tracker (untreated cells). Then, BIX-01294- or chaetocin-pretreated cells were mixed (1:1) with untreated cells, and the mixture was injected into the tail vein of NSG mice (5×10^6 cells/mouse). Five mice were used for each combination and a negative control mouse received only RPMI. After 3 h, both populations of labeled cells in the spleen and bone marrow were determined by flow cytometry. Numbers indicate the percentage of cells per sample analyzed. **d** Graphs show the percentage of untreated or BIX-01294-pretreated cells that homed into the bone marrow or spleen. Numbers were normalized according to the total number of cells/ml in that organ and the percentage of green or red cells and the number of cells/ml injected. **e** Graphs show the percentage of untreated or chaetocin-pretreated cells that homed into the bone marrow or spleen. *P*-values are indicated by asterisks (*$P < 0.05$; **$P < 0.01$; ***$P < 0.001$).

B-ALL (but not T-ALL) cells respond to decitabine (which promotes DNA demethylation) treatment [35]. Our results suggest that T- and B-ALL cells might use different migratory mechanisms to reach and colonize other tissues, and confirm that different epigenetic pathways may be lineage-specific. In agreement with cell proliferation changes induced by CXCL12, we observed that short times of CXCL12 stimulation might promote T- and B-ALL cell proliferation, although H3K9 methylation induced by CXCL12 might occur at shorter times and in response to other biomechanical or migratory stimuli.

ALL cells express several chemokine receptors, including CXCR4, which is associated with worse outcomes in pediatric patients [36]. Furthermore, it has been reported that CXCR4 promotes tumorigenicity and transcriptional changes in multiple cell types [37]. There is a correlation between ALL infiltration in vivo and the levels of CXCR4, CCR7, and ZAP70 (Zeta-chain-associated protein kinase 70) [38]. Our data provide evidence for CXCR4 as a major mediator in the H3K9 methylation induced by CXCL12. Although CXCR7 influences the signaling induced by CXCR4 [39], we did not find any significant effect blocking CXCR7 on the CXCL12-mediated H3K9 methylation. In addition, a recent study showed that the CXCR7/CXCR4 heterodimer regulates the histone demethylase JMJD2D and induces H3K9 and H3K36 demethylation [40], which aligns with our observations that the upregulation of H3K9 methylation in T-ALL cells is independent of CXCR7 signaling.

Mechanistically, PKC is a molecular pathway involved in the CXCL12 signaling of immune cells [41]. Several PKC isoforms,

including PKCζ, PKCα, and PKCβ, influence the chemotaxis and in vivo engraftment of CD34 + cells towards CXCL12 [42]. It has been reported that PMA and CXCL12 induce different migration and morphology in normal T-cells [43]. Here, we described that PMA stimulation promoted similar H3K9 methylation in T- and B-ALL cells, whilst CXCL12-stimulated H3K9 methylation only in T-ALL cells. This suggests that PKC activation might be sufficient to induce this epigenetic change in both cell types, although only T-ALL cells might activate this pathway in response to CXCL12. The BCR controls the CXCR4 internalization and signaling in B-cells that might explain the different responsiveness observed to CXCL12 stimulation in B-ALL cells [44]. Also, it has been reported that cortactin is important for CXCR4 internalization upon CXCL12 stimulation in T- but not in B-ALL cells [45]. Our findings also indicated that CXCL12-mediated H3K9 methylation was dependent on conventional PKC activity. Interestingly, CXCR7 does not regulate Ca2 mobilization [39]. This evidence could explain why conventional PKC activity and CXCR4, but not CXCR7, would be necessary to induce H3K9 methylation in T-ALL cells. It has been reported that most of these isoforms are in the cytosol of T-lymphocytes [43], we observed that PKCβ might localize in the nucleus of T-ALL cells, whilst PKCα showed more cytoplasmic localization. This aligned with previous reports showing the nuclear localization of PKC isoforms and their role on gene expression, immune cell differentiation and phosphorylating nuclear components, such as transcription factors, lamins and histones [46, 47]. PKC activity may therefore be a key element of H3K9 methylation machinery.

So far, cancer cells present altered histone modifications and other epigenetic changes, which correlate with aberrant genomic expression features according to the chromatin structure [48]. H3K9 methylation is widely involved in gene silencing and transcriptional repression [16]. The study of the transcriptome and methylome is critical to identify the progression of ALL in pediatric patients [49]. It has been reported that CXCL12 regulates LIC (leukemia initiating cell) biology in protective niches to resist conventional therapies [50, 51]. By using ChIP-seq, we observed that fast stimulation of ALL cells with CXCL12 induced an increment in the number of H3K9me3 peaks without significant correlation at a transcriptional level. This discrepancy between gene transcription and H3K9 methylation variance has been previously reported [52] and could reflect a direct effect of the chromatin on the nuclear mechanics rather than its transcriptional role at longer times or during leukemia maintenance and progression.

Physical barriers induce nuclear and chromatin changes in cancer cells [53], and increasing evidence demonstrates that the chromatin contributes to the mechanical response of the nucleus [20]. Interestingly, we observed that both T- and B-ALL cells also redistributed H3K9me3 marker at the nuclear front of migrating cells, even when B-ALL cells did not upregulate H3K9 methylation in response to CXCL12. This suggests that CXCL12 affected the chromatin compaction of T-ALL cells and, on the other hand, the chromatin distribution during constricted cell migration might occur independently of the leukemia cell type. This agrees with the idea of constricted migration causes DNA damage and affects the cell cycle of tumor cells [54]. In our study, we determined that CXCL12 promoted effective changes in the mechanical deformability response of nuclei from T-ALL cells. The role of H3K9 methylation in the invasiveness of multiple cancer cells has been previously suggested [55, 56]. Furthermore, it has been reported a link between H3K9 methylation activity and transendothelial migration of ALL cells [57]. CXCL12/CXCR4 interaction is required for the chemotaxis of T-ALL cells into the BM and disease progression in mouse models. Targeting CXCR4 with inhibitors or antagonisms, such as POL5551 and plerixafor, blocks ALL engraftment in vivo and increase the efficacy of conventional treatments [58, 59]; however, conventional treatments upregulate CXCR4 in ALL cells and treatments against CXCL12 and CXCR4 may cause side effects on other cell receptors involved in cell migration and adhesion [60]. Since H3K9 methylation regulated the cell migration and nuclear deformability of T-ALL, blockage of this process may be a promising therapy for patients. Here, we found that blocking suv39h1 and G9a activities in T-ALL cells reduced their capacity to reach the BM and the spleen. It is noteworthy that other cell receptors might regulate leukemia cell dissemination, including integrins [61], and G9a is a promising therapeutic target in blood cancers [62] and might contribute to altering the epigenetic landscape of ALL in the migration process in response to other external stimuli. Previous studies have indicated that H3K9 methyltransferase inhibitors block the growth of tumor cells in xenograft models [63–66]. Of particular note is that these studies were performed on established tumors and drug administration for longer periods rather than defining the direct role of these treatments on direct cell invasion. Our results showed that the use of H3K9 methyltransferase inhibitors might reflect a direct impact on leukemia cell migration. This aligns with previous anti-tumor effects of these inhibitors on cancer cells, such as oxidative stress and cell death and opens potential implications in a complex metastatic situation, which includes a sequence of events related to cell adhesion, migration, survival, and tumor niche engraftment. Together, we might speculate that the use of H3K9 methyltransferase inhibitors might represent a therapeutic option to block different stages of T-ALL infiltration and progression.

REFERENCES

1. Pui CH, Robison LL, Look AT. Acute lymphoblastic leukaemia. Lancet. 2008;371:1030–43.
2. Aifantis I, Raetz E, Buonamici S. Molecular pathogenesis of T-cell leukemia and lymphoma. Nat Rev Immunol. 2008;8:380–90.
3. Pui CH, Jeha S. New therapeutic strategies for the treatment of acute lymphoblastic leukaemia. Nat Rev Drug Disco. 2007;6:149–65.
4. Moser B, Loetscher P. Lymphocyte traffic control by chemokines. Nat Immunol. 2001;2:123–128.
5. Sugiyama T, Kohara H, Noda M, Nagasawa T. Maintenance of the hematopoietic stem cell pool by CXCL12-CXCR4 chemokine signaling in bone marrow stromal cell niches. Immunity. 2006;25:977–88.
6. de Lourdes Perim A, Amarante MK, Guembarovski RL, de Oliveira CE, Watanabe MA. CXCL12/CXCR4 axis in the pathogenesis of acute lymphoblastic leukemia (ALL): a possible therapeutic target. Cell Mol Life Sci. 2015;72:1715–23.
7. Pitt LA, Tikhonova AN, Hu H, Trimarchi T, King B, Gong Y, et al. CXCL12-producing vascular endothelial niches control acute T cell leukemia maintenance. Cancer Cell. 2015;27:755–68.
8. Scupoli MT, Donadelli M, Cioffi F, Rossi M, Perbellini O, Malpeli G, et al. Bone marrow stromal cells and the upregulation of interleukin-8 production in human T-cell acute lymphoblastic leukemia through the CXCL12/CXCR4 axis and the NF-kappaB and JNK/AP-1 pathways. Haematologica. 2008;93:524–32.
9. Cancilla D, Rettig MP, DiPersio JF. Targeting CXCR4 in AML and ALL. Front Oncol. 2020;10:1672.
10. Hong Z, Wei Z, Xie T, Fu L, Sun J, Zhou F, et al. Targeting chemokines for acute lymphoblastic leukemia therapy. J Hematol Oncol. 2021;14:48.
11. Rea S, Eisenhaber F, O'Carroll D, Strahl BD, Sun ZW, Schmid M. et al. Regulation of chromatin structure by site-specific histone H3 methyltransferases. Nature. 2000;406:593–9.
12. Friedl P, Wolf K, Lammerding J. Nuclear mechanics during cell migration. Curr Opin Cell Biol. 2011;23:55–64.
13. Pfeifer CR, Irianto J, Discher DE. Nuclear mechanics and cancer cell migration. Adv Exp Med Biol. 2019;1146:117–30.
14. Stephens AD, Banigan EJ, Marko JF. Chromatin's physical properties shape the nucleus and its functions. Curr Opin Cell Biol. 2019;58:76–84.
15. Schumann K, Lammermann T, Bruckner M, Legler DF, Polleux J, Spatz JP, et al. Immobilized chemokine fields and soluble chemokine gradients cooperatively shape migration patterns of dendritic cells. Immunity. 2010;32:703–13.
16. Nakayama J, Rice JC, Strahl BD, Allis CD, Grewal SI. Role of histone H3 lysine 9 methylation in epigenetic control of heterochromatin assembly. Science. 2001;292:110–3.

17. Kidiyoor GR, Li Q, Bastianello G, Bruhn C, Giovannetti I, Mohamood A, et al. ATR is essential for preservation of cell mechanics and nuclear integrity during interstitial migration. Nat Commun. 2020;11:4828.
18. Bendall LJ, Baraz R, Juarez J, Shen W, Bradstock KF. Defective p38 mitogen-activated protein kinase signaling impairs chemotaxic but not proliferative responses to stromal-derived factor-1alpha in acute lymphoblastic leukemia. Cancer Res. 2005;65:3290–8.
19. Pajerowski JD, Dahl KN, Zhong FL, Sammak PJ, Discher DE. Physical plasticity of the nucleus in stem cell differentiation. Proc Natl Acad Sci USA. 2007;104:15619–24.
20. Stephens AD, Banigan EJ, Adam SA, Goldman RD, Marko JF. Chromatin and lamin A determine two different mechanical response regimes of the cell nucleus. Mol Biol Cell. 2017;28:1984–96.
21. Le Berre M, Aubertin J, Piel M. Fine control of nuclear confinement identifies a threshold deformation leading to lamina rupture and induction of specific genes. Integr Biol (Camb). 2012;4:1406–14.
22. Jost TR, Borga C, Radaelli E, Romagnani A, Perruzza L, Omodho L, et al. Role of CXCR4-mediated bone marrow colonization in CNS infiltration by T cell acute lymphoblastic leukemia. J Leukoc Biol. 2016;99:1077–87.
23. Melo RCC, Longhini AL, Bigarella CL, Baratti MO, Traina F, Favaro P. et al. CXCR7 is highly expressed in acute lymphoblastic leukemia and potentiates CXCR4 response to CXCL12. PLoS One. 2014;9:e85926
24. Wang JF, Park IW, Groopman JE. Stromal cell-derived factor-1alpha stimulates tyrosine phosphorylation of multiple focal adhesion proteins and induces migration of hematopoietic progenitor cells: roles of phosphoinositide-3 kinase and protein kinase C. Blood. 2000;95:2505–13.
25. Lai YS, Chen JY, Tsai HJ, Chen TY, Hung WC. The SUV39H1 inhibitor chaetocin induces differentiation and shows synergistic cytotoxicity with other epigenetic drugs in acute myeloid leukemia cells. Blood. Cancer J. 2015;5:e313.
26. Lu C, Klement JD, Yang D, Albers T, Lebedyeva IO, Waller JL. et al. SUV39H1 regulates human colon carcinoma apoptosis and cell cycle to promote tumor growth. Cancer Lett. 2020;476:87–96.
27. Irianto J, Xia Y, Pfeifer CR, Greenberg RA, Discher DE. As a nucleus enters a small pore, chromatin stretches and maintains integrity, even with DNA breaks. Biophys J. 2017;112:446–9.
28. Vargas P, Terriac E, Lennon-Dumenil AM, Piel M. Study of cell migration in microfabricated channels. J Vis Exp. 2014;84:e51099.
29. Cannon JL, Oruganti SR, Vidrine DW. Molecular regulation of T-ALL cell infiltration into the CNS. Oncotarget. 2017;8:84626–7.
30. Frishman-Levy L, Izraeli S. Advances in understanding the pathogenesis of CNS acute lymphoblastic leukemia and potential for therapy. Br J Haematol. 2017;176:157–67.
31. Vadillo E, Dorantes-Acosta E, Pelayo R, Schnoor M. T cell acute lymphoblastic leukemia (T-ALL): New insights into the cellular origins and infiltration mechanisms common and unique among hematologic malignancies. Blood Rev. 2018;32:36–51.
32. Gomez AM, Martinez C, Gonzalez M, Luque A, Melen GJ, Martínez J, et al. Chemokines and relapses in childhood acute lymphoblastic leukemia: A role in migration and in resistance to antileukemic drugs. Blood Cells Mol Dis. 2015;55:220–7.
33. Bradstock KF, Makrynikola V, Bianchi A, Shen W, Hewson J, Gottlieb DJ. Effects of the chemokine stromal cell-derived factor-1 on the migration and localization of precursor-B acute lymphoblastic leukemia cells within bone marrow stromal layers. Leukemia. 2000;14:882–8.
34. Kato I, Niwa A, Heike T, Fujino H, Saito MK, Umeda K, et al. Identifcation of hepatic niche harboring human acute lymphoblastic leukemic cells via the SDF-1/CXCR4 axis. PLoS ONE. 2011;6:e27042.
35. Kuang SQ, Fang Z, Zweidler-McKay PA, Yang H, Wei Y, Gonzalez-Cervantes EA, et al. Epigenetic inactivation of Notch-Hes pathway in human B-cell acute lymphoblastic leukemia. PLoS One. 2013;8:e61807.
36. Crazzolara R, Kreczy A, Mann G, Heitger A, Eibl G, Fink FM. et al. High expression of the chemokine receptor CXCR4 predicts extramedullary organ infiltration in childhood acute lymphoblastic leukaemia. Br J Haematol. 2001;115:545–53.
37. Bao Y, Wang Z, Liu B, Lu X, Xiong Y, Shi J, et al. A feed-forward loop between nuclear translocation of CXCR4 and HIF-1alpha promotes renal cell carcinoma metastasis. Oncogene. 2019;38:881–95.
38. Alsadeq A, Fedders H, Vokuhl C, Belau NM, Zimmermann M, Wirbelauer T, et al. The role of ZAP70 kinase in acute lymphoblastic leukemia infiltration into the central nervous system. Haematologica. 2017;102:346–55.
39. Levoye A, Balabanian K, Baleux F, Bachelerie F, Lagane B. CXCR7 heterodimerizes with CXCR4 and regulates CXCL12-mediated G protein signaling. Blood. 2009;113:6085–93.
40. Song ZY, Wang F, Cui SX, Gao ZH. Qu XJ.CXCR7/CXCR4 heterodimer-induced histone demethylation: a new mechanism of colorectal tumorigenesis. Oncogene. 2019;38:1560–75.
41. Altman A, Kong KF. Protein kinase C enzymes in the hematopoietic and immune systems. Annu Rev Immunol. 2016;34:511–38.
42. Petit I, Goichberg P, Spiegel A, Peled A, Brodie C, Seger R. et al. Atypical PKC-zeta regulates SDF-1-mediated migration and development of human CD34+ progenitor cells. J Clin Invest. 2005;115:168–76.
43. Wei SY, Lin TE, Wang WL, Lee PL, Tsai MC, Chiu JJ. Protein kinase C-δ and -β coordinate flow-induced directionality and deformation of migratory human blood T-lymphocytes. J Mol Cell Biol. 2014;6:458–72.
44. Guinamard R, Signoret N, Ishiai M, Marsh M, Kurosaki T, Ravetch JV. B cell antigen receptor engagement inhibits stromal cell-derived factor (SDF)-1alpha chemotaxis and promotes protein kinase C (PKC)-induced internalization of CXCR4. J Exp Med. 1999;189:1461–6.
45. Velázquez-Avila M, Balandrán JC, Ramírez-Ramírez D, Velázquez-Avila M, Sandoval A, Felipe-López A, et al. High cortactin expression in B-cell acute lymphoblastic leukemia is associated with increased transendothelial migration and bone marrow relapse. Leukemia. 2019;33:1337–48.
46. Poli A, Ratti S, Finelli C, Mongiorgi S, Clissa C, Lonetti A, et al. Nuclear translocation of PKC-alpha is associated with cell cycle arrest and erythroid differentiation in myelodysplastic syndromes (MDSs). FASEB J. 2018;32:681–92.
47. Edens LJ, Dilsaver MR, Levy DL. PKC-mediated phosphorylation of nuclear lamins at a single serine residue regulates interphase nuclear size in Xenopus and mammalian cells. Mol Biol Cell. 2017;28:1389–99.
48. Esteller M. Epigenetics in cancer. N. Engl J Med. 2008;358:1148–59.
49. Almamun M, Levinson BT, van Swaay AC, Johnson NT, McKay SD, Arthur GL, et al. Integrated methylome and transcriptome analysis reveals novel regulatory elements in pediatric acute lymphoblastic leukemia. Epigenetics. 2015;10:882–90.
50. Konopleva MY, Jordan CT. Leukemia stem cells and microenvironment: biology and therapeutic targeting. J Clin Oncol. 2011;29:591–9.
51. Passaro D, Irigoyen M, Catherinet C, Gachet S, Da Costa C, Lasgi C, et al. CXCR4 is required for Leukemia-Initiating Cell activity in T cell acute lymphoblastic leukemia. Cancer Cell. 2015;27:769–79.
52. Nava MM, Miroshnikova YA, Biggs LC, Whitefield DB, Metge F, Boucas J, et al. Heterochromatin-driven nuclear softening protects the genome against mechanical stress-induced damage. Cell. 2020;181:800–17.
53. Makhija E, Jokhun DS, Shivashankar GV. Nuclear deformability and telomere dynamics are regulated by cell geometric constraints. Proc Natl Acad Sci USA. 2016;113:E32–40.
54. Pfeifer CR, Xia Y, Zhu K, Liu D, Irianto J, García VMM, et al. Constricted migration increases DNA damage and independently represses cell cycle. Mol Biol Cell. 2018;29:1948–62.
55. Zhang X, Cook PC, Zindy E, Williams CJ, Jowitt TA, Streuli CH, et al. Integrin alpha4beta1 controls G9a activity that regulates epigenetic changes and nuclear properties required for lymphocyte migration. Nucleic Acids Res. 2016;44:3031–44.
56. Gerlitz G, Bustin M. Efficient cell migration requires global chromatin condensation. J Cell Sci. 2010;123:2207–17.
57. Madrazo E, Ruano D, Abad L, Alonso-Gómez E, Sánchez-Valdepeñas C, González-Murillo A. et al. G9a Correlates with VLA-4 integrin and influences the migration of childhood acute lymphoblastic leukemia cells. Cancers (Basel). 2018;10:325
58. Sison EA, Magoon D, Li L, Annesley CE, Romagnoli B, Douglas GJ, et al. POL5551, a novel and potent CXCR4 antagonist, enhances sensitivity to chemotherapy in pediatric ALL. Oncotarget. 2015;6:30902–18.
59. Randhawa S, Cho BS, Ghosh D, Sivina M, Koehrer S, Müschen M, et al. Effects of pharmacological and genetic disruption of CXCR4 chemokine receptor function in B-cell acute lymphoblastic leukaemia. Br J Haematol. 2016;174:425–36.
60. Barbieri F, Bajetto A, Thellung S, Würth R, Florio T. Drug design strategies focusing on the CXCR4/CXCR7/CXCL12 pathway in leukemia and lymphoma. Expert Opin Drug Disco. 2016;11:1093–109.
61. Redondo-Muñoz J, García-Pardo A, Teixidó J. Molecular players in hematologic tumor cell trafficking. Front Immunol. 2019;10:156.
62. San José-Enériz E, Agirre X, Rabal O, Vilas-Zornoza A, Sanchez-Arias JA, Miranda E, et al. Discovery of first-in-class reversible dual small molecule inhibitors against G9a and DNMTs in hematological malignancies. Nat Commun. 2017;8:15424.
63. Dong C, Wu Y, Yao J, Wang Y, Yu Y, Rychahou PG, et al. G9a interacts with Snail and is critical for Snail-mediated E-cadherin repression in human breast cancer. J Clin Invest. 2012;122:1469–86.
64. Yokoyama M, Chiba T, Zen Y, Oshima M, Kusakabe Y, Noguchi Y, et al. Histone lysine methyltransferase G9a is a novel epigenetic target for the treatment of hepatocellular carcinoma. Oncotarget. 2017;8:21315–26.
65. Isham CR, Tibodeau JD, Jin W, Xu R, Timm MM, Bible KC. Chaetocin: a promising new antimyeloma agent with in vitro and in vivo activity mediated via imposition of oxidative stress. Blood. 2007;109:2579–88.

66. Jung HJ, Seo I, Casciello F, Jacquelin S, Lane SW, Suh SI, et al. The anticancer effect of chaetocin is enhanced by inhibition of autophagy. Cell Death Dis. 2016;7: e2098.

ACKNOWLEDGEMENTS

The authors thank the Microscopy Unit and the Flow Cytometry Core Unit of Instituto de Investigación Biosanitaria Gregorio Marañón (IiSGM) for assistance with confocal, videomicroscopy and flow cytometry analyses. The UCM-Genomic CAI Unit for their assistance with the microarray experiments. We thank Dr. Ignacio Casal, Joaquín Teixidó, Alicia García-Arroyo and María Montoya for insightful and critical comments. This research was supported by a FPI Scholarship 2018 (Ministerio de Ciencia e Innovacion/MICINN, Agencia Estatal de Investigacion/AEI y Fondo Europeo de Desarrollo Regional/FEDER) to R. G.N.; an undergraduate fellowship "Beca de Introducción a la Investigación" (Asociación Española Contra el Cáncer) to C.O.P.; and by grants from Asociación Pablo Ugarte to M.R., Gilead Sciences International Scholar in Hematology/Oncology (Gilead), 2020 Leonardo Grant for Researchers and Cultural Creators (BBVA Foundation) and SAF2017-86327-R (Ministerio de Ciencia e Innovacion/MICINN, Agencia Estatal de Investigacion/AEI y Fondo Europeo de Desarrollo Regional/FEDER) to J.R.M.

AUTHOR CONTRIBUTIONS

EM carried out biochemical and imaging experiments and contributed to the interpretation of biological data. RGN performed biochemical and in vivo studies. COP contributed to biochemical and imaging experiments. AGM provided clinically annotated multiple ALL samples and contributed to in vivo experiments and the interpretation of clinical data. MGL carried out the bioinformatics analysis of ChIP-seq and microarray data samples and contributed to the interpretation of data. MR designed part of the studies, provided ALL samples, and contributed to the interpretation of clinical data. JRM designed the studies, supervised the project, and wrote the manuscript with the input of all authors.

COMPETING INTERESTS

The authors declare no competing interests.

ADDITIONAL INFORMATION

Supplementary information The online version contains supplementary material available at https://doi.org/10.1038/s41388-021-02168-8.

Correspondence and requests for materials should be addressed to Javier Redondo-Muñoz.

Reprints and permission information is available at http://www.nature.com/reprints

Publisher's note Springer Nature remains neutral with regard to jurisdictional claims in published maps and institutional affiliations.

G9a se correlaciona con la integrina VLA-4 e influye en la migración de células de leucemia linfoblástica aguda infantil

La leucemia linfoblástica aguda (LLA) es el cáncer pediátrico más común. A medida que avanza la LLA, las células leucémicas cruzan la barrera endotelial y se infiltran en otros tejidos. Las enzimas epigenéticas representan nuevas dianas terapéuticas en las neoplasias malignas hematológicas y podrían contribuir a la capacidad de las células para migrar a través de barreras físicas. Aunque muchas moléculas impulsan este proceso, el papel del núcleo y sus componentes sigue sin estar claro. Aquí informamos, por primera vez, de que la expresión de G9a (una metiltransferasa de histonas relacionada con el silenciamiento génico) se correlaciona con la expresión de la subunidad de integrina α4 en niños con LLA. Hemos demostrado que el agotamiento de G9a o su inhibición con BIX01294 anula la capacidad de las células LLA para migrar a través de una monocapa endotelial. Además, las células tratadas con BIX01294 y silenciadas para G9a presentaron núcleos más grandes y un fenotipo más adherente que las células control en monocapas endoteliales. El bloqueo de G9a no afectó al citoesqueleto celular ni a la expresión de integrina de LLA las líneas celulares, y solo su silenciamiento redujo ligeramente la polimerización de actina F. De manera similar a la migración transendotelial, la inhibición de G9a perjudicó la migración celular inducida por la integrina VLA-4 (α4β1) de células primarias y líneas de células LLA a través de espacios estrechos *in vitro*. Nuestros resultados sugieren una conexión celular entre G9a y VLA-4, que subyace en funciones novedosas de G9a durante la migración de células LLA.

Elena Madrazo, David Ruano, Lorea Abad, Estefanía Alonso-Gómez Carmen Sánchez-Valdepeñas, África González-Murillo, Manuel Ramírez, Javier Redondo-Muñoz. Cancers (Basel). 2018 Sep 12;10(9):325. doi: 10.3390/cancers10090325.

cancers

MDPI

Article

G9a Correlates with VLA-4 Integrin and Influences the Migration of Childhood Acute Lymphoblastic Leukemia Cells

Elena Madrazo [1], David Ruano [2], Lorea Abad [2], Estefanía Alonso-Gómez [1], Carmen Sánchez-Valdepeñas [2], África González-Murillo [3,4], Manuel Ramírez [2,4] and Javier Redondo-Muñoz [1,5,*]

1 Department of Immunology, Hospital 12 de Octubre Health Research Institute (imas12), School of Medicine, Complutense University, 28040 Madrid, Spain; emadrazo@ucm.es (E.M.); e.alonso.gmz@gmail.com (E.A.-G.)
2 Department of Pediatric Hematology & Oncology, Hospital Universitario Niño Jesús, 28009 Madrid, Spain; druano64@hotmail.com (D.R.); lorea.abad@salud.madrid.org (L.A.); carmen.sanchez.val@gmail.com (C.S.-V.); manuel.ramirez@salud.madrid.org (M.R.)
3 Oncolohematology Unit, Hospital Universitario Niño Jesús, 28009 Madrid, Spain; africa.gonzalez@salud.madrid.org
4 Health Research Institute La Princesa, 28006 Madrid, Spain
5 Lydia Becker Institute of Immunology and Inflammation, Manchester Collaborative Centre for Inflammation Research, University of Manchester, Manchester M13 9PL, UK
* Correspondence: javredon@ucm.es; Tel.: +34-91394-1385

Received: 2 August 2018; Accepted: 11 September 2018; Published: 12 September 2018

Abstract: Acute lymphoblastic leukemia (ALL) is the most common pediatric cancer. As ALL progresses, leukemic cells cross the endothelial barrier and infiltrate other tissues. Epigenetic enzymes represent novel therapeutic targets in hematological malignancies, and might contribute to cells' capacity to migrate across physical barriers. Although many molecules drive this process, the role of the nucleus and its components remain unclear. We report here, for the first time, that the expression of G9a (a histone methyltransferase related with gene silencing) correlates with the expression of the integrin subunit α4 in children with ALL. We have demonstrated that G9a depletion or its inhibition with BIX01294 abrogated the ability of ALL cells to migrate through an endothelial monolayer. Moreover, G9a-depleted and BIX01294-treated cells presented bigger nuclei and more adherent phenotype than control cells on endothelial monolayers. Blocking G9a did not affect the cell cytoskeleton or integrin expression of ALL cell lines, and only its depletion reduced slightly F-actin polymerization. Similarly to the transendothelial migration, G9a inhibition impaired the cell migration induced by the integrin VLA-4 (α4β1) of primary cells and ALL cell lines through narrow spaces in vitro. Our results suggest a cellular connection between G9a and VLA-4, which underlies novel functions of G9a during ALL cell migration.

Keywords: VLA-4; G9a; acute lymphoblastic leukemia; epigenetics; migration

1. Introduction

Acute lymphoblastic leukemia (ALL), the most common cancer in children, is characterized by the accumulation of hematopoietic B- or T-cell precursors, which eventually infiltrate the bone marrow or thymus and secondary organs, resulting in leukemia progression [1,2]. ALL patients are stratified according to multiple subtypes defined by genetic abnormalities, such as chromosomal translocations, chromosomal deletions, amplifications, fusions, etc. [3]. Risk-tailored therapy protocols can cure most children with ALL but non-responding and relapsed pediatric ALL patients (20% of total) have poor

prognosis and are the leading cause of cancer mortality at that age [4]. Most relapses occur in patients with no identifiable genetic alterations, i.e., the intermediate risk group [5]. ALL cells present specific genetic and epigenetic changes, which open new avenues to stratify patients and develop more effective therapies [6,7]. It has been reported that the methylation of specific histones is linked to cancer cell invasion [8,9]. One of these enzymes, the histone methyltransferase G9a catalyzes H3K9 methylation (a heterochromatin marker) [10], and is critical in lymphocyte development and leukemogenesis [11]; and its inhibition promotes apoptosis in acute leukemias [12]. The integrin α4β1 (CD49d/CD29, very late antigen-4, VLA-4) is a cell receptor that binds fibronectin, VCAM-1, osteopontin and other protein such as MMPs [13–15]. The expression of VLA-4 in pediatric ALL patients is associated with poor outcome and relapse-free survival (RFS) probabilities [16]. VLA-4 adhesion promotes G9a activity and H3K9 methylation during Jurkat (a T-ALL cell line) and normal lymphocyte cell migration [17]; however, the interplay between VLA-4 and G9a, and how they contribute to ALL dissemination, has not been described before.

The function and molecular connections of G9a during ALL cell migration are not known. These are important issues since G9a might represent a therapeutic target in ALL. We described a correlation between the gene expression of G9a and the α4 subunit of VLA-4 in samples from patients with ALL but not in healthy donors. Furthermore, G9a activity is critical during ALL transendothelial migration and ALL migration in response to VLA-4 adhesion. Together, our findings describe, for the first time, that G9a might play a direct role on ALL cell migration.

2. Results

2.1. Patient Characteristics

We studied samples from 50 children patients (age 1–14 years old) with a diagnosis of ALL, including patients carrying any genomic translocation and other bioclinical parameters. Major karyotypic and clinical characteristics, including sex, risk stratification, WBC (white blood cell) count, blasts in BM (bone marrow) and MRD (minimal residual disease) after induction are summarized in Table 1.

Table 1. Clinical and biological characteristics of the studied ALL patients.

Variable	Characteristics	Number of Cases	Percentage (%)
Gender	Male	27	54
	Female	23	46
Risk group	1 (LR [1])	11	22
	2 (IR [1])	32	64
	3 (HR [1])	7	14
WBC [1] (>50,000 cells/mm^3)	Positive	6	12
	Negative	44	88
MRD [1] after induction	Positive	22	44
	Negative	28	56
Extramedullary disease	Positive	22	44
	Negative	28	56
Blast in BM [1]	Positive	25	50
	Negative	25	50
ETV6/RUNX1	Positive	15	30
	Negative	32	64
	ND [1]	3	6

Table 1. *Cont.*

Variable	Characteristics	Number of Cases	Percentage (%)
BCR/ABL	Positive	2	4
	Negative	47	94
	ND [1]	1	2
MLL rearrangements	Positive	2	4
	Negative	47	94
	ND [1]	1	2
Hyperdiploidy	Positive	13	26
	Negative	36	72
	ND [1]	1	2
Relapse	Positive	7	14
	Negative	41	82
	ND [1]	2	4
Death	Positive	6	12
	Negative	43	86
	ND [1]	1	2

[1] Abbreviations: ALL, acute lymphoblastic leukemia; BCR, breakpoint cluster region; ABL, Abelson; MLL, mixed-lineage leukemia; LR, low risk; IR, intermediate risk; HR, high risk; WBC, white blood cells count at diagnosis; MRD, minimal residual disease after induction; BM, bone marrow; ND Not determined.

2.2. The Expression of G9a Correlates with α4 Integrin Expression in ALL Cells

The histone H3 is methylated by several enzymes from suv39h family, including Suv39h1 and G9a [18]. To elucidate the expression pattern of both histone H3K9 methyltransferases in childhood ALL, samples from pediatric patients with primary ALL and 10 samples from healthy donors were determined by using RT-qPCR. ITGA-4 (the integrin subunit α4), G9a and Suv39h1 expression was detected in all of the samples analyzed. We observed a significant Pearson correlation between ITGA-4 and G9a levels (p = 0.0206) but not with Suv39h1 (p = 0.1524) (Figure 1a and Figure S1a). Moreover, we did not find any correlation between G9a and ITGA-4 in a small cohort of healthy donors (Figure S1b). To further analyze the expression level of G9a according to the clinical risk grade groups, all patients were divided into three subgroups (1-low; 2-intermediate; and 3-high risk). We confirmed a tendency for high ITGA-4 expression levels to associate with high-risk group (Figure 1b). Interestingly, we found that G9a expression exhibited an opposite trend to ITGA-4 with clinical risk grade in ALL cells (Figure 1c). By determining the correlation between ITGA-4 and G9a levels within the different risk groups, we observed that intermediate-risk group presented a significant correlation between G9a and VLA-4 expression (Figure 1d). We stratified the patients according to their G9a expression into lower (LE) or higher (HE) than the median (Median = 0.6001) groups, confirming that the low-risk group showed more patients with HE of G9a whilst the high-risk group presented the opposite tendency (Table 2). Our results suggest that G9a and ITGA-4 levels present an opposite trend according to the different risk groups and may act jointly in children with an intermediate stage of ALL.

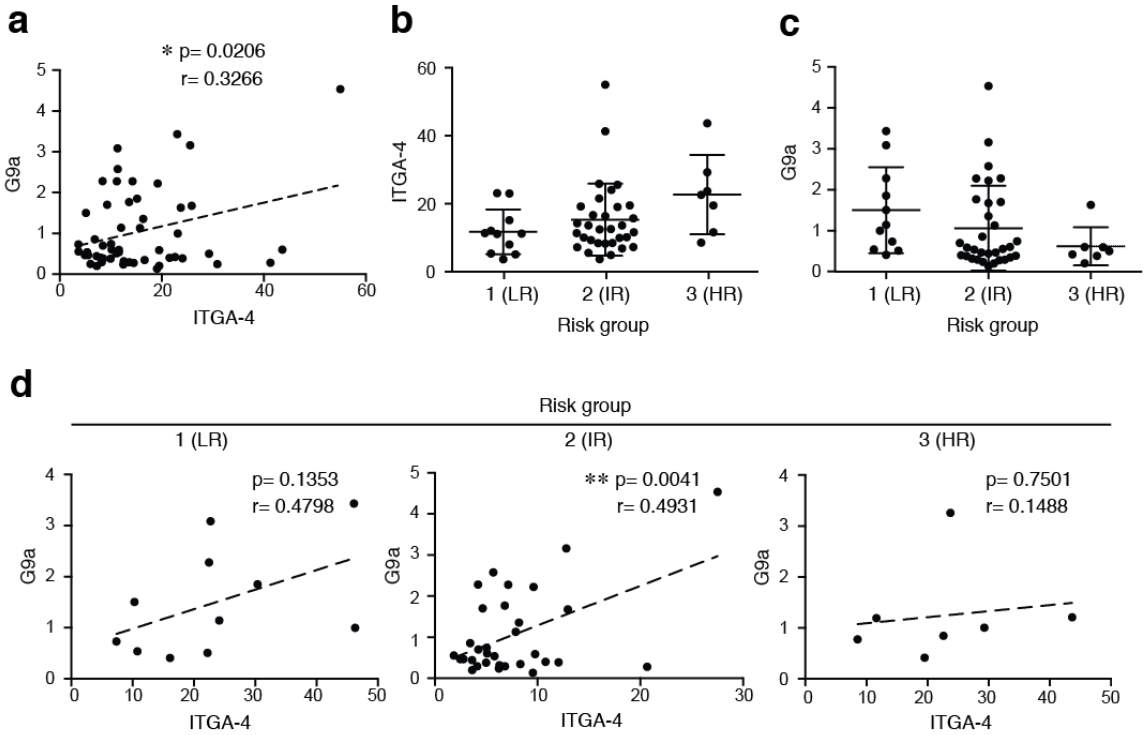

Figure 1. Expression and correlation of ITGA-4 and G9a in children patients of ALL. (**a**) ITGA-4 and G9a expression analyzed by RT-qPCR. Expression levels were normalized by TBP and graph shows the mean of children ALL patients ($n = 50$). Pearson's correlation coefficient (r) and p-value between ITGA-4 and G9a are shown. * $p < 0.05$; (**b**,**c**) Patients were divided according to their risk groups (LR, low risk; IR, intermediate risk; HR, high risk) and ITGA-4 (**b**) and G9a (**c**) expression analyzed; (**d**) Patients were divided as in (**b**) and Pearson's correlation coefficient (r) and p-value between VLA-4 and G9a are shown. ** $p < 0.01$.

Table 2. G9a expression according to risk group.

Risk Group	G9a LE [1]	G9a HE [1]	Percentage (%)
1	3	8	27.3/72.7
2	17	15	53.1/46.9
3	5	2	71.4/28.6

[1] Abbreviations: LE, low expression (lower than the median); HE, high expression (higher than the median).

2.3. G9a Depletion Abrogates ALL Transendothelial Migration

Dissemination of ALL cells requires the extravasation of leukemia cells from the blood vessels across the endothelial barrier in a process known as transendothelial migration (TEM) [19]. To analyze the role of G9a in a more physiological context, we determined the cell capacity of two G9a depleted cell lines to cross a monolayer of human umbilical vein endothelial cells (HUVEC). HUVEC cells were stained with CFSE (which do not interfere with the TEM process) and the integrity of the monolayer was confirmed by staining for Zo-1, an endothelial cell-cell junctions marker. Firstly, we verified that control or G9a depleted cells were able to attach onto HUVEC cell monolayer (Figure 2a). We used the specific G9a inhibitor BIX01294, to block G9a activity for 1 h and 48 h, with no effects on cell attachment onto HUVEC cells (Figure S2a). By analyzing the nuclear shape of ALL cells onto HUVEC cells, we determined that G9a depletion or inhibition promoted a significant increment of the nuclear area of ALL cells (Figure 2b–d and Figure S2b).

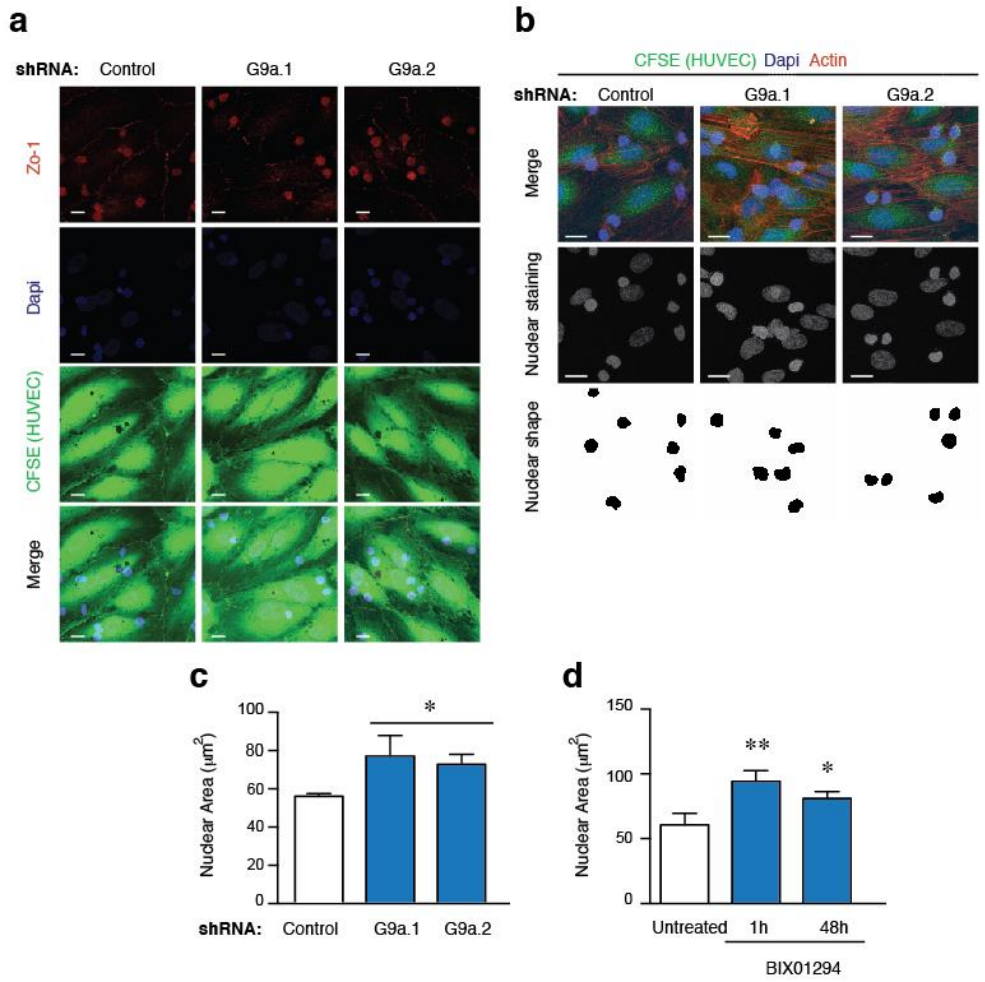

Figure 2. G9a depletion increases the nuclear area of ALL cells. (**a**) HUVEC cells were grown to confluency, labelled with CFSE and stimulated with TNFα for 16 h. Control or G9a depleted Jurkat cells were plated on TNFα-activated HUVEC cells. Cells were fixed, permeabilized and analyzed to visualized their nuclei (DAPI, blue), F-actin (Phalloidin, cyan), and endothelial junctions (Zo-1, red); (**b**) Control and G9a depleted Jurkat cells were cultured on CFSE labelled HUVEC activated with TNFα, fixed and stained for DAPI (blue) and F-actin (red). Nuclear shapes were determined; (**c**) Graph shows the nuclear areas quantified from (**b**); Mean $n = 3$ replicates ± SD. Bar = 10 μm. * $p < 0.05$; (**d**) Graph shows the nuclear areas from untreated or BIX10924 treated Jurkat at cells cultured on TNFα-activated HUVEC. Mean $n = 3$ replicates ± SD. * $p < 0.05$; ** $p < 0.01$.

We next investigated the contribution of G9a expression to ALL migration across HUVEC cells. Firstly, we confirmed by time-lapse that control cells were able to pass through the endothelial barrier (Video 1–3 in supplementary material) whilst G9a depleted cells remained crawling and extending multiple protrusions (Video 4 and 5 in supplementary material and Figure 3a). Interestingly, tracking of G9a depleted cells showed that they moved by crawling on endothelial monolayer more than control cells (Figure 3b). We confirmed that control cells showed higher levels of H3K9me2/3 staining compared to G9a depleted cells attached to HUVEC (Figure 3c). Then, we defined the position and migration of control or G9a depleted cells relative to the endothelial cell monolayer and quantified the number of cells crawling or showing paracellular (through cell-cell junctions) or transcellular (inducing an invagination in a single HUVEC cell) TEM. We found that control Jurkat cells used transcellular and paracellular TEM routes; however, G9a depletion reduced significantly the number of cells undergoing both TEM types and increased the number of crawling cells (Figure 3c,d). Furthermore, by using BIX01294 we determined that blocking G9a for 1 h and 48 h also presented a significant increment

in the number of crawling cells (Figure S3a,b). Together, these results indicate that G9a controls the ability of ALL to cross the endothelial barrier and extravasate into tissues.

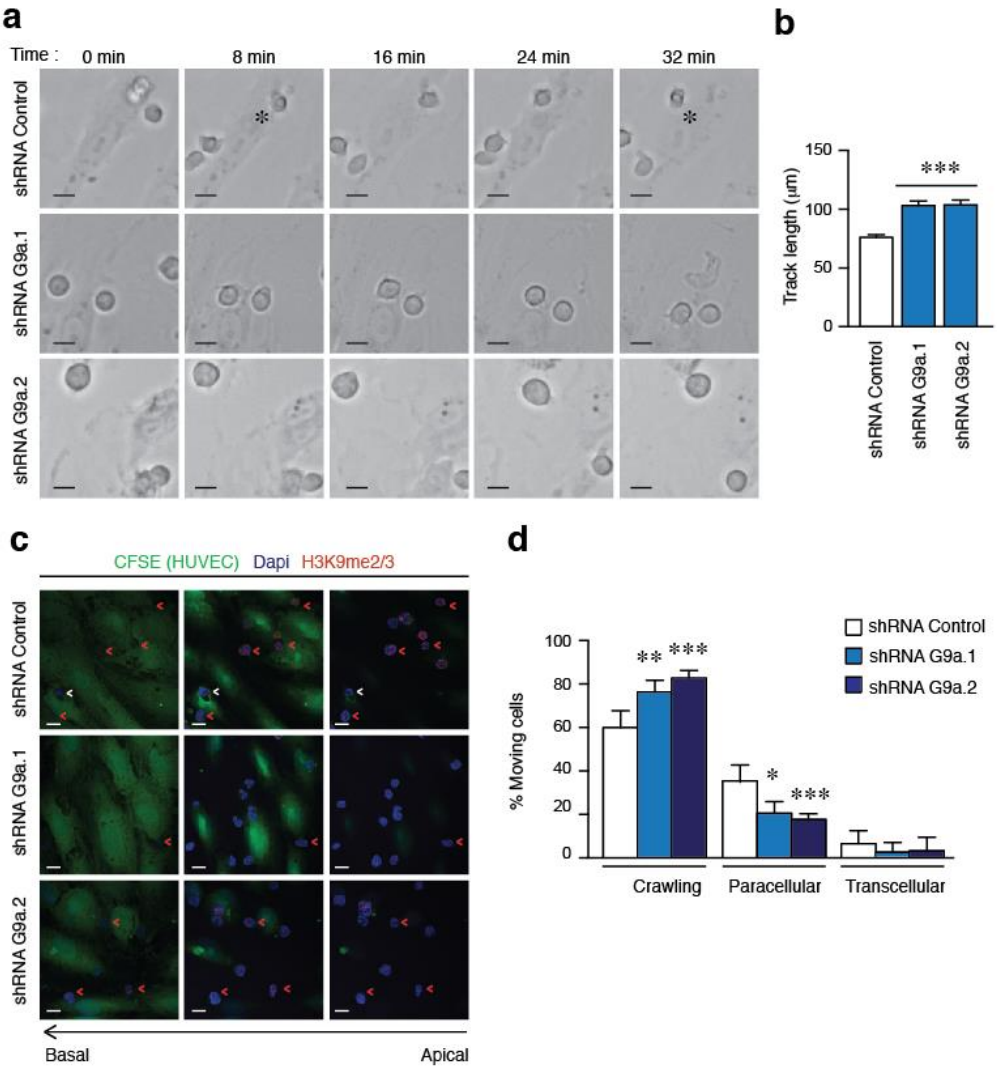

Figure 3. G9a depletion abrogates the TEM of ALL cells. (**a**) Representative images of control or G9a depleted Jurkat cells migrating on TNFα-activated HUVEC cells. Cells were tracked through time. Asterisk indicates a transmigrating cell. Bar = 10 μm (**b**) Control or G9a depleted Jurkat cells were labelled with CFSE to track their movement on TNFα-activated HUVEC monolayer. Graph shows the quantification of track lengths. Mean $n = 200$ cells ± SEM. *** $p < 0.001$; (**c**) Control or G9a depleted Jurkat cells were plated on TNFα-activated HUVEC cells labelled with CFSE. After 30 min, cells were fixed, permeabilized and analyzed to visualize their nuclei (blue), F-actin (cyan), and H3K9me2/3 (red). White arrows indicate cells undergoing transcellular TEM. Red arrows indicate cells crossing through cell-cell junctions in paracellular TEM; (**d**) Graph shows the percentage of control or G9a depleted cells crawling or performing TEM. Mean $n = 5$ ± SD. Bar = 10 μm. * $p < 0.05$; ** $p < 0.01$; *** $p < 0.001$.

2.4. G9a Activity Does Not Affect Integrin Expression and Only Partially the Actin Polymerization in ALL Cells

We have previously shown that VLA-4 adhesion does not mediate G9a upregulation [17], however the effect of G9a inhibition on VLA-4 is currently unknown. We treated B- and T-ALL cell lines with BIX01294 for 1 h and then analyzed the expression of the integrin subunit α4. We detected variable expression levels of the integrin subunits without any down-regulation of these upon G9a inhibition compared with control cells (Figure 4a). Furthermore, by using a previously validated stable G9a depleted Jurkat cell line shRNA construct we only detected a slight reduction of the

levels of α4 and β1 in G9a depleted Jurkat cells compared to control cells (Figure 4b). It has been described that G9a depletion does not affect cell adhesion [17]; however, we sought to examine the effect of G9a on F-actin polymerization. Remarkably, G9a inhibition did not diminished the levels of F-actin in any ALL cell lines (Figure 4c), whilst G9a depleted cells presented a reduction in the internal levels of polymerized actin (Figure 4d). Then, we analyzed the cellular morphology of G9a depleted cells cultured on VCAM-1. ERM (ezrin/radixin/moesin) proteins localizes at the rear pole of migrating lymphocytes [20]. Remarkably, control cells were able to polarize and present long trailing edge (stained for p-ERM) while G9a depletion promoted more rounded morphologies (Figure 4e,f). Moreover, G9a inhibition also affected the cellular morphology promoting more rounded forms (Figure S4a,b). Together, these results suggest that G9a targeting was not directly involved in integrin expression although it might be functionally relevant for ALL morphology and migration.

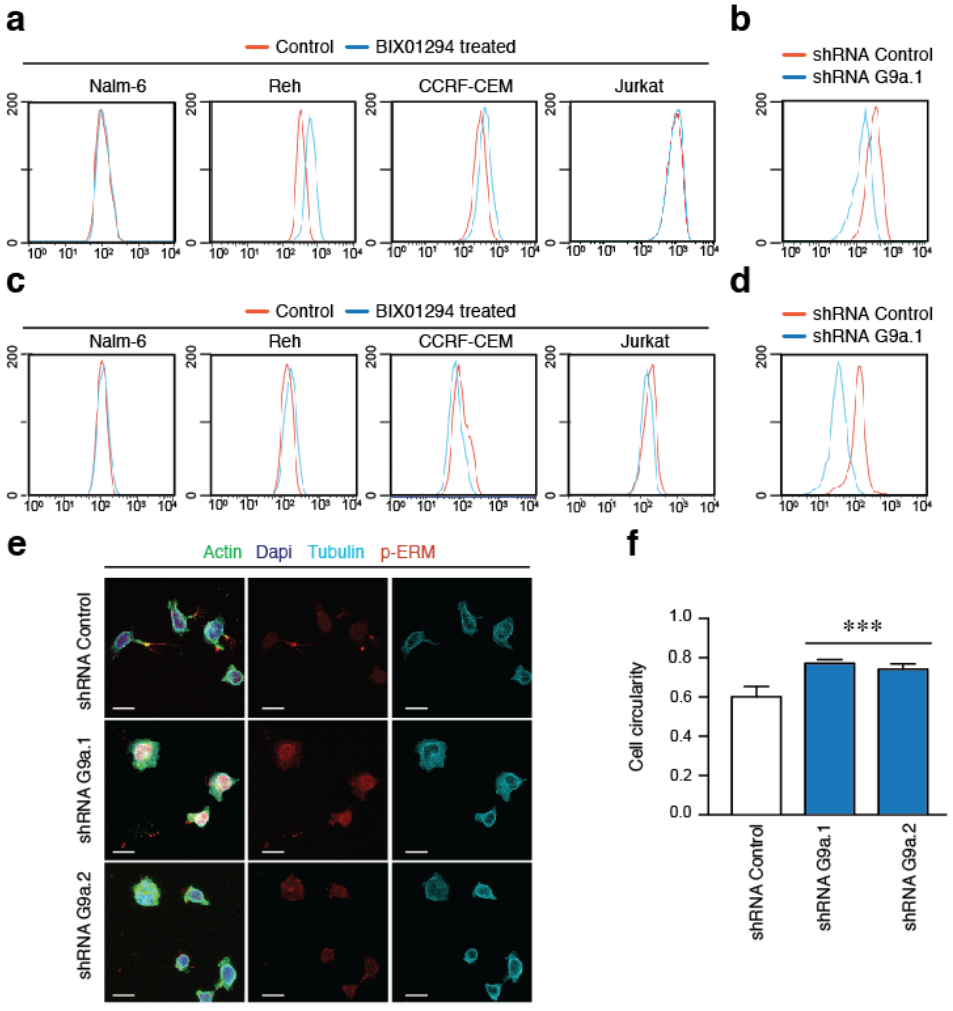

Figure 4. G9a does not affect integrin expression although might regulate cell morphology. (**a**) B- (Nalm-6 and Reh) and T- (Jurkat and CCRF-CEM) ALL cell lines were incubated with BIX01294 for 1h. Then, the expression of α4 subunits was determined by flow cytometry. Grey area represents untreated cells and green line BIX01294 treated cells; (**b**) The expression of the integrin subunit α4 was determined in control or G9a depleted Jurkat cells. Grey area represents control and green line G9a depleted cells; (**c**) B- and T-ALL cells lines were treated with BIX01294 for 1 h. Then, cells were fixed, permeabilized and their F-actin levels quantified by phalloidin staining; (**d**) Control and G9a depleted cells were processed as in (**c**) to quantified the levels of F-actin; (**e**) Control or G9a depleted Jurkat cells were cultured on VCAM1 (2 μg/mL) for 20 min. Cells were fixed and stained for tubulin (cyan) and trailing edge (phospho-ERM) marker; (**f**) Graph shows the rounded shape (circularity) of control or depleted cells for G9a in (**e**); Mean $n = 3$ replicates ± SD. Bar = 10 μm. *** $p < 0.001$.

2.5. G9a Activity Modulates VLA-4-Mediated ALL Cell Migration

HUVEC cells express many molecules that contribute to TEM of normal and leukemic cells [21]. To discriminate how G9a is functionally involved in the VLA-4-mediated migration of ALL cells, we compared the ability of primary samples and ALL cell lines to cross through 3 μm pore transwells. All the ALL cell lines migrated robustly in response to serum, and this migration was enhanced when the transwell was previously coated with the ligand of VLA-4, VCAM-1. We confirmed the effect of G9a inhibition with BIX01294 in diminishing the migration induced by VLA-4 adhesion (Figure 5a–d). Likewise, when we studied migration of primary samples upon VLA-4 adhesion, we observed a significant increment in the migration index when cells attached to VCAM-1 (Figure 5e). Consistent with ALL cell lines, primary ALL cells treated with BIX01294 also reduced significantly the migration induced by VLA-4 adhesion (Figure 5e). Together, these results indicate that G9a activity is required during ALL cell movement.

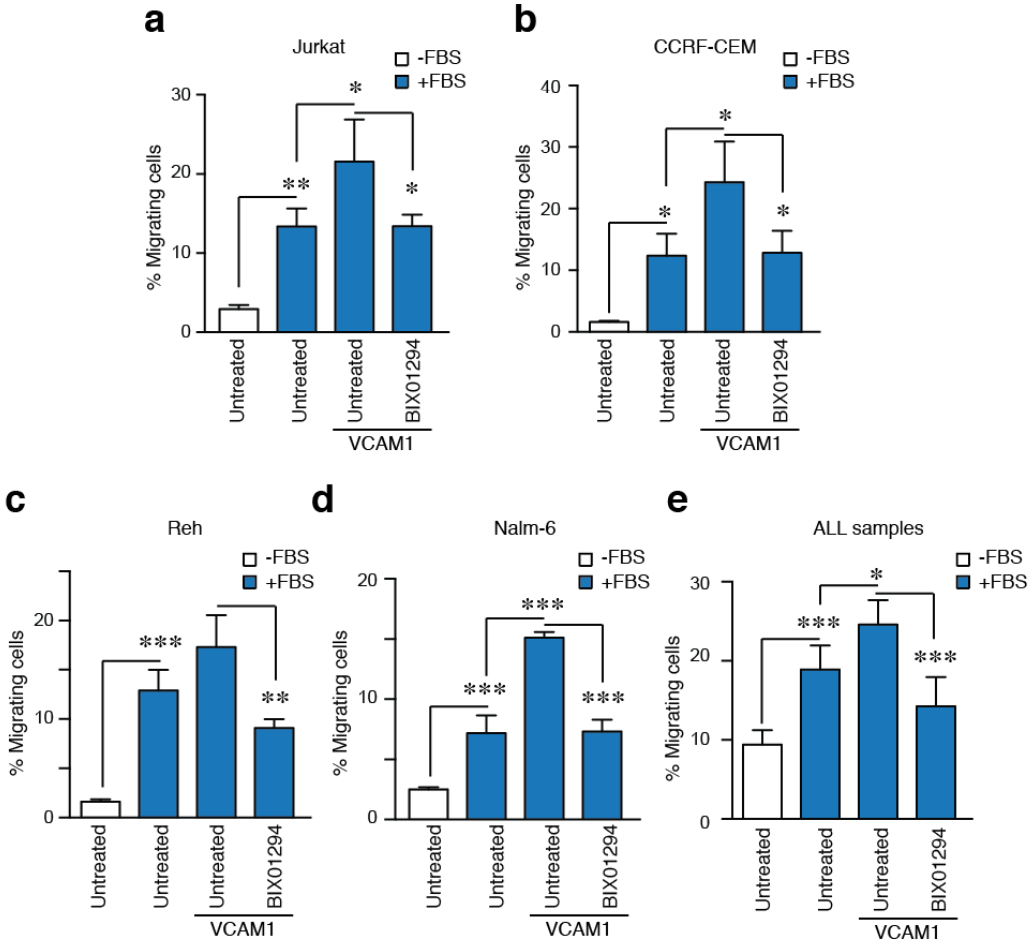

Figure 5. G9a inhibition impairs ALL cell squeezing induced by VLA-4 adhesion. (**a**) Jurkat; (**b**) CCRF-CEM; (**c**) Reh; (**d**) Nalm-6; and (**e**) primary samples from ALL patients were plated on upper chambers of Transwells of 3 μm of pore size. In some cases, the filter was previously coated with VCAM-1 (10 μg/mL). Serum was added at the bottom chamber to promote cell migration for 3 h. Then, cells were collected from the bottom chamber, stained and quantified. Mean $n = 3 \pm$ SD (for **a**–**d**) and Mean $n = 5 \pm$ SD (for **e**). * $p < 0.05$; ** $p < 0.01$; *** $p < 0.001$.

3. Discussion

Cell trafficking into other tissues is critical during ALL dissemination, as the infiltration of leukemic cells into specific reservoirs, such as the CNS or testis, protects ALL cells from conventional therapies and promotes relapses in patients [22,23]. In this study, we have defined, for the first time

the interplay between the integrin VLA-4 and the histone methyltransferase G9a in ALL cell migration. Overall, we aimed to gain more insight into the clinical relevance of G9a during the migration of leukemic cells of children with ALL.

Current advances suggest a therapeutic role of epigenetic enzymes, such as DNA methyltransferases and histone deacetylases, with promising results for leukemia patients [6,24]. For instance, it has been suggested that the inhibition of the histone H3K27 demethylase UTX shows promising antitumor effects in T-ALL, while the activity of H3K27 methyltransferase EZH2 acts as tumor suppressor in ALL mouse models [25,26]. Other critical enzymes involved in tumor progression are the H3K9 methyltransferases. Suv39h1 activity controls cell migration in breast and colorectal carcinoma cells [27], while the depletion of suv39h2 induces apoptosis and cell death in ALL cells [28]. G9a is a histone methyltransferase overexpressed in multiple cancers and clear functions during lymphocyte development [11]. Recently, it has been published how G9a inhibition impairs cell cancer division and promotes cell death by inducing interferon-mediated genes and immunogenic response in several hematological malignancies, including AML and ALL [29]. In a complementary study, BIX01294 treatment upregulates p21 and pro-apoptotic members of Bcl-2 family [12]. Although these findings highlight the anti-tumor characteristics of G9a inhibitors, we now show in the present study that G9a inhibition might be relevant in ALL treatment not only by priming ALL for death, but also inhibiting the ability of leukemia cells to infiltrate other tissues.

The expression of VLA-4 is controversial in acute leukemias. In AML patients VLA-4 is a favorable marker associated with better prognosis [30]. In contrast, its expression is associated with poor prognosis in children, but not in adult, ALL patients [16,31]. Although the small number of healthy donors limits any conclusion about whether in normal lymphocytes G9a correlates or not with VLA-4, our results confirm a positive correlation between VLA-4 and G9a. In contrast to VLA-4, G9a expression presents an opposite trend with the clinical risk grade of patients, and when we stratified the patients according to their clinical risk, only the intermediate risk group presents a positive correlation between both molecules. In support of this, others have previously shown that basal levels of G9a or H3K9 methylation do not correlate with the tumor progression [29], although G9a targeting clearly might be relevant in the clinic. Our present results extend these previous findings, confirming that probably the functional connections between the integrin and G9a are more relevant in ALL than the expression of both molecules. H3K9 demethylases LSD1 and JMJD1A are related to tumor progression and metastasis in several cancer types, including colorectal and leukemias [32,33], as the balance between methylases and demethylases are critical for epigenetic changes, exploring these enzymes as potential therapeutic targets will have clinical interest in the future.

Our results also show that blocking the expression of G9a also resulted in a reduction of TEM in ALL cells. TEM of normal and leukemic cells involves several adhesive molecules, including selectins, ICAM-1, VCAM-1, PECAM-1 and others [21]. The functions of VLA-4 are central for the dissemination and drug resistance in ALL cells, and VLA-4 inhibition with blocking antibodies (Natalizumab) or small molecules (TBC3486) sensitizes leukemic cells to conventional therapies and improves survival in vivo models [34,35]. Recently, it has been shown that targeting VLA-4 with antisense drugs fails to improve survival in mouse model of ALL [36], supporting the idea that blocking the integrin and its molecular pathways has to continue being improved. Several molecules, such as myosin IIA, RhoA and Rap1b, translate integrins signals into cytoskeletal changes affecting the cell capacity to squeeze through HUVEC cells [37,38]. Also, other factors, such as MIP-β, contribute to the ability of the cells to cross the endothelial barrier [39]. Unlike these previous studies focusing on intracellular pathways, we show here that G9a, a nuclear component, could affect the nuclear morphology and migration of ALL cells onto a HUVEC monolayer.

The cell cytoskeleton and nuclear components are critical for nuclear deformability and cancer cell migration [40–42]. Moreover, integrins control the nuclear changes by translating external stimuli into the nucleus [43]. The effect of G9a inhibition on cell migration can be mediated by changes at gene transcription, nuclear deformability and intracellular signal levels. It has been previously demonstrated

that G9a regulates several cell receptors, including integrins [44,45]. Although we have seen changes in cell morphology, they did not correspond to integrin expression changes or F-actin polymerization. The role of the nucleus during cell migration might be evaluated by forcing lymphocytes to move across pores sizes that require high nuclear deformability [42]. Our data clearly establish that G9a function was critical for ALL cell migration through narrow spaces across primary samples from patients and cell lines. We hypothesize that G9-mediated alterations of the chromatin structure may impair cell migration by affecting the physical properties of the nucleus and its connections with the cytoskeleton. The actin cytoskeleton is critical for cancer cell migration [46], and how its interactions with the nucleus regulate the nuclear deformability and transendothelial migration [47,48]. In agreement with this, it has been suggested that nuclear lobes and their cytoskeletal connections control the nuclear deformability of migrating neutrophils and lymphocytes [49]. Therefore, G9a induced mechanisms would be attractive for targeting leukemia dissemination and further pre-clinical evaluation of G9a inhibitors.

In summary, our results demonstrate novel cellular and functional connections between G9a and the ALL cell capacity to infiltrate in response to microenvironmental signals. Our observations indicate that targeting G9a clearly affects ALL cell migration, which might contribute to leukemia infiltration and dissemination through the patient's body. In this context, studying the pathological relevance of G9a in ALL cell migration would be interesting to determine new therapeutic options in this leukemia.

4. Materials and Methods

4.1. Patients and Samples

A total of 50 ALL patients under 14 years old were retrospectively included in this study. ALL diagnosis and treatment was defined according to SEHOP-Pethema 2013 (Spanish Program for the Treatment of Hematologic Diseases). Primary human PBL were isolated from buffy coats of healthy anonymous donors (Blood Bank, Hospital Gregorio Marañón) after depletion of the monocyte fraction with CD14 microbeads. All guardians gave written informed consent. Patients were tested with conventional karyotyping and molecular studies using standard procedures. The total cohort of the study (n = 50) included seven relapses and six deaths. Patient characteristics are provided in Table 1.

4.2. Ethics Approval and Consent to Participate

Samples were obtained with informed consent for research purposes, and the procedures were approved by the Institutional Review Boards of the Hospital General Universitario Gregorio Marañón (Epicon) and the Hospital Universitario Niño Jesús (R0070/15).

4.3. Cell Lines

The B- and T-ALL cell lines Jurkat, CCRF-CEM, Nalm6 and REH were obtained from Dr. Ramírez and cultured in RPMI 1640 with L-glutamine and 125 mM Hepes (Sigma Aldrich, St. Louis, MO, USA) with 10% fetal bovine serum (FBS, Sigma-Aldrich). HUVEC cells were obtained from Prof. Martin Humphries (The University of Manchester, Manchester, UK) and cultured in EBM-2 Endothelial Growth Basal Medium (Lonza, Walkersville, MD, USA). HUVECs were used up to the third passage. All cells were maintained in 5% CO_2 at 37 °C.

4.4. Reagents and Antibodies

The mouse antibody anti-H3K9me2/3 (#5327), and the rabbit antibody -phospho-ERM (#3726) were from Cell Signaling (Danvers, MA, USA). The mouse antibody anti-β-tubulin (#T5201) was from Sigma-Aldrich. The antibody anti-α4 (HP2/1) was a gift from Prof. Sánchez-Madrid (Hospital de la Princesa, Universidad Autónoma de Madrid). The anti-ZO-1 antibody was from SantaCruz (Santa Cruz, CA, USA) (#sc-33725). Tetramethylrhodamine (TRITC)-Phalloidin, Alexa 647-Phalloidin,

CellTrace™ CFSE, secondary antibodies Alexa-488, -594, -647 for immunofluorescence analysis and DAPI were obtained from Thermo Scientific (Waltham, MA, USA). VCAM1 was obtained from Peprotech. BIX01294 was from Abcam (Cambridge, UK).

4.5. RT- Real-Time PCR (qPCR)

Total RNA was extracted using the RNeasy kit (Qiagen, Valencia, CA, USA), and cDNA was synthesized from 1.0 µg of total RNA using SuperScript II First-Strand Synthesis System and oligo(dT) from Invitrogen (Thermo Scientific, Waltham, MA, USA). cDNA concentrations were quantified using a NanoDrop ND-1000 Spectrophotometer (Fisher Scientific, Pittsburgh, PA, USA). Oligonucleotides for selected genes were designed according to the Roche software (Universal Human Probe Roche Library, see supplementary material Table S1). Quantitative real-time PCR (qRT-PCR) was performed on a Roche LightCycler® 480 following the manufacturer's instructions. Assays were made in triplicates and results normalized according to the expression levels of TBP (Roche Real Time Ready Single Assay ID 101145). Melt curve analysis was performed at the end of PCR to confirm the presence of a single, specific product. The results were expressed using the $\Delta\Delta C_t$ method for quantification.

4.6. Production of Lentivirus

G9a was depleted with two different short hairpin RNA sequences. The previously reported shRNA G9a.1 [15] and G9a.2: (5′-GGACCTTCATCTGCGAGTATG-3′), which was purchased from Sigma-Aldrich and inserted in the pVenus lentiviral transfer vector (pVLVTHM). The recombinant lentiviruses were generated by transient transfection of 293T cells using Pei according to manufacturer's protocol. Briefly, subconfluent HEK293T cells were co-transfected with the pVLVTHM vector and the packaging vectors pPsPax2, pMD2G. After 24 h, the medium was replaced with fresh medium 10 mM sodium butyrate and media changed after 6 h. 48 h later virus containing supernatants were harvested and filtered through 0.45 µm pore-sized membranes. Infection was performed by adding the lentiviral containing media to Jurkat cells at 1×10^6 cells/mL, with 10 µg/mL Polybrene (Millipore, Zug, Switzerland). The media was changed after 24 h, and cells were passaged over two weeks. Stably infected cells were sorted by FACS based upon GFP fluorescence.

4.7. Immunofluorescence and Transendothelial Cell Migration

For stainings in 2D, control or G9a depleted Jurkat cells were cultured for 20 min on VCAM-1 (5 µg/mL). Cells were fixed in 4% formaldehyde (10 min), permeabilized with 0.5% Tx-100 in PBS (5 min), blocked in 10% fetal bovine serum and incubated with appropriated primary antibodies for 1 h at RT. After several washes, samples with incubated with secondary antibodies (1 h at RT). Samples were washed and mounted in Dako.

For transendothelial migration, HUVEC were plated on fibronectin-coated plates and confluent monolayers were stimulated with 15 ng/mL TNF-α, for 16 h prior to the assay. Then, HUVEC cells were labeled with CFSE and, after several washes, Control or G9a Jurkat cells were added to monolayer and allowed to transmigrate for 20 min. Cells were fixed, permeabilized and stained with appropriated antibodies. Images were acquired using a SP5 and SPE confocal microscopes (Leica, Wetzlar, Germany) with an ACS-APO 40× NA 1.30 oil immersion objective. We labeled control or G9a depleted cells with CFSE and cultured them on TNF-α stimulated HUVEC monolayer. Timelapes images were acquired with a TE2000 PFS microscope (Nikon, Tokyo, Japan) using a 20×/0.5 Plan Fluor objective and the Sedat filter set Chroma (89,000). The images were collected every 1 min over 30 min using a Cascade II EMCCD camera (Photometrics, Tucson, AZ, USA). Quantification of cell and nuclear circularity were determined using ImageJ (NIH, Bethesda, MA, USA). Track length was determined using Imaris (Bitplane, Zürich, Switzerland).

4.8. Flow Cytometry Analysis

Integrin VLA-4 expression was carried out by indirect immunofluorescence. Cells were blocked with human IgG (50 μg/mL; 30 min), incubated with HP2/1 (5–10 μg/mL; 30 min), followed by an appropriated fluorochrome-conjugated secondary antibody for 30 min (Jackson ImmunoResearch, West Grove, PA, USA). Between incubations, the preparations were washed with PBS. Flow cytometry was performed with a FacSort (Beckman Coulter, Brea, CA, USA) and data were analyzed using the BD CellQuest Pro software (BD Biosciences, Erembodegem, Belgium). To determine the content of polymerized actin (F-actin), cells were fixed with paraformaldehyde 4% in PBS for 15 min, permeabilized with Triton X-100 for 5 min and stained with (Alexa 647)-phalloidin (Molecular-Probes, Eugene, OR, USA). Cells were incubated at 22 °C for 10 min, washed twice with phosphate-buffered saline (PBS), and subjected to flow cytometry.

4.9. Transwell Invasion

We used transwell plate inserts (Corning Costar, 6.5 mm diameter, 3 μm pore sizes). In some cases, the filter was coated with 5 μg/mL of VCAM-1. 100 μL of a cell suspension (2×10^5 cells/well) in serum free medium, preincubated or not with BIX01294, was added to the upper chamber. 600 μL of complete medium with serum was added to the bottom chamber to promote the cell migration. The chambers were incubated in a CO_2 incubator at 37 °C for 6 h. Migrated cells from the lower chamber were collected, stained and quantified.

4.10. Statistical Analysis

Student *t* test (two tailed Mann-Whitney non-parametric test) or ANOVA (two tailed Kruskal-Wallis non-parametric test) were used for between-group analysis. For all analyses, statistical calculations were performed using Prism 6.0 Software (GraphPad Software, Inc. La Jolla, CA, USA), and p-values < 0.05 were considered statistically significant.

5. Conclusions

Here, we provide the first evidence for the functional involvement of G9a activity in the migration of primary ALL cells from patients. Although we observed a correlation between the integrin VLA-4 and the expression of G9a, the number of patients and healthy donors is not sufficient to conclude the potential interest of G9a as biomarker in this pathology and further studies might be conducted in the future. This study provide direct evidence that G9a depletion or inhibition disrupts cell polarity and cell capacity to extravasate endothelial barriers or squeeze through narrow spaces. Taken together, our findings indicate that G9a contributes to leukemia cell migration and might be considered a potential therapeutic target to block cancer cell dissemination.

Supplementary Materials: The following are available online at http://www.mdpi.com/2072-6694/10/9/325/s1. The supplementary material enclosed to this manuscript includes: one Supplementary Table S1, five Supplementary Videos, and four Supplementary Figures. Figure S1: Correlation between SUV39H1 and ITGA4 in ALL patients and between G9a and ITGA4 in healthy donors. Figure S2: Cell attachment and nuclear spreading of Jurkat cells treated with BIX01294 on a monolayer of HUVEC cells. Figure S3. Transendothelial migration of Jurkat cells treated with BIX01294. Figure S4. Cell polarity of Jurkat cells treated with BIX01294. Table S1. Oligonucleotides for selected genes.

Author Contributions: E.M., E.A.-G., and J.R.-M. performed the experiments. L.A., Á.G.-M., D.R. and M.R. isolated ALL samples and performed the genetic and clinical classification. M.R. and J.R.-M. analyzed all data. J.R.-M. designed the study and wrote the manuscript with the input of M.R.

Funding: E.M. and E.A.-G. were supported by a fellowship for Fondo de Garantía de Empleo Juvenil from Comunidad de Madrid. M.R. is funded by Asociación Pablo Ugarte. J.R.-M. is funded by Gilead Sciences (International Scholar in Hematology/Oncology) and the Spanish Ministry of Economy and Competitiveness (RYC-2015-18497 and SAF2017-86327-R).

Acknowledgments: We thank Martin Humphries (University of Manchester) for HUVEC cells, and Francisco Sánchez-Madrid for the HP2/1 antibody. Special thanks to Adam Hurlstone (University of Manchester) for editing suggestions. We really appreciate the help and assistance of Paloma Sánchez-Mateos, Rafael Samaniego, Amaya Puig-Kröger and all members of the Immuno-Oncology research laboratory (Instituto de Investigación Biomédica Gregorio Marañón). The confocal studies were performed in the Instituto de Investigación Biomédica Gregorio Marañón and the Bioimaging Facility (University of Manchester). The Bioimaging Facility microscopes were purchased with grants from Wellcome Trust and the University of Manchester Strategic Fund. The authors thank members of the Department of Immunology, University Complutense of Madrid for critical feedback and insightful comments.

Conflicts of Interest: The authors declare no conflict of interest. The funders had no roles in the design of the study; in the collection, analyses or interpretation of data; in the writing of the manuscript, or in the decision to publish the results.

References

1. Inaba, H.; Greaves, M.; Mullighan, C.G. Acute lymphoblastic leukaemia. *Lancet* **2013**, *381*, 1943–1955. [CrossRef]
2. Hunger, S.P.; Mullighan, C.G. Acute lymphoblastic leukemia in children. *N. Engl. J. Med.* **2015**, *373*, 1541–1552. [CrossRef] [PubMed]
3. Moorman, A.V. New and emerging prognostic and predictive genetic biomarkers in B-cell precursor acute lymphoblastic leukemia. *Haematologica* **2016**, *101*, 407–416. [CrossRef] [PubMed]
4. Bhojwani, D.; Pui, C.H. Relapsed childhood acute lymphoblastic leukaemia. *Lancet Oncol.* **2013**, *14*, e205–e217. [CrossRef]
5. Conter, V.; Bartram, C.R.; Valsecchi, M.G.; Schrauder, A.; Panzer-Grümayer, R.; Möricke, A.; Aricò, M.; Zimmermann, M.; Mann, G.; De Rossi, G.; et al. Molecular response to treatment redefines all prognostic factors in children and adolescents with B-cell precursor acute lymphoblastic leukemia: Results in 3184 patients of the AIEOP-BFM ALL 2000 study. *Blood* **2010**, *115*, 3206–3214. [CrossRef] [PubMed]
6. Almamun, M.; Levinson, B.T.; van Swaay, A.C.; Johnson, N.T.; McKay, S.D.; Arthur, G.L.; Davis, J.W.; Taylor, K.H. Integrated methylome and transcriptome analysis reveals novel regulatory elements in pediatric acute lymphoblastic leukemia. *Epigenetics* **2015**, *10*, 882–890. [CrossRef] [PubMed]
7. Van Vlierberghe, P.; Pieters, R.; Beverloo, H.B.; Meijerink, J.P. Molecular-genetic insights in paediatric T-cell acute lymphoblastic leukaemia. *Br. J. Haematol.* **2008**, *143*, 153–168. [CrossRef] [PubMed]
8. Gerlitz, G.; Bustin, M. The role of chromatin structure in cell migration. *Trends Cell Biol.* **2011**, *21*, 6–11. [CrossRef] [PubMed]
9. Gerlitz, G.; Bustin, M. Efficient cell migration requires global chromatin condensation. *J. Cell Sci.* **2010**, *123*, 2207–2217. [CrossRef] [PubMed]
10. Shinkai, Y.; Tachibana, M. H3K9 methyltransferase G9a and the related molecule GLP. *Genes Dev.* **2011**, *25*, 781–788. [CrossRef] [PubMed]
11. Scheer, S.; Zaph, C. The Lysine Methyltransferase G9a in Immune Cell Differentiation and Function. *Front. Immunol.* **2017**, *8*, 429. [CrossRef] [PubMed]
12. Huang, Y.; Zou, Y.; Lin, L.; Ma, X.; Huang, X. Effect of BIX-01294 on proliferation, apoptosis and histone methylation of acute T lymphoblastic leukemia cells. *Leuk. Res.* **2017**, *62*, 34–39. [CrossRef] [PubMed]
13. Hemler, M.E.; Elices, M.J.; Parker, C.; Takada, Y. Structure of the integrin VLA-4 and its cell-cell and cell-matrix adhesion functions. *Immunol. Rev.* **1990**, *114*, 45–65. [CrossRef] [PubMed]
14. Redondo-Muñoz, J.; Ugarte-Berzal, E.; García-Marco, J.A.; del Cerro, M.H.; van den Steen, P.E.; Opdenakker, G.; Terol, M.J.; García-Pardo, A. α4β1 integrin and 190-kDa CD44v constitute a cell surface docking complex for gelatinase B/MMP-9 in chronic leukemic but not in normal B cells. *Blood* **2008**, *112*, 169–178. [CrossRef] [PubMed]
15. Bayless, K.J.; Davis, G.E. Identification of dual α4β1 integrin binding sites within a 38 amino acid domain in the N-terminal thrombin fragment of human osteopontin. *J. Biol. Chem.* **2001**, *276*, 13483–13489. [CrossRef] [PubMed]
16. Shalapour, S.; Hof, J.; Kirschner-Schwabe, R.; Bastian, L.; Eckert, C.; Prada, J.; Henze, G.; von Stackelberg, A.; Seeger, K. High VLA-4 expression is associated with adverse outcome and distinct gene expression changes in childhood B-cell precursor acute lymphoblastic leukemia at first relapse. *Haematologica* **2011**, *96*, 1627–1635. [CrossRef] [PubMed]

17. Zhang, X.; Cook, P.C.; Zindy, E.; Williams, C.J.; Jowitt, T.A.; Streuli, C.H.; MacDonald, A.S.; Redondo-Muñoz, J. Integrin α4β1 controls G9a activity that regulates epigenetic changes and nuclear properties required for lymphocyte migration. *Nucleic Acids Res.* **2016**, *44*, 3031–3044. [CrossRef] [PubMed]
18. Mozzetta, C.; Boyarchuk, E.; Pontis, J.; Ait-Si-Ali, S. Sound of silence: The properties and functions of repressive Lys methyltransferases. *Nat. Rev. Mol. Cell Biol.* **2015**, *16*, 499–513. [CrossRef] [PubMed]
19. Nourshargh, S.; Hordijk, P.L.; Sixt, M. Breaching multiple barriers: Leukocyte motility through venular walls and the interstitium. *Nat. Rev. Mol. Cell Biol.* **2010**, *11*, 366–378. [CrossRef] [PubMed]
20. Lee, J.H.; Katakai, T.; Hara, T.; Gonda, H.; Sugai, M.; Shimizy, A. Roles of p-ERM and Rho-ROCK signaling in lymphocyte polarity and uropod formation. *J. Cell Biol.* **2004**, *167*, 327–337. [CrossRef] [PubMed]
21. Ley, K.; Laudanna, C.; Cybulsky, M.I.; Nourshargh, S. Getting to the site of inflammation: The leukocyte adhesion cascade updated. *Nat. Rev. Immunol.* **2007**, *7*, 678–689. [CrossRef] [PubMed]
22. Gaynes, J.S.; Jonart, L.M.; Zamora, E.A.; Naumann, J.A.; Gossai, N.P.; Gordon, P.M. The central nervous system microenvironment influences the leukemia transcriptome and enhances leukemia chemo-resistance. *Haematologica* **2017**, *102*, e136–e139. [CrossRef] [PubMed]
23. Chiarini, F.; Lonetti, A.; Evangelisti, C.; Buontempo, F.; Orsini, E.; Evangelisti, C.; Cappellini, A.; Neri, L.M.; McCubrey, J.A.; Martelli, A.M. Advances in understanding the acute lymphoblastic leukemia bone marrow microenvironment: From biology to therapeutic targeting. *Biochim. Biophys. Acta* **2016**, *1863*, 449–463. [CrossRef] [PubMed]
24. Benyoucef, A.; Palii, C.G.; Wang, C.; Porter, C.J.; Chu, A.; Dai, F.; Tremblay, V.; Rakopoulos, P.; Singh, K.; Huang, S.; et al. UTX inhibition as selective epigenetic therapy against TAL1-driven T-cell acute lymphoblastic leukemia. *Genes Dev.* **2016**, *30*, 508–521. [CrossRef] [PubMed]
25. Montaño, A.; Forero-Castro, M.; Marchena-Mendoza, D.; Benito, R.; Hernández-Rivas, J.M. New challenges in targeting signaling pathways in acute lymphoblastic leukemia by NGS approaches: An update. *Cancers* **2018**, *10*, 110. [CrossRef] [PubMed]
26. Simon, C.; Chagraoui, J.; Krosl, J.; Gendron, P.; Wilhelm, B.; Lemieux, S.; Boucher, G.; Chagnon, P.; Drouin, S.; Lambert, R.; et al. A key role for EZH2 and associated genes in mouse and human adult T-cell acute leukemia. *Genes Dev.* **2012**, *26*, 651–656. [CrossRef] [PubMed]
27. Yokoyama, Y.; Hieda, M.; Nishioka, Y.; Matsumoto, A.; Higashi, S.; Kimura, H.; Yamamoto, H.; Mori, M.; Matsuura, S.; Matsuura, N. Cancer-associated upregulation of histone H3 lysine 9 trimethylation promotes cell motility in vitro and drives tumor formation in vivo. *Cancer Sci.* **2013**, *104*, 889–895. [CrossRef] [PubMed]
28. Mutonga, M.; Tamura, K.; Malnassy, G.; Fulton, N.; de Albuquerque, A.; Hamamoto, R.; Stock, W.; Nakamura, Y.; Alachkar, H. Targeting Suppressor of Variegation 3-9 Homologue 2 (SUV39H2) in Acute Lymphoblastic Leukemia (ALL). *Transl. Oncol.* **2015**, *8*, 368–375. [CrossRef] [PubMed]
29. San José-Enériz, E.; Agirre, X.; Rabal, O.; Vilas-Zornoza, A.; Sanchez-Arias, J.A.; Miranda, E.; Ugarte, A.; Roa, S.; Paiva, B.; Estella-Hermoso de Mendoza, A.; et al. Discovery of first-in-class reversible dual small molecule inhibitors against G9a and DNMTs in hematological malignancies. *Nat. Commun.* **2017**, *8*, 15424. [CrossRef] [PubMed]
30. Bae, M.H.; Oh, S.H.; Park, C.J.; Lee, B.R.; Kim, Y.J.; Cho, Y.U.; Jang, S.; Lee, J.H.; Kim, N.; Park, S.H.; et al. VLA-4 and CXCR4 expression levels show contrasting prognostic impact (favorable and unfavorable; respectively) in acute myeloid leukemia. *Ann. Hematol.* **2015**, *94*, 1631–1638. [CrossRef] [PubMed]
31. Ko, S.Y.; Park, C.J.; Park, S.H.; Cho, Y.U.; Jang, S.; Seo, E.J.; Kim, N.; Kim, D.Y.; Koh, K.N.; Im, H.J.; et al. High CXCR4 and low VLA-4 expression predicts poor survival in adults with acute lymphoblastic leukemia. *Leuk. Res.* **2014**, *38*, 65–70. [CrossRef] [PubMed]
32. Peng, K.; Su, G.; Ji, J.; Yang, X.; Miao, M.; Mo, P.; Li, M.; Xu, J.; Li, W.; Yu, C. Histone demethylase JMJD1A promotes colorectal cancer growth and metastasis by enhancing Wnt/β-catenin signaling. *J. Biol. Chem.* **2018**, *293*, 10606–10619. [CrossRef] [PubMed]
33. Zou, Z.K.; Huang, Y.Q.; Zou, Y.; Zheng, X.K.; Ma, X.D. Silencing of LSD1 gene modulates histone methylation and acetylation and induces the apoptosis of JeKo-1 and MOLT-4 cells. *Int. J. Mol. Med.* **2017**, *40*, 319–328. [CrossRef] [PubMed]
34. Hsieh, Y.T.; Gang, E.J.; Geng, H.; Park, E.; Huantes, S.; Chudziak, D.; Dauber, K.; Schaefer, P.; Scharman, C.; Shimada, H.; et al. Integrin alpha4 blockade sensitizes drug resistant pre-B acute lymphoblastic leukemia to chemotherapy. *Blood* **2013**, *121*, 1814–1818. [CrossRef] [PubMed]

35. Hsieh, Y.T.; Gang, E.J.; Shishido, S.N.; Kim, H.N.; Pham, J.; Khazal, S.; Osborne, A.; Esguerra, Z.A.; Kwok, E.; Jang, J.; et al. Effects of the small-molecule inhibitor of integrin α4, TBC3486, on pre-B-ALL cells. *Leukemia* **2014**, *28*, 2101–2104. [CrossRef] [PubMed]
36. Duchartre, Y.; Bachl, S.; Kim, H.N.; Gang, E.J.; Lee, S.; Liu, H.C.; Shung, K.; Xu, R.; Kruse, A.; Tachas, G.; et al. Effects of CD49d-targeted antisense-oligonucleotide on α4 integrin expression and function of acute lymphoblastic leukemia cells: Results of in vitro and in vivo studies. *PLoS ONE* **2017**, *12*, e0187684. [CrossRef] [PubMed]
37. Wigton, E.J.; Thompson, S.B.; Long, R.A.; Jacobelli, J. Myosin-IIA regulates leukemia engraftment and brain infiltration in a mouse model of acute lymphoblastic leukemia. *J. Leukoc. Biol.* **2016**, *100*, 143–153. [CrossRef] [PubMed]
38. Infante, E.; Heasman, S.J.; Ridley, A.J. Statins inhibit T-acute lymphoblastic leukemia cell adhesion and migration through Rap1b. *J. Leukoc. Biol.* **2011**, *89*, 577–586. [CrossRef] [PubMed]
39. Ma, Y.R.; Ma, Y.H. MIP-1α enhances Jurkat cell transendothelial migration by up-regulating endothelial adhesion molecules VCAM-1 and ICAM-1. *Leuk. Res.* **2014**, *38*, 1327–1331. [CrossRef] [PubMed]
40. McGregor, A.L.; Hsia, C.R.; Lammerding, J. Squish and squeeze—The nucleus as a physical barrier during migration in confined environments. *Curr. Opin. Cell Biol.* **2016**, *40*, 32–40. [CrossRef] [PubMed]
41. Liu, L.; Luo, Q.; Sun, J.; Song, G. Nucleus and nucleus-cytoskeleton connections in 3D cell migration. *Exp. Cell Res.* **2016**, *348*, 56–65. [CrossRef] [PubMed]
42. Wolf, K.; Te Lindert, M.; Krause, M.; Alexander, S.; Te Riet, J.; Willis, A.L.; Hoffman, R.M.; Figdor, C.G.; Weiss, S.J.; Friedl, P. Physical limits of cell migration: Control by ECM space and nuclear deformation and tuning by proteolysis and traction force. *J. Cell Biol.* **2013**, *201*, 1069–1084. [CrossRef] [PubMed]
43. Madrazo, E.; Conde, A.C.; Redondo-Muñoz, J. Inside the cell: Integrins as new governors of nuclear alterations? *Cancers* **2017**, *9*, 82. [CrossRef] [PubMed]
44. Tan, Y.; Tajik, A.; Chen, J.; Jia, Q.; Chowdhury, F.; Wang, L.; Chen, J.; Zhang, S.; Hong, Y.; Yi, H.; et al. Matrix softness regulates plasticity of tumour-repopulating cells via H3K9 demethylation and Sox2 expression. *Nat. Commun.* **2014**, *5*, 4619. [CrossRef] [PubMed]
45. Hu, L.; Zang, M.D.; Wang, H.X.; Zhang, B.G.; Wang, Z.Q.; Fan, Z.Y.; Wu, H.; Li, J.F.; Su, L.P.; Yan, M.; et al. G9A promotes gastric cancer metastasis by upregulating ITGB3 in a SET domain-independent manner. *Cell Death Dis.* **2018**, *9*, 278. [CrossRef] [PubMed]
46. Yamaguchi, H.; Condeelis, J. Regulation of the actin cytoskeleton in cancer cell migration and invasion. *Biochim. Biophys. Acta* **2007**, *1773*, 642–652. [CrossRef] [PubMed]
47. Cao, X.; Moeendarbary, E.; Isermann, P.; Davidson, P.M.; Wang, X.; Chen, M.B.; Burkart, A.K.; Lammerding, J.; Kamm, R.D.; Shenoy, V.B. A chemomechanical model for nuclear morphology and stresses during cell transendothelial migration. *Biophys. J.* **2016**, *111*, 1541–1552. [CrossRef] [PubMed]
48. Barzilai, S.; Yadav, S.K.; Morrell, S.; Roncato, F.; Klein, E.; Stoler-Barak, L.; Golani, O.; Feigelson, S.W.; Zemel, A.; Nourshargh, S.; et al. Leukocytes breach endothelial barriers by insertion of nuclear lobes and disassembly of endothelial actin filaments. *Cell Rep.* **2017**, *18*, 685–699. [CrossRef] [PubMed]
49. Alon, R.; van Buul, J.D. Leukocyte breaching of endothelial barriers: The actin link. *Trends Immunol.* **2017**, *38*, 606–615. [CrossRef] [PubMed]

El análisis de seguimiento de partículas múltiples en núcleos aislados revela el fenotipo mecánico de las células leucémicas

El núcleo está compuesto fundamentalmente por láminas y membranas nucleares que encierran la cromatina, los componentes nucleoesqueléticos y el nucleoplasma en suspensión. Las conexiones funcionales de esta red integran estímulos externos en señales celulares, incluidas fuerzas físicas para respuestas mecánicas del núcleo. Canónicamente, las características morfológicas del núcleo, como la forma y el tamaño, han servido a los patólogos para estratificar y diagnosticar a los pacientes con cáncer; sin embargo, las nuevas técnicas biofísicas deben aprovechar los parámetros físicos para mejorar el diagnóstico del cáncer. Mediante el uso de la técnica de seguimiento de partículas múltiples (MPT) en gránulos de cromatina, diseñamos un algoritmo basado en SURF (características robustas aceleradas) para estudiar las propiedades mecánicas de núcleos aislados y en células vivas. Hemos determinado la rigidez aparente al cizallamiento, la viscosidad y la densidad óptica del núcleo, y cómo influye la estructura de la cromatina en estos valores biofísicos. Además, utilizamos nuestro análisis MPT-SURF para estudiar las propiedades mecánicas aparentes de núcleos aislados de pacientes con leucemia linfoblástica aguda. Encontramos que las células de leucemia exhibieron diferencias mecánicas en comparación con los linfocitos normales. Curiosamente, los núcleos aislados de células de leucemia de alto riesgo mostraron una mayor viscosidad que sus homólogos de linfocitos normales, mientras que los núcleos de células de pacientes en recaída presentaron una mayor densidad que los de linfocitos normales o células de leucemia de riesgo estándar y alto. En conjunto, aquí presentamos cómo el análisis MPT-SURF de los gránulos de cromatina nuclear define características fenotípicas mecánicas nucleares, que podrían ser clínicamente relevantes.

Diego Herráez-Aguilar, **Elena Madrazo**, Horacio López-Menéndez, Manuel Ramírez, Francisco Monroy, Javier Redondo-Muñoz. Sci Rep. 2020 Apr 21;10(1):6707. doi: 10.1038/s41598-020-63682-5.

SCIENTIFIC REPORTS
nature research

OPEN

Multiple particle tracking analysis in isolated nuclei reveals the mechanical phenotype of leukemia cells

Diego Herráez-Aguilar[1,2], Elena Madrazo[3], Horacio López-Menéndez[1,4], Manuel Ramírez[5,6], Francisco Monroy[1,4*] & Javier Redondo-Muñoz[3,7*]

The nucleus is fundamentally composed by lamina and nuclear membranes that enclose the chromatin, nucleoskeletal components and suspending nucleoplasm. The functional connections of this network integrate external stimuli into cell signals, including physical forces to mechanical responses of the nucleus. Canonically, the morphological characteristics of the nucleus, as shape and size, have served for pathologists to stratify and diagnose cancer patients; however, novel biophysical techniques must exploit physical parameters to improve cancer diagnosis. By using multiple particle tracking (MPT) technique on chromatin granules, we designed a SURF (Speeded Up Robust Features)-based algorithm to study the mechanical properties of isolated nuclei and in living cells. We have determined the apparent shear stiffness, viscosity and optical density of the nucleus, and how the chromatin structure influences on these biophysical values. Moreover, we used our MPT-SURF analysis to study the apparent mechanical properties of isolated nuclei from patients of acute lymphoblastic leukemia. We found that leukemia cells exhibited mechanical differences compared to normal lymphocytes. Interestingly, isolated nuclei from high-risk leukemia cells showed increased viscosity than their counterparts from normal lymphocytes, whilst nuclei from relapsed-patient's cells presented higher density than those from normal lymphocytes or standard- and high-risk leukemia cells. Taken together, here we presented how MPT-SURF analysis of nuclear chromatin granules defines nuclear mechanical phenotypic features, which might be clinically relevant.

The nucleus is a central cellular organelle that must alter its physical properties during cellular functions, including gene expression, cell migration, and development in homeostasis and human diseases[1]. The nucleus is composed by the nuclear envelope, nucleoskeletal components, and the nucleoplasm, which contains the DNA and its associated molecules forming the chromatin[2]. The nuclear envelope is mainly composed by nuclear membranes, A- (lamin A and C) and B- (lamin B) lamin types, and other structural proteins that connect the nucleus with the cytoskeleton as LINC complexes[3]. Lamin A/C levels and its ratio to lamin B levels control nuclear deformability and stiffness[4,5]. It has been reported that other nuclear components, as LINC and F-actin binding proteins, control nuclear shape and rigidity[6]. In general, these nuclear changes correlate with more invasive phenotype of tumor cells and higher genomic instability upon cell migration[7,8].

Chromatin organization is modulated by epigenetic changes that promote chromatin compaction and decondensation according to electrostatic interactions and configurational entropy[9–11]. Several biophysical techniques support that the chromatin conformation alterations contributes to the morphology and the biophysical behavior of the nucleus[12–16] Abnormalities in nuclear shape and organization occur in a wide range of human pathologies,

[1]Department of Physical Chemistry, Complutense University, 28040, Madrid, Spain. [2]Faculty of Experimental Sciences, Francisco de Vitoria University (UFV), 28223, Pozuelo de Alarcón, Madrid, Spain. [3]Department of Immunology, Hospital 12 de Octubre Health Research Institute (imas12), School of Medicine, Complutense University, 28040, Madrid, Spain. [4]Translational Biophysics, Hospital Doce de Octubre Health Research Institute (imas12), 28041, Madrid, Spain. [5]Oncolohematology. Hospital Universitario Niño Jesús, Madrid, Spain. [6]Health Research Institute La Princesa, Madrid, Spain. [7]Lydia Becker Institute of Immunology and Inflammation, Manchester Collaborative Centre for Inflammation Research, University of Manchester, Manchester, M13 9PL, UK. *email: monroy@ucm.es; javredon@ucm.es

including cancer[17,18]. Likewise, nuclear morphology has been still used for diagnoses in many biopsies by pathologists[19,20]. Whereas several studies have improved nuclear morphometric experiments to stratify cancer cells[21], the functional links between the biophysical properties of nuclei from cancer cells and their value in clinics remain elusive.

In the case of acute lymphoblastic leukemia (ALL), novel strategies for prevention and early detection have pointed the critical role of genetic changes leading to nuclear modifications on the molecular pathogenicity of the neoplastic cells[22]. ALL is the most common pediatric malignancy and the leading cause of death in children with cancer[23]. However, it is not known how the nuclei of ALL cells differ from normal peripheral blood lymphocytes (PBL).

In this study, we used a multiple particle tracking (MPT) analysis of chromatin granules to determine coarse-grained descriptors of nuclear mechanics in isolated nuclei from leukemia cells. MPT technique is broadly recognized as a key technology for quantitative analysis of intracellular mechanics[24,25]. Based on the microrheology concept[26], we have exploited MPT with time-lapsed microscopy images as a phenotyping method with mechanical markers expanded on the principles of micromechanical cell mapping[27,28]. The robustness of MPT relies on the efficiency of the tracking algorithm to ensure the correspondence of the multiple objects and an adequate frame-of-reference for drift-correction between consecutive slides[24,27,29]. We have developed a novel MPT-method based on the SURF algorithm[30] which determine *in situ* the apparent rheological properties of the cell nucleus by tracking the mobility of nuclear granules. This paper focusses on the relative variations of the apparent nuclear viscosities between different phenotypes in isolated nuclei although we have resolved also the mechanical descriptors in intact cells. By using primary samples obtained from patients with ALL, we observed that leukemia cells present a different density than normal lymphocytes. Moreover, we were able to identify that isolated nuclei from high-risk ALL cells show higher viscosity than standard-risk or normal lymphocytes. Together, our analysis of biophysical traits of chromatin granules defines the mechanical phenotype of isolated nuclei from leukemia cells that might be relevant to stratify patients.

Results

Chromatin mobility by Multiple Particle Tracking enhanced upon Speeded-Up Robust Feature detection (MPT-SURF). Chromatin is packed in nucleosomes folded into 30 nm helical fiber, and this into higher dynamic chromosome territories[31]. Due to its heterogeneity, we considered the possibility to probe coarse-grained chromatin dynamics undergoing confined Brownian motion in a viscoelastic environment[32]. We measured the diffusing trajectories of single granules of chromatin (chromatin "spots") localized in the equatorial plane of isolated nuclei from Jurkat (a T-ALL cell line) cells (Fig. 1a). To track the positions of the centroids in real time ($r_i(t)$), we designed an adapted SURF (Speeded Up Robust Features) algorithm, which we integrated in a custom-made MPT scheme programmed in Mathematica (Supplementary Notes 1–4 and Supplementary Figs S1 and S2). The MPT-SURF method removed spurious motions due to possible drifts to resolve the collective movement of these particles (Supplementary Fig. S3). We selected for MPT-SURF analysis those granules with diameters between $0.5 - 1.5\ \mu m$ (Fig. 1b). We also confirmed that the relative size and the optical density of these chromatin granules remained steady during measurements (Supplementary Fig. S4), without any significant change (Supplementary Fig. S5).

The Brownian movement of nuclear granules identified was characterized by a Gaussian profile of displacements (Fig. 1c), which defines diffusing trajectories of mean squared displacements in terms of lag times τ, these are $MSD = \Delta h^2(\tau) = \sum_j \left[r_j(t+\tau) - r_j(t)\right]^2$ (with the averaging sum extended over all the positions in a time series). We used Jurkat cells (a T-ALL cell line) to isolate the cell nucleus and obtained the Brownian displacements from chromatin spots ($n = 72$) (Fig. 1d). Each trajectory was found nearly-free diffusive at enough short-times, where was fitted to the 2D free-diffusion equation[24]:

$$\Delta h^2_{\tau \to 0} = 4 D_{eff} \tau \tag{1}$$

with D_{eff} being an effective diffusion coefficient calculated for the corresponding chromatin spot ($MSD \sim \tau^1$ at $\tau \ll 1s$; Fig. 1d and Supplementary Fig. S6a–c). To test MPT-SURF for performance with *ex-cell* measurements in isolated nuclei, we compared the MPT-SURF analysis in intact Jurkat cells or isolated nuclei (Supplementary Note S4.4). Both types of measurements (ex-cell/in-cell) rendered the Brownian trajectories with the limiting free-diffusion behavior expected at short times (Supplementary Fig. S6b,c); at $\tau \ll 1s$, we observed $MSD \sim \tau^1$ and $RMSD \sim \tau^{1/2}$, as expected. Chromatin diffusivity is hindered by the viscoelastic environment[32], as we confirmed in our system by the evident confinement of the trajectories (Supplementary Fig. S6b). In addition, we detected hyper-diffusive displacements at long times that correspond to a free-diffusivity breakout ($MSD \sim \tau^\alpha$ with $\alpha > 1$ at $\tau > 1s$; Fig. 1d, Supplementary Fig. S6c). Together, these results indicate that MPT-SURF algorithm enables for detecting Brownian trajectories of chromatin spots with well-defined features expected to remain steady during measurements.

Apparent chromatin microviscosity as a probe of interphase nuclear mechanics. We determined the distribution of apparent viscosities η_{app} obtained for each chromatin spot displacement from the Stokes-Einstein relationship[33,34],

$$D_{eff} = \frac{k_B T}{6\pi \eta_{app} R} \tag{2}$$

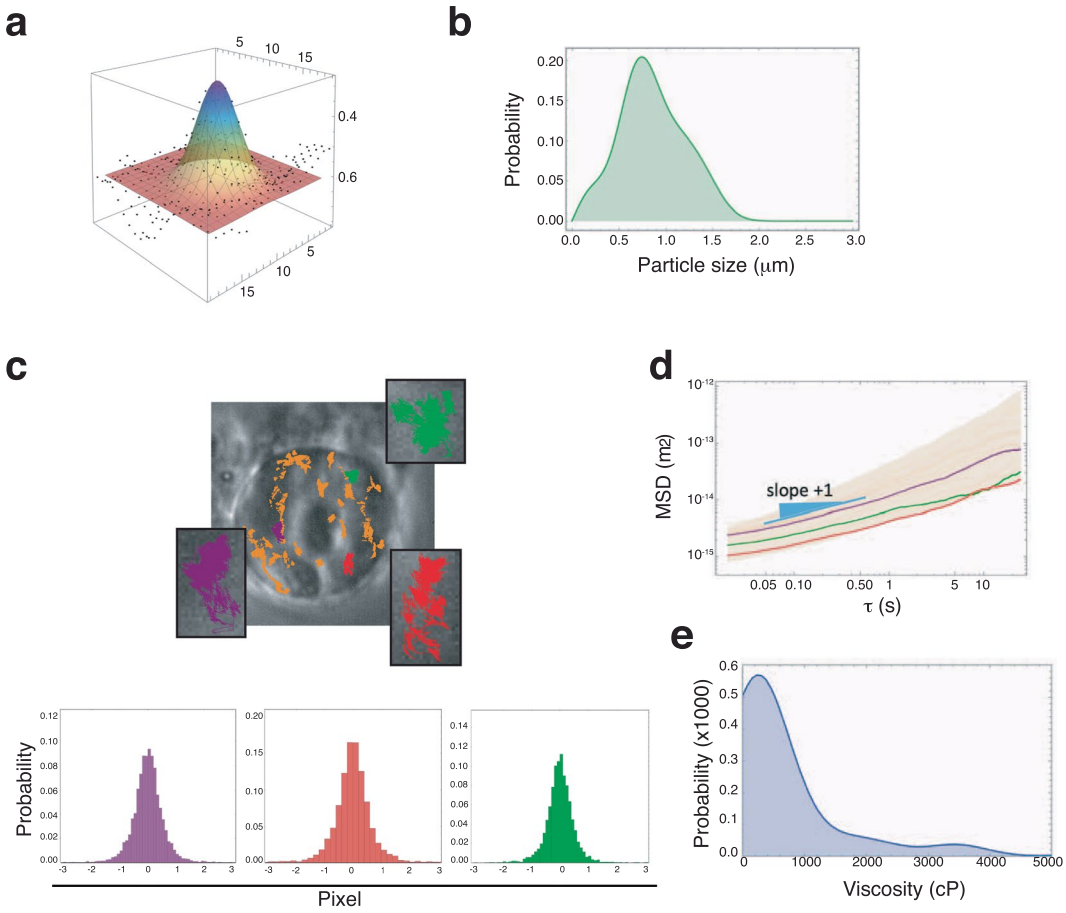

Figure 1. Description of the experimental rationale used for particle tracking microrheology with chromatin grains. **(a)** Spatial profile of a typical chromatin grain with the best fit to a 2D-Gaussian profile. To be eligible for microrheological analysis, a given dynamical trajectory is obligated to conserve apparent grain dimensions. **(b)** Typical distribution of grain sizes in a nucleus, specifically that of Fig. 1c. **(c)** Brownian trajectories of selected chromatin grains in a nucleus from Jurkat cell. Three particular trajectories (insets in green, red and purple) were zoomed to show their Brownian nature characterized by a Gaussian distribution of the displacements. **(d)** Variability band of the mean square displacements (MSD trajectories) as calculated from the Brownian trajectories as a function of the lag time (τ). All trajectories were found almost parallel, with a slope unity at short times compatible with free-diffusivity ($MSD \sim \tau$) and an intercept given by the diffusion coefficient D_{eff} (see Eq. 1). Variability depended on the different grain sizes (see Fig. 1b), and tthe different environmental microviscosity sensed by every one of those particles. The three highlighted trajectories correspond to the three selected grains in Fig. 1c (equal colors). **(e)** Distribution of the measured values of the apparent viscosities η_{app} using Eq. (2) with the values of the diffusion coefficient calculated from the best fits with Eq. (1) to the data in Fig. 1d. The apparent particle size R was assumed to equal the measured grain size (Fig. 1a).

where k_B is the Boltzmann's constant, t the absolute temperature, and R the apparent size of the chromatin spot determined as an optical radius by fitting its intensity profile to a Gaussian function. We defined the apparent viscosity from the tracks of the chromatin spots (including the most probable expectation and the standard deviation; $n \gg 50$, typically) (Fig. 1e). We calculated that the characteristic uncertainty on this phenotypical descriptor (apparent microviscosity) was 30–35% of the averaged value in a single nucleus (summing up experimental error plus data variance due to chromatin heterogeneity). We did not find significant differences between isolated nuclei or these in intact Jurkat cells (Supplementary Fig. S6d). Together, our findings suggest that MPT-SURF analysis of nuclear spots allows to measure the apparent chromatin viscoelasticity in an isolated nucleus.

Chromatin microrheology reveals the n ucleus mechanics as a Voigt-like body with a regulated viscoelasticity. We focused on the frequency dependence of the apparent viscoelastic parameters obtained from an effective fluctuation-dissipation scheme[25,35,36], which defines the apparently linear mechanic response of the nucleus. Given the complex value of the linear viscoelastic modulus[35] $\widetilde{G}(\omega) = G'(\omega) + iG''(\omega)$, with apparent values of the storage modulus $G'(\omega)$, loss modulus $G''(\omega) = \omega\eta(\omega)$ and shear viscosity $\eta(\omega)$ expressed as a function of the frequency of the chromatin motions (ω), the generalized Stokes-Einstein relationship in Eq. (2) can be rewritten as follows[35,37]:

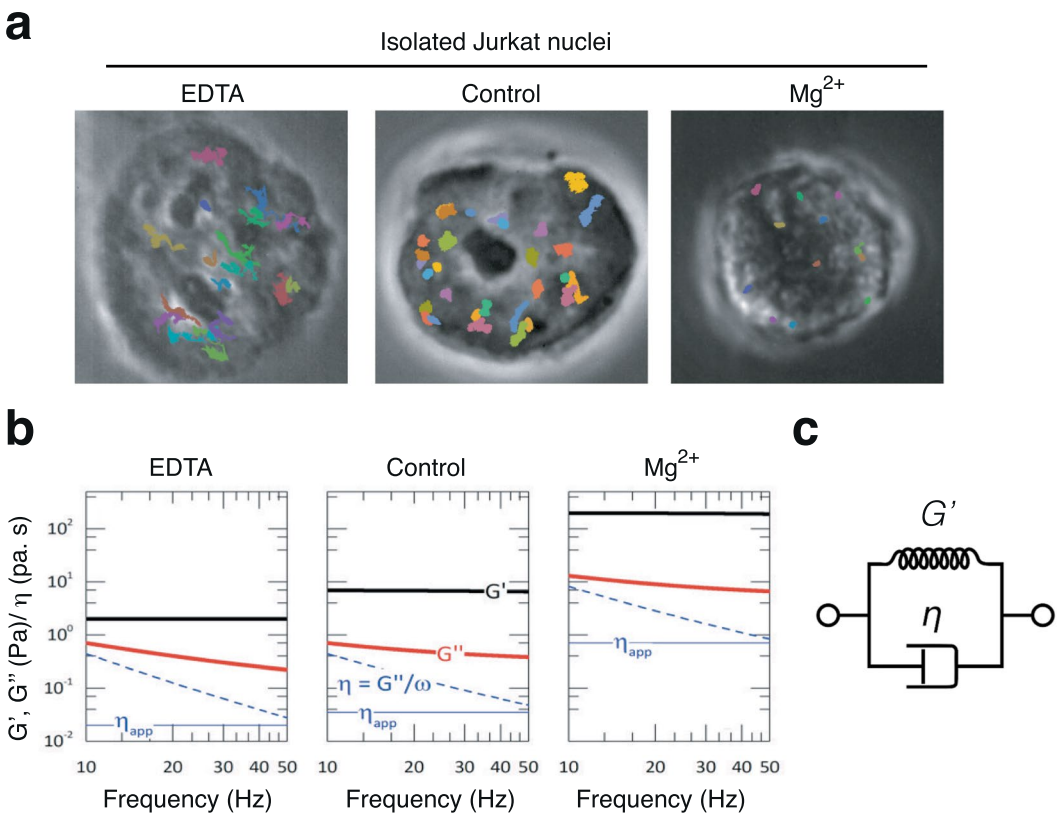

Figure 2. Chromatin viscoelasticity of isolated nuclei from Jurkat cells. (**a**) Representative phase contrast images of Jurkat nuclei analyzed by adding $MgCl_2$ or EDTA. (**b**) Experimental values of the viscoelastic moduli of a representative chromatin grain in a Jurkat nucleus as a function of the shearing frequency (inverse Brownian time; $\omega = 1/\tau$); $G'(\omega)$ were the shear rigidity modulus (black lines), and $G''(\omega) = \omega\eta$ the loss modulus (red lines), which was determined by the frequency-dependence of the effective viscosity $\eta(\omega)$ (dashed blue lines). Straight blue lines show the constant values of apparent viscosity measured from the Brownian diffusivities. The apparent viscosity η_{app} defined the instantaneous limit of the dynamic viscosity $\eta(\omega)$ at high ω, which represented the short-time limit of free-diffusivity (see Fig. 1d). (**c**) The Voigt-like rheological model described the chromatin as an elastic spring of rigidity G' coupled in parallel with a damping element of viscosity η., which represented together a soft viscoelastic body with a mechanical e lowest.

$$\widetilde{G}(s) = \frac{k_B T}{\pi R s \langle \tilde{r}^2(s) \rangle} \tag{3}$$

where $\widetilde{G}(s)$ is the Laplace transform of $\widetilde{G}(\omega)$, and $\tilde{r}^2(s)$ the Laplace transform of the diffusive trajectory $r(t)^2$, with s being the Laplace frequency (see Methods). The thermal force involved was weak, therefore the passive microrheological response detected by MPT-SURF was guaranteed in the linear region of the strain-stress relationship that underlies Eq. (3). Using this microrheological relationship, we studied the apparent viscoelasticity of isolated nuclei incubated at different conditions (Fig. 2a). Figure 2b shows a representative frequency dependence of the viscoelastic parameters calculated by MPT-SURF; $G'(\omega)$ was obtained as the real part of the complex modulus $\widetilde{G}(\omega)$, $G''(\omega)$ was the imaginary part, and the shear viscosity $\eta(\omega) = G''(\omega)/\omega$ was compared with the value of the apparent viscosity η_{app}, as measured from the effective diffusion coefficient (See Eq. (2)). In the Fourier frequency domain probed in the experiments (corresponding to the inverse times of the Brownian trajectories tracked), the apparent value of the storage modulus in isolated nuclei remained essentially constant (typical value $G' = 8 \pm 3P$ a; $N = 17$) (Fig. 2b; central panel). This value was similar to the low rigidity of the cytoplasm[33] and compatible with the shear rigidity of soft biological gels[38,39]. The apparent value of the loss modulus was constant with a lower value, $G'' \approx G'/10$, which slightly decreased with increasing frequencies. Due to the rheological behavior observed ($G' \gg G'' \sim \omega^0$), we identified the chromatin as a Kelvin-Voigt material constituted by an elastic element (the shear rigidity) coupled in parallel with a viscous damper (the shear viscosity) (Fig. 2c). In this Voigt-like system, viscoelasticity was such that viscous losses were significantly smaller than rigidity ($G'' \ll G'$), which defined viscous creep as the preferred rheological channel to undergo chromatin deformations. Chromatin motion might depend on the viscous channel undergoing displacements at a velocity limited by the local viscosity. Therefore, we focused on the apparent viscosity η_{app} as the rheological descriptor with a phenotypical value. We defined that the dynamic value of the shear viscosity decreased with frequency, and reached a limiting value

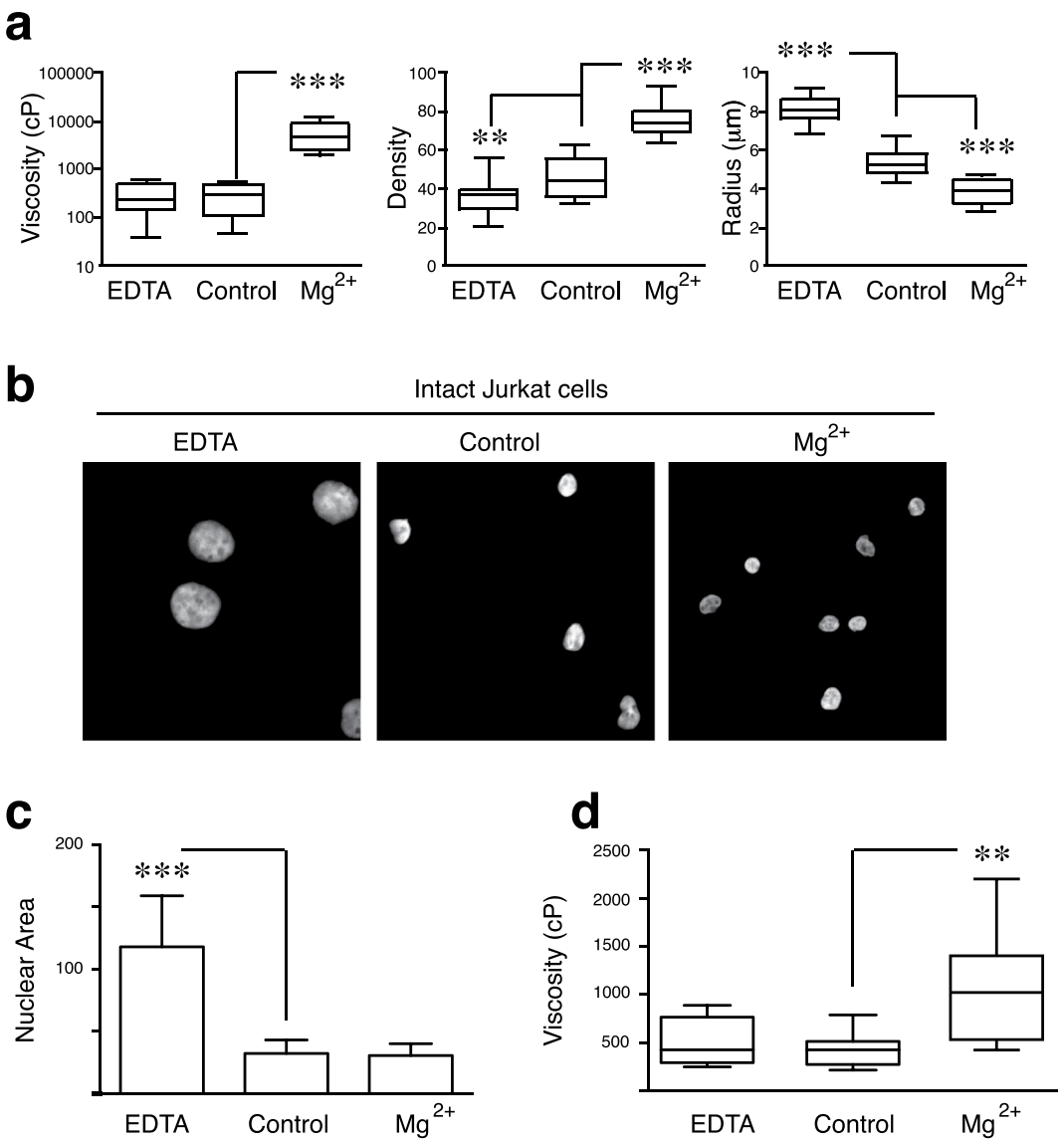

Figure 3. Viscosity alterations induced by osmotic stress of nuclei upon isolation or in intact cells. (**a**) Comparative statistics of the averaged values of the apparent viscosity, optical density and radius measured for a population of Jurkat nuclei at the three different conditions considered. (**b**) Jurkat cells were cultured in the presence of $MgCl_2$ (7.5 mM) or EDTA (1 mM) for 24 h. Then, cells were fixed, stained with Hoechst and analyzed by confocal microscopy. (**c**) Graph shows the nuclear areas from (**b**). (**d**) The apparent nuclear viscosity for a population of Jurkat cells cultured as in (**b**) were analyzed by MPT-SURF. $^{**}P < 0.01$.

$\eta(\omega) \rightarrow \eta_{app}$ at high ω, which was compatible with the apparent value determined from the diffusive part of MSD trajectories (Fig. 2b; central panel). Moreover, we confirmed by MPT-SURF that nuclei after isolation or in intact cells showed similar viscosity (Supplementary Fig. S6). We also measured the nuclear area from isolated nuclei and in intact cells (Supplementary Fig. S7). As we expected from previous reports[40], the isolation process induced nuclear shrinking, although this did not affect the microrheology quantification. Figure 2a shows that nuclei incubated with EDTA swelled in comparison to control (untreated) nuclei, whilst the presence of Mg^{2+} induced nuclear shrinking. Together, our results suggest that MPT-SURF might serve to characterize the mechanical phenotype of isolated nuclei under different conditions.

Effect of osmotic stress in acute lymphoblastic leukemia cells. As expected from Fig. 2a, the addition of Mg^{2+} to isolated nuclei promoted nuclear shrinking, significantly smaller area, and bigger viscosity and density than control (untreated) nuclei (Fig. 3a). In contrast, EDTA promoted nuclear swelling and reduced the nuclear density compared to untreated conditions; however, no statistically differences of the viscosity were detected (Fig. 3a). To address whether these osmotic effects on intact cells might promote *in situ* nuclear changes detected by MPT-SURF, we cultured Jurkat cells in high (Mg^{2+}) or low (EDTA) levels of divalent cations, which have been reported to increase heterochromatin levels in breast cancer cells[41]. Firstly, we demonstrated that

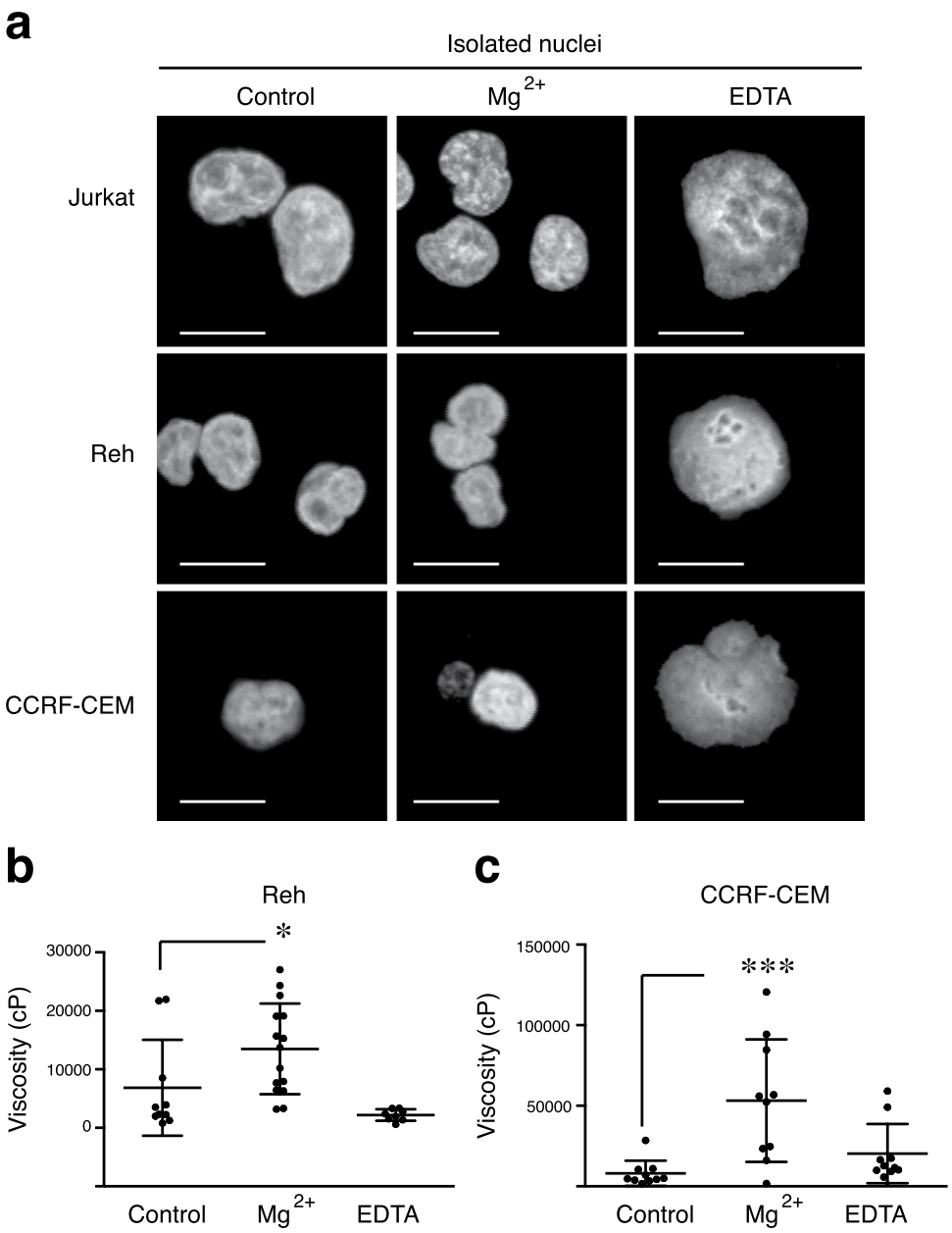

Figure 4. Swelling and shriking conditions promote change in the nuclear shape and viscoelasticity of ALL cell lines. (**a**) Representative images of isolated nuclei from Jurkat and CCRF-CEM (T-ALL) and Reh (B-ALL) cells upon $MgCl_2$ or EDTA addition for 5 min. Then, nuclei were fixed, stained with Hoechst and analyzed by confocal microscopy. (**b**,**c**) Comparative statistics of the averaged values of the apparent viscosity measured for a population of Reh (Fig. 3b) or CCRF-CEM (Fig. 3c) nuclei at the three different conditions considered. *P < 0.05.

Mg^{2+} addition did not alter the nuclear area of Jurkat cells, whilst EDTA treatment significantly increased it (Fig. 3b,c). Using MPT-SURF measurements, we analyzed the viscosity for nuclei of Jurkat cells treated with Mg^{2+} (Supplementary Fig. S8). For isolated nuclei, the diffusing trajectories displayed a very relevant drop after treatment with Mg^{2+}, which revealed significantly slower chromatin mobilities upon osmotic compaction (Supplementary Fig. S8). We confirmed that Mg^{2+}-treatment of isolated nuclei of Jurkat cells promoted higher apparent nuclear viscosity than control cells, whilst EDTA addition didn't show any difference (Fig. 3d).

We expanded our analyses to other B-ALL (Reh) and T-ALL (CCRF-CEM) leukemia cell lines to demonstrate the value of the MPT-SURF analysis of the nuclear microrheology as a quantitative probe of mechanical phenotype. We confirmed that the addition of Mg^{2+} diminished the nuclear morphology, whilst EDTA increased the nuclear shape compared to control conditions of ALL cell lines studied (Fig. 4a). By tracking nuclear chromatin spots from isolated nuclei, we quantified the apparent viscosity of Reh and CCRF-CEM cells. We confirmed that Mg^{2+} addition increased slightly the nuclear viscosity of Reh cells (Fig. 4b) and significantly of CCRF-CEM cells

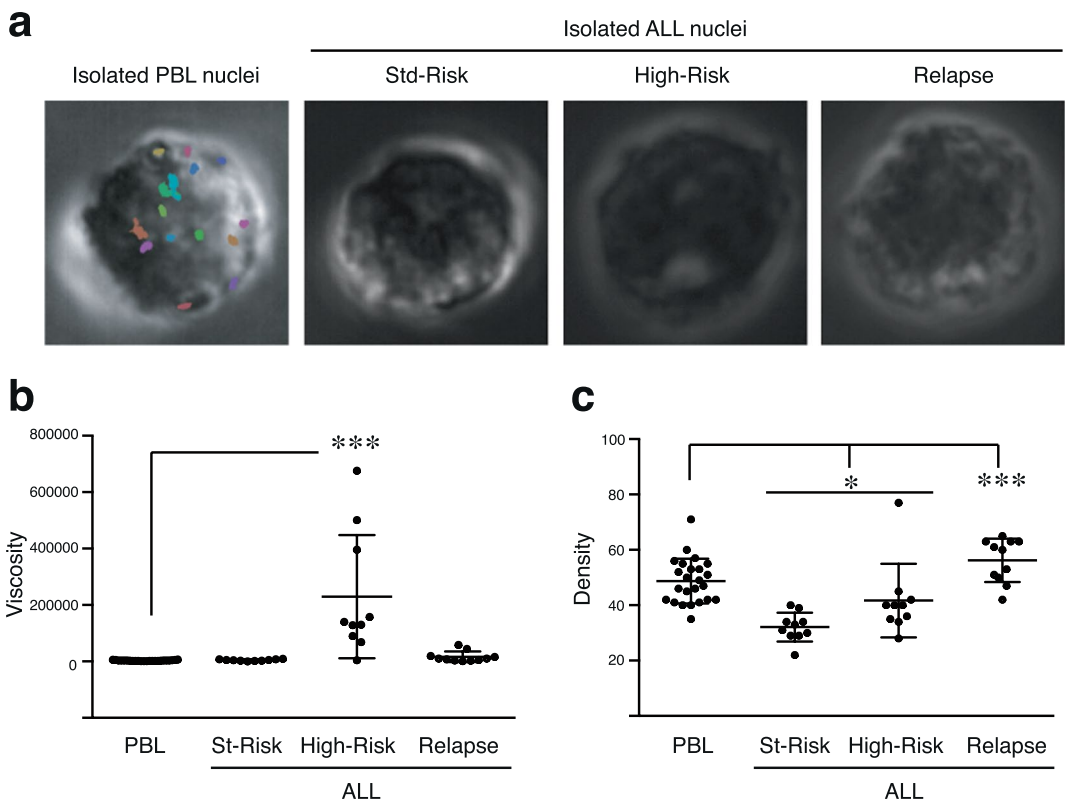

Figure 5. ALL cells present different biomechanical properties according to their clinical feature meassured by passive microrheology. (**a**) Representative phase contrast images of isolated nuclei from normal (PBL) and leukemic ALL cells. ALL cells were stratified according to SHEOP-PETHEMA 2013 in Standard- (St) or High- (High) risk groups and relapsed ALL cells. (**b**) The apparent viscosity from nuclei in Fig. 4a was determined by passive microrheology. (**c**) The optical density from nuclei in Fig. 4a was measured by passive microrheology. *P < 0.05; ***P < 0.001.

(Fig. 4c). Together, our data demonstrate the general value of MPT-SURF as a probe to detect chromatin compaction/fluidization in the nucleus of a leukemia cell.

Mechanical phenotype of isolated nuclei of primary leukemic cells. ALL patients are commonly stratified according to age, genetic abnormalities, leukocytes in blood count, type of ALL, MRD (minimal residual disease) after induction, etc[42]. To further understand the clinical relevance of MPT-SURF technique, we isolated nuclei from PBL, or cancer ALL cells from patients stratified according to SEHOP-PETHEMA (Spanish Program for the Treatment of Hematologic Diseases) 2013 protocol in standard-or high-risk groups (Fig. 5a). Isolated nuclei of high-risk group of ALL cells presented a significant higher viscosity compared to the other conditions (Fig. 5b). Then, we explored by MPT-SURF the *in situ* nuclear viscosity of intact ALL cells from patients. We observed that cells from a high-risk stratified patient presented a trend to higher nuclear viscosity than standard-risk or relapse ALL cells (Supplementary Fig. S9). Remarkably, isolated nuclei from relapsed ALL cells had higher nuclear density than normal PBL, whilst standard- and high-risk group showed significant lower nuclear density (Fig. 5c). Together, these data indicate that leukemic cells present aberrant mechanical properties in their nuclei that might be related to clinical aggressiveness and/or resistance to chemotherapy.

Discussion

Chromatin compaction depends on histone packing and intranuclear electrostatic forces[31]. Dynamic changes in chromatin structure control its organization and mobility[43], and promote auxetic nuclei[44]. Previously, several studies have defined how lamins control the nuclear stiffness and influence on several cell functions (as cell cycle, differentiation, etc.) involved in human pathologies[4–8]. Chromatin viscosity is an emerging actor that contributes to the nuclear mechanics of the cell[45]. Here, we have developed a fast and performant MPT-SURF algorithm that enables for detecting Brownian trajectories of chromatin spots and determining the viscoelastic properties associated to the chromatin configuration of isolated nuclei from normal and leukemia cells.

Nuclear isolation might influence on the chromatin structure and disrupt cytoskeletal bridges between the nucleus and the cell body. Interestingly, nuclear isolation induces a stress-stiffening in the nuclei[40]; however, it has been extensively reported that the nuclear alterations still allow to measure changes in the physical properties of nuclei isolated or in intact cells[45–47]. It has been reported different methods for single nucleus isolation that allows to study the contribution of the chromatin on the mechanical properties of the nucleus as an independent entity[48–51]. Here, we present a MPT-SURF analysis that can be used on fresh biological samples and allow us to

determine the mechanical phenotype of isolated nuclei as a parametric setting constituted by the nuclear viscosity, the stiffness and the optical density.

Although the dynamic viscosity of cells has been widely studied[52,53], the nuclear viscosity of isolated nuclei remains still quite unexplored. Here, we have focused on the local Brownian-like displacements in isolated nuclei of nuclear granules and their apparent diffusion in a soft medium within seconds. These small fluctuations were thermally driven, as deduced from the Gaussian distribution of the displacements and the viscoelastic character of heterogeneous nucleus with dense "spots" undergoing confined Brownian motion. Our results align with the rheological behavior revealed in experiments of protein mobility in chromatin measured by fluorescence correlation spectroscopy (FCS)[32]. Accordingly, previous findings support that the temperature, pH, and salt conditions control the elastic material behavior and volume changes of isolated nuclei[54]. A conceptually similar method has been used with integral nuclei of human HeLa cells using fluorescently labelled histones to track chromatin displacements[55].

We have confirmed that nuclear shrinking under Mg^{2+} addition causes significant chromatin condensation followed by a high increase of the chromatin viscosity. Conversely, Mg^{2+} depletion (by EDTA) produces visible nuclear swelling. Our results demonstrate the dynamical equivalence between the diffusing behavior of the chromatin granules tracked in both isolated and *in situ* nuclei; although MPT-SURF analysis determined that osmotic stress in living cells promoted smaller mechanical changes than in isolated nuclei. Probably, this is due to regulation mechanisms in the whole cell, through mechanosensitive ion channels able to regulate the nuclear compaction and heterochromatin formation due to changes in the composition of the extracellular medium[41]. Also, we cannot discard the contribution of the cytoskeleton in living cells, which is a major actor in nuclear deformation and strain recovery[56]. Interestingly, we did not observe statistically significant decrease of the nuclear viscosity upon EDTA addition in isolated nuclei nor intact cells, although we observed that some specimens fluidized. This difference in the average viscosity might be due to the heterogeneous distribution of the EDTA-disentangled chromatin (most possibly euchromatin that is not specifically selected in our method as mobile spots), and to the spatial distribution of the chromatin in chromosomal territories and topologically associating domains (TADs)[57]. In general, using intact cells instead of isolated nuclei present the advantage of a more physiological context, which preserves the cytoskeletal and cellular connections; although it makes more difficult to discern the contribution of each component and, in our system, to identify particular properties according the clinical stage of the sample.

It is known that the biomechanical properties of cancer cells can define their phenotype[58,59]. Cancer cells respond to physical forces presented in the tumor environment by controlling the mechanical properties of their nuclei[60]. Interestingly, invasive phenotypes of cancer cells are often softer than normal cells in order to migrate through endothelial barriers and invade other tissues[61]. Recently, it has been reported that the mechanical properties of the nucleus depend on the substrate elasticity and the invasiveness of the cancer cells[62]. In this scenario, new biophysical techniques must be implemented to obtain a quantitative diagnosis independent of the subjective view or interpretation of the pathologists[63]. We found higher nuclear viscosity of high-risk ALL cells than normal PBL. Interestingly, for nuclear density we observed lower values in Standard- and High-Risk ALL cells than in PBL, whilst the relapsed ALL cells presented an increment in the density. A plausible explanation for the differences found is that ALL cells might present an aberrant chromosomal density compared to normal PBL. The implementation of new technologies for diagnoses usually requires further validation by increasing the number of samples, using different subsets of patients and healthy donors. Together, our results present quantitative differences in the viscosity and density of isolated nuclei from leukemia cells with different prognosis. Given the clinical interest for diagnosis, our findings facilitate the possibility to develop new tools for prognosis prediction of cancer cells.

Methods

Primary samples and cell lines. The ALL cell lines Jurkat, CCRF-CEM, Reh were obtained from Dr. Ramírez and cultured in RPMI 1640 with L-glutamine and 125 μM Hepes (Sigma Aldrich, St. Louis, MO, USA) with 10% fetal bovine serum (FBS, Sigma-Aldrich). Primary human PBL were isolated from buffy coats of healthy anonymous donors (Blood Bank, Hospital Gregorio Marañón) after depletion of the monocyte fraction with CD14 microbeads. Primary samples from ALL patients under 14 years old were obtained with informed consent for research purposes, and the procedures were approved by the Institutional Review Boards of the Hospital General Universitario Gregorio Marañón (Epicon) and the Hospital Universitario Niño Jesús (R0070/15). ALL diagnosis and treatment were defined according to SEHOP-PETHEMA 2013 (Spanish Program for the Treatment of Hematologic Diseases).

Immunofluorescence. Nuclei from Jurkat cells were isolated using a hypotonic buffer A (10 mM HEPES, 10 mM KCl, 1.5 mM $MgCl_2$, 0.34 M sucrose, 10% (v/v) glycerol, 1 mM DTT and Roche protease inhibitor) and 0.5% of NP-40 followed by vortexing for 15 sec and centrifugation for 5 min at 4°C 3,500 g. Nuclei were resuspended in TKMC buffer (50 mM Tris pH 7.5, 25 mM KCl, 3 mM $MgCl_2$, 3 mM $CaCl_2$, and proteinase inhibitors) and sedimented onto poly-Lysine coated slides (Thermo Scientific). Nuclei were incubated or not with EDTA, 3 mM (swelling condition) or $MgCl_2$ 3 mM (shrinking condition) for 5 min. Then, nuclei were fixed with 4% formaldehyde in PBS (10 min), permeabilized with 0.5% Tx-100 in PBS (5 min) and stained by Hoechst 33342. For intact cells, Jurkat cells were cultured in the presence or not of EDTA (1 mM) or $MgCl_2$ (7.5 mM) for 24 h. Then, cells were analyzed by MPT-SURF or fixed, permeabilized and the nucleus stained by Hoechst 33342. Nuclear shape was analyzed by SPE confocal microscopy with an objective ACS-APO 40x NA 1.30 oil immersion. Quantification of nuclear area were determined with Fiji.

Time-lapse Video Microscopy (TLVM). Intact cells or isolated nuclei from cells cultured in suspension were washed in isotonic conditions and diluted in TKM buffer. Then, isolated nuclei were deposited onto poly-Lysine coated glass slides and imaged in a phase contrast inverted microscope (NikonEclipse2000Ti) equipped with a 100 W TI-12 DH Pillar Illuminator, an LWD 0.52 collimator, and a 100× oil immersion objective (PlanApoVC, N.A. 1.4; Nikon). Tracking movies of nuclear particles from at least 6 isolated nuclei or cells were captured with a FASTCAM SA3 camera (Photron), with an effective pixel size of 50×50 nm^2. To provide optimal signal-to-noise ratio (SNR), the movies were recorded during 10 s of tracking time at a sampling frequency of 512 Hz (5120 frames).

Multiple particle tracking of nuclear particles using Speed-Up Robust Feature detection (MPT-SURF). Time-resolved images from nuclei were analyzed with an MPT-SURF code generated with Mathematica software (Wolfram Research) available as Supplementary Information (Supplementary Notes 1–3). Dense nuclear grains were identified as highly-contrasted objects with a symmetric 2D-Gaussian intensity profile of intensity significantly larger than the averaged background (see Supplementary Note 1). The instantaneous position of every nuclear particle was identified as the position of the maximum of the fitted Gaussian profile; for a particle *i* placed in a Cartesian frame of reference, we recorded as a function of time *t*: *(i)* two-dimensional coordinate $r_i(t) = (x_i, y_i)$ (corresponding to center of the Gaussian profile), *(ii)* a circular-like diameter $D_i(t)$ (corresponding to the Gaussian full width at the half maximum), and *(iii)* the intensity $I_i(t)$ (as the integrated area of the 2D-Gaussian profile). Spot-tracer displacements between two consecutive frames were evaluated by using the SURF feature detection algorithm[30] (see Supplementary Notes 2, 3 for further description). The instantaneous centroid of these spots was evaluated as the position of the center-of-mass at a given time t, this is $r_0(t) = \sum_i r_i(t) I_i(t) / \sum_i I_i(t)$, using the optical density I_i as a weighting factor. Troubleshooting was performed by discarding spots with consecutive coordinates varying larger than a 50% of the previous displacement, and more than 10% in the apparent size characteristics (both diameter D_i and intensity I_i). Larger variations in the apparent size were interpreted as either spurious spot exchanges, or off-plane defocusing giving rise to actual 3D-contributions to the particle displacements. Finally, a coordinate drift correction was performed to the whole set of coordinates at every frame by applying a geometrical rigid transform, *via* singular-value decomposition, which maximized the alignment of the tracers between two consecutive frames and preserves both size and shape. The 2D-acceptable Brownian trajectories drift-corrected by the motion of the center of mass $r_i'(t) = r_i(t) - r_0(t)$ where then processed to get the trajectory of mean square displacements as a function of the lag time τ; for the particle *i*, these is $MSD_i(\tau) = \sum_j \left[r_i'\left(t_j + \tau\right) - r_i'\left(t_j\right) \right]^2 / n$, where the sum was calculated along a given time series $t_j = j\delta t$, with $j = 1, 2 \ldots n$ describing the discrete steps of timelength δt. Then, by exploiting the 2D-diffusion equation $MSD_i(\tau) = 4D_{eff}\tau$, the diffusion coefficient corresponding to every trajectory was computed as the slope D_{eff} of the linear fit. Further, the apparent viscosity η_{app} was estimated using the Stokes-Einstein relationship for sticking conditions, $D_{eff} = k_B T / 6\pi\eta_{app} R$, where $k_B T$ is the thermal energy, and $R = D/2$ the apparent size of the nuclear particle. The average value calculated in a given specimen over a collection of acceptable nuclear particles (normally higher than 10), was the quantity assumed with phenotyping value (average value in Fig. 1e).

Laplace-transform microrheology. The Laplace-transform must be performed to evaluate the viscoelastic modulus from the generalized fluctuation-dissipation relationship in Eq. (3). However, rather than a direct evaluation with a high computational cost and a high error from numerical approximations, we accounted both for the shear modulus moduli and the phase angle in polar notation $\widetilde{G}(i\omega) = G_d(\omega)\, exp[i\delta(\omega)]$ through the approximate analytic relation[70]; for the modulus, we get:

$$G_d(\omega) \approx \frac{2k_B T}{3\pi R \langle \Delta R^2(\tau) \rangle \, \Gamma\left(1 + \frac{d \, ln \, \langle \Delta R^2(\tau) \rangle}{d \, ln \, \tau}\right)}$$

where $\tau = 1/\omega$ and Γ being the gamma function; and for the phase:

$$\delta(\omega) \approx \frac{\pi}{2}\left(\frac{d \, lnG_d(\omega)}{dln(\omega)}\right)$$

Statistical analysis. Student t test (two tailed Mann-Whitney non-parametric test) or ANOVA (two tailed Kruskal-Wallis non-parametric test) were used for between-group analysis. For all analyses, statistical calculations were performed using Prism 6.0 Software (GraphPad Software, Inc. La Jolla, CA, USA), and p-values <0.05 were considered statistically significant.

Software availability. The software generated for the microrheological analysis is available from Dr. D. Herráez-Aguilar and F. Monroy upon request.

Written informed consent was obtained from the parents or legal guardians of all participants and from the participants themselves if aged 12 or more years.

Received: 18 March 2019; Accepted: 2 April 2020;
Published online: 21 April 2020

References

1. Zwerger, M., Ho, C. Y. & Lammerding, J. Nuclear mechanics in disease. *Annu. Rev. Biomed. Eng.* **13**, 397–428, https://doi.org/10.1146/annurev-bioeng-071910-124736 (2011).
2. Burke, B. & Stewart, C. L. Functional architecture of the cell's nucleus in development, aging, and disease. *Curr. Top. Dev. Biol.* **109**, 1–52, https://doi.org/10.1016/B978-0-12-397920-9.00006-8 (2014).
3. Ungricht, R. & Kutay, U. Mechanisms and functions of nuclear envelope remodeling. *Nat. Rev. Mol. Cell Biol.* **18**, 229–245, https://doi.org/10.1038/nrm.2016.153 (2017).
4. Swift, J. *et al*. Nuclear lamin-A scales with tissue stiffness and enhances matrix-directed differentiation. *Science* **341**, 1240104, https://doi.org/10.1126/science.1240104 (2013).
5. Swift, J. & Discher, D. E. The nuclear lamina is mechano-responsive to ECM elasticity in mature tissue. *J. Cell Sci.* **127**, 3005–3015, https://doi.org/10.1242/jcs.149203 (2014).
6. Wang, N., Tytell, J. D. & Ingber, D. E. Mechanotransduction at a distance: mechanically coupling the extracellular matrix with the nucleus. *Nat. Rev. Mol. Cell Biol.* **10**, 75–82, https://doi.org/10.1038/nrm2594 (2009).
7. Sakthivel, K. M. & Sehgal, P. A Novel Role of Lamins from Genetic Disease to Cancer Biomarkers. *Oncol. Rev.* **10**, 309, https://doi.org/10.4081/oncol.2016.309 (2016).
8. Denais, C. M. *et al*. Nuclear envelope rupture and repair during cancer cell migration. *Science* **352**, 353–358, https://doi.org/10.1126/science.aad7297 (2016).
9. Lherbette, M. *et al*. Atomic Force Microscopy micro-rheology reveals large structural inhomogeneities in single cell-nuclei. *Sci. Rep.* **7**, 8116, https://doi.org/10.1038/s41598-017-08517-6 (2017).
10. Bloomfield, V. A. DNA condensation by multivalent cations. *Biopolymers* **44**, 269–82, 10.1002/(SICI)1097-0282(1997)44:3<269::AID-BIP6>3.0.CO;2-T (1997).
11. Emanuel, M., Radja, N. H., Henriksson, A. & Schiessel, H. The physics behind the larger scale organization of DNA in eukaryotes. *Phys. Biol.* **6**, 025008, https://doi.org/10.1088/1478-3975/6/2/025008 (2009).
12. Irianto, J., Xia, Y., Pfeifer, C. R., Greenberg, R. A. & Discher, D. E. As a nucleus enters a small pore, chromatin stretches and maintains integrity, even with DNA breaks. *Biophys. J.* **112**, 446–449, https://doi.org/10.1016/j.bpj.2016.09.047 (2017).
13. Spagnol, S. T., Armiger, T. J. & Dahl, K. N. Mechanobiology of Chromatin and the Nuclear Interior. *Cell Mol. Bioeng.* **9**, 268–276, https://doi.org/10.1007/s12195-016-0444-9 (2016).
14. Mazumder, A., Roopa, T., Basu, A., Mahadevan, L. & Shivashankar, G. V. Dynamics of chromatin decondensation reveals the structural integrity of a mechanically prestressed nucleus. *Biophys. J.* **95**, 3028–3035, https://doi.org/10.1529/biophysj.108.132274 (2008).
15. Chalut, K. J. *et al*. Chromatin decondensation and nuclear softening accompany Nanog downregulation in embryonic stem cells. *Biophys. J.* **103**, 2060–2070, https://doi.org/10.1016/j.bpj.2012.10.015 (2012).
16. Stephens, A. D. *et al*. Chromatin histone modifications and rigidity affect nuclear morphology independent of lamins. *Mol. Biol. Cell* **29**, 220–233, https://doi.org/10.1091/mbc.E17-06-0410 (2018).
17. Zink, D., Fischer, A. H. & Nickerson, J. A. Nuclear structure in cancer cells. *Nat. Rev. Cancer* **4**, 677–87, https://doi.org/10.1038/nrc1430 (2004).
18. Lever, E. & Sheer, D. The role of nuclear organization in cancer. *J. Pathol.* **220**, 114–125, https://doi.org/10.1002/path.2651 (2010).
19. Papanicolaou, G. N. & Traut, H. F. The diagnostic value of vaginal smears in carcinoma of the uterus. 1941. *Arch. Pathol. Lab. Med.* **121**, 211–224, https://doi.org/10.1016/S0002-9378(16)40621-6 (1997).
20. Grys, B. T. *et al*. Machine learning and computer vision approaches for phenotypic profiling. *J. Cell Biol.* **216**, 65–71, https://doi.org/10.1083/jcb.201610026 (2017).
21. Gann, P. H. *et al*. Development of a nuclear morphometric signature for prostate cancer risk in negative biopsies. *PLoS One* **8**, e69457, https://doi.org/10.1371/journal.pone.0069457 (2013).
22. Inaba, H., Greaves, M. & Mullighan, C. G. Acute lymphoblastic leukaemia. *Lancet* **381**, 1943–1955, https://doi.org/10.1016/S0140-6736(12)62187-4 (2013).
23. Jaqaman, K. *et al*. Robust single-particle tracking in live-cell time-lapse sequences. *Nat. Methods* **5**, 695–702, https://doi.org/10.1038/nmeth.1237 (2008).
24. Chenouard, N. *et al*. Objective comparison of particle tracking methods. *Nat. Methods* **11**, 281–9, https://doi.org/10.1038/nmeth.2808 (2014).
25. Mason, T., Ganesan, K., van Zanten, J. H., Wirtz, D. & Kuo, S. C. Particle tracking microrheology of complex fluids. *Phys. Rev. Lett.* **79**, 3282–3285, https://doi.org/10.1103/PhysRevLett.79.3282 (1997).
26. Yamada, S., Wirtz, D. & Kuo, S. C. Mechanics of living cells measured by laser tracking microrheology. *Biophys. J.* **78**, 1736–1747, https://doi.org/10.1016/S0006-3495(00)76725-7 (2000).
27. Tseng, Y., Kole, T. P. & Wirtz, D. Micromechanical mapping of live cells by multiple particle tracking microrheology. *Biophys. J.* **83**, 3162–3176 (2002).
28. Vig, D. K., Hamby, A. E. & Wolgemuth, C. W. On the quantification of cellular velocity fields. *Biophys. J.* **110**, 1469–1475, https://doi.org/10.1016/j.bpj.2016.02.032, (2016).
29. Zidovska, A., Weitz, D. A. & Mitchison, T. J. Micron-scale coherence in interphase chromatin dynamics. *Proc. Natl Acad. Sci. USA* **110**, 15555–15560, https://doi.org/10.1073/pnas.1220313110 (2013).
30. Bay, H., Ess, A., Tuytelaars, T. & Van Gool, L. SURF: Speeded-up robust features. *Comput. Vis. Image Underst.* **10**, 346–359, https://doi.org/10.1016/j.cviu.2007.09.014, (2008).
31. Korolev, N., Fan, Y., Lyubartsev, A. P. & Nordenskiöld, L. Modelling chromatin structure and dynamics: status and prospects. *Curr. Opin. Struct. Biol.* **22**, 151–9, https://doi.org/10.1016/j.sbi.2012.01.006 (2012).
32. Erdel, F., Baum, M. & Rippe, K. The viscoelastic properties of chromatin and the nucleoplasm revealed by scale-dependent protein mobility. *J. Phys. Cond. Matter* **27**, 064115, https://doi.org/10.1088/0953-8984/27/6/064115 (2015).
33. Einstein, A. Zur theorie der brownschen bewegung. *Ann. Phys.* **324**, 371, https://doi.org/10.1002/andp.19063240208 (1906).
34. Frey, E. & Kroy, K. Brownian motion: A paradigm of soft matter and biological physics. *Ann. Phys.* **14**, 20–50, https://doi.org/10.1002/andp.200410132 (2005).
35. Mason, T. G. & Weitz, D. A. Optical measurements of frequency-dependent linear viscoelastic moduli of complex fluids. *Phys. Rev. Lett.* **74**, 1250–1253, https://doi.org/10.1103/PhysRevLett.74.1250 (1995).
36. Tschoegl, N.W. The Phenomenological Theory of Linear Viscoelastic Behavior: An introduction. *Springer-Verlag New York*, https://doi.org/10.1007/978-3-642-73602-5 (1989).
37. Gittes, F., Schnurr, B., MacKintosh, F. C. & Schmidt, C. F. Determining microscopic viscoelasticity in flexible and semiflexible polymer networks from thermal fluctuations. *Macromolecules* **30**, 7781–7792, https://doi.org/10.1021/ma970555n (1997).
38. Guo, M. *et al*. Probing the stochastic, motor-driven properties of the cytoplasm using force spectrum microscopy. *Cell* **158**, 822–832, https://doi.org/10.1016/j.cell.2014.06.051 (2014).
39. Chen, D. T. N., Wen, Q., Janmey, P. A., Crocker, J. C. & Yodh, A. G. Rheology of Soft Materials. *Annu. Rev. Condens. Matter Phys.* **1**, 301–322, https://doi.org/10.1146/annurev-conmatphys-070909-104120 (2010).
40. Dahl, K. N., Engler, A. J., Pajerowski, J. D. & Discher, D. E. Power-law rheology of isolated nuclei with deformation mapping of nuclear substructures. *Biophys. J. 2005* **89**, 2855–64, https://doi.org/10.1529/biophysj.105.062554 (2005).

41. Stephens, A. D., *et al*. Physicochemical mechanotransduction alters nuclear shape and mechanics via heterochromatin formation. *Mol Biol Cell*, mbcE19050286T, https://doi.org/10.1091/mbc.E19-05-0286-T, (2019).
42. Moorman, A. V. New and emerging prognostic and predictive genetic biomarkers in B-cell precursor acute lymphoblastic leukemia. *Haematologica* **101**, 407–416, https://doi.org/10.3324/haematol.2015.141101 (2016).
43. Booth-Gauthier, E. A., Alcoser, T. A., Yang, G. & Dahl, K. N. Force-induced changes in subnuclear movement and rheology. *Biophys. J.* **103**, 2423–31, https://doi.org/10.1016/j.bpj.2012.10.039 (2012).
44. Pagliara, S. *et al*. Auxetic nuclei in embryonic stem cells exiting pluripotency. *Nat. Mater.* **13**, 638–644, https://doi.org/10.1038/nmat3943 (2014).
45. Guilluy, C. *et al*. Isolated nuclei adapt to force and reveal a mechanotransduction pathway in the nucleus. *Nat. Cell Biol.* **16**, 376–81, https://doi.org/10.1038/ncb2927 (2014).
46. Verstraeten, V. L. & Lammerding, J. Experimental techniques for study of chromatin mechanics in intact nuclei and living cells. *Chromosome Res.* **16**, 499–510, https://doi.org/10.1007/s10577-008-1232-8 (2008).
47. Liu, H. *et al*. *In situ* mechanical characterization of the cell nucleus by atomic force microscopy. *ACS Nano* **8**, 3821–3828, https://doi.org/10.1021/nn500553z (2014).
48. Stephens, A. D., Banigan, E. J., Adam, S. A., Goldman, R. D. & Marko, J. F. Chromatin and lamin A determine two different mechanical response regimes of the cell nucleus. *Mol. Biol. Cell* **28**, 1984–1996, https://doi.org/10.1091/mbc.E16-09-0653 (2017).
49. Wang, P. *et al*. WDR5 modulates cell motility and morphology and controls nuclear changes induced by a 3D environment. *Proc. Natl Acad. Sci. USA* **115**, 8581–8586, https://doi.org/10.1073/pnas.1719405115 (2018).
50. Schreiner, S. M., Koo, P. K., Zhao, Y., Mochrie, S. G. & King, M. C. The tethering of chromatin to the nuclear envelope supports nuclear mechanics. *Nat. Commun.* **6**, 7159, https://doi.org/10.1038/ncomms8159 (2015).
51. Pajerowski, J. D., Dahl, K. N., Zhong, F. L., Sammak, P. J. & Discher, D. E. Physical plasticity of the nucleus in stem cell differentiation. *Proc. Natl Acad. Sci. USA* **104**, 15619–15624, https://doi.org/10.1073/pnas.0702576104 (2007).
52. Kalwarczyk, T. *et al*. Comparative analysis of viscosity of complex liquids and cytoplasm of mammalian cells at the nanoscale. *Nano Lett.* **11**, 2157–2163, https://doi.org/10.1021/nl2008218 (2011).
53. Spagnol, S. T. & Dahl, K. N. Spatially Resolved Quantification of Chromatin Condensation through Differential Local Rheology in Cell Nuclei Fluorescence Lifetime Imaging. *PLoS One* **11**, e0146244, https://doi.org/10.1371/journal.pone.0146244 (2016).
54. Chan, C. J., Li, W., Cojoc, G. & Guck, J. Volume Transitions of Isolated Cell Nuclei Induced by Rapid Temperature Increase. *Biophys. J.* **112**, 1063–1076, https://doi.org/10.1016/j.bpj.2017.01.022 (2017).
55. Ivanovska, I. L. *et al*. Cross-linked matrix rigidity and soluble retinoids synergize in nuclear lamina regulation of stem cell differentiation. *Mol. Biol. Cell* **28**, 2010–2022, https://doi.org/10.1091/mbc.E17-01-0010 (2017).
56. Wang, X. *et al*. Mechanical stability of the cell nucleus - roles played by the cytoskeleton in nuclear deformation and strain recovery. *J Cell Sci* **131**, https://doi.org/10.1242/jcs.209627 (2018).
57. Dixon, J. R., Gorkin, D. U. & Ren, B. Chromatin Domains: The Unit of Chromosome Organization. *Mol. Cell* **62**, 668–80, https://doi.org/10.1016/j.molcel.2016.05.018 (2016).
58. Kumar, S. & Weaver, V. M. Mechanics, malignancy, and metastasis: the force journey of a tumor cell. *Cancer Metastasis Rev.* **28**, 113–127, https://doi.org/10.1007/s10555-008-9173-4 (2009).
59. Lee, G. Y. & Lim, C. T. Biomechanics approaches to studying human diseases. *Trends Biotechnol.* **25**, 111–8, https://doi.org/10.1016/j.tibtech.2007.01.005 (2007).
60. Buxboim, A., Ivanovska, I. L. & Discher, D. E. Matrix elasticity, cytoskeletal forces and physics of the nucleus: how deeply do cells 'feel' outside and in? *J. Cell Sci.* **123**, 297–308, https://doi.org/10.1242/jcs.041186 (2010).
61. Wirtz, D., Konstantopoulos, K. & Searson, P. C. The physics of cancer: the role of physical interactions and mechanical forces in metastasis. *Nat. Rev. Cancer* **11**, 512–522, https://doi.org/10.1038/nrc3080 (2011).
62. Abidine, Y. *et al*. Mechanosensitivity of cancer cells in contact with soft substrates using AFM. *Biophys. J.* **114**, 1165–1175, https://doi.org/10.1016/j.bpj.2018.01.005 (2018).
63. Uhler, C. & Shivashankar, G. V. Nuclear mechanopathology and cancer diagnosis. *Trends Cancer* **4**, 320–331, https://doi.org/10.1016/j.trecan.2018.02.009 (2018).

Acknowledgements

We really appreciate the help and assistance of M. Ramírez's lab to purify primary samples from patients with ALL and L.H. Moleiro for lab training with TLVM. The confocal studies were performed in the Unidad de Microscopía Confocal (Instituto de Investigación Biomédica Gregorio Marañón). This work was supported in part by Agencia Estatal de Investigación under grants RYC-2015-18497 and SAF2017-86327-R (to J.R.M.) and FIS2015-70339C2-1-R (to F.M.), and by Comunidad de Madrid S2013/MIT-2807 and S2018/NMT-4389 (to F.M.) and Y2018/BIO-5207 to (J.R.M. and F.M.). M.R. is funded by Asociación Pablo Ugarte.

Author contributions

D.H.A. conceived and conducted the experiments, designed the software for analysis and wrote the manuscript; E.M. conducted the experiments; H.L.M. helped with software/hardware update and optimization for experimental approaches. M.R. isolated and provided the primary samples.; F.M. and J.R.M. designed the study, conceived the experiments and wrote the manuscript. All authors reviewed the manuscript.

Competing interests

The authors declare no competing interests.

Additional information

Supplementary information is available for this paper at https://doi.org/10.1038/s41598-020-63682-5.

Correspondence and requests for materials should be addressed to F.M. or J.R.-M.

Reprints and permissions information is available at www.nature.com/reprints.

Publisher's note Springer Nature remains neutral with regard to jurisdictional claims in published maps and institutional affiliations.

DISCUSIÓN

La LLA se caracteriza por la acumulación de células tumorales en sangre y su posterior infiltración en otros tejidos, como el SNC, ganglios linfáticos, médula ósea o testículos entre otros. La migración celular e invasión de otros tejidos es un proceso fundamental para la diseminación de las LLA. Para que esto ocurra es necesario que las células tengan la capacidad de adherirse y cruzar el endotelio desde los vasos sanguíneos hasta estos nichos (Sison & Brown, 2011). Las interacciones entre los receptores de las células de LLA y el microambiente en estos nichos dirigen la migración y la proliferación de las células leucémicas, promoviendo la resistencia contra las terapias convencionales y las recaídas (Chiarini et al., 2016). Los mecanismos empleados por las células de LLA para invadir tejidos son múltiples (figura 16), incluyendo la interacción de los receptores celulares (como las integrinas y los receptores de quimioquinas) con sus ligandos presentes en los nichos metastásicos y la matriz extracelular (Gómez et al., 2015; Ma et al., 2014).

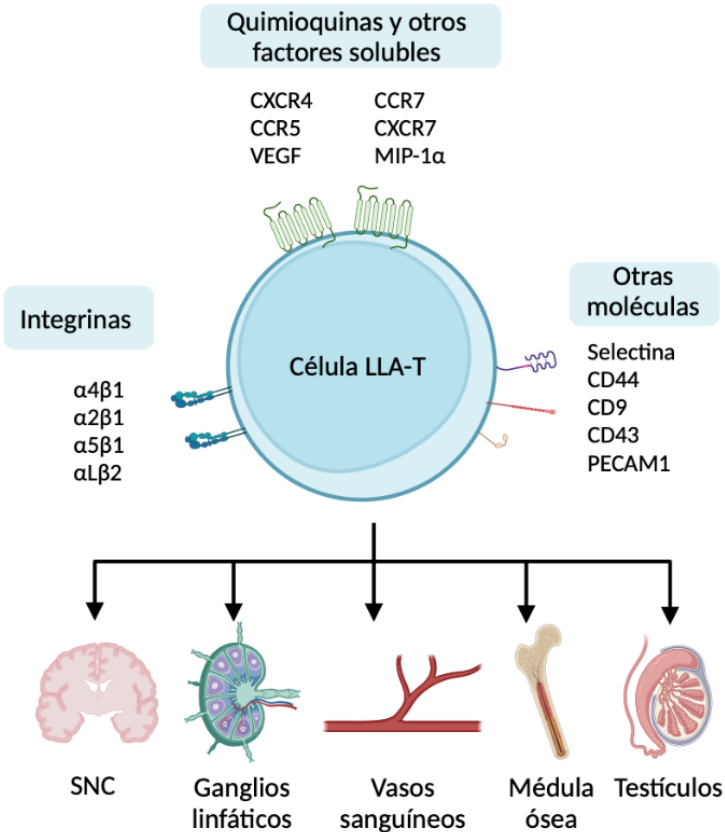

Figura 16. Mecanismos principales de la migración de las células de LLA (adaptado de Redondo-Muñoz et al., 2019). Existen múltiples receptores de superficie celular y moléculas solubles que impulsan el movimiento celular de LLA. Las células de LLA pueden permanecer en la MO o colonizar varios órganos extramedulares, como el sistema nervioso central (SNC), los ganglios linfáticos o los testículos. En general, las integrinas β1 (α4β1, α2β1, α5β1) y la integrina αLβ2 son fundamentales para el alojamiento de las células de LLA en la MO y para su infiltración en la mayoría de los órganos extramedulares. El receptor de quimioquinas CXCR4 media la infiltración de células LLA en MO, hígado, pulmón y SNC, mientras que CCR7

controla la infiltración de LLA en SNC y ganglios linfáticos. Otras moléculas que podrían contribuir a la migración de LLA incluyen MIP-1α, VEGF, PECAM-1 o CD44 (para MO).

Recientemente se ha descrito al núcleo celular como un componente celular que tiene una función fundamental en el proceso de migración (Szczesny & Mauck, 2017). El núcleo es un orgánulo celular que tiene que alterar sus propiedades físicas durante algunas funciones celulares como la expresión génica o la migración (Zwerger et al., 2011). Las anomalías en la morfología y organización nuclear ocurren en muchas patologías, y en algunos casos se ha podido utilizar como método de diagnóstico (Grys et al., 2017). Las modificaciones epigenéticas desempeñan un papel fundamental en la regulación transcripcional del ADN, y, en consecuencia, los patrones de expresión anormales conducen al desarrollo y mantenimiento de diferentes tipos de cáncer (Sharma et al., 2010). Aunque las mutaciones somáticas en muchos tumores pueden marcar el inicio de su desarrollo, estudios recientes sugieren que las alteraciones epigenéticas pueden marcar también el origen de algunos tumores, y que, en conjunto, las alteraciones genéticas y epigenéticas interactúan en todas las etapas del desarrollo y progresión del cáncer (Chi et al., 2010). Algunos patrones epigenéticos de modificación de histonas pueden actuar como factores pronósticos de algunos tumores (Yokoyama et al., 2014), como la pérdida de las marcas epigenéticas H4K16ac y H4K20me3 que está presente en muchos tipos de cáncer, como en el carcinoma cutáneo (Fraga et al., 2005) o cáncer de próstata (Behbahani et al., 2012). Otro ejemplo es metiltransferasa de H3K27 (EZH2) que ha actuado en modelos animales como supresor tumoral (Simon et al., 2012). Además, recientemente se ha descrito que la metilación de H3K9 tiene un papel determinante en la supervivencia en LMA (Monaghan et al., 2019). En el caso de la LLA se ha comprobado que algunas modificaciones de histonas pueden tener un papel importante en su desarrollo y progresión (Fathi et al., 2020). Por todo ello, en esta tesis hemos querido estudiar el papel de una de estas modificaciones epigenéticas (H3K9me3) y comprobar si los mecanismos implicados en la metilación de esta histona pudieran conducir a alguna posible diana terapéutica para el tratamiento de la LLA. Como mencionamos en la figura 18, las señales que inducen la migración e invasión de los linfocitos se basan fundamentalmente en la activación por quimioquinas y en la adhesión mediada por receptores linfocitarios, por lo que nos planteamos cómo podrían relacionarse estos estímulos con los cambios epigenéticos y nucleares característicos de la LLA.

Las quimioquinas son una familia de moléculas que gobiernan la localización de leucocitos a diferentes órganos, incluido el SNC (Gómez et al., 2015). Recientemente se ha visto, que las células de un órgano específico pueden secretar quimioquinas que reclutan a leucocitos que expresan el receptor específico en sus membranas (Zlotnik et al., 2011). Además, se ha demostrado que las quimioquinas pueden proporcionar un apoyo antiapoptótico a las células tumorales, prolongando su supervivencia y potenciando la resistencia a la quimioterapia (Rollins, 2006). En estudios realizados sobre los niveles de expresión de receptores de quimioquinas en pacientes con recaídas en LLA, se ha visto que hay algunos receptores de quimioquinas que están significativamente más altos que otros, como son CXCR3 (Gómez et al.,

2015) y CXCR4 (Pitt et al., 2015). Como ya hemos visto en la introducción, CXCR4 es el receptor principal de CXCL12, el cuál es el principal quimioatrayente para las células madre hematopoyéticas (HSC) en el microambiente de la médula ósea, y desempeña un papel fundamental en la localización, proliferación y supervivencia de las células de LLA en la médula ósea, el hígado, el SNC, etc. (Agarwal et al., 2016). Dado que tanto CXCL12 como el núcleo celular son factores claves en la invasión y progresión de la LLA, nos planteamos si CXCL12 pudiese tener alguna relación con cambios epigenéticos que estuvieran modificando la morfología y deformabilidad del nuclear, afectando así a la migración de las células de LLA. En nuestros resultados observamos que al estimular a las células de LLA con CXCL12, se induce un aumento de la metilación de H3K9 en minutos en las células de LLA-T que no ocurre en las células de LLA-B. Estas diferencias entre las LLA-T y B sugieren que ambos linajes estarían usando diferentes mecanismos en la migración para infiltrarse en otros tejidos y que para ello estarían empleando distintas vías epigenéticas. Algunas diferencias en la etapa epigenética entre ambos linajes de LLA ya han sido descritas, como la hipermetilación de los factores de Notch (Kuang et al., 2013) o la respuesta al tratamiento con decitabina (desmetilación del ADN) de las células de LLA-B pero no de T (Roolf et al., 2018).

Niveles altos de expresión de CXCR4 se asocian con una infiltración extramedular en pacientes pediátricos, y, por lo tanto, con peor pronóstico (Hong et al., 2021). Se ha demostrado que la localización nuclear de CXCR4 desempeña un papel fundamental en la metástasis y en un mal pronóstico en múltiples tipos de cáncer (Bao et al., 2019). Además, se ha estudiado como CXCR4 está implicado en algunos mecanismos de regulación epigenética en algunos tumores, como en el cáncer de mama o el melanoma (Ramos et al, 2011). Nuestros resultados revelan que el bloqueo de CXCR4 es capaz de inhibir la metilación de H3K9 inducida por CXCL12. Actualmente se conoce que el receptor CXCR7 también tiene afinidad por CXCL12 (Bachelerie et al., 2014), y se ha sugerido que la heterodimerización de CXCR4 y CXCR7 es un mecanismo para modular la función de CXCR4 en algunas leucemias (Decaillot et al., 2011; Melo et al., 2014). Sin embargo, aunque se ha estudiado que CXCR7 correlaciona en muchos casos con cambios en la respuesta de CXCL12 durante algunos procesos de tumorigénesis (Levoye et al., 2009), no hemos encontrado ningún efecto significativo en el que CXCR7 pueda estar implicado en la metilación de H3K9 inducida por CXCL12. A parte de que la afinidad de CXCL12 por CXCR4 es 10 veces mayor que por CXCR7 (Burns et al., 2006), recientemente se ha estudiado que CXCR7 podría cooperar con CXCR4 para formar heterodímeros. El heterodímero CXCR4/CXCR7 impulsa la tumorigénesis mediante la regulación de la demetilasa JMJD2DA que induce la desmetilación de H3K9 y H3K36 en LLA (Song et al, 2019), lo que encajaría con nuestros resultados de que el incremento de la metilación de H3K9 en las células de LLA-T es independiente de la señalización de CXCR7.

El eje CXCR4/CXCL12 promueve la migración celular a través de múltiples vías de señalización, incluida la activación de PKC. Se ha descrito que la migración inducida por CXCL12 de progenitores CD34+ y de células LLA-B depende de la activación de PKC, y que la isoforma PKC-ζ atípica induce la motilidad de las células progenitoras (Wang et al., 2000). También se ha

demostrado que las isoformas PKC-α y PKC-β están implicadas en la quimiotaxis, proliferación y diferenciación de las células progenitoras dentro de la MO (Petit et al., 2005). Con nuestros resultados hemos comprobado que al bloquear las PKC convencionales disminuye la metilación de H3K9 inducida por CXCL12 en las células de LLA-T. Las PKC convencionales poseen en la región reguladora el dominio C2 de unión a calcio, el cual es necesario para la activación de la enzima (Steingberg, 2008). Curiosamente, el receptor de quimioquinas CXCR7 no desencadena la movilización de calcio intracelular, sin embargo, CXCR4 sí (Levoye et al., 2008). Todo esto encaja con nuestros resultados descritos anteriormente sobre la independencia de CXCR7 en la metilación de H3K9 inducida por CXCL12. PMA y CXCL12 son dos potentes activadores de la adhesión y migración de los linfocitos T, pero se ha descubierto que inducen distinta morfología y migración en células T (Wei et al., 2014). Nuestros datos muestran que CXCL12 induce un aumento de la metilación de H3K9 solo en células de LLA-T, sin embargo, PMA induce el aumento de H3K9me2/3 tanto en células de LLA-T como LLA-B. Esto sugiere que la activación de la vía de PKC podría ser suficiente para inducir este cambio epigenético en ambos tipos de células de LLA, sin embargo, activar este cambio a través de CXCL12 solo se puede dar en las células de LLA-T. También hemos comprobado que el bloqueo de la actividad de PKC convencionales reducía la migración en respuesta a CXCL12 de las células de LLA-T. Se ha descrito que la mayoría de las isoformas de las PKC se encuentran a nivel citoplasmático (Wei et al., 2014), pero quisimos estudiar la localización de estas PKC convencionales buscando si alguna de ella destacaba a nivel nuclear. Observamos que mientras PKCα presentaba una localización citoplasmática exclusivamente, PKCβ presentaba tanto una localización citoplasmática como nuclear. Ya se había descrito otros casos en los que otras isoformas de PKC presentaban una translocación nuclear (Poli et al., 2017). El abordaje de como estas PKC nucleares llevan a cabo funciones reguladoras a nivel de la expresión génica podría representar una posible diana terapéutica en pacientes con LLA.

La metilación de H3K9 es un marcador canónico de heterocromatina, por lo que está implicada en el silenciamiento génico y la represión transcripcional (Esteller, 2008). Mediante el estudio por ChIP-seq comprobamos que CXCL12 induce un incremento de los picos de H3K9me3 en todo el genoma, pero sin una correlación significativa a nivel transcripcional, lo que sugiere que la importancia de este cambio epigenético podría ser más determinante en la mecánica nuclear que en a nivel de transcripción génica. Previamente ya había sido descrito que los cambios en la estructura de la cromatina son necesarios como función protectora del material genético en respuesta a las deformaciones celulares (Nava et al., 2020). Al comprobar que el aumento de la metilación de H3K9 se daba en todo el genoma, decidimos estudiar como estaba afectando la inducción con CXCL12 al nivel de compactación de la cromatina a nivel global. Comprobamos que los cambios en la cromatina inducidos por CXCL12 tienen un impacto directo en las propiedades mecánicas y en la deformabilidad del núcleo en células de LLA-T, al alterar el tratamiento con CXCL12 los valores de respuesta mecánicos debido a fuerzas externas. Estos resultados se correlacionan con estudios anteriores donde se había comprobado como marcas epigenéticas características de células cancerosas como H3K9me3, provocaban que las

deformaciones mecánicas indujeran la ruptura nuclear y daños en el ADN (Stephen et al., 2017). Además, también hemos visto que estos cambios en la compactación de la cromatina inducidos por CXCL12 son capaces de provocar cambios en la profileración en las células de LLA, por lo que CXCL12 estaría siendo un apoyo importante a la supervivencia y proliferación de las células de LLA, como ya se había comprobado previamente (Bendall et al., 2005).

Teniendo en cuenta la importancia de la metilación de H3K9 en las células de LLA, nos resultó interesante estudiar moduladores de este marcador epigenético como posible estrategia terapéutica. La metilación en H3K9 por las metiltransferasas G9a y SUV39H1 está asociada con la inhibición de genes supresores de tumores (Lai et al., 2015), por ello, numerosos estudios lo las han propuesto como posibles dianas terapéuticas contra algunos tipos de cáncer (Saha & Muntean, 2021). Además, se ha estudiado cómo algunas de estas metiltransferasas están implicadas en la progresión y migración de las células leucémicas, (Madrazo et al., 2018) (Chu et al., 2020). G9a y SUV39h1 dos metiltransferasas de H3K9 que están implicadas en el desarrollo de los linfocitos y se encuentra sobreexpresada en muchos tipos de tumores. En los últimos años se ha descrito cómo ambas metiltransferasas están implicadas en algunos tipos de leucemias agudas, por ejemplo, en el caso de G9a se ha demostrado cómo el tratamiento con BIX-01294 (inhibidor de G9a) inhibe la proliferación e induce la apoptosis en células de LLA-T (Huang et al., 2017). En nuestros resultados, hemos demostrado que bloqueando ambas metiltransferasas inhibimos el aumento de metilación en H3K9 y la compactación de la cromatina inducida por CXCL12. La condensación de la cromatina tiene un papel estructural durante el movimiento y la morfología del núcleo, que son necesarios para una migración celular eficiente (Gerlitz & Bustin, 2010). Las constricciones nucleares están relacionadas con la migración celular e implican la redistribución de los componentes nucleares, incluidos los marcadores de histonas (Irianto et al., 2017). Al estudiar como afectaba a las células de LLA-T la estimulación con CXCL12 vimos que las células que están migrando presentan unos niveles de metilación de H3K9 mayores en las zonas que están sometidas a la compresión nuclear activa, lo que encajaría con nuestros resultados previos ya que serían las zonas con mayor grado de compactación de la cromatina. Además, hemos visto que tanto en las células de LLA-T como B se produce una redistribución del marcador H3K9me2/3 en el frente nuclear de las células en migración, esto sugiere que esta redistribución es independiente de la respuesta a CXCL12 y es consecuencia del proceso de migración, ya se había estudiado que el proceso de la migración celular causa daños en el ADN y afecta al ciclo células de las células tumorales (Pfeifer et al., 2018). Comprobamos mediante ensayos de migración a través de poros y microcanales con constricciones, cómo era posible bloquear la migración de las células de LLA-T inducida por CXCL12 con inhibidores de las metiltransferasas G9a y SUV39H1. Nuestros resultados en ensayos *in vivo* demuestran que la inhibición de la actividad de G9a y SUV39H1 reduce la capacidad de las células de LLA-T de llegar a la médula ósea y al bazo. Previamente ya se había descrito en distintos estudios cómo la inhibición de ambas metiltransferasas podía aumentar la supervivencia en los modelos *in vivo* en distintos tipos de leucemias (San José-Enériz et al., 2017) y frenar el desarrollo y la metástasis en otros tipos de tumores como el de mama (Dong et a., 2012). Dado que la metilación de H3K9

inducida por CXCL12 regula la migración celular y la deformabilidad nuclear de LLA-T, nuestros resultados sugieren que las metiltransferasas de H3K9, G9a y SUV39H1 podrían convertirse en unas dianas terapéuticas interesantes para bloquear la infiltración y el desarrollo de la LLA-T.

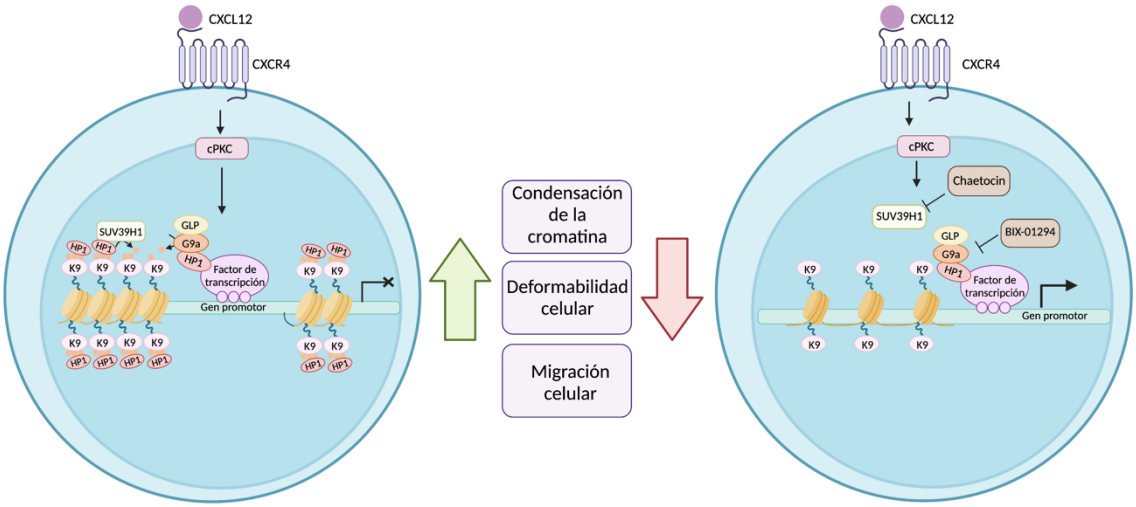

Figura 17. Cambios epigenéticos producidos por CXCL12 en células de LLA-T y como afecta al comportamiento celular.

Viendo el importante papel que tienen las metiltransferasas de H3K9 en la migración de las células de LLA-T tanto en modelos *in vitro* como *in vivo*, nos planteamos cómo podrían estar ocurriendo el proceso de extravasación de los vasos sanguíneos de las células de LLA. Este proceso es conocido como migración transendotelial (MTE) (Muller et al., 2016). Durante este proceso se reorganiza la estructura de la cromatina y cambian las propiedades viscoelásticas y la rigidez del núcleo, lo que favorece la migración de estas células 2D y 3D (Zhang et al., 2016). Hemos observamos como las células silenciadas o inhibidas para G9a con incapaces de atravesar la barrera endotelial, y además presentan un aumento significativo del área. La MTE de células normales y leucémicas involucra a varias moléculas adhesivas como selectinas, VCAM-1, ICAM-1, entre otras (Ley et al., 2007). Hasta ahora, se había demostrado como algunos tratamientos que tienen como diana terapéutica estas moléculas de adhesión, como Natalizumab (inhibición de VLA-4 con anticuerpos bloqueadores), podían aplicarse a terapias convencionales para frenar la diseminación de las células leucémicas y mejorar la supervivencia en modelos in vivo (Hsieh et al., 2013). Sin embargo, en un estudio realizado recientemente en el que han usado un fármaco antisentido de VLA-4 no se han obtenido resultados *in vivo* que puedan traducirse como una opción terapéutica para los pacientes con LLA (Duchartre et al., 2017). Teniendo en cuenta tanto la implicación de G9a como de la integrina VLA-4 en la migración transendotelial nos planteamos la posible relación que podría haber entre ambas. Nuestros resultados indican que hay una correlación significativa entre VLA-4 y G9a en los pacientes infantiles con LLA, que no ocurre en donantes sanos. Cuando segregamos los pacientes por grupos de riesgo observamos una tendencia opuesta entre las expresiones de ambas moléculas, la expresión alta de VLA-4 se

asocia con los pacientes de alto riesgo, sin embargo, con la expresión de G9a ocurre lo contrario. En el caso de los pacientes de riesgo intermedio si presentan una correlación positiva entre la expresión de G9a y VLA-4. Esta tendencia opuesta en la expresión de ambas moléculas nos lleva a pensar que podría ser más importante en la LLA la conexión funcional que existe entre ambas moléculas, que sus niveles de expresión. Curiosamente, en otro estudio publicado (Zhang et al., 2016) han demostrado que G9a se asocia con la lámina B1 cuando las células se cultivan sobre VCAM1 (principal ligando de VLA-4), por lo que la una relación entre G9a y VLA-4 podría vincularse a través de la envoltura nuclear y la cromatina, y contribuir a los cambios de las propiedades físicas del núcleo.

Ya hemos dicho que el núcleo, debido a su gran tamaño y su rigidez, actúa como barrera física cuando las células encuentran poros de un tamaño más pequeño al de su diámetro nuclear, produciendo que la migración sea menos efectiva. El tamaño y la rigidez del núcleo van a depender de los niveles de las proteínas de la lámina nuclear A/C y de la organización de la cromatina (McGregor et al., 2016). Se ha demostrado que G9a es capaz de regular distintos receptores celulares, y entre ellos se encuentran las integrinas (Tan et al., 2014). Por ello, el efecto que observábamos al inhibir G9a sobre la migración podría estar mediado por cambios en la transcripción de los genes, la deformabilidad nuclear y los niveles de señales intracelulares. Hemos visto en esta tesis que los cambios en la morfología inducidos por el silenciamiento o inhibición de G9a no se corresponden con cambios en la expresión de la integrina ni en la polimerización de F actina, sin embargo, si podrían tener un papel importante en la migración celular. Nuestros resultados demuestran que la función de G9a es fundamental para la migración de las células de LLA a través de tamaños de poros que requieren de una alta deformabilidad nuclear. Por lo tanto, los mecanismos inducidos por G9a y sus conexiones con el citoesqueleto para generar una gran deformabilidad nuclear serían atractivos para abordar la diseminación de la leucemia y una mayor evaluación preclínica de los inhibidores de G9a.

La capacidad de deformación del núcleo celular, como ya hemos mencionado en varias ocasiones, es de vital importancia en el proceso de migración de la LLA, por lo que quisimos valorar si podría ser un parámetro a valorar a nivel diagnostico. Hasta ahora hemos estudiado como se estaban produciendo estas modificaciones a nivel molecular, sin embargo, también nos planteamos estudiar las propiedades biomecánicas nucleares para tener una visión más intregadora de este proceso. El núcleo celular está compuesto fundamentalmente por la cromatina, los componentes nucleoesqueléticos y el nucleoplasma, los cuales están envueltos por láminas y membranas nucleares. La compactación de la cromatina depende del empaquetamiento de las histonas y de las fuerzas electrostáticas intranucleares (Korolev et al., 2012). Hasta hace unos años, la mayoría de los estudios relacionaban la rigidez y otras propiedades biomecánicas del núcleo celular con las láminas que rodean al resto de componentes nucleares (Swift et al., 2013; Denais et al., 2016). Sin embargo, otros estudios emergentes han situado a la cromatina como el componente nuclear encargado de la viscosidad del núcleo, y por tanto a las propiedades biomecánicas de la célula (Guilluy et al., 2014; Stephens

et al., 2018). Debido a que en los linfocitos el núcleo celular es de gran tamaño en proporción al resto del cuerpo celular, decidimos estudiar las propiedades biomecánicas nucleares de células de diferentes subtipos de LLA y compararla con linfocitos sanos. Para ello desarrollamos un algoritmo MPT-SURF que permite detectar las trayectorias brownianas de puntos de cromatina y determinar las propiedades viscoelásticas asociadas a la cromatina. Algunos parámetros biofísicos como la viscosidad han sido estudiados en múltiples ocasiones tanto a nivel celular (Kalwarczyk et al., 2011; Spagnol & Dahl, 2016), como a nivel nuclear (Guilluy et al., 2014). Para realizar estos ensayos hemos realizado un aislamiento nuclear previo, ya que pese a que se ha demostrado que el aislamiento nuclear induce un endurecimiento por estrés en los núcleos (Dahl et al., 2005), se ha visto que es posible medir cambios en las propiedades físicas tanto en núcleos aislados como en células intactas (Verstraeten & Lammerding, 2008). Para confirmar que mediante el análisis MTP-SURF íbamos a ser capaces de determinar cambios mecánicos en los núcleos estudiados, tanto aislados como en células intactas, les provocamos cambios sometiéndolos a estrés osmótico. Está descrito que la adición o privación de cationes provoca un cambio en la conformación de la cromatina y en el tamaño del núcleo celular (Allahverdi et al., 2015). Como esperábamos, hemos observamos que mediante la adicción de Mg^{2+} se provoca la condensación de la cromatina y, por tanto, una reducción del tamaño nuclear y un aumento significativo de la viscosidad de la cromatina. Por el contrario, el agotamiento de Mg^{2+} producido por la adicción de EDTA provoca una hinchazón nuclear; aunque sin cambios significativos de la viscosidad nuclear. Probablemente esto ocurra debido a la distribución heterogénea de la cromatina descondensada con EDTA, y a otros factores nucleares que puedan afectar la viscosidad nuclear.

Distintos autores han postulado que las propiedades biomecánicas de las células tumorales pueden definir su fenotipo (Kumar & Weaver, 2009). Una vez validada nuestra aproximación experimental, analizamos muestras primarias de pacientes con intención de determinar cambios biofísicos asociados al fenotipo o características clínicas. Hemos obtenido una viscosidad significativamente mayor en las células de LLA de alto riesgo que en linfocitos normales. En cuanto a la densidad nuclear, también observamos valores bajos en las células de LLA de riesgo estándar y de alto riesgo, mientras que las células de pacientes de LLA tras recaída presentaban unos valores más altos. Nuestros resultados confirman estudios realizados previamente, donde se había demostrado diferencias en las propiedades mecánicas de células normales y tumorales; mostrando que estas últimas son más blandas y con un mayor potencial metastásico (Cross et al., 2007; Wirtz et al., 2011). Además, una explicación plausible de las diferencias encontradas es que las células de LLA podrían presentar una densidad cromosómica aberrante en comparación con el PBL normal. Por lo tanto, nuestros resultados presentan diferencias cuantitativas en las viscosidad y densidad en los núcleos asilados de diferentes fenotipos de LLA comparados con PBL sanos. Y esto, podría facilitar la posibilidad de desarrollar nuevas herramientas para la predicción del pronóstico de células tumorales.

CONCLUSIONES

1. La quimioquina CXCL12 induce la metilación de H3K9 de forma rápida y reversible tanto en pacientes como en líneas celulares de LLA- T, pero no en LLA-B.

2. La metilación de H3K9 inducida por CXCL12 se produce a nivel global en todo el genoma, pero sin cambios significativos a nivel transcripcional.

3. La metilación de H3K9 inducida por CXCL12 provoca la condensación de la cromatina y un cambio en las propiedades mecánicas y la deformabilidad del núcleo de células de LLA-T.

4. El receptor de quimioquinas CXCR4 es el receptor clave en el proceso de metilación de H3K9 inducida por CXCL12. Además, la actividad de PKC convencionales resulta necesaria para que tengan lugar estos cambios nucleares en las células de LLA-T.

5. Las metiltransferasas G9a y SUV39H1 controlan los cambios epigenéticos y la compactación de la cromatina inducida por CXCL12 en células de LLA-T.

6. La inhibición de las metiltransferasas de H3K9 afecta a la deformabilidad nuclear inducida por CXCL12 y reduce la migración de células LLA-T in vitro y en modelos in vivo.

7. Existe una correlación entre la expresión de la integrina VLA-4 y la metiltransferasa G9a en pacientes pediátricos con LLA.

8. La inhibición de G9a interrumpe la polaridad y la capacidad celular para extravasar barreras endoteliales o atravesar espacios estrechos en células de LLA.

9. El análisis MPT-SURF es capaz de detectar cambios en la compactación de la cromatina midiendo las propiedades viscoelásticas del núcleo celular en células de LLA sometidas a estrés osmótico.

10. Las células leucémicas presentan propiedades mecánicas aberrantes en sus núcleos que podrían estar relacionadas con su agresividad clínica y su resistencia a la quimioterapia.

11. Las células de LLA presentan diferencias cuantitativas en la viscosidad y densidad de sus núcleos dependiendo de su fenotipo.

BIBLIOGRAFÍA

1. Adam, S. A. (2017). The nucleoskeleton. *Cold Spring Harbor Perspectives in Biology*, *9*(2). https://doi.org/10.1101/cshperspect.a023556

2. Agarwal, P., Li, H., Paterson, A. J., He, J., Nagasawa, T., & Bhatia, R. (2016). Role of CXCL12-expressing bone marrow populations in leukemic stem cell regulation. *Blood*, *128*(22), 26–26. https://doi.org/10.1182/blood.v128.22.26.26

3. Aifantis, I., Raetz, E., & Buonamici, S. (2008). Molecular pathogenesis of T-cell leukaemia and lymphoma. *Nature Reviews. Immunology*, *8*(5), 380–390. https://doi.org/10.1038/nri2304

4. Allahverdi, A., Chen, Q., Korolev, N., & Nordenskiöld, L. (2015). Chromatin compaction under mixed salt conditions: opposite effects of sodium and potassium ions on nucleosome array folding. *Scientific Reports*, *5*(1), 8512. https://doi.org/10.1038/srep08512

5. Arber, D. A., Orazi, A., Hasserjian, R., Thiele, J., Borowitz, M. J., Le Beau, M. M., Bloomfield, C. D., Cazzola, M., & Vardiman, J. W. (2016). The 2016 revision to the World Health Organization classification of myeloid neoplasms and acute leukemia. *Blood*, *127*(20), 2391–2405. https://doi.org/10.1182/blood-2016-03-643544

6. Aristizabal, M. J., Anreiter, I., Halldorsdottir, T., Odgers, C. L., McDade, T. W., Goldenberg, A., Mostafavi, S., Kobor, M. S., Binder, E. B., Sokolowski, M. B., & O'Donnell, K. J. (2020). Biological embedding of experience: A primer on epigenetics. *Proceedings of the National Academy of Sciences of the United States of America*, *117*(38), 23261–23269. https://doi.org/10.1073/pnas.1820838116

7. Baccarelli, A., & Bollati, V. (2009). Epigenetics and environmental chemicals. *Current Opinion in Pediatrics*, *21*(2), 243–251. https://doi.org/10.1097/mop.0b013e32832925cc

8. Bachelerie, F., Ben-Baruch, A., Burkhardt, A. M., Combadiere, C., Farber, J. M., Graham, G. J., Horuk, R., Sparre-Ulrich, A. H., Locati, M., Luster, A. D., Mantovani, A., Matsushima, K., Murphy, P. M., Nibbs, R., Nomiyama, H., Power, C. A., Proudfoot, A. E. I., Rosenkilde, M. M., Rot, A., … Zlotnik, A. (2014). International Union of Basic and Clinical Pharmacology. [corrected]. LXXXIX. Update on the extended family of chemokine receptors and introducing a new nomenclature for atypical chemokine receptors. *Pharmacological Reviews*, *66*(1), 1–79. https://doi.org/10.1124/pr.113.007724

9. Bannister, A. J., & Kouzarides, T. (2005). Reversing histone methylation. *Nature*, *436*(7054), 1103–1106. https://doi.org/10.1038/nature04048

10. Bannister, A. J., & Kouzarides, T. (2011a). Regulation of chromatin by histone modifications. *Cell Research*, *21*(3), 381–395. https://doi.org/10.1038/cr.2011.22

11. Bannister, A. J., & Kouzarides, T. (2011b). Regulation of chromatin by histone modifications. *Cell Research*, *21*(3), 381–395. https://doi.org/10.1038/cr.2011.22

12. Bao, Y., Wang, Z., Liu, B., Lu, X., Xiong, Y., Shi, J., Li, P., Chen, J., Zhang, Z., Chen, M., Wang, L., & Wu, Z. (2019). A feed-forward loop between nuclear translocation of CXCR4 and HIF-1α promotes renal cell carcinoma metastasis. *Oncogene*, *38*(6), 881–895. https://doi.org/10.1038/s41388-018-0452-4

13. Barreiro, O., & Sánchez-Madrid, F. (2009a). Molecular basis of leukocyte-endothelium interactions during the inflammatory response. *Revista Espanola de Cardiologia*, *62*(5), 552–562. https://doi.org/10.1016/s1885-5857(09)71837-7

14. Barreiro, O., & Sánchez-Madrid, F. (2009b). Molecular basis of leukocyte–endothelium interactions during the inflammatory response. *Revista Espanola de Cardiologia (English Ed.)*, *62*(5), 552–562. https://doi.org/10.1016/s1885-5857(09)71837-7

15. Barreiro, O., Vicente-Manzanares, M., Urzainqui, A., Yáñez-Mó, M., & Sánchez-Madrid, F. (2004). Interactive protrusive structures during leukocyte adhesion and transendothelial migration. *Frontiers in Bioscience*, *9*(1–3), 1849–1863. https://doi.org/10.2741/1285

16. Bassan, R., & Hoelzer, D. (2011). Modern therapy of acute lymphoblastic leukemia. *Journal of Clinical Oncology: Official Journal of the American Society of Clinical Oncology*, *29*(5), 532–543. https://doi.org/10.1200/JCO.2010.30.1382

17. Behbahani, T. E., Kahl, P., von der Gathen, J., Heukamp, L. C., Baumann, C., Gütgemann, I., Walter, B., Hofstädter, F., Bastian, P. J., von Ruecker, A., Müller, S. C., Rogenhofer, S., & Ellinger, J. (2012). Alterations of global histone H4K20 methylation during prostate carcinogenesis. *BMC Urology*, *12*(1), 5. https://doi.org/10.1186/1471-2490-12-5

18. Belson, M., Kingsley, B., & Holmes, A. (2007). Risk factors for acute leukemia in children: A review. *Environmental Health Perspectives*, *115*(1), 138–145. https://doi.org/10.1289/ehp.9023

19. Bendall, L. (2005). Chemokines and their receptors in disease. *Histology and Histopathology*, *20*(3), 907–926. https://doi.org/10.14670/HH-20.907

20. Bendall, L. J., Baraz, R., Juarez, J., Shen, W., & Bradstock, K. F. (2005). Defective p38 mitogen-activated protein kinase signaling impairs chemotaxic but not proliferative responses to stromal-derived factor-1alpha in acute lymphoblastic leukemia. *Cancer Research*, *65*(8), 3290–3298. https://doi.org/10.1158/0008-5472.CAN-04-3402

21. Bene, M. C., Castoldi, G., Knapp, W., Ludwig, W. D., Matutes, E., Orfao, A., & van't Veer, M. B. (1995). Proposals for the immunological classification of acute leukemias. European Group for the Immunological Characterization of Leukemias (EGIL). *Leukemia*, *9*(10), 1783–1786. https://pubmed.ncbi.nlm.nih.gov/7564526/

22. Bennett, J. M., Catovsky, D., Daniel, M. T., Flandrin, G., Galton, D. A., Gralnick, H. R., & Sultan, C. (1976). Proposals for the classification of the acute leukaemias. French American-British (FAB) co-operative group. *British Journal of Haematology*, *33*(4), 451–458. https://doi.org/10.1111/j.1365-2141.1976.tb03563.x

23. Bone, C. R., & Starr, D. A. (2016). Nuclear migration events throughout development. *Journal of Cell Science*, *129*(10), 1951–1961. https://doi.org/10.1242/jcs.179788

24. Brunning, R. D. (2003). Classification of acute leukemias. *Seminars in Diagnostic Pathology*, *20*(3), 142–153. https://doi.org/10.1016/s0740-2570(03)00031-5

25. Bule, P., Aguiar, S. I., Aires-Da-Silva, F., & Dias, J. N. R. (2021). Chemokine-directed tumor microenvironment modulation in cancer immunotherapy. *International Journal of Molecular Sciences*, *22*(18), 9804. https://doi.org/10.3390/ijms22189804

26. Buonamici, S., Trimarchi, T., Klinakis, A., Reavie, L., Mar, B. G., Gehrie, E., Kuan, E. L., Randolph, G. J., Bromberg, J., & Aifantis, I. (2008). Knockdown of CCR7 or its ligands causes a loss of central nervous system involvement in Notch1 induced T-ALL. *Blood*, *112*(11), 199–199. https://doi.org/10.1182/blood.v112.11.199.199

27. Buonamici, S., Trimarchi, T., Ruocco, M. G., Reavie, L., Cathelin, S., Mar, B. G., Klinakis, A., Lukyanov, Y., Tseng, J.-C., Sen, F., Gehrie, E., Li, M., Newcomb, E., Zavadil, J., Meruelo, D., Lipp, M., Ibrahim, S., Efstratiadis, A., Zagzag, D., … Aifantis, I. (2009). CCR7 signalling as an essential regulator of CNS infiltration in T-cell leukaemia. *Nature*, *459*(7249), 1000–1004. https://doi.org/10.1038/nature08020

28. Bürger, B., Zimmermann, M., Mann, G., Kühl, J., Löning, L., Riehm, H., Reiter, A., & Schrappe, M. (2003). Diagnostic cerebrospinal fluid examination in children with acute lymphoblastic leukemia: significance of low leukocyte counts with blasts or traumatic lumbar puncture. *Journal of Clinical Oncology: Official Journal of the American Society of Clinical Oncology*, *21*(2), 184–188. https://doi.org/10.1200/JCO.2003.04.096

29. Campana, D. (2012). Minimal residual disease monitoring in childhood acute lymphoblastic leukemia. *Current Opinion in Hematology*, *19*(4), 313–318. https://doi.org/10.1097/moh.0b013e3283543d5c

30. Casciello, F., Windloch, K., Gannon, F., & Lee, J. S. (2015). Functional role of G9a histone methyltransferase in cancer. *Frontiers in Immunology*, *6*, 487. https://doi.org/10.3389/fimmu.2015.00487

31. Chambers, J., & Rabbitts, T. H. (2015). LMO2 at 25 years: a paradigm of chromosomal translocation proteins. *Open Biology*, *5*(6), 150062. https://doi.org/10.1098/rsob.150062

32. Chang, B., Chen, Y., Zhao, Y., & Bruick, R. K. (2007a). JMJD6 is a histone arginine demethylase. *Science (New York, N.Y.)*, *318*(5849), 444–447. https://doi.org/10.1126/science.1145801

33. Chang, B., Chen, Y., Zhao, Y., & Bruick, R. K. (2007b). JMJD6 is a histone arginine demethylase. *Science (New York, N.Y.)*, *318*(5849), 444–447. https://doi.org/10.1126/science.1145801

34. Chang, W., Worman, H. J., & Gundersen, G. G. (2015). Accessorizing and anchoring the LINC complex for multifunctionality. *The Journal of Cell Biology*, *208*(1), 11–22. https://doi.org/10.1083/jcb.201409047

35. Chen, M.-W., Hua, K.-T., Kao, H.-J., Chi, C.-C., Wei, L.-H., Johansson, G., Shiah, S.-G., Chen, P.-S., Jeng, Y.-M., Cheng, T.-Y., Lai, T.-C., Chang, J.-S., Jan, Y.-H., Chien, M.-H., Yang, C.-J., Huang, M.-S., Hsiao, M., & Kuo, M.-L. (2010). H3K9 histone methyltransferase G9a promotes lung cancer invasion and metastasis by silencing the cell adhesion molecule Ep-CAM. *Cancer Research*, *70*(20), 7830–7840. https://doi.org/10.1158/0008-5472.CAN-10-0833

36. Chen, R., Kang, R., Fan, X.-G., & Tang, D. (2014a). Release and activity of histone in diseases. *Cell Death & Disease*, *5*(8), e1370. https://doi.org/10.1038/cddis.2014.337

37. Chen, R., Kang, R., Fan, X.-G., & Tang, D. (2014b). Release and activity of histone in diseases. *Cell Death & Disease*, *5*(8), e1370. https://doi.org/10.1038/cddis.2014.337

38. Cheng, Y., He, C., Wang, M., Ma, X., Mo, F., Yang, S., Han, J., & Wei, X. (2019). Targeting epigenetic regulators for cancer therapy: mechanisms and advances in clinical trials. *Signal Transduction and Targeted Therapy*, *4*(1), 62. https://doi.org/10.1038/s41392-019-0095-0

39. Chi, P., Allis, C. D., & Wang, G. G. (2010). Covalent histone modifications--miswritten, misinterpreted and mis-erased in human cancers. *Nature Reviews. Cancer*, *10*(7), 457–469. https://doi.org/10.1038/nrc2876

40. Chiarini, F., Lonetti, A., Evangelisti, C., Buontempo, F., Orsini, E., Evangelisti, C., Cappellini, A., Neri, L. M., McCubrey, J. A., & Martelli, A. M. (2016). Advances in understanding the acute lymphoblastic leukemia bone marrow microenvironment: From biology to therapeutic targeting. *Biochimica et Biophysica Acta*, *1863*(3), 449–463. https://doi.org/10.1016/j.bbamcr.2015.08.015

41. Chiotaki, R., Polioudaki, H., & Theodoropoulos, P. A. (2014). Differential nuclear shape dynamics of invasive andnon-invasive breast cancer cells are associated with actin cytoskeleton organization and stability. *Biochemistry and Cell Biology*, *92*(4), 287–295. https://doi.org/10.1139/bcb-2013-0120

42. Chu, Y., Chen, Y., Guo, H., Li, M., Wang, B., Shi, D., Cheng, X., Guan, J., Wang, X., Xue, C., Cheng, T., Shi, J., & Yuan, W. (2020). SUV39H1 regulates the progression of MLL-AF9-induced acute myeloid leukemia. *Oncogene*, *39*(50), 7239–7252. https://doi.org/10.1038/s41388-020-01495-6

43. Crazzolara, R., Kreczy, A., Mann, G., Heitger, A., Eibl, G., Fink, F. M., Möhle, R., & Meister, B. (2001). High expression of the chemokine receptor CXCR4 predicts extramedullary organ infiltration in childhood acute lymphoblastic leukaemia: High CXCR4 Expression Predicts Organ Infiltration in Childhood ALL. *British Journal of Haematology*, *115*(3), 545–553. https://doi.org/10.1046/j.1365-2141.2001.03164.x

44. Crazzolara, Roman, Jöhrer, K., Johnstone, R. W., Greil, R., Kofler, R., Meister, B., & Bernhard, D. (2002). Histone deacetylase inhibitors potently repress CXCR4 chemokine receptor expression and function in acute lymphoblastic leukaemia. *British Journal of Haematology*, *119*(4), 965–969. https://doi.org/10.1046/j.1365-2141.2002.03955.x

45. Cross, S. E., Jin, Y.-S., Tondre, J., Wong, R., Rao, J., & Gimzewski, J. K. (2008). AFM-based analysis of human metastatic cancer cells. *Nanotechnology*, *19*(38), 384003. https://doi.org/10.1088/0957-4484/19/38/384003

46. Dahl, K. N., Engler, A. J., Pajerowski, J. D., & Discher, D. E. (2005). Power-law rheology of isolated nuclei with deformation mapping of nuclear substructures. *Biophysical Journal*, *89*(4), 2855–2864. https://doi.org/10.1529/biophysj.105.062554

47. Davidson, P. M., & Lammerding, J. (2014). Broken nuclei--lamins, nuclear mechanics, and disease. *Trends in Cell Biology*, *24*(4), 247–256. https://doi.org/10.1016/j.tcb.2013.11.004

48. de Barrios, O., & Parra, M. (2021). Epigenetic control of infant B cell precursor acute lymphoblastic leukemia. *International Journal of Molecular Sciences*, *22*(6), 3127. https://doi.org/10.3390/ijms22063127

49. De Marchi, E., Baldassari, F., Bononi, A., Wieckowski, M. R., & Pinton, P. (2013). Oxidative stress in cardiovascular diseases and obesity: role of p66Shc and protein kinase C. *Oxidative Medicine and Cellular Longevity*, *2013*, 564961. https://doi.org/10.1155/2013/564961

50. Deak, D., Gorcea-Andronic, N., Sas, V., Teodorescu, P., Constantinescu, C., Iluta, S., Pasca, S., Hotea, I., Turcas, C., Moisoiu, V., Zimta, A.-A., Galdean, S., Steinheber, J., Rus, I., Rauch, S., Richlitzki, C., Munteanu, R., Jurj, A., Petrushev, B., … Tomuleasa, C. (2021). A narrative review of central nervous system involvement in acute leukemias. *Annals of Translational Medicine*, *9*(1), 68. https://doi.org/10.21037/atm-20-3140

51. DeAngelo, D. J., Stevenson, K. E., Dahlberg, S. E., Silverman, L. B., Couban, S., Supko, J. G., Amrein, P. C., Ballen, K. K., Seftel, M. D., Turner, A. R., Leber, B., Howson-Jan, K., Kelly, K., Cohen, S., Matthews, J. H., Savoie, L., Wadleigh, M., Sirulnik, L. A., Galinsky, I., … Stone, R. M. (2015). Long-term outcome of a pediatric-inspired regimen used for adults aged 18-50 years with newly diagnosed acute lymphoblastic leukemia. *Leukemia*, *29*(3), 526–534. https://doi.org/10.1038/leu.2014.229

52. Décaillot, F. M., Kazmi, M. A., Lin, Y., Ray-Saha, S., Sakmar, T. P., & Sachdev, P. (2011). CXCR7/CXCR4 heterodimer constitutively recruits beta-arrestin to enhance cell migration. *The Journal of Biological Chemistry*, *286*(37), 32188–32197. https://doi.org/10.1074/jbc.M111.277038

53. Denais, C. M., Gilbert, R. M., Isermann, P., McGregor, A. L., te Lindert, M., Weigelin, B., Davidson, P. M., Friedl, P., Wolf, K., & Lammerding, J. (2016). Nuclear envelope rupture and repair during cancer cell migration. *Science (New York, N.Y.)*, *352*(6283), 353–358. https://doi.org/10.1126/science.aad7297

54. Dinmohamed, A. G., Szabó, A., van der Mark, M., Visser, O., Sonneveld, P., Cornelissen, J. J., Jongen-Lavrencic, M., & Rijneveld, A. W. (2016). Improved survival in adult patients with acute lymphoblastic leukemia in the Netherlands: a population-based study on treatment, trial participation and survival. *Leukemia*, *30*(2), 310–317. https://doi.org/10.1038/leu.2015.230

55. Dong, C., Wu, Y., Yao, J., Wang, Y., Yu, Y., Rychahou, P. G., Evers, B. M., & Zhou, B. P. (2012). G9a interacts with Snail and is critical for Snail-mediated E-cadherin repression in human breast cancer. *The Journal of Clinical Investigation*, *122*(4), 1469–1486. https://doi.org/10.1172/JCI57349

56. Dores, G. M., Devesa, S. S., Curtis, R. E., Linet, M. S., & Morton, L. M. (2012). Acute leukemia incidence and patient survival among children and adults in the United States, 2001-2007. *Blood*, *119*(1), 34–43. https://doi.org/10.1182/blood-2011-04-347872

57. Duchartre, Y., Bachl, S., Kim, H. N., Gang, E. J., Lee, S., Liu, H.-C., Shung, K., Xu, R., Kruse, A., Tachas, G., Bonig, H., & Kim, Y.-M. (2017). Effects of CD49d-targeted antisense-oligonucleotide on α4 integrin expression and function of acute lymphoblastic leukemia cells: Results of in vitro and in vivo studies. *PloS One*, *12*(11), e0187684. https://doi.org/10.1371/journal.pone.0187684

58. Dunne, J. L., Ballantyne, C. M., Beaudet, A. L., & Ley, K. (2002). Control of leukocyte rolling velocity in TNF-alpha-induced inflammation by LFA-1 and Mac-1. *Blood*, *99*(1), 336–341. https://doi.org/10.1182/blood.v99.1.336

59. Dupin, I., & Etienne-Manneville, S. (2011). Nuclear positioning: mechanisms and functions. *The International Journal of Biochemistry & Cell Biology*, *43*(12), 1698–1707. https://doi.org/10.1016/j.biocel.2011.09.004

60. Dupont, C., Armant, D. R., & Brenner, C. A. (2009). Epigenetics: definition, mechanisms and clinical perspective. *Seminars in Reproductive Medicine*, *27*(5), 351–357. https://doi.org/10.1055/s-0029-1237423

61. Elsevier. (s/f). *Las principales funciones ejercidas por la migración del leucocito desde la sangre a los tejidos*. Elsevier Connect. Recuperado el 5 de septiembre de 2022, de https://www.elsevier.com/es-es/connect/medicina/inmunologia-funciones-migracion-del-leucocito

62. Emadi, A., & Law, J. Y. (s/f). *Acute Lymphoblastic Leukemia (ALL)*. MSD Manual Professional Edition. Recuperado el 14 de septiembre de 2022, de https://www.msdmanuals.com/professional/hematology-and-oncology/leukemias/acute-lymphoblastic-leukemia-all

63. Erdel, F., Baum, M., & Rippe, K. (2015). The viscoelastic properties of chromatin and the nucleoplasm revealed by scale-dependent protein mobility. *Journal of Physics. Condensed Matter: An Institute of Physics Journal*, *27*(6), 064115. https://doi.org/10.1088/0953-8984/27/6/064115

64. Esteller, M. (2008). Epigenetics in cancer. *The New England Journal of Medicine*, *358*(11), 1148–1159. https://doi.org/10.1056/NEJMra072067

65. Estève, P.-O., Patnaik, D., Chin, H. G., Benner, J., Teitell, M. A., & Pradhan, S. (2005). Functional analysis of the N- and C-terminus of mammalian G9a histone H3 methyltransferase. *Nucleic Acids Research*, *33*(10), 3211–3223. https://doi.org/10.1093/nar/gki635

66. Fraga, M. F., Ballestar, E., Villar-Garea, A., Boix-Chornet, M., Espada, J., Schotta, G., Bonaldi, T., Haydon, C., Ropero, S., Petrie, K., Iyer, N. G., Pérez-Rosado, A., Calvo, E., Lopez, J. A., Cano, A., Calasanz, M. J., Colomer, D., Piris, M. Á., Ahn, N., … Esteller, M. (2005). Loss of acetylation at Lys16 and trimethylation at Lys20 of histone H4 is a common hallmark of human cancer. *Nature Genetics*, *37*(4), 391–400. https://doi.org/10.1038/ng1531

67. Fathi, E., Farahzadi, R., Montazersaheb, S., & Bagheri, Y. (2021). Epigenetic modifications in acute lymphoblastic leukemia: From cellular mechanisms to therapeutics. *Current Gene Therapy*, *21*(1), 60–71. https://doi.org/10.2174/1566523220999201111194554

68. Fullmer, A., O'Brien, S., Kantarjian, H., & Jabbour, E. (2009). Novel therapies for relapsed acute lymphoblastic leukemia. *Current Hematologic Malignancy Reports*, *4*(3), 148–156. https://doi.org/10.1007/s11899-009-0021-6

69. García-Castro, M. I., Anderson, R., Heasman, J., & Wylie, C. (1997). Interactions between germ cells and extracellular matrix glycoproteins during migration and gonad assembly in the mouse embryo. *The Journal of Cell Biology*, *138*(2), 471–480. https://doi.org/10.1083/jcb.138.2.471

70. Garcia-Pardo, A., Wayner, E. A., Carter, W. G., & Ferreira, O. C., Jr. (1990). Human B lymphocytes define an alternative mechanism of adhesion to fibronectin. The interaction of the alpha 4 beta 1 integrin with the LHGPEILDVPST sequence of the type III connecting segment is sufficient to promote cell attachment. *The Journal of Immunology*, *144*(9), 3361–3366. http://www.jimmunol.org/content/144/9/3361.abstract

71. García-Ramírez, I., Bhatia, S., Rodríguez-Hernández, G., González-Herrero, I., Walter, C., González de Tena-Dávila, S., Parvin, S., Haas, O., Woessmann, W., Stanulla, M., Schrappe, M., Dugas, M., Natkunam, Y., Orfao, A., Domínguez, V., Pintado, B., Blanco, O., Alonso-López, D., De Las Rivas, J., … Sánchez-García, I. (2018). Lmo2 expression defines tumor cell

identity during T-cell leukemogenesis. *The EMBO Journal*, *37*(14). https://doi.org/10.15252/embj.201798783

72. Gerlitz, G., & Bustin, M. (2010). Efficient cell migration requires global chromatin condensation. *Journal of Cell Science*, *123*(Pt 13), 2207–2217. https://doi.org/10.1242/jcs.058271

73. Goldberg, A. D., Allis, C. D., & Bernstein, E. (2007). Epigenetics: a landscape takes shape. *Cell*, *128*(4), 635–638. https://doi.org/10.1016/j.cell.2007.02.006

74. Gómez, A. M., Martínez, C., González, M., Luque, A., Melen, G. J., Martínez, J., Hortelano, S., Lassaletta, Á., Madero, L., & Ramírez, M. (2015). Chemokines and relapses in childhood acute lymphoblastic leukemia: A role in migration and in resistance to antileukemic drugs. *Blood Cells, Molecules & Diseases*, *55*(3), 220–227. https://doi.org/10.1016/j.bcmd.2015.07.001

75. González-Herrero, I., Rodríguez-Hernández, G., Luengas-Martínez, A., Isidro-Hernández, M., Jiménez, R., García-Cenador, M., García-Criado, F., Sánchez-García, I., & Vicente-Dueñas, C. (2018). The making of leukemia. *International Journal of Molecular Sciences*, *19*(5), 1494. https://doi.org/10.3390/ijms19051494

76. Gordon, J. A. R., Grandy, R. A., Lian, J. B., Stein, J. L., van Wijnen, A. J., & Stein, G. S. (2013). Chromatin. En S. Maloy & K. Hughes (Eds.), *Brenner's Encyclopedia of Genetics* (pp. 538–541). Elsevier.

77. Grabovsky, V., Feigelson, S., Chen, C., Bleijs, D. A., Peled, A., Cinamon, G., Baleux, F., Arenzana-Seisdedos, F., Lapidot, T., van Kooyk, Y., Lobb, R. R., & Alon, R. (2000). Subsecond induction of α4 integrin clustering by immobilized chemokines stimulates leukocyte tethering and rolling on endothelial vascular cell adhesion molecule 1 under flow conditions. *The Journal of Experimental Medicine*, *192*(4), 495–506. https://doi.org/10.1084/jem.192.4.495

78. Grys, B. T., Lo, D. S., Sahin, N., Kraus, O. Z., Morris, Q., Boone, C., & Andrews, B. J. (2017). Machine learning and computer vision approaches for phenotypic profiling. *The Journal of Cell Biology*, *216*(1), 65–71. https://doi.org/10.1083/jcb.201610026

79. Guan, H., Miao, H., Ma, N., Lu, W., & Luo, B. (2017). Correlations between Epstein-Barr virus and acute leukemia. *Journal of Medical Virology*, *89*(8), 1453–1460. https://doi.org/10.1002/jmv.24797

80. Guil, S., & Esteller, M. (2009). DNA methylomes, histone codes and miRNAs: tying it all together. *The International Journal of Biochemistry & Cell Biology*, *41*(1), 87–95. https://doi.org/10.1016/j.biocel.2008.09.005

81. Guilluy, C., Osborne, L. D., Van Landeghem, L., Sharek, L., Superfine, R., Garcia-Mata, R., & Burridge, K. (2014). Isolated nuclei adapt to force and reveal a mechanotransduction pathway in the nucleus. *Nature Cell Biology*, *16*(4), 376–381. https://doi.org/10.1038/ncb2927

82. Gundersen, G. G., & Worman, H. J. (2013). Nuclear positioning. *Cell*, *152*(6), 1376–1389. https://doi.org/10.1016/j.cell.2013.02.031

83. H., V. (2012). Unravelling Glycobiology by NMR Spectroscopy. En *Glycosylation*. InTech.

84. Hamidi, H., & Ivaska, J. (2018). Every step of the way: integrins in cancer progression and metastasis. *Nature Reviews. Cancer*, *18*(9), 533–548. https://doi.org/10.1038/s41568-018-0038-z

85. Harasawa, H., Yamada, Y., Hieshima, K., Jin, Z., Nakayama, T., Yoshie, O., Shimizu, K., Hasegawa, H., Hayashi, T., Imaizumi, Y., Ikeda, S., Soda, H., Soda, H., Atogami, S., Takasaki, Y., Tsukasaki, K., Tomonaga, M., Murata, K., Sugahara, K., … Kamihira, S. (2006). Survey of chemokine receptor expression reveals frequent co-expression of skin-homing CCR4 and CCR10 in adult T-cell leukemia/lymphoma. *Leukemia & Lymphoma*, *47*(10), 2163–2173. https://doi.org/10.1080/10428190600775599

86. Hasegawa, H., Nomura, T., Kohno, M., Tateishi, N., Suzuki, Y., Maeda, N., Fujisawa, R., Yoshie, O., & Fujita, S. (2000). Increased chemokine receptor CCR7/EBI1 expression

enhances the infiltration of lymphoid organs by adult T-cell leukemia cells. *Blood*, *95*(1), 30–38. https://doi.org/10.1182/blood.v95.1.30

87. Hergeth, S. P., & Schneider, R. (2015). The H1 linker histones: multifunctional proteins beyond the nucleosomal core particle. *EMBO Reports*, *16*(11), 1439–1453. https://doi.org/10.15252/embr.201540749

88. Hieda, M., Matsuura, N., & Kimura, H. (2015). Histone modifications associated with cancer cell migration and invasion. *Methods in Molecular Biology (Clifton, N.J.)*, *1238*, 301–317. https://doi.org/10.1007/978-1-4939-1804-1_16

89. Hill, J. A., Giralt, S., Torgerson, T. R., & Lazarus, H. M. (2019). CAR-T - and a side order of IgG, to go? - Immunoglobulin replacement in patients receiving CAR-T cell therapy. *Blood Reviews*, *38*(100596), 100596. https://doi.org/10.1016/j.blre.2019.100596

90. Holland, M., Castro, F. V., Alexander, S., Smith, D., Liu, J., Walker, M., Bitton, D., Mulryan, K., Ashton, G., Blaylock, M., Bagley, S., Connolly, Y., Bridgeman, J., Miller, C., Krishnan, S., Dempsey, C., Masurekar, A., Stern, P., Whetton, A., & Saha, V. (2011). RAC2, AEP, and ICAM1 expression are associated with CNS disease in a mouse model of pre-B childhood acute lymphoblastic leukemia. *Blood*, *118*(3), 638–649. https://doi.org/10.1182/blood-2010-09-307330

91. Hong, Z., Wei, Z., Xie, T., Fu, L., Sun, J., Zhou, F., Jamal, M., Zhang, Q., & Shao, L. (2021). Targeting chemokines for acute lymphoblastic leukemia therapy. *Journal of Hematology & Oncology*, *14*(1), 48. https://doi.org/10.1186/s13045-021-01060-y

92. Hsieh, Y.-T., Jiang, E., Pham, J., Kim, H.-N., Abdel-Azim, H., Khazal, S., Bug, G., Spohn, G., Bonig, H., & Kim, Y.-M. (2013). VLA4 blockade in acute myeloid leukemia. *Blood*, *122*(21), 3944–3944. https://doi.org/10.1182/blood.v122.21.3944.3944

93. Huang, Y., Zou, Y., Lin, L., Ma, X., & Huang, X. (2017). Effect of BIX-01294 on proliferation, apoptosis and histone methylation of acute T lymphoblastic leukemia cells. *Leukemia Research*, *62*, 34–39. https://doi.org/10.1016/j.leukres.2017.09.015

94. Huguet, F., Leguay, T., Raffoux, E., Thomas, X., Beldjord, K., Delabesse, E., Chevallier, P., Buzyn, A., Delannoy, A., Chalandon, Y., Vernant, J.-P., Lafage-Pochitaloff, M., Chassevent, A., Lhéritier, V., Macintyre, E., Béné, M.-C., Ifrah, N., & Dombret, H. (2009). Pediatric-inspired therapy in adults with Philadelphia chromosome-negative acute lymphoblastic leukemia: the GRAALL-2003 study. *Journal of Clinical Oncology: Official Journal of the American Society of Clinical Oncology*, *27*(6), 911–918. https://doi.org/10.1200/JCO.2008.18.6916

95. Hunger, S. P., & Mullighan, C. G. (2015). Acute lymphoblastic leukemia in children. *The New England Journal of Medicine*, *373*(16), 1541–1552. https://doi.org/10.1056/NEJMra1400972

96. Hynes, R. O. (1992). Integrins: versatility, modulation, and signaling in cell adhesion. *Cell*, *69*(1), 11–25. https://doi.org/10.1016/0092-8674(92)90115-s

97. Imai, Y., Shimaoka, M., & Kurokawa, M. (2010). Essential roles of VLA-4 in the hematopoietic system. *International Journal of Hematology*, *91*(4), 569–575. https://doi.org/10.1007/s12185-010-0555-3

98. Inoue, M., Nakayamada, H., Tokuyama, S., & Ueda, H. (1997). Peripheral non-opioid analgesic effects of kyotorphin in mice. *Neuroscience Letters*, *236*(1), 60–62. https://doi.org/10.1016/s0304-3940(97)00760-x

99. Irianto, J., Xia, Y., Pfeifer, C. R., Greenberg, R. A., & Discher, D. E. (2017). As a nucleus enters a small pore, chromatin stretches and maintains integrity, even with DNA breaks. *Biophysical journal*, *112*(3), 446–449. https://doi.org/10.1016/j.bpj.2016.09.047

100. Ishikawa, T., & Ali-Osman, F. (1993). Glutathione-associated cis-diamminedichloroplatinum(II) metabolism and ATP-dependent efflux from leukemia cells. Molecular characterization of glutathione-platinum complex and its biological significance. *The Journal of Biological Chemistry*, *268*(27), 20116–20125. https://doi.org/10.1016/s0021-9258(20)80702-9

101. Jacobsen, K., Kravitz, J., Kincade, P. W., & Osmond, D. G. (1996). Adhesion receptors on bone marrow stromal cells: in vivo expression of vascular cell adhesion molecule-1 by reticular cells and sinusoidal endothelium in normal and gamma-irradiated mice. *Blood*, *87*(1), 73–82. https://doi.org/10.1182/blood.v87.1.73.bloodjournal87173

102. Jang, W., Park, J., Kwon, A., Choi, H., Kim, J., Lee, G. D., Han, E., Jekarl, D. W., Chae, H., Han, K., Yoon, J.-H., Lee, S., Chung, N.-G., Cho, B., Kim, M., & Kim, Y. (2019). CDKN2B downregulation and other genetic characteristics in T-acute lymphoblastic leukemia. *Experimental & Molecular Medicine*, *51*(1), 1–15. https://doi.org/10.1038/s12276-018-0195-x

103. Janssens, R., Struyf, S., & Proost, P. (2018). The unique structural and functional features of CXCL12. *Cellular & Molecular Immunology*, *15*(4), 299–311. https://doi.org/10.1038/cmi.2017.107

104. Jenuwein, T., & Allis, C. D. (2001). Translating the histone code. *Science (New York, N.Y.)*, *293*(5532), 1074–1080. https://doi.org/10.1126/science.1063127

105. Jiffar, T., Kurinna, S., Suck, G., Carlson-Bremer, D., Ricciardi, M. R., Konopleva, M., Andreeff, M., & Ruvolo, P. P. (2004). PKC alpha mediates chemoresistance in acute lymphoblastic leukemia through effects on Bcl2 phosphorylation. *Leukemia*, *18*(3), 505–512. https://doi.org/10.1038/sj.leu.2403275

106. Kalwarczyk, T., Tabaka, M., & Holyst, R. (2012). Biologistics--diffusion coefficients for complete proteome of Escherichia coli. *Bioinformatics (Oxford, England)*, *28*(22), 2971–2978. https://doi.org/10.1093/bioinformatics/bts537

107. Kato, M., & Manabe, A. (2018). Treatment and biology of pediatric acute lymphoblastic leukemia. *Pediatrics International: Official Journal of the Japan Pediatric Society*, *60*(1), 4–12. https://doi.org/10.1111/ped.13457

108. Kemp, B. E., & Pearson, R. B. (1990). Protein kinase recognition sequence motifs. *Trends in Biochemical Sciences*, *15*(9), 342–346. https://doi.org/10.1016/0968-0004(90)90073-k

109. Kessenbrock, K., Plaks, V., & Werb, Z. (2010). Matrix metalloproteinases: regulators of the tumor microenvironment. *Cell*, *141*(1), 52–67. https://doi.org/10.1016/j.cell.2010.03.015

110. Kikkawa, U., & Nishizuka, Y. (1986). The role of protein kinase C in transmembrane signalling. *Annual Review of Cell Biology*, *2*(1), 149–178. https://doi.org/10.1146/annurev.cb.02.110186.001053

111. Kindler, T., Cornejo, M. G., Scholl, C., Liu, J., Leeman, D. S., Haydu, J. E., Fröhling, S., Lee, B. H., & Gilliland, D. G. (2008). K-RasG12D-induced T-cell lymphoblastic lymphoma/leukemias harbor Notch1 mutations and are sensitive to gamma-secretase inhibitors. *Blood*, *112*(8), 3373–3382. https://doi.org/10.1182/blood-2008-03-147587

112. Korolev, N., Fan, Y., Lyubartsev, A. P., & Nordenskiöld, L. (2012). Modelling chromatin structure and dynamics: status and prospects. *Current Opinion in Structural Biology*, *22*(2), 151–159. https://doi.org/10.1016/j.sbi.2012.01.006

113. Kouzarides, T. (2007). Chromatin modifications and their function. *Cell*, *128*(4), 693–705. https://doi.org/10.1016/j.cell.2007.02.005

114. Kuang, S.-Q., Fang, Z., Zweidler-McKay, P. A., Yang, H., Wei, Y., Gonzalez-Cervantes, E. A., Boumber, Y., & Garcia-Manero, G. (2013). Epigenetic inactivation of Notch-Hes pathway in human B-cell acute lymphoblastic leukemia. *PloS One*, *8*(4), e61807. https://doi.org/10.1371/journal.pone.0061807

115. Kulaeva, O. I., Hsieh, F.-K., & Studitsky, V. M. (2010). RNA polymerase complexes cooperate to relieve the nucleosomal barrier and evict histones. *Proceedings of the National Academy of Sciences of the United States of America*, *107*(25), 11325–11330. https://doi.org/10.1073/pnas.1001148107

116. Kumar, S., & Weaver, V. M. (2009). Mechanics, malignancy, and metastasis: the force journey of a tumor cell. *Cancer Metastasis Reviews*, *28*(1–2), 113–127. https://doi.org/10.1007/s10555-008-9173-4

117. Kuo, M. H., Brownell, J. E., Sobel, R. E., Ranalli, T. A., Cook, R. G., Edmondson, D. G., Roth, S. Y., & Allis, C. D. (1996). Transcription-linked acetylation by Gcn5p of histones H3 and H4 at specific lysines. *Nature*, *383*(6597), 269–272. https://doi.org/10.1038/383269a0

118. Lai, Y.-S., Chen, J.-Y., Tsai, H.-J., Chen, T.-Y., & Hung, W.-C. (2015). The SUV39H1 inhibitor chaetocin induces differentiation and shows synergistic cytotoxicity with other epigenetic drugs in acute myeloid leukemia cells. *Blood Cancer Journal*, *5*(5), e313. https://doi.org/10.1038/bcj.2015.37

119. Lausten-Thomsen, U., Madsen, H. O., Vestergaard, T. R., Hjalgrim, H., Nersting, J., & Schmiegelow, K. (2011). Prevalence of t(12;21)[ETV6-RUNX1]-positive cells in healthy neonates. *Blood*, *117*(1), 186–189. https://doi.org/10.1182/blood-2010-05-282764

120. Lee-Sherick, A. B., Linger, R. M. A., Gore, L., Keating, A. K., & Graham, D. K. (2010). Targeting paediatric acute lymphoblastic leukaemia: novel therapies currently in development: Review. *British Journal of Haematology*, *151*(4), 295–311. https://doi.org/10.1111/j.1365-2141.2010.08282.x

121. Levoye, A., Balabanian, K., Baleux, F., Bachelerie, F., & Lagane, B. (2009). CXCR7 heterodimerizes with CXCR4 and regulates CXCL12-mediated G protein signaling. *Blood*, *113*(24), 6085–6093. https://doi.org/10.1182/blood-2008-12-196618

122. Ley, K., Laudanna, C., Cybulsky, M. I., & Nourshargh, S. (2007). Getting to the site of inflammation: the leukocyte adhesion cascade updated. *Nature Reviews. Immunology*, *7*(9), 678–689. https://doi.org/10.1038/nri2156

123. Liu, J., Dou, X., Chen, C., Chen, C., Liu, C., Xu, M. M., Zhao, S., Shen, B., Gao, Y., Han, D., & He, C. (2020). N 6-methyladenosine of chromosome-associated regulatory RNA regulates chromatin state and transcription. *Science (New York, N.Y.)*, *367*(6477), 580–586. https://doi.org/10.1126/science.aay6018

124. Luger, K. (2015). Nucleosomes: Structure and function. *Encyclopedia of Life Sciences*. https://www.academia.edu/11345141/Nucleosomes_Structure_and_Function

125. Ma, S., Shi, Y., Pang, Y., Dong, F., Cheng, H., Hao, S., Xu, J., Zhu, X., Yuan, W., Cheng, T., & Zheng, G. (2014). Notch1-induced T cell leukemia can be potentiated by microenvironmental cues in the spleen. *Journal of Hematology & Oncology*, *7*(1), 71. https://doi.org/10.1186/s13045-014-0071-7

126. Madrazo, E., Ruano, D., Abad, L., Alonso-Gómez, E., Sánchez-Valdepeñas, C., González-Murillo, Á., Ramírez, M., & Redondo-Muñoz, J. (2018). G9a correlates with VLA-4 integrin and influences the migration of childhood acute lymphoblastic leukemia cells. *Cancers*, *10*(9). https://doi.org/10.3390/cancers10090325

127. Maison, C., Bailly, D., Quivy, J.-P., & Almouzni, G. (2016). The methyltransferase Suv39h1 links the SUMO pathway to HP1α marking at pericentric heterochromatin. *Nature Communications*, *7*(1), 12224. https://doi.org/10.1038/ncomms12224

128. Malard, F., & Mohty, M. (2020). Acute lymphoblastic leukaemia. *Lancet*, *395*(10230), 1146–1162. https://doi.org/10.1016/S0140-6736(19)33018-1

129. Mariño-Ramírez, L., Kann, M. G., Shoemaker, B. A., & Landsman, D. (2005). Histone structure and nucleosome stability. *Expert Review of Proteomics*, *2*(5), 719–729. https://doi.org/10.1586/14789450.2.5.719

130. Martínez-Laperche, C., Gómez-García, A. M., Lassaletta, Á., Moscardó, C., Vivanco, J. L., Molina, J., Fuster, J. L., Couselo, J. M., de Toledo, J. S., Bureo, E., Madero, L., & Ramírez, M. (2013). Detection of occult cerebrospinal fluid involvement during maintenance therapy identifies a group of children with acute lymphoblastic leukemia at high risk for relapse. *American Journal of Hematology*, *88*(5), 359–364. https://doi.org/10.1002/ajh.23407

131. Martín-Lorenzo, A., Auer, F., Chan, L. N., García-Ramírez, I., González-Herrero, I., Rodríguez-Hernández, G., Bartenhagen, C., Dugas, M., Gombert, M., Ginzel, S., Blanco, O., Orfao, A., Alonso-López, D., Rivas, J. D. L., García-Cenador, M. B., García-Criado, F. J., Müschen, M., Sánchez-García, I., Borkhardt, A., … Hauer, J. (2018). Loss of Pax5 exploits

Sca1-BCR-ABLp190 susceptibility to confer the metabolic shift essential for pB-ALL. *Cancer Research*, *78*(10), 2669–2679. https://doi.org/10.1158/0008-5472.can-17-3262

132. McCormack, M. P., Young, L. F., Vasudevan, S., de Graaf, C. A., Codrington, R., Rabbitts, T. H., Jane, S. M., & Curtis, D. J. (2010). The Lmo2 oncogene initiates leukemia in mice by inducing thymocyte self-renewal. *Science (New York, N.Y.)*, *327*(5967), 879–883. https://doi.org/10.1126/science.1182378

133. McEver, R. P., & Zhu, C. (2010). Rolling cell adhesion. *Annual Review of Cell and Developmental Biology*, *26*(1), 363–396. https://doi.org/10.1146/annurev.cellbio.042308.113238

134. Kumar, S., & Weaver, V. M. (2009). Mechanics, malignancy, and metastasis: the force journey of a tumor cell. *Cancer Metastasis Reviews*, *28*(1–2), 113–127. https://doi.org/10.1007/s10555-008-9173-4

135. Melcher, M., Schmid, M., Aagaard, L., Selenko, P., Laible, G., & Jenuwein, T. (2000). Structure-function analysis of SUV39H1 reveals a dominant role in heterochromatin organization, chromosome segregation, and mitotic progression. *Molecular and Cellular Biology*, *20*(10), 3728–3741. https://doi.org/10.1128/MCB.20.10.3728-3741.2000

136. Mellado, M., Rodríguez-Frade, J. M., Mañes, S., & Martínez-A, C. (2001). Chemokine signaling and functional responses: the role of receptor dimerization and TK pathway activation. *Annual Review of Immunology*, *19*(1), 397–421. https://doi.org/10.1146/annurev.immunol.19.1.397

137. Melo, R. de C. C., Longhini, A. L., Bigarella, C. L., Baratti, M. O., Traina, F., Favaro, P., de Melo Campos, P., & Saad, S. T. O. (2014). CXCR7 is highly expressed in acute lymphoblastic leukemia and potentiates CXCR4 response to CXCL12. *PloS One*, *9*(1), e85926. https://doi.org/10.1371/journal.pone.0085926

138. Miller, M. C., & Mayo, K. H. (2017). Chemokines from a structural perspective. *International Journal of Molecular Sciences*, *18*(10). https://doi.org/10.3390/ijms18102088

139. Miller, K. D., Nogueira, L., Devasia, T., Mariotto, A. B., Yabroff, K. R., Jemal, A., Kramer, J., & Siegel, R. L. (2022). Cancer treatment and survivorship statistics, 2022. *CA: A Cancer Journal for Clinicians*, *72*(5), 409–436. https://doi.org/10.3322/caac.21731

140. Morgan, B. A., Mittman, B. A., & Smith, M. M. (1991). The highly conserved N-terminal domains of histones H3 and H4 are required for normal cell cycle progression. *Molecular and Cellular Biology*, *11*(8), 4111–4120. https://doi.org/10.1128/mcb.11.8.4111-4120.1991

141. Moser, B., Wolf, M., Walz, A., & Loetscher, P. (2004). Chemokines: multiple levels of leukocyte migration control. *Trends in Immunology*, *25*(2), 75–84. https://doi.org/10.1016/j.it.2003.12.005

142. Moyano, J. V., Carnemolla, B., Albar, J. P., Leprini, A., Gaggero, B., Zardi, L., & Garcia-Pardo, A. (1999). Cooperative role for activated alpha4 beta1 integrin and chondroitin sulfate proteoglycans in cell adhesion to the heparin III domain of fibronectin. Identification of a novel heparin and cell binding sequence in repeat III5. *The Journal of Biological Chemistry*, *274*(1), 135–142. https://doi.org/10.1074/jbc.274.1.135

143. Müller, A., Homey, B., Soto, H., Ge, N., Catron, D., Buchanan, M. E., McClanahan, T., Murphy, E., Yuan, W., Wagner, S. N., Barrera, J. L., Mohar, A., Verástegui, E., & Zlotnik, A. (2001). Involvement of chemokine receptors in breast cancer metastasis. *Nature*, *410*(6824), 50–56. https://doi.org/10.1038/35065016

144. Muller, W. A. (2013). Getting leukocytes to the site of inflammation. *Veterinary Pathology*, *50*(1), 7–22. https://doi.org/10.1177/0300985812469883

145. Muller, William A. (2016). Transendothelial migration: unifying principles from the endothelial perspective. *Immunological Reviews*, *273*(1), 61–75. https://doi.org/10.1111/imr.12443

146. Mullighan, C. G., Zhang, J., Harvey, R. C., Collins-Underwood, J. R., Schulman, B. A., Phillips, L. A., Tasian, S. K., Loh, M. L., Su, X., Liu, W., Devidas, M., Atlas, S. R., Chen, I.-M., Clifford, R. J., Gerhard, D. S., Carroll, W. L., Reaman, G. H., Smith, M., Downing, J. R., … Willman, C. L. (2009). JAK mutations in high-risk childhood acute lymphoblastic leukemia. *Proceedings of the National Academy of Sciences of the United States of America*, *106*(23), 9414–9418. https://doi.org/10.1073/pnas.0811761106

147. Mullighan, C. G. (2010). Genetic variation and the risk of acute lymphoblastic leukemia. *Leukemia Research*, *34*(10), 1269–1270. https://doi.org/10.1016/j.leukres.2010.05.013

148. Munshi, A., Shafi, G., Aliya, N., & Jyothy, A. (2009a). Histone modifications dictate specific biological readouts. *Yi Chuan Xue Bao [Journal of Genetics and Genomics]*, *36*(2), 75–88. https://doi.org/10.1016/s1673-8527(08)60094-6

149. Munshi, A., Shafi, G., Aliya, N., & Jyothy, A. (2009b). Histone modifications dictate specific biological readouts. *Yi Chuan Xue Bao [Journal of Genetics and Genomics]*, *36*(2), 75–88. https://doi.org/10.1016/s1673-8527(08)60094-6

150. Nava, M. M., Miroshnikova, Y. A., Biggs, L. C., Whitefield, D. B., Metge, F., Boucas, J., Vihinen, H., Jokitalo, E., Li, X., García Arcos, J. M., Hoffmann, B., Merkel, R., Niessen, C. M., Dahl, K. N., & Wickström, S. A. (2020). Heterochromatin-driven nuclear softening protects the genome against mechanical stress-induced damage. *Cell*, *181*(4), 800-817.e22. https://doi.org/10.1016/j.cell.2020.03.052

151. Navarrete-Meneses, M. D. P., & Pérez-Vera, P. (2017). Alteraciones epigenéticas en leucemia linfoblástica aguda. *Boletin medico del Hospital Infantil de Mexico*, *74*(4), 243–264. https://doi.org/10.1016/j.bmhimx.2017.02.005

152. Ness, K. K., Armenian, S. H., Kadan-Lottick, N., & Gurney, J. G. (2011). Adverse effects of treatment in childhood acute lymphoblastic leukemia: general overview and implications for long-term cardiac health. *Expert Review of Hematology*, *4*(2), 185–197. https://doi.org/10.1586/ehm.11.8

153. Newton, A. C. (1995). Protein kinase C: structure, function, and regulation. *The Journal of Biological Chemistry*, *270*(48), 28495–28498. https://doi.org/10.1074/jbc.270.48.28495

154. Nguyen, D. P., Garcia Alai, M. M., Kapadnis, P. B., Neumann, H., & Chin, J. W. (2009). Genetically encoding N(epsilon)-methyl-L-lysine in recombinant histones. *Journal of the American Chemical Society*, *131*(40), 14194–14195. https://doi.org/10.1021/ja906603s

155. Nishizuka, Y. (1984). The role of protein kinase C in cell surface signal transduction and tumour promotion. *Nature*, *308*(5961), 693–698. https://doi.org/10.1038/308693a0

156. Nishizuka, Y. (1986). Studies and perspectives of protein kinase C. *Science (New York, N.Y.)*, *233*(4761), 305–312. https://doi.org/10.1126/science.3014651

157. Nishizuka, Y. (1988). The molecular heterogeneity of protein kinase C and its implications for cellular regulation. *Nature*, *334*(6184), 661–665. https://doi.org/10.1038/334661a0

158. Nomiyama, H., Osada, N., & Yoshie, O. (2013). Systematic classification of vertebrate chemokines based on conserved synteny and evolutionary history. *Genes to Cells: Devoted to Molecular & Cellular Mechanisms*, *18*(1), 1–16. https://doi.org/10.1111/gtc.12013

159. Nonomura, C., Kikuchi, J., Kiyokawa, N., Ozaki, H., Mitsunaga, K., Ando, H., Kanamori, A., Kannagi, R., Fujimoto, J., Muroi, K., Furukawa, Y., & Nakamura, M. (2008). CD43, but not P-selectin glycoprotein ligand-1, functions as an E-selectin counter-receptor in human pre-B-cell leukemia NALL-1. *Cancer Research*, *68*(3), 790–799. https://doi.org/10.1158/0008-5472.CAN-07-1459

160. Nordlund, J., & Syvänen, A.-C. (2018). Epigenetics in pediatric acute lymphoblastic leukemia. *Seminars in Cancer Biology*, *51*, 129–138. https://doi.org/10.1016/j.semcancer.2017.09.001

161. Osborn, L., Hession, C., Tizard, R., Vassallo, C., Luhowskyj, S., Chi-Rosso, G., & Lobb, R. (1989). Direct expression cloning of vascular cell adhesion molecule 1, a cytokine-induced

endothelial protein that binds to lymphocytes. *Cell*, *59*(6), 1203–1211. https://doi.org/10.1016/0092-8674(89)90775-7

162. Passaro, D., Irigoyen, M., Catherinet, C., Gachet, S., Da Costa De Jesus, C., Lasgi, C., Tran Quang, C., & Ghysdael, J. (2015). CXCR4 is required for leukemia-initiating cell activity in T cell acute lymphoblastic leukemia. *Cancer Cell*, *27*(6), 769–779. https://doi.org/10.1016/j.ccell.2015.05.003

163. Peters, A. H. F. M., Kubicek, S., Mechtler, K., O'Sullivan, R. J., Derijck, A. A. H. A., Perez-Burgos, L., Kohlmaier, A., Opravil, S., Tachibana, M., Shinkai, Y., Martens, J. H. A., & Jenuwein, T. (2003). Partitioning and plasticity of repressive histone methylation states in mammalian chromatin. *Molecular Cell*, *12*(6), 1577–1589. https://doi.org/10.1016/s1097-2765(03)00477-5

164. Petit, I., Goichberg, P., Spiegel, A., Peled, A., Brodie, C., Seger, R., Nagler, A., Alon, R., & Lapidot, T. (2005). Atypical PKC-ζ regulates SDF-1–mediated migration and development of human CD34+ progenitor cells. *The Journal of Clinical Investigation*, *115*(1), 168–176. https://doi.org/10.1172/jci200521773

165. Pfeifer, C. R., Xia, Y., Zhu, K., Liu, D., Irianto, J., García, V. M. M., Millán, L. M. S., Niese, B., Harding, S., Deviri, D., Greenberg, R. A., & Discher, D. E. (2018). Constricted migration increases DNA damage and independently represses cell cycle. *Molecular Biology of the Cell*, *29*(16), 1948–1962. https://doi.org/10.1091/mbc.E18-02-0079

166. Pitt, L. A., Tikhonova, A. N., Hu, H., Trimarchi, T., King, B., Gong, Y., Sanchez-Martin, M., Tsirigos, A., Littman, D. R., Ferrando, A. A., Morrison, S. J., Fooksman, D. R., Aifantis, I., & Schwab, S. R. (2015). CXCL12-producing vascular endothelial niches control acute T cell leukemia maintenance. *Cancer Cell*, *27*(6), 755–768. https://doi.org/10.1016/j.ccell.2015.05.002

167. Plow, E. F., Haas, T. A., Zhang, L., Loftus, J., & Smith, J. W. (2000). Ligand binding to integrins. *The Journal of Biological Chemistry*, *275*(29), 21785–21788. https://doi.org/10.1074/jbc.R000003200

168. Poli, A., Ratti, S., Finelli, C., Mongiorgi, S., Clissa, C., Lonetti, A., Cappellini, A., Catozzi, A., Barraco, M., Suh, P.-G., Manzoli, L., McCubrey, J. A., Cocco, L., & Follo, M. Y. (2018). Nuclear translocation of PKC-α is associated with cell cycle arrest and erythroid differentiation in myelodysplastic syndromes (MDSs). *FASEB Journal: Official Publication of the Federation of American Societies for Experimental Biology*, *32*(2), 681–692. https://doi.org/10.1096/fj.201700690R

169. Poulard, C., Baulu, E., Lee, B. H., Pufall, M. A., & Stallcup, M. R. (2018). Increasing G9a automethylation sensitizes B acute lymphoblastic leukemia cells to glucocorticoid-induced death. *Cell Death & Disease*, *9*(10), 1038. https://doi.org/10.1038/s41419-018-1110-z

170. Proudfoot, A. E. I. (2002). Chemokine receptors: multifaceted therapeutic targets. *Nature Reviews. Immunology*, *2*(2), 106–115. https://doi.org/10.1038/nri722

171. Pui, C.-H. (2006). Central nervous system disease in acute lymphoblastic leukemia: prophylaxis and treatment. *Hematology*, *2006*(1), 142–146. https://doi.org/10.1182/asheducation-2006.1.142

172. Pui, C.-H., Carroll, W. L., Meshinchi, S., & Arceci, R. J. (2011). Biology, risk stratification, and therapy of pediatric acute leukemias: an update. *Journal of Clinical Oncology: Official Journal of the American Society of Clinical Oncology*, *29*(5), 551–565. https://doi.org/10.1200/JCO.2010.30.7405

173. Pui, C.-H., & Howard, S. C. (2008). Current management and challenges of malignant disease in the CNS in paediatric leukaemia. *The Lancet Oncology*, *9*(3), 257–268. https://doi.org/10.1016/S1470-2045(08)70070-6

174. Pui, C.-H., Mullighan, C. G., Evans, W. E., & Relling, M. V. (2012). Pediatric acute lymphoblastic leukemia: where are we going and how do we get there? *Blood*, *120*(6), 1165–1174. https://doi.org/10.1182/blood-2012-05-378943

175. Pui, C.-H., Nichols, K. E., & Yang, J. J. (2019). Somatic and germline genomics in paediatric acute lymphoblastic leukaemia. *Nature Reviews. Clinical Oncology*, *16*(4), 227–240. https://doi.org/10.1038/s41571-018-0136-6

176. Pui, C.-H., Robison, L. L., & Look, A. T. (2008). Acute lymphoblastic leukaemia. *Lancet*, *371*(9617), 1030–1043. https://doi.org/10.1016/S0140-6736(08)60457-2

177. Pullen, J., Shuster, J. J., Link, M., Borowitz, M., Amylon, M., Carroll, A. J., Land, V., Look, A. T., McIntyre, B., & Camitta, B. (1999). Significance of commonly used prognostic factors differs for children with T cell acute lymphocytic leukemia (ALL), as compared to those with B-precursor ALL. A Pediatric Oncology Group (POG) study. *Leukemia*, *13*(11), 1696–1707. https://doi.org/10.1038/sj.leu.2401555

178. Qian, M., Zhao, X., Devidas, M., Yang, W., Gocho, Y., Smith, C., Gastier-Foster, J. M., Li, Y., Xu, H., Zhang, S., Jeha, S., Zhai, X., Sanda, T., Winter, S. S., Dunsmore, K. P., Raetz, E. A., Carroll, W. L., Winick, N. J., Rabin, K. R., … Yang, J. J. (2019). Genome-wide association study of susceptibility loci for T-cell acute lymphoblastic leukemia in children. *Journal of the National Cancer Institute*, *111*(12), 1350–1357. https://doi.org/10.1093/jnci/djz043

179. Qiuping, Z., Jei, X., Youxin, J., Wei, J., Chun, L., Jin, W., Qun, W., Yan, L., Chunsong, H., Mingzhen, Y., Qingping, G., Kejian, Z., Zhimin, S., Qun, L., Junyan, L., & Jinquan, T. (2004). CC chemokine ligand 25 enhances resistance to apoptosis in CD4+ T cells from patients with T-cell lineage acute and chronic lymphocytic leukemia by means of livin activation. *Cancer Research*, *64*(20), 7579–7587. https://doi.org/10.1158/0008-5472.CAN-04-0641

180. Qiuping, Z., Qun, L., Chunsong, H., Xiaolian, Z., Baojun, H., Mingzhen, Y., Chengming, L., Jinshen, H., Qingping, G., Kejian, Z., Zhimin, S., Xuejun, Z., Junyan, L., & Jinquan, T. (2003). Selectively increased expression and functions of chemokine receptor CCR9 on CD4+ T cells from patients with T-cell lineage acute lymphocytic leukemia. *Cancer Research*, *63*(19), 6469–6477.

181. Quinn, K. E., Mackie, D. I., & Caron, K. M. (2018). Emerging roles of atypical chemokine receptor 3 (ACKR3) in normal development and physiology. *Cytokine*, *109*, 17–23. https://doi.org/10.1016/j.cyto.2018.02.024

182. Raboso-Gallego, J., Casado-García, A., Isidro-Hernández, M., & Vicente-Dueñas, C. (2019). Epigenetic priming in childhood acute lymphoblastic leukemia. *Frontiers in Cell and Developmental Biology*, *7*, 137. https://doi.org/10.3389/fcell.2019.00137

183. Redondo-Muñoz, J., García-Pardo, A., & Teixidó, J. (2019a). Molecular players in hematologic tumor cell trafficking. *Frontiers in Immunology*, *10*, 156. https://doi.org/10.3389/fimmu.2019.00156

184. Redondo-Muñoz, J., García-Pardo, A., & Teixidó, J. (2019b). Molecular players in hematologic tumor cell trafficking. *Frontiers in Immunology*, *10*, 156. https://doi.org/10.3389/fimmu.2019.00156

185. Reiter, A., Schrappe, M., Ludwig, W. D., Hiddemann, W., Sauter, S., Henze, G., Zimmermann, M., Lampert, F., Havers, W., & Niethammer, D. (1994). Chemotherapy in 998 unselected childhood acute lymphoblastic leukemia patients. Results and conclusions of the multicenter trial ALL-BFM 86. *Blood*, *84*(9), 3122–3133. https://doi.org/10.1182/blood.v84.9.3122.bloodjournal8493122

186. Rice, J. C., Briggs, S. D., Ueberheide, B., Barber, C. M., Shabanowitz, J., Hunt, D. F., Shinkai, Y., & Allis, C. D. (2003a). Histone methyltransferases direct different degrees of methylation to define distinct chromatin domains. *Molecular Cell*, *12*(6), 1591–1598. https://doi.org/10.1016/s1097-2765(03)00479-9

187. Rice, J. C., Briggs, S. D., Ueberheide, B., Barber, C. M., Shabanowitz, J., Hunt, D. F., Shinkai, Y., & Allis, C. D. (2003b). Histone methyltransferases direct different degrees of methylation to define distinct chromatin domains. *Molecular Cell*, *12*(6), 1591–1598. https://doi.org/10.1016/s1097-2765(03)00479-9

188. RNTI-SEHOP. (s/f). *Registro Español de Tumores Infantiles RETI-SEHOP*. Www.uv.es. Recuperado el 13 de septiembre de 2022, de https://www.uv.es/rnti/index.html

189. Rodríguez-Hernández, G., Hauer, J., Martín-Lorenzo, A., Schäfer, D., Bartenhagen, C., García-Ramírez, I., Auer, F., González-Herrero, I., Ruiz-Roca, L., Gombert, M., Okpanyi, V., Fischer, U., Chen, C., Dugas, M., Bhatia, S., Linka, R. M., Garcia-Suquia, M., Rascón-Trincado, M. V., Garcia-Sanchez, A., … Borkhardt, A. (2017). Infection exposure promotes ETV6-RUNX1 precursor B-cell leukemia via impaired H3K4 demethylases. *Cancer Research*, *77*(16), 4365–4377. https://doi.org/10.1158/0008-5472.CAN-17-0701

190. Rollins, B. J. (2006). Inflammatory chemokines in cancer growth and progression. *European Journal of Cancer (Oxford, England: 1990)*, *42*(6), 760–767. https://doi.org/10.1016/j.ejca.2006.01.002

191. Roolf, C., Richter, A., Konkolefski, C., Knuebel, G., Sekora, A., Krohn, S., Stenzel, J., Krause, B. J., Vollmar, B., Murua Escobar, H., & Junghanss, C. (2018). Decitabine demonstrates antileukemic activity in B cell precursor acute lymphoblastic leukemia with MLL rearrangements. *Journal of Hematology & Oncology*, *11*(1). https://doi.org/10.1186/s13045-018-0607-3

192. Ruiz-Aparicio, P. F., Vanegas, N.-D. P., Uribe, G. I., Ortiz-Montero, P., Cadavid-Cortés, C., Lagos, J., Flechas-Afanador, J., Linares-Ballesteros, A., & Vernot, J.-P. (2020). Dual targeting of stromal cell support and leukemic cell growth by a peptidic PKC inhibitor shows effectiveness against B-ALL. *International Journal of Molecular Sciences*, *21*(10), 3705. https://doi.org/10.3390/ijms21103705

193. Saha, N., & Muntean, A. G. (2021). Insight into the multi-faceted role of the SUV family of H3K9 methyltransferases in carcinogenesis and cancer progression. *Biochimica et Biophysica Acta. Reviews on Cancer*, *1875*(1), 188498. https://doi.org/10.1016/j.bbcan.2020.188498

194. Salomon, D. R., Crisa, L., Mojcik, C. F., Ishii, J. K., Klier, G., & Shevach, E. M. (1997). Vascular cell adhesion molecule-1 is expressed by cortical thymic epithelial cells and mediates thymocyte adhesion. Implications for the function of alpha4beta1 (VLA4) integrin in T-cell development. *Blood*, *89*(7), 2461–2471. https://europepmc.org/article/MED/9116290

195. Salomon, D. R., Mojcik, C. F., Chang, A. C., Wadsworth, S., Adams, D. H., Coligan, J. E., & Shevach, E. M. (1994). Constitutive activation of integrin alpha 4 beta 1 defines a unique stage of human thymocyte development. *The Journal of Experimental Medicine*, *179*(5), 1573–1584. https://doi.org/10.1084/jem.179.5.1573

196. San José-Enériz, E., Agirre, X., Rabal, O., Vilas-Zornoza, A., Sanchez-Arias, J. A., Miranda, E., Ugarte, A., Roa, S., Paiva, B., Estella-Hermoso de Mendoza, A., Alvarez, R. M., Casares, N., Segura, V., Martín-Subero, J. I., Ogi, F.-X., Soule, P., Santiveri, C. M., Campos-Olivas, R., Castellano, G., … Prosper, F. (2017). Discovery of first-in-class reversible dual small molecule inhibitors against G9a and DNMTs in hematological malignancies. *Nature Communications*, *8*(1), 15424. https://doi.org/10.1038/ncomms15424

197. Sánchez-Martín, L., Sánchez-Mateos, P., & Cabañas, C. (2013). CXCR7 impact on CXCL12 biology and disease. *Trends in Molecular Medicine*, *19*(1), 12–22. https://doi.org/10.1016/j.molmed.2012.10.004

198. Schäfer, D., Olsen, M., Lähnemann, D., Stanulla, M., Slany, R., Schmiegelow, K., Borkhardt, A., & Fischer, U. (2018). Five percent of healthy newborns have an ETV6-RUNX1 fusion as revealed by DNA-based GIPFEL screening. *Blood*, *131*(7), 821–826. https://doi.org/10.1182/blood-2017-09-808402

199. Schimmel, L., Heemskerk, N., & van Buul, J. D. (2017). Leukocyte transendothelial migration: A local affair. *Small GTPases*, *8*(1), 1–15. https://doi.org/10.1080/21541248.2016.1197872

200. Schmidt, J.-A., Hornhardt, S., Erdmann, F., Sánchez-García, I., Fischer, U., Schüz, J., & Ziegelberger, G. (2021). Risk factors for childhood leukemia: Radiation and

beyond. *Frontiers in Public Health*, *9*, 805757. https://doi.org/10.3389/fpubh.2021.805757

201. Schrappe, M., Valsecchi, M. G., Bartram, C. R., Schrauder, A., Panzer-Grümayer, R., Möricke, A., Parasole, R., Zimmermann, M., Dworzak, M., Buldini, B., Reiter, A., Basso, G., Klingebiel, T., Messina, C., Ratei, R., Cazzaniga, G., Koehler, R., Locatelli, F., Schäfer, B. W., … Conter, V. (2011). Late MRD response determines relapse risk overall and in subsets of childhood T-cell ALL: results of the AIEOP-BFM-ALL 2000 study. *Blood*, *118*(8), 2077–2084. https://doi.org/10.1182/blood-2011-03-338707

202. Schrappe, M., Hunger, S. P., Pui, C.-H., Saha, V., Gaynon, P. S., Baruchel, A., Conter, V., Otten, J., Ohara, A., Versluys, A. B., Escherich, G., Heyman, M., Silverman, L. B., Horibe, K., Mann, G., Camitta, B. M., Harbott, J., Riehm, H., Richards, S., … Zimmermann, M. (2012). Outcomes after induction failure in childhood acute lymphoblastic leukemia. *The New England Journal of Medicine*, *366*(15), 1371–1381. https://doi.org/10.1056/NEJMoa1110169

203. Shah, N. N., & Fry, T. J. (2019). Mechanisms of resistance to CAR T cell therapy. *Nature Reviews. Clinical Oncology*, *16*(6), 372–385. https://doi.org/10.1038/s41571-019-0184-6

204. Shahbazian, M. D., Zhang, K., & Grunstein, M. (2005). Histone H2B ubiquitylation controls processive methylation but not monomethylation by Dot1 and Set1. *Molecular Cell*, *19*(2), 271–277. https://doi.org/10.1016/j.molcel.2005.06.010

205. Shalapour, S., Hof, J., Kirschner-Schwabe, R., Bastian, L., Eckert, C., Prada, J., Henze, G., von Stackelberg, A., & Seeger, K. (2011). High VLA-4 expression is associated with adverse outcome and distinct gene expression changes in childhood B-cell precursor acute lymphoblastic leukemia at first relapse. *Haematologica*, *96*(11), 1627–1635. https://doi.org/10.3324/haematol.2011.047993

206. Sharma, S., Kelly, T. K., & Jones, P. A. (2010). Epigenetics in cancer. *Carcinogenesis*, *31*(1), 27–36. https://doi.org/10.1093/carcin/bgp220

207. Shaw, S. K., Bamba, P. S., Perkins, B. N., & Luscinskas, F. W. (2001). Real-time imaging of vascular endothelial cadherin during leukocyte transmigration across endothelium. *The Journal of Immunology*, *167*(4), 2323–2330. https://doi.org/10.4049/jimmunol.167.4.2323

208. Shen, Z., Gu, X., Mao, W., Yin, L., Yang, L., Zhang, Z., Liu, K., Wang, L., & Huang, Y. (2018). Influence of pre-transplant minimal residual disease on prognosis after Allo-SCT for patients with acute lymphoblastic leukemia: systematic review and meta-analysis. *BMC Cancer*, *18*(1), 1–12. https://doi.org/10.1186/s12885-018-4670-5

209. Shi, Y., Riese, D. J., 2nd, & Shen, J. (2020). The role of the CXCL12/CXCR4/CXCR7 chemokine axis in cancer. *Frontiers in Pharmacology*, *11*, 574667. https://doi.org/10.3389/fphar.2020.574667

210. Shinkai, Y., & Tachibana, M. (2011). H3K9 methyltransferase G9a and the related molecule GLP. *Genes & Development*, *25*(8), 781–788. https://doi.org/10.1101/gad.2027411

211. Shirozu, M., Nakano, T., Inazawa, J., Tashiro, K., Tada, H., Shinohara, T., & Honjo, T. (1995). Structure and chromosomal localization of the human stromal cell-derived factor 1 (SDF1) gene. *Genomics*, *28*(3), 495–500. https://doi.org/10.1006/geno.1995.1180

212. Simon, C., Chagraoui, J., Krosl, J., Gendron, P., Wilhelm, B., Lemieux, S., Boucher, G., Chagnon, P., Drouin, S., Lambert, R., Rondeau, C., Bilodeau, A., Lavallée, S., Sauvageau, M., Hébert, J., & Sauvageau, G. (2012). A key role for *EZH2* and associated genes in mouse and human adult T-cell acute leukemia. *Genes & Development*, *26*(7), 651–656. https://doi.org/10.1101/gad.186411.111

213. Sison, E. A. R., & Brown, P. (2011a). The bone marrow microenvironment and leukemia: biology and therapeutic targeting. *Expert Review of Hematology*, *4*(3), 271–283. https://doi.org/10.1586/ehm.11.30

214. Sison, E. A. R., & Brown, P. (2011b). The bone marrow microenvironment and leukemia: biology and therapeutic targeting. *Expert Review of Hematology*, *4*(3), 271–283. https://doi.org/10.1586/ehm.11.30

215. Sneider, A., Hah, J., Wirtz, D., & Kim, D.-H. (2019). Recapitulation of molecular regulators of nuclear motion during cell migration. *Cell Adhesion & Migration*, *13*(1), 50–62. https://doi.org/10.1080/19336918.2018.1506654

216. Song, Y., Wu, F., & Wu, J. (2016a). Targeting histone methylation for cancer therapy: enzymes, inhibitors, biological activity and perspectives. *Journal of Hematology & Oncology*, *9*(1), 49. https://doi.org/10.1186/s13045-016-0279-9

217. Song, Y., Wu, F., & Wu, J. (2016b). Targeting histone methylation for cancer therapy: enzymes, inhibitors, biological activity and perspectives. *Journal of Hematology & Oncology*, *9*(1). https://doi.org/10.1186/s13045-016-0279-9 Song, Z.-Y., Wang, F., Cui, S.-X., Gao, Z.-H., & Qu, X.-J. (2019). CXCR7/CXCR4 heterodimer-induced histone demethylation: a new mechanism of colorectal tumorigenesis. *Oncogene*, *38*(9), 1560–1575. https://doi.org/10.1038/s41388-018-0519-2

218. Sotiroudis, T. G., Kyriakidis, S. M., Baltas, L. G., Ktenas, T. B., Zevgolis, V. G., & Evangelopoulos, A. E. (1989). Phosphorylase Kinase and Protein Kinase C: Functional Similarities. En *Receptors, Membrane Transport and Signal Transduction* (pp. 55–66). Springer Berlin Heidelberg.

219. Spagnol, S. T., Armiger, T. J., & Dahl, K. N. (2016). Mechanobiology of chromatin and the nuclear interior. *Cellular and Molecular Bioengineering*, *9*(2), 268–276. https://doi.org/10.1007/s12195-016-0444-9

220. Steinberg, S. F. (2008). Structural basis of protein kinase C isoform function. *Physiological Reviews*, *88*(4), 1341–1378. https://doi.org/10.1152/physrev.00034.2007

221. Steinherz, P. G., Gaynon, P. S., Breneman, J. C., Cherlow, J. M., Grossman, N. J., Kersey, J. H., Johnstone, H. S., Sather, H. N., Trigg, M. E., Uckun, F. M., & Bleyer, W. A. (1998). Treatment of patients with acute lymphoblastic leukemia with bulky extramedullary disease and T-cell phenotype or other poor prognostic features: randomized controlled trial from the Children's Cancer Group. *Cancer*, *82*(3), 600–612. https://doi.org/10.1002/(sici)1097-0142(19980201)82:3<600:aid-cncr24>3.0.co;2-4

222. Stephens, A. D., Banigan, E. J., Adam, S. A., Goldman, R. D., & Marko, J. F. (2017). Chromatin and lamin A determine two different mechanical response regimes of the cell nucleus. *Molecular Biology of the Cell*, *28*(14), 1984–1996. https://doi.org/10.1091/mbc.E16-09-0653

223. Stephens, A. D., Liu, P. Z., Banigan, E. J., Almassalha, L. M., Backman, V., Adam, S. A., Goldman, R. D., & Marko, J. F. (2018). Chromatin histone modifications and rigidity affect nuclear morphology independent of lamins. *Molecular Biology of the Cell*, *29*(2), 220–233. https://doi.org/10.1091/mbc.e17-06-0410

224. Stock, W. (2010). Adolescents and young adults with acute lymphoblastic leukemia. *Hematology*, *2010*(1), 21–29. https://doi.org/10.1182/asheducation-2010.1.21

225. Stone, M. J., Hayward, J. A., Huang, C., E Huma, Z., & Sanchez, J. (2017). Mechanisms of regulation of the chemokine-receptor network. *International Journal of Molecular Sciences*, *18*(2), 342. https://doi.org/10.3390/ijms18020342

226. Storring, J. M., Minden, M. D., Kao, S., Gupta, V., Schuh, A. C., Schimmer, A. D., Yee, K. W. L., Kamel-Reid, S., Chang, H., Lipton, J. H., Messner, H. A., Xu, W., & Brandwein, J. M. (2009). Treatment of adults with BCR-ABL negative acute lymphoblastic leukaemia with a modified paediatric regimen. *British Journal of Haematology*, *146*(1), 76–85. https://doi.org/10.1111/j.1365-2141.2009.07712.x

227. Swerdlow, S. H., & International Agency for Research on Cancer. (2008). *WHO classification of tumours of haematopoietic and lymphoid tissues: Vol. 2: International Agency for Research on Cancer* (4a ed.). IARC.

228. Swift, J., Ivanovska, I. L., Buxboim, A., Harada, T., Dingal, P. C. D. P., Pinter, J., Pajerowski, J. D., Spinler, K. R., Shin, J.-W., Tewari, M., Rehfeldt, F., Speicher, D. W., & Discher, D. E. (2013). Nuclear lamin-A scales with tissue stiffness and enhances matrix-directed differentiation. *Science (New York, N.Y.)*, *341*(6149), 1240104. https://doi.org/10.1126/science.1240104

229. Szczesny, S. E., & Mauck, R. L. (2017a). The nuclear option: Evidence implicating the cell nucleus in mechanotransduction. *Journal of Biomechanical Engineering*, *139*(2), 021006. https://doi.org/10.1115/1.4035350

230. Szczesny, S. E., & Mauck, R. L. (2017b). The nuclear option: Evidence implicating the cell nucleus in mechanotransduction. *Journal of Biomechanical Engineering*, *139*(2), 021006. https://doi.org/10.1115/1.4035350

231. Tachibana, M., Ueda, J., Fukuda, M., Takeda, N., Ohta, T., Iwanari, H., Sakihama, T., Kodama, T., Hamakubo, T., & Shinkai, Y. (2005). Histone methyltransferases G9a and GLP form heteromeric complexes and are both crucial for methylation of euchromatin at H3-K9. *Genes & Development*, *19*(7), 815–826. https://doi.org/10.1101/gad.1284005

232. Tamaru, H. (2010). Confining euchromatin/heterochromatin territory: jumonji crosses the line. *Genes & Development*, *24*(14), 1465–1478. https://doi.org/10.1101/gad.1941010

233. Tan, Y., Tajik, A., Chen, J., Jia, Q., Chowdhury, F., Wang, L., Chen, J., Zhang, S., Hong, Y., Yi, H., Wu, D. C., Zhang, Y., Wei, F., Poh, Y.-C., Seong, J., Singh, R., Lin, L.-J., Doğanay, S., Li, Y., … Wang, N. (2014). Matrix softness regulates plasticity of tumour-repopulating cells via H3K9 demethylation and Sox2 expression. *Nature Communications*, *5*(1), 4619. https://doi.org/10.1038/ncomms5619

234. Tanaka, K. (2012). Higher involvement of subtelomere regions for chromosome rearrangements in leukemia and lymphoma and in irradiated leukemic cell line. *Indian journal of science and technology*, *5*(1), 1–11. https://doi.org/10.17485/ijst/2012/v5i1.1

235. Tasian, S. K., Loh, M. L., & Hunger, S. P. (2015). Childhood acute lymphoblastic leukemia: Integrating genomics into therapy: Childhood ALL Genomics. *Cancer*, *121*(20), 3577–3590. https://doi.org/10.1002/cncr.29573

236. Tebbi, C. K. (2021). Etiology of acute leukemia: A review. *Cancers*, *13*(9), 2256. https://doi.org/10.3390/cancers13092256

237. Teicher, B. A., & Fricker, S. P. (2010). CXCL12 (SDF-1)/CXCR4 pathway in cancer. *Clinical Cancer Research: An Official Journal of the American Association for Cancer Research*, *16*(11), 2927–2931. https://doi.org/10.1158/1078-0432.CCR-09-2329

238. Terwilliger, T., & Abdul-Hay, M. (2017). Acute lymphoblastic leukemia: a comprehensive review and 2017 update. *Blood Cancer Journal*, *7*(6), e577–e577. https://doi.org/10.1038/bcj.2017.53

239. Trepat, X., Chen, Z., & Jacobson, K. (2012). Cell migration. *Comprehensive Physiology*, *2*(4), 2369–2392. https://doi.org/10.1002/cphy.c110012

240. Trojer, P., & Reinberg, D. (2006a). Histone lysine demethylases and their impact on epigenetics. *Cell*, *125*(2), 213–217. https://doi.org/10.1016/j.cell.2006.04.003

241. Trojer, P., & Reinberg, D. (2006b). Histone lysine demethylases and their impact on epigenetics. *Cell*, *125*(2), 213–217. https://doi.org/10.1016/j.cell.2006.04.003

242. Tsai, H.-I., Wu, Y., Huang, R., Su, D., Wu, Y., Liu, X., Wang, L., Xu, Z., Pang, Y., Sun, C., He, C., Shu, F., Zhu, H., Wang, D., Cheng, F., Huang, L., & Chen, H. (2022). PHF6 functions as a tumor suppressor by recruiting methyltransferase SUV39H1 to nucleolar region and offers a novel therapeutic target for PHF6-muntant leukemia. *Acta Pharmaceutica Sinica. B*, *12*(4), 1913–1927. https://doi.org/10.1016/j.apsb.2021.10.025

243. Turner, M. D., Nedjai, B., Hurst, T., & Pennington, D. J. (2014). Cytokines and chemokines: At the crossroads of cell signalling and inflammatory disease. *Biochimica et Biophysica Acta*, *1843*(11), 2563–2582. https://doi.org/10.1016/j.bbamcr.2014.05.014

244. Ulvmar, M. H., Hub, E., & Rot, A. (2011). Atypical chemokine receptors. *Experimental Cell Research*, *317*(5), 556–568. https://doi.org/10.1016/j.yexcr.2011.01.012

245. Van Vlierberghe, P., & Ferrando, A. (2012). The molecular basis of T cell acute lymphoblastic leukemia. *The Journal of Clinical Investigation*, *122*(10), 3398–3406. https://doi.org/10.1172/JCI61269

246. Van Vlierberghe, P., van Grotel, M., Beverloo, H. B., Lee, C., Helgason, T., Buijs-Gladdines, J., Passier, M., van Wering, E. R., Veerman, A. J. P., Kamps, W. A., Meijerink, J. P. P., & Pieters, R. (2006). The cryptic chromosomal deletion del(11)(p12p13) as a new activation mechanism of LMO2 in pediatric T-cell acute lymphoblastic leukemia. *Blood*, *108*(10), 3520–3529. https://doi.org/10.1182/blood-2006-04-019927

247. Verstraeten, V. L. R. M., & Lammerding, J. (2008). Experimental techniques for study of chromatin mechanics in intact nuclei and living cells. *Chromosome Research: An International Journal on the Molecular, Supramolecular and Evolutionary Aspects of Chromosome Biology*, *16*(3), 499–510. https://doi.org/10.1007/s10577-008-1232-8

248. Walport, L. J., Hopkinson, R. J., Chowdhury, R., Schiller, R., Ge, W., Kawamura, A., & Schofield, C. J. (2016a). Arginine demethylation is catalysed by a subset of JmjC histone lysine demethylases. *Nature Communications*, *7*, 11974. https://doi.org/10.1038/ncomms11974

249. Walport, L. J., Hopkinson, R. J., Chowdhury, R., Schiller, R., Ge, W., Kawamura, A., & Schofield, C. J. (2016b). Arginine demethylation is catalysed by a subset of JmjC histone lysine demethylases. *Nature Communications*, *7*, 11974. https://doi.org/10.1038/ncomms11974

250. Wang, J., Chen, S., Xiao, W., Li, W., Wang, L., Yang, S., Wang, W., Xu, L., Liao, S., Liu, W., Wang, Y., Liu, N., Zhang, J., Xia, X., Kang, T., Chen, G., Cai, X., Yang, H., Zhang, X., … Zhou, P. (2018). CAR-T cells targeting CLL-1 as an approach to treat acute myeloid leukemia. *Journal of Hematology & Oncology*, *11*(1), 7. https://doi.org/10.1186/s13045-017-0553-5

251. Wang X.-J., Yuan W.-P., & Cheng T. (2012). Function of histone methyltransferases in HSC regulation and leukemogenesis. *Zhonghua xue ye xue za zhi*, *33*(9), 781–784. https://doi.org/10.3760/cma.j.issn.0253-2727.2012.09.026

252. Verstraeten, V. L. R. M., & Lammerding, J. (2008). Experimental techniques for study of chromatin mechanics in intact nuclei and living cells. *Chromosome Research: An International Journal on the Molecular, Supramolecular and Evolutionary Aspects of Chromosome Biology*, *16*(3), 499–510. https://doi.org/10.1007/s10577-008-1232-8

253. Webb, B. L., Hirst, S. J., & Giembycz, M. A. (2000). Protein kinase C isoenzymes: a review of their structure, regulation and role in regulating airways smooth muscle tone and mitogenesis: Protein kinase C. *British Journal of Pharmacology*, *130*(7), 1433–1452. https://doi.org/10.1038/sj.bjp.0703452

254. Wei, S.-Y., Lin, T.-E., Wang, W.-L., Lee, P.-L., Tsai, M.-C., & Chiu, J.-J. (2014). Protein kinase C-δ and -β coordinate flow-induced directionality and deformation of migratory human blood T-lymphocytes. *Journal of Molecular Cell Biology*, *6*(6), 458–472. https://doi.org/10.1093/jmcb/mju050

255. Wilson, A., & Trumpp, A. (2006). Bone-marrow haematopoietic-stem-cell niches. *Nature Reviews. Immunology*, *6*(2), 93–106. https://doi.org/10.1038/nri1779

256. Wirtz, D., Konstantopoulos, K., & Searson, P. C. (2011). The physics of cancer: the role of physical interactions and mechanical forces in metastasis. *Nature Reviews. Cancer*, *11*(7), 512–522. https://doi.org/10.1038/nrc3080

257. Wolf, K., Te Lindert, M., Krause, M., Alexander, S., Te Riet, J., Willis, A. L., Hoffman, R. M., Figdor, C. G., Weiss, S. J., & Friedl, P. (2013). Physical limits of cell migration: control by ECM space and nuclear deformation and tuning by proteolysis and traction force. *The Journal of Cell Biology*, *201*(7), 1069–1084. https://doi.org/10.1083/jcb.201210152

258. Wolffe, A. P. (1997). Histones, nucleosomes and the roles of chromatin structure in transcriptional control. *Biochemical Society Transactions*, *25*(2), 354–358. https://doi.org/10.1042/bst0250354

259. Woo, H., Dam Ha, S., Lee, S. B., Buratowski, S., & Kim, T. (2017). Modulation of gene expression dynamics by co-transcriptional histone methylations. *Experimental & Molecular Medicine*, *49*(4), e326–e326. https://doi.org/10.1038/emm.2017.19

260. Xu, L., Wang, J., Liu, Y., Xie, L., Su, B., Mou, D., Wang, L., Liu, T., Wang, X., Zhang, B., Zhao, L., Hu, L., Ning, H., Zhang, Y., Deng, K., Liu, L., Lu, X., Zhang, T., Xu, J., … Chen, H. (2019). CRISPR-edited stem cells in a patient with HIV and acute Lymphocytic leukemia. *The New England Journal of Medicine*, *381*(13), 1240–1247. https://doi.org/10.1056/NEJMoa1817426

261. Xu, H., Wu, M., Ma, X., Huang, W., & Xu, Y. (2021). Function and mechanism of novel histone posttranslational modifications in health and disease. *BioMed Research International*, *2021*, 6635225. https://doi.org/10.1155/2021/6635225

262. Yan, L., Rosen, N., & Arteaga, C. (2011). Targeted cancer therapies. *Chinese Journal of Cancer*, *30*(1), 1–4. https://doi.org/10.5732/cjc.010.10553

263. Yang, J., Li, J., Zhang, X., Lv, F., Guo, X., Wang, Q., Wang, L., Chen, D., Zhou, X., Ren, J., & Lu, P. (2018). A feasibility and safety study of CD19 and CD22 chimeric antigen receptors-modified T cell cocktail for therapy of B cell acute lymphoblastic leukemia. *Blood*, *132*(Supplement 1), 277–277. https://doi.org/10.1182/blood-2018-99-11441

264. Yokoyama, Y., Matsumoto, A., Hieda, M., Shinchi, Y., Ogihara, E., Hamada, M., Nishioka, Y., Kimura, H., Yoshidome, K., Tsujimoto, M., & Matsuura, N. (2014). Loss of histone H4K20 trimethylation predicts poor prognosis in breast cancer and is associated with invasive activity. *Breast Cancer Research: BCR*, *16*(3), R66. https://doi.org/10.1186/bcr3681

265. Yu, L., Cecil, J., Peng, S.-B., Schrementi, J., Kovacevic, S., Paul, D., Su, E. W., & Wang, J. (2006). Identification and expression of novel isoforms of human stromal cell-derived factor 1. *Gene*, *374*, 174–179. https://doi.org/10.1016/j.gene.2006.02.001

266. Zarbock, A., Ley, K., McEver, R. P., & Hidalgo, A. (2011). Leukocyte ligands for endothelial selectins: specialized glycoconjugates that mediate rolling and signaling under flow. *Blood*, *118*(26), 6743–6751. https://doi.org/10.1182/blood-2011-07-343566

267. Zhang, L., Yu, B., Hu, M., Wang, Z., Liu, D., Tong, X., Leng, J., Zhou, B., Hu, Y., Wu, R., Ding, Q., & Zhang, Q. (2011). Role of Rho-ROCK signaling in MOLT4 cells metastasis induced by CCL25. *Leukemia Research*, *35*(1), 103–109. https://doi.org/10.1016/j.leukres.2010.07.039

268. Zhang, X., Cook, P. C., Zindy, E., Williams, C. J., Jowitt, T. A., Streuli, C. H., MacDonald, A. S., & Redondo-Muñoz, J. (2016). Integrin α4β1 controls G9a activity that regulates epigenetic changes and nuclear properties required for lymphocyte migration. *Nucleic Acids Research*, *44*(7), 3031–3044. https://doi.org/10.1093/nar/gkv1348

269. Zhao, Z., & Shilatifard, A. (2019). Epigenetic modifications of histones in cancer. *Genome Biology*, *20*(1), 245. https://doi.org/10.1186/s13059-019-1870-5

270. Zhou, B., Leng, J., Hu, M., Zhang, L., Wang, Z., Liu, D., Tong, X., Yu, B., Hu, Y., Deng, C., Liu, Y., & Zhang, Q. (2010). Ezrin is a key molecule in the metastasis of MOLT4 cells induced by CCL25/CCR9. *Leukemia Research*, *34*(6), 769–776. https://doi.org/10.1016/j.leukres.2009.11.025

271. Zhou, W., Guo, S., Liu, M., Burow, M. E., & Wang, G. (2019). Targeting CXCL12/CXCR4 axis in tumor immunotherapy. *Current Medicinal Chemistry*, *26*(17), 3026–3041. https://doi.org/10.2174/0929867324666170830111531

272. Zhou, Y.-Q., Liu, D.-Q., Chen, S.-P., Sun, J., Zhou, X.-R., Xing, C., Ye, D.-W., & Tian, Y.-K. (2019). The role of CXCR3 in neurological diseases. *Current Neuropharmacology*, *17*(2), 142–150. https://doi.org/10.2174/1570159X15666171109161140

273. Zlotnik, A., Burkhardt, A. M., & Homey, B. (2011). Homeostatic chemokine receptors and organ-specific metastasis. *Nature Reviews. Immunology*, *11*(9), 597–606. https://doi.org/10.1038/nri304

274. Zlotnik, A., & Yoshie, O. (2000). Chemokines: a new classification system and their role in immunity. *Immunity*, *12*(2), 121–127. https://doi.org/10.1016/s1074-7613(00)80165-x

275. Zuckerman, T., & Rowe, J. M. (2014). Pathogenesis and prognostication in acute lymphoblastic leukemia. *F1000 Prime Reports*, *6*, 59. https://doi.org/10.12703/P6-59

276. Zwerger, M., Ho, C. Y., & Lammerding, J. (2011a). Nuclear mechanics in disease. *Annual Review of Biomedical Engineering*, *13*(1), 397–428. https://doi.org/10.1146/annurev-bioeng-071910-124736

277. Zwerger, M., Ho, C. Y., & Lammerding, J. (2011b). Nuclear mechanics in disease. *Annual Review of Biomedical Engineering*, *13*(1), 397–428. https://doi.org/10.1146/annurev-bioeng-071910-124736

ANEXOS

PUBLICACIONES OBTENIDAS DURANTE LA TESIS DOCTORAL

1. Publicaciones relacionadas con la tesis doctoral

Elena Madrazo, David Ruano, Lorea Abad, Estefanía Alonso-Gómez Carmen Sánchez-Valdepeñas, África González-Murillo, Manuel Ramírez, Javier Redondo-Muñoz. G9a correlates with VLA-4 integrin and influences the migration of childhood acute lymphoblastic leukemia cells. **Cancers (Basel), Sep 2018**. doi: 10.3390/cancers10090325.

Diego Herráez-Aguilar, **Elena Madrazo**, Horacio López-Menéndez, Manuel Ramírez, Francisco Monroy, Javier Redondo-Muñoz. Multiple particle tracking analysis in isolated nuclei reveals the mechanical phenotype of leukemia cells. **Scientific Reports, Apr 2020.** doi: 10.1038/s41598-020-63682-5.

Elena Madrazo #, Raquel González-Novo #, Cándido Ortiz-Placín, Mario García de Lacoba, África González-Murillo, Manuel Ramírez, Javier Redondo-Muñoz. Fast H3K9 methylation promoted by CXCL12 contributes to nuclear changes and invasiveness of T-acute lymphoblastic leukemia cells. **Oncogene, Feb 2022.** doi: 10.1038/s41388-021-02168-8.

2. Otras publicaciones durante la tesis doctoral

Elena Madrazo, Andrea Cordero Conde, Javier Redondo-Muñoz. Inside the Cell: Integrins as New Governors of Nuclear Alterations? **Review Cancers (Basel), Jul 2017.** doi: 10.3390/cancers9070082.

Pengbo Wang, Marcel Dreger, **Elena Madrazo,** Craig J Williams, Rafael Samaniego, Nigel W Hodson, Francisco Monroy, Esther Baena, Paloma Sánchez-Mateos, Adam Hurlstone, Javier Redondo-Muñoz. WDR5 modulates cell motility and morphology and controls nuclear changes induced by a 3D environment. **PNAS, Aug 2018.** doi: 10.1073/pnas.1719405115.

Marcel Dreger, **Elena Madrazo**, Adam Hurlstone , Javier Redondo-Muñoz. Novel contribution of epigenetic changes to nuclear dynamics. **Review Nucleus, Dec 2019**. doi: 10.1080/19491034.2019.1580100.

.